

**SUBSECTION 2.5.2: VIBRATORY GROUND MOTION
TABLE OF CONTENTS**

2.5.2	VIBRATORY GROUND MOTION	2.5.2-1
2.5.2.1	Seismicity	2.5.2-2
2.5.2.2	Geologic Structures and EPRI Seismic Source Model for the Site Region	2.5.2-16
2.5.2.3	Correlation of Seismicity with Geologic Structures and EPRI Sources	2.5.2-21
2.5.2.4	Probabilistic Seismic Hazard Analysis and Controlling Earthquakes	2.5.2-21
2.5.2.5	Seismic Wave Transmission Characteristics of the Site	2.5.2-82
2.5.2.6	Ground Motion Response Spectra	2.5.2-92
2.5.2.7	References	2.5.2-93

SUBSECTION 2.5.2 LIST OF TABLES

<u>Number</u>	<u>Title</u>
2.5.2-201	Conversion between Body-Wave (mb) and Moment (Mw) Magnitudes
2.5.2-202	Seismicity Catalog for the Phase 1 Investigation Region [22°N to 35°N, 100°W to 65°W] for which the Events are Rmb Magnitude Greater than or Equal to 3.0 or Intensity [Int] Greater than or Equal to IV(4)
2.5.2-203	Seismicity Catalog for the Phase 2 Investigation Region [15°N to 24°N, 100°W to 65°W] for which the Events are Mw Magnitude Greater than or Equal to 6.0
2.5.2-204	Seismicity Events Recommended for Recurrence Analysis within the Gulf of Mexico
2.5.2-205	Region 2 Matrix of Detection Probabilities; Modified to Extend the Matrix to Year 2007
2.5.2-206	Matrix of Detection Probabilities for the Gulf of Mexico
2.5.2-207	Summary of EPRI Seismic Sources within the Site Region
2.5.2-208	Mean and Fractile Seismic Hazard Data for Crystal River Site from EPRI-SOG Study and Units 6 & 7 Study
2.5.2-209	Summary of Supplemental Sources and Truncated Woodward-Clyde Source
2.5.2-210	Geographic Coordinates of Supplemental Sources and Truncated Woodward-Clyde Source
2.5.2-211	Geographic Coordinates of Updated Charleston Seismic Source (UCSS) Model Sources
2.5.2-212	Comparison of Post-EPRI Magnitude Estimates for the 1886 Charleston Earthquake
2.5.2-213	Comparison of Talwani and Schaeffer and UCSS Age Constraints on Charleston-Area Paleoliquefaction Events
2.5.2-214	List of Experts Contacted as part of Cuba and Northern Caribbean Source Model SSHAC Level 2 Process
2.5.2-215	Significant Earthquakes in the Cuba and Northern Caribbean Region, 1500 to 2008
2.5.2-216	Empirical Relations between Rupture Area (A) and Moment Magnitude (Mw) and Rupture Length (L) and Mw Used to Determine Mmax for Cuba and Northern Caribbean Sources
2.5.2-217	Summary of Cuba and Northern Caribbean Source Model
2.5.2-218	Geographic Coordinates of Cuba Source

SUBSECTION 2.5.2 LIST OF TABLES (CONT.)

<u>Number</u>	<u>Title</u>
2.5.2-219	Geographic Coordinates of Cuba and Northern Caribbean Model Line Sources
2.5.2-220	Mean and Fractile Rock Seismic Hazard Curves
2.5.2-221	Mean Hard Rock UHRS Accelerations (g)
2.5.2-222	Percent Contribution to Deaggregation
2.5.2-223	Controlling Magnitudes and Distances from Deaggregation
2.5.2-224	Assigned Strong Motion Durations in P-SHAKE
2.5.2-225	HF and LF Horizontal 1E-04 Rock Spectra, Amplification Factors, Site Spectra, and Raw and Smoothed Envelope Spectra
2.5.2-226	HF and LF horizontal 1E-05 Rock Spectra, Amplification Factors, Site Spectra, and Raw and Smoothed Envelope Spectra
2.5.2-227	Horizontal 1E-04 and 1E-05 Site Spectra, Values of AR and DF, and GMRS
2.5.2-228	Smooth 1E-04, 1E-05, and 1E-06 Spectra at GMRS Elevation
2.5.2-229	V/H Ratios, Vertical 1E-04 and 1E-05 Site Spectra, Values of AR and DF, and GMRS

SUBSECTION 2.5.2 LIST OF FIGURES

<u>Number</u>	<u>Title</u>
2.5.2-201	Seismicity in the Study Region, Phase 1 and Phase 2
2.5.2-202	Supplemental Areas of Incompleteness Regions, Gulf of Mexico, Near Florida, and Near Atlantic, South of the Boundary of EPRI Incompleteness Regions
2.5.2-203	EPRI Seismic Source Zones and Updated Charleston Seismic Source (UCSS) Model Sources
2.5.2-204	EPRI and Supplemental Source Zones — Bechtel
2.5.2-205	EPRI and Supplemental Source Zones — Dames & Moore
2.5.2-206	EPRI and Supplemental Source Zones — Law Engineering
2.5.2-207	EPRI and Supplemental Source Zones — Rondout Associates
2.5.2-208	EPRI and Supplemental Source Zones — Weston Geophysical
2.5.2-209	EPRI and Supplemental Source Zones — Woodward-Clyde
2.5.2-210	Historical Seismicity from EPRI Earthquake Catalog and from Updated Catalog (Through 2007) in Southeastern United States
2.5.2-211	Earthquake Occurrence Rates for EPRI Catalog and for Updated Catalog Extended Through 2007 for Florida Test Region
2.5.2-212	Gulf Coast Crustal Divisions from Kanter
2.5.2-213	Passive Margin Basins on Continental and Transitional Crust from Bally et al.
2.5.2-214	Plate Reconstruction Showing Stretched Continental Crust from Pindell and Kennan
2.5.2-215	Extended Continental Crust from Dunbar and Sawyer
2.5.2-216	Thick Transitional Crust from Sawyer et al.
2.5.2-217	Updated Charleston Seismic Source (UCSS) Model Sources
2.5.2-218	Updated Charleston Seismic Source (UCSS) Logic Tree with Weights for Each Branch
2.5.2-219	Tectonic Features and Significant Earthquakes of Cuba and the Northern Caribbean
2.5.2-220	Fault Map of Cuba from Garcia et al.

SUBSECTION 2.5.2 LIST OF FIGURES (CONT.)

<u>Number</u>	<u>Title</u>
2.5.2-221	Seismicity in the Cuba and Northern Caribbean Region, 1500–2008
2.5.2-222	Kinematic Illustrations Showing Interactions of Sepentrional and Northern Hispaniola Faults at Depth
2.5.2-223	Selected Rupture Zones of Major Earthquakes on the Central North America-Caribbean Plate Boundary from Dolan and Bowman
2.5.2-224	Cuba and Northern Caribbean Seismic Source Model Sources
2.5.2-225	Mean and Fractile Rock PGA Seismic Hazard Curves
2.5.2-226	Mean and Fractile Rock 25 Hz Seismic Hazard Curves, Rock
2.5.2-227	Mean and Fractile Rock 10 Hz Seismic Hazard Curves, Rock
2.5.2-228	Mean and Fractile Rock 5 Hz Seismic Hazard Curves, Rock
2.5.2-229	Mean and Fractile Rock 2.5 Hz Seismic Hazard Curves, Rock
2.5.2-230	Mean and Fractile Rock 1 Hz Seismic Hazard Curves, Rock
2.5.2-231	Mean and Fractile Rock 0.5 Hz Seismic Hazard Curves, Rock
2.5.2-232	Mean and Median Rock UHRS for 1E-04, 1E-05, and 1E-06
2.5.2-233	M and R Deaggregation for 1 and 2.5 Hz at 1E-04 Annual Frequency of Exceedence
2.5.2-234	M and R Deaggregation for 5 and 10 Hz at 1E-04 Annual Frequency of Exceedence
2.5.2-235	M and R Deaggregation for 1 and 2.5 Hz at 1E-05 Annual Frequency of Exceedence
2.5.2-236	M and R Deaggregation for 5 and 10 Hz at 1E-05 Annual Frequency of Exceedence
2.5.2-237	M and R Deaggregation for 1 and 2.5 Hz at 1E-06 Annual Frequency of Exceedence
2.5.2-238	M and R Deaggregation for 5 and 10 Hz at 1E-06 Annual Frequency of Exceedence

SUBSECTION 2.5.2 LIST OF FIGURES (CONT.)

<u>Number</u>	<u>Title</u>
2.5.2-239	HF and LF Rock Spectra Anchored to Mean UHRS Values from Hazard Calculation for 1E-04 Spectra
2.5.2-240	HF and LF Rock Spectra Anchored to Mean UHRS Values from Hazard Calculation for 1E-05 Spectra
2.5.2-241	HF and LF Rock Spectra Anchored to Mean UHRS Values from Hazard Calculation for 1E-06 Spectra
2.5.2-242	Input Base Case Shear Wave Velocity Profile
2.5.2-243	Input Median Shear Wave Velocity Profile (+/- One Standard Deviation) for Randomization Process
2.5.2-244	Strain Dependent Degradation Curves for Natural Soils (<150 feet)
2.5.2-245	Strain Dependent Damping Ratio Properties for Natural Soils (<150 feet)
2.5.2-246	Randomized Shear Wave Velocity Profiles, Median Shear Wave Velocity Profile and the Input Median Profile Used For Randomization
2.5.2-247	Median of Site Amplification Factor at GMRS Horizon (El. – 35 feet) from Analyses of the 60 Modified Random Profiles with the 1E-04 LF Input Motion
2.5.2-248	Maximum Strains Versus Depth that are Calculated for the 60 Profiles and their Median (Thick Red Line) with the 1E-04 LF Input Motion
2.5.2-249	Median of Site Amplification Factor at GMRS Horizon (El. – 35 feet) from Analyses of the 60 Modified Random Profiles with the 1E-04 HF Input Motion
2.5.2-250	Maximum Strains Versus Depth that are Calculated for the 60 Profiles and their Median (Thick Red Line) with the 1E-04 HF Input Motion
2.5.2-251	Median of Site Amplification Factor at GMRS Horizon (El. – 35 feet) from Analyses of the 60 Modified Random Profiles with the 1E-05 LF Input Motion
2.5.2-252	Maximum Strains Versus Depth that are Calculated for the 60 Profiles and their Median (Thick Red Line) with the 1E-05 LF Input Motion
2.5.2-253	Median of Site Amplification Factor at GMRS Horizon (El. – 35 feet) from Analyses of the 60 Modified Random Profiles with the 1E-05 HF Input

Turkey Point Units 6 & 7
COL Application
Part 2 — FSAR

SUBSECTION 2.5.2 LIST OF FIGURES (CONT.)

<u>Number</u>	<u>Title</u>
	Motion
2.5.2-254	Maximum Strains Versus Depth that are Calculated for the 60 Profiles and their Median (Thick Red Line) with the 1E-05 HF Input Motion
2.5.2-255	Median Maximum Strain Profiles (Full Soil Column) (Sheet 1 of 2)
2.5.2-255	Median Maximum Strain Profiles (Upper 800 feet) (Sheet 2 of 2)
2.5.2-256	Median Profiles of Strain-Compatible Soil Damping (Full Soil Column) (Sheet 1 of 2)
2.5.2-256	Median Profiles of Strain-Compatible Soil Damping (Upper 800 feet) (Sheet 2 of 2)
2.5.2-257	Comparison of Median Soil Amplification Factors at GMRS Horizon for LF and HF 1E-04 and 1E-05 Input Motions
2.5.2-258	HF and LF Horizontal 1E-04 and 1E-05 Site Spectra
2.5.2-259	Smoothed Horizontal 1E-04 and 1E-05 Site Spectra
2.5.2-260	Smoothed Horizontal 1E-04 and 1E-05 Site Spectra and GMRS
2.5.2-261	Smoothed Vertical 1E-04 and 1E-05 Site Spectra and GMRS

2.5.2 VIBRATORY GROUND MOTION

PTN COL 2.5-2

This subsection provides a detailed description of the vibratory ground motion assessment for Units 6 & 7. This assessment uses the guidance from RG 1.208. RG 1.208 incorporates developments in ground motion estimation models; updated models for seismic sources; methods for determining site response; and new methods for defining a site-specific, performance-based earthquake ground motion that satisfy the requirements of 10 CFR 100.23. Identification and characterization of seismic sources lead to the determination of safe shutdown earthquake (SSE) ground motion. This subsection develops the site-specific ground motion response spectrum (GMRS) characterized by horizontal and vertical response spectra determined as free-field motions on the ground surface using performance-based procedures.

The GMRS represents the first part in development of a SSE for a site as a characterization of the regional and local seismic hazard. The GMRS is used to determine the adequacy of the certified seismic design response spectra for the DCD (RG 1.208). The certified seismic design response spectra (CSDRS) is the SSE ground motion for the site, the vibratory ground motion for which certain structures, systems, and components are designed to remain functional, pursuant to Appendix S to 10 CFR Part 50.

The starting point for the GMRS assessment is the probabilistic seismic hazard analysis (PSHA) conducted by the Electric Power Research Institute (EPRI) for the seismicity owners group (SOG). The EPRI-SOG seismic hazard study is based on the evaluation of seismicity, seismic source models, and ground motion attenuation relationships ([Reference 245](#)).

[Subsection 2.5.2.1](#) documents the review and update of the available EPRI earthquake catalog. The earthquake data are reviewed and used to update the EPRI catalog in Phase 1 of the seismicity update. A Phase 2 catalog of earthquakes is completed and used as a supplement to the EPRI seismicity catalog for the large distant, frequent earthquakes of the Caribbean region.

[Subsections 2.5.2.2](#) through [2.5.2.4](#) describe seismic source models and ground motion characterizations.

[Subsection 2.5.2.5](#) summarizes information about the seismic wave transmission characteristics of the site with reference to more detailed discussion of all engineering aspects of the subsurface in [Subsection 2.5.4](#).

Subsection 2.5.2.6 describes development of the horizontal GMRS ground motion for the site. Following RG 1.208, the selected ground motion is based on the risk-consistent/performance-based approach. Site-specific horizontal ground motion amplification factors are developed using site-specific estimates of subsurface soil and rock properties. These amplification factors are then used to scale the hard rock spectra to develop uniform hazard response spectra (UHRS) accounting for site-specific conditions using Approach 2A of NUREG/CR-6728 (**Reference 308**).

Subsection 2.5.2.6 also describes vertical GMRS, developed by scaling the horizontal GMRS by a frequency-dependent vertical-to-horizontal (V:H) factor.

PTN COL 2.5-1
PTN COL 2.5-2

2.5.2.1 Seismicity

The seismic hazard analysis conducted by EPRI (**Reference 245**) relied, in part, on an analysis of historical seismicity in the Central and Eastern United States (CEUS) to estimate seismicity parameters (rates of seismic activity, Gutenberg-Richter b-values, and maximum magnitude) for individual seismic sources. The historical earthquake catalog used in the EPRI seismic hazard analysis was complete through 1984. Given the location of Units 6 & 7 at the southeast edge of the EPRI-SOG seismic hazard study region, the earthquake data for the site region for all time through mid-February 2008 were reviewed and used to update the EPRI catalog. These earthquakes were cataloged in Phase 1 of the seismicity update (see **Subsection 2.5.2.1.2**). It was also recognized that there was some potential for a relatively significant contribution to seismic hazard at the site from the large distant, frequent earthquakes of the Caribbean region. The EPRI seismic hazard methodology did not incorporate contributions to the seismic hazard from sources in the Caribbean region and in the Gulf of Mexico except along its immediate coast. Therefore, special attention in the update of the EPRI catalog was given to earthquakes throughout the Gulf of Mexico and the Caribbean region. A Phase 2 catalog of earthquakes was completed as a supplement to the EPRI seismicity catalog for the region for moment magnitude (M_w) 3.0 and larger earthquakes occurring in the Caribbean south of the Phase 1 catalog coverage (see **Subsection 2.5.2.1.3**).

2.5.2.1.1 1988 EPRI Regional Earthquake Catalog

Many seismic networks record earthquakes in the CEUS. An effort was made during the EPRI seismic hazard study to combine available data on historical earthquakes and to develop a homogeneous earthquake catalog that contained

Turkey Point Units 6 & 7
COL Application
Part 2 — FSAR

all recorded earthquakes for the region. “Homogeneous” means that estimates of body-wave magnitude (m_b) for all earthquakes are consistent, duplicate earthquakes have been removed, non-earthquakes (e.g., mine blasts and sonic booms) have been eliminated, and significant events in the historical record have not been missed. The EPRI earthquake catalog (Reference 246) is the basis on which seismicity parameters such as earthquake recurrence rates and maximum magnitude are estimated.

2.5.2.1.2 Updated Seismicity Data (Phase 1)

The Phase 1 earthquake catalog used in the study region (see Figure 2.5.2-201) is an updated catalog to determine whether regional earthquake patterns and seismicity parameters developed from the EPRI catalog (Reference 246) remained unchanged. RG 1.206 specifies that earthquakes of modified Mercalli intensity (MMI) greater than or equal to IV or magnitude greater than or equal to 3.0 should be listed “that have been reported within 200 miles (320 kilometers) of the site.” The centerline of Units 6 & 7 was taken as 25.4241° N and 80.3332° W. In updating the EPRI earthquake catalog, a latitude-longitude window of 22° to 35° N, 100° to 65° W was used. This large window, called the Phase 1 seismicity investigation region, incorporates the 200 miles (320 kilometers) radius “site region” and all seismic sources north of the Caribbean contributing significantly to earthquake hazard at the site.

Given the location of the site at the southeast edge of the EPRI-SOG seismic hazard study region, the earthquake data for the site region for all time through mid-February 2008 were reviewed and used to update the EPRI catalog. Thirty-four regional seismicity catalogs were considered in the development of the Phase 1 seismicity catalog. The earthquake catalogs used for this initial update are:

- Advanced National Seismic System (ANSS) (Reference 204)
- Central U.S. Catalog (OWN) (Reference 307)
- Cuba Catalog (CUBA) (Reference 205)
- Decade of North America Geology (DNA) (Reference 307)
- Earthquake History of the U.S. (EQH) (Reference 307)
- Updated Engdahl (NENG) (Reference 249)

Turkey Point Units 6 & 7
COL Application
Part 2 — FSAR

- Engdahl and Villasenor (EV02) ([Reference 250](#))
- Electric Power Research Institute ([Reference 246](#))
- Frohlich and Davis (FD02) ([Reference 253](#))
- Gutenberg and Richter (G-R) ([Reference 307](#))
- Incorporated Research Institute for Seismology (IRIS) ([Reference 264](#))
- Panamerican Institute of Geography and History (IPGH) ([Reference 307](#))
- International Seismological Centre (ISC) ([Reference 265](#))
- Middle America Seismograph Consortium (MIDAS) ([Reference 284](#))
- Missouri-Tennessee Regional Data, 1974–1994 (SLU) ([Reference 307](#))
- NEIC Mexico, Central America and Caribbean, 1900–1979 (MCAC) ([Reference 289](#))
- NEIC Preliminary Determination of Epicenters (PDE, PDE-W, PDE-Q) ([Reference 292](#))
- NEIC Eastern, Central, and Mountain States of U.S. (SRA) ([Reference 288](#))
- NEIC Significant U.S. Earthquakes (USHIS) ([Reference 340](#))
- Mexico Composite Catalog ([Reference 307](#))
- National Geophysical Data Center ([Reference 307](#))
- Perez (PEREZ) ([Reference 298](#))
- Puerto Rico Seismic Network (PRSN) ([Reference 305](#))
- Regional Catalog for the Caribbean Sea (CARIB) ([Reference 307](#))
- Southeastern U.S. Seismic Network (SEUSN) ([Reference 341](#))
- Southeast Blacksburg Catalog (BLA) ([Reference 307](#))
- Historical U.S., 1568–1984 (STO) ([Reference 307](#))

Turkey Point Units 6 & 7
COL Application
Part 2 — FSAR

- Tennessee Earthquake Information Center (TEIC) (Reference 307)
- Regional Data from Trinidad (TRN) (Reference 307)
- U.S. Network Catalog (USN) (Reference 307)
- Utsu Catalog (UTS) (Reference 307)
- Villasenor and Engdahl (VE07) (Reference 332)
- Villasenor et al. (ISSv) (Reference 333)
- Wysession et al. (Reference 338)

No events were found in either the MCAC (Reference 289) or VE07 (Reference 332) catalogs. In the event of duplicate entries for a given earthquake in the remaining 32 catalogs, earthquake location and size were selected with the following order of preference: first the EPRI catalog, then special studies of regional earthquakes, then routine listings from regional catalogs, and finally routine listings from global catalogs.

For the purpose of developing earthquake recurrence statistics in the Phase 1 investigation region, it was necessary to eliminate dependent events (that is, foreshocks, aftershocks, and secondary events of an apparent seismicity cluster). The EPRI earthquake catalog distinguishes MAIN (independent) events from non-MAIN (dependent) events. Guided by the EPRI characterization of MAIN vs. non-MAIN, as well as by apparent spatial and temporal similarity between events, dependent events were identified and removed from the Phase 1 update to the EPRI catalog. The remaining events in the Phase 1 investigation region were assessed to be equivalent to EPRI MAIN events.

2.5.2.1.2.1 Assessment of Best Estimate and Uniform Magnitude

For the EPRI-SOG methodology, two types of magnitudes are required for each event in the catalog: (1) best, or expected, estimate of body-wave magnitude ($E[m_b]$, also referred to as Emb in the 1988 EPRI study; Reference 246); and (2) uniform magnitude (m_b^* , also referred to as Rmb in the 1988 EPRI study; Reference 246). These magnitudes were applied in the Phase 1 earthquake catalog where the EPRI catalog was considered in the development of the reevaluated earthquake catalog.

Best Estimate Magnitude Emb

Various magnitude types may be available for a given event. Each available magnitude was considered in the evaluation of Emb for that event. If a body-wave magnitude (m_b) was available, it was adopted directly. Other magnitudes were converted to additional estimates of Emb using the Equation 4-1 and Table 4-1 in the 1988 EPRI study (Reference 246):

$$\text{Emb} = 0.253 + 0.907 \cdot M_d \quad \text{Equation 2.5.2-1}$$

$$\text{Emb} = 0.655 + 0.812 \cdot M_L \quad \text{Equation 2.5.2-2}$$

$$\text{Emb} = 2.302 + 0.618 \cdot M_S \quad \text{Equation 2.5.2-3}$$

Where, M_d is duration (or coda) magnitude, M_L is “local” magnitude, and M_S is surface-wave magnitude.

If no explicit magnitudes are available for an event, an available maximum intensity value (I_0) was converted to Emb, using a relationship from Table 4-1 in the 1988 EPRI study (Reference 246):

$$\text{Emb} = 0.709 + 0.599 \cdot I_0 \quad \text{Equation 2.5.2-4}$$

The EPRI PSHA study expressed maximum magnitude (M_{\max}) values in terms of body-wave magnitude (m_b), whereas most modern seismic hazard analyses describe M_{\max} in terms of moment magnitude (M_w). To provide a consistent comparison between magnitude scales, body-wave magnitude was related to moment magnitude using the arithmetic average of three equations, or their inversions, presented by Atkinson and Boore (Reference 210), Frankel et al. (Reference 252), and EPRI (Reference 244). Throughout the discussion in Subsections 2.5.2.2 and 2.5.2.3, the largest values of M_{\max} distributions assigned by the Earth Science Teams (EST) (Reference 247) to seismic sources are presented for both magnitude scales (m_b and M_w). For example, EPRI m_b values of M_{\max} are followed by the equivalent M_w value. Conversion values from m_b to M_w and M_w to m_b are provided in Table 2.5.2-201. Body-wave magnitudes converted from moment magnitudes in this fashion were considered estimates of Emb.

For each event the final Emb was taken as the largest estimate of Emb.

Uniform Magnitude m_b

The EPRI-SOG seismic hazard methodology modifies the m_b values to develop a uniform magnitude, m_b^* , to assess an unbiased estimate of seismicity recurrence parameters. EPRI Equation 4-2 (Reference 246) indicates that the equation from which m_b^* is estimated from $E[m_b]$ and the standard deviation of m_b , σ_{mb} , (referred to as Smb in the 1988 EPRI study; Reference 246) is:

$$m_b^* = E[m_b] + (1/2) \cdot \ln(10) \cdot b \cdot \sigma_{mb}^2 \quad \text{Equation 2.5.2-5}$$

Where,

$$b = 1.0$$

Based on an examination of the EPRI-SOG catalog, particularly σ_{mb} (Smb) values listed as related to the various size measures from which they were determined, values for σ_{mb} (Smb) were estimated for each earthquake in the updated catalog, and m_b^* (Rmb) values were calculated (Equation 2.5.2-5) for each event added to the updated earthquake catalog.

The result of the above process was a homogeneous earthquake update of the EPRI earthquake catalog (Reference 246) for earthquakes occurring within the Phase 1 seismicity investigation window (Table 2.5.2-202). For the purpose of earthquake recurrence analysis, all events added for the update are assumed to be independent events.

2.5.2.1.3 Caribbean Seismicity Data (Phase 2)

Occurrence of large earthquakes in the region south of the Phase 1 coverage suggested that additional examination of earthquakes in the Caribbean region was needed (see Figure 2.5.2-201). The original EPRI-SOG analysis indicated that earthquake recurrence parameters had not been evaluated for the Caribbean region. The occurrence of recent moderate-large earthquakes in the Caribbean region indicated the potential for a significant contribution to seismic hazard at the site from sources in this region. This required a careful evaluation of Caribbean seismicity, both before and after the development of the EPRI earthquake catalog.

In order to investigate the potential of the Caribbean region to contribute to the seismic hazard of the site, it was necessary to consider a larger area of investigation. A latitude-longitude window of 15° to 24° N, 100° to 65° W was used to create a new catalog supplement to the EPRI seismicity catalog. This large window, called the Phase 2 seismicity investigation window, incorporates all

Turkey Point Units 6 & 7
COL Application
Part 2 — FSAR

events with $M_w \geq 3.0$ (Table 2.5.2-203) and all Caribbean seismic sources that would be expected to contribute significantly to the earthquake hazard of the site. The Phase 2 seismicity catalog combined with the seismicity catalog described in Subsection 2.5.2.1.2, allows an improved characterization of the seismicity within the project seismicity investigation window.

There are many earthquake catalogs covering the Phase 2 seismicity investigation window, but no single published catalog includes everything for assessing earthquake occurrence. Thus, several regional and global catalogs were combined to make a new catalog supplement. These parent catalogs cover different time, space, and magnitude ranges and have different accuracy in important earthquake parameters. Duplicate entries from the several parent catalogs were removed under a process that included selection of preferred entries for location and size parameters from among the many catalogs investigated to yield an initial catalog.

Twenty-three significant regional seismicity catalogs were considered in the development of the Phase 2 seismicity catalog within the Units 6 & 7 investigation region. The earthquake catalogs used for this phase of the update are:

- Advanced National Seismic System (ANSS) (Reference 204)
- Cuba Catalog (CUBA) (Reference 205)
- Decade of North America Geology (DNA) (Reference 307)
- Earthquake History of the U.S. (EQH) (Reference 307)
- Updated Engdahl (NENG) (Reference 249)
- Engdahl and Villasenor, 2002 (EV02) (Reference 250)
- Gutenberg and Richter (G-R) (Reference 307)
- Panamerican Institute of Geography and History (IPGH) (Reference 307)
- International Seismological Centre (ISC) (Reference 265)
- Middle America Seismograph Consortium (MIDAS) (Reference 284)
- NEIC Mexico, Central America and Caribbean, 1900–1979 (MCAC) (Reference 289)

Turkey Point Units 6 & 7
COL Application
Part 2 — FSAR

- NEIC Preliminary Determination of Epicenters (PDE, PDE-W, PDE-Q) ([Reference 292](#))
- NEIC Significant Worldwide Earthquakes (NOAA) ([Reference 307](#))
- Mexico Composite Catalog ([Reference 307](#))
- National Geophysical Data Center ([Reference 307](#))
- Perez (PEREZ) ([Reference 298](#))
- Puerto Rico Seismic Network (PRSN) ([Reference 305](#))
- Regional Catalog for the Caribbean Sea (CARIB) ([Reference 307](#))
- Regional Data from Trinidad (TRN) ([Reference 307](#))
- U.S. Network Catalog (USN) ([Reference 307](#))
- Villasenor and Engdahl, 2007 (VE07) ([Reference 332](#))
- Villasenor et al., 1997 (ISSv) ([Reference 333](#))
- Wyss et al., 1995 ([Reference 338](#))

In the event of duplicate entries in the 23 catalogs, the earthquakes cataloged were those selected based on a regionally defined preference order for Phase 2 of the seismicity update.

After a uniform initial catalog was compiled (see [Subsection 2.5.2.1.3.1](#)), foreshocks and aftershocks were eliminated using the 1974 window method of Gardner and Knopoff ([Reference 256](#)). Dependent shocks, classified as those that fall within the space and time intervals of the mainshock and are of smaller magnitudes, were eliminated to obtain a data set of mainshocks, which were assumed to show a Poisson distribution. The Gardner-Knopoff ([Reference 256](#)) method was proposed to be an alternative technique for removing dependent events when the earthquake catalog has variable quality station coverage in different regions and time periods ([Reference 314](#)).

Dependent or “related” events of a mainshock were identified within distance-time windows as a function of the location, time, and magnitude of the mainshock. The first earthquake in the catalog was declared provisionally as a mainshock event, and then all its equal or smaller magnitude related events were identified and

eliminated as aftershocks from the catalog. The next earthquake in the rest of the catalog was then declared as the next provisional mainshock event, and this cluster removal procedure was repeated, this time considering related events both before and after this mainshock. Equal or smaller magnitude related events occurring before the mainshock were marked for deletion as foreshocks—possibly including a previously assumed mainshock, that may now be identified as a foreshock of our current provisional mainshock—and equal or smaller magnitude related events occurring after the mainshock were marked for deletion as aftershocks. This procedure was repeated through the entire earthquake catalog. A listing of selected values for the shape of envelope has been given in Table 1 of Reference 256 by Gardner and Knopoff. There is also an upper-bound linear relationship between distance and magnitude that is used in a similar way to the time bounds. The original table proposed by Gardner and Knopoff (Reference 256) was extended to magnitude 3.0 by interpolating it in the form of the following relationships:

$$\text{Location Distance (km)} = 10^{(0.1238M + 0.983)} \quad \text{Equation 2.5.2-6}$$

$$\begin{aligned} \text{Time (days)} &= 10^{(0.032M + 2.7389)} \text{ for } M \geq 6.5 && \text{Equation 2.5.2-7} \\ &= 10^{(0.5409M - 0.547)} \text{ for } M < 6.5 \end{aligned}$$

where, we assumed “M” is equivalent to moment magnitude M_w . As an example, any earthquake within 918 days after a $M_w = 7.0$ earthquake, and with an epicenter location within about 71 kilometers of the epicenter of the $M_w = 7.0$ mainshock, was identified as an aftershock. For $M_w \geq 6.5$, the slope of the time window is less than $M_w < 6.5$ to conform with improved estimates of the shape of the envelope given by Gardner and Knopoff (Reference 256).

Figure 2.5.2-201 shows Units 6 & 7 and its associated site region, the defined latitude-longitude windows, both the original EPRI catalog earthquakes and updated seismicity data for the Phase 1 and Phase 2 investigation regions. These earthquake catalogs are used later in Subsection 2.5.2.4 to develop earthquake recurrence parameters for the Gulf of Mexico and Caribbean region for use in the PSHA of the site.

2.5.2.1.3.1 Uniform Magnitude M_w

In the Phase 2 earthquake catalog, moment magnitude (M_w) was used as the unifying magnitude because it is the most commonly used magnitude in recent seismic hazard studies.

Converting Magnitude Sizes to M_w

Various magnitude types may be available for a given event. Each available magnitude was considered in the evaluation of M_w for that event. If a moment magnitude (M_w) was available, it was adopted directly. Other magnitudes were converted to estimates of M_w using the Equation 2.5.2-8.

Global average relationships between M_S and $\log M_0$ (logarithm of the seismic moment) were used in which the independent variable is $\log M_0$ based on the assumption that the slope of the regression is 1 for small and 2/3 for large values of M_0 (Reference 240). The following global $\log M_0$ – M_S relation was used to convert surface wave magnitude to seismic moment for all events:

$$\begin{aligned} \log M_0 &= 19.24 + M_S & M_S < 5.3 \\ \log M_0 &= 30.20 - \sqrt{92.45 - 11.4M_S} & 5.3 \leq M_S \leq 6.8 \\ \log M_0 &= 16.14 + 1.5M_S & M_S > 6.8 \end{aligned} \quad \text{Equation 2.5.2-8}$$

Moment magnitudes were estimated from seismic moment for all events as a linear transformation of the logarithm of the seismic moment M_0 given by (Reference 269):

$$M_w = (2/3) \log M_0 - 10.7 \quad \text{Equation 2.5.2-9}$$

in which M_0 is in dyne-cm units (10^{-7} Nm).

A new linear relationship to compute M_S from m_b , valid in the interval $4.0 < m_b < 6.0$ and $3.1 < M_S < 6.7$, was applied by the following linear regression (Reference 254):

$$M_S = 1.37 m_b - 2.34 \quad \text{Equation 2.5.2-10}$$

2.5.2.1.4 Final Earthquake Catalogs

The objective of compiling a Units 6 & 7 earthquake catalog was to develop an improved characterization of seismicity for all time within the seismicity investigation region (15°N to 35°N , 100°W to 65°W) with which to not only compare to the EPRI-SOG seismicity catalog, as it had been used in the development of the seismic source characterization for the EPRI-SOG seismic hazard study, but also to suggest and facilitate characterization of possible additional seismic sources to the south of the original EPRI-SOG CEUS study region. The final earthquake catalog consists of two separate catalogs. The

Turkey Point Units 6 & 7
COL Application
Part 2 — FSAR

earthquake catalog for the Phase 1 seismicity investigation region (22°N to 35°N, 100°W to 65°W) is primarily the earthquakes in the EPRI-SOG catalog supplemented by earthquakes from several additional earthquake catalogs.

[Table 2.5.2-202](#) lists the earthquakes for the Phase 1 investigation region for which the events are Rmb magnitude ≥ 3.0 or intensity $I_0 \geq IV$ through mid-February 2008. The earthquake catalog for the Phase 2 seismicity investigation region (15°N to 24°N, 100°W to 65°W) is a composite of several earthquake catalogs appropriate for Cuba and the Caribbean for events that have moment magnitude $M_w \geq 3.0$ for all years through mid-March 2008. [Table 2.5.2-203](#) lists the earthquakes for the Phase 2 investigation region for the larger events of moment magnitude $M_w \geq 6.0$. Note that there is a 2-degree overlap in the Phase 1 and Phase 2 regions of the Units 6 & 7 seismicity investigation region—between 22°N and 24°N. As elaborated later in discussions about the seismic sources, different magnitude types were required for characterization of the EPRI-SOG sources in the northern portion of the investigation region, as compared to the Caribbean sources in the southern portion. The 2-degree overlap of the coverage of the two phases of seismicity update allowed for completeness and consistency of seismicity characterization of each subregion. In the plot of seismicity for the seismicity investigation region in [Figure 2.5.2-201](#) the seismicity of Phase 2 is presented in the 2-degree overlay area to fully encompass Cuba seismicity.

The distribution of epicenters indicated that the largest density of earthquakes was located along the Caribbean transform fault zones.

Within the updated earthquake catalog there are two new moderate seismic events in the Gulf of Mexico that are significant for an updated characterization of the regional seismicity. These are (1) a M_w 5.1 (m_b 5.6) earthquake that occurred on February 10, 2006, offshore of the Louisiana coast within the Gulf of Mexico and (2) a M_w 5.8 (m_b 5.9) earthquake that occurred on September 10, 2006, off the Florida coast within the Gulf of Mexico.

A moment-tensor source can be used to model the surface waves generated by the February 10, 2006, earthquake if the earthquake centroid is placed within a few miles of the earth's surface in a medium with a very low shear modulus. The explanation for the February 10 earthquake that is currently in best agreement with the observed seismic data is a gravity-driven displacement surface within a thick shallow sedimentary wedge ([Reference 293](#)).

The focal mechanism for the September 10, 2006, earthquake indicates a reverse sense of motion, and the earthquake depth is reported as 14 to 19 miles (22 to

31 kilometers) (Reference 290). This mechanism is that of an earthquake caused by tectonically driven stresses within the earth's crust.

2.5.2.1.5 Periods of Completeness for the Offshore Florida Earthquakes

The EPRI seismic hazard methodology (Reference 246) uses estimates of periods of completeness for the reporting of earthquakes as a function of magnitude. This methodology employs a matrix of probability of detection of earthquakes for an area for selected ranges of time-before-present and magnitude. The purpose of this subsection is to develop detection probability matrices for the areas in the Gulf of Mexico and off the coast of Florida where such information is not available in the original EPRI parameterization (Reference 243), but is necessary for the complete characterization of updated EPRI-SOG seismic sources (see Figure 2.5.2-202). Matrices for three regions—referred to as “Gulf of Mexico,” “Near Florida,” and “Near Atlantic”—are used later in Subsection 2.5.2.4 to develop EPRI-consistent earthquake recurrence parameters for use in the PSHA of the site.

Gulf of Mexico

Table 2.5.2-204 lists the 26 earthquakes within the Gulf of Mexico seismicity recurrence region, considered EPRI MAIN or independent events that were used to develop the matrix of detection probability for this area. This matrix was prepared to be consistent with the 1988 EPRI seismic hazard methodology. Generation of the matrix of detection probability used, as a conservative guideline, the adjacent EPRI matrices of detection probability available onshore. The 1988 EPRI seismic hazard study used a detailed analysis of United States demographics and history, number, quality, and distribution of seismographic instruments to develop matrices of probability of completeness as a function of time period, gridded area, and magnitude interval. Given uneven population distributions over time and uneven deployment of seismographic networks these completeness probability matrices also vary by location. EPRI “Incompleteness Regions” 2 and 3 are closest to the Gulf of Mexico seismicity recurrence region (Reference 243, Table 5-1) — see Figure 2.5.2-202.

It was assumed that the probabilities of earthquake detection for the Gulf of Mexico are less than those given for onshore coastal locations for comparable time periods. The procedure followed for estimating detection probabilities for the Gulf of Mexico was, therefore, to start with an available EPRI matrix, suggesting the lowest probabilities along the shoreline—that is, EPRI Incompleteness Region

Turkey Point Units 6 & 7
COL Application
Part 2 — FSAR

2, as it has lower detection probabilities than Incompleteness Region 3—and to assume lower probabilities of detection within the Gulf of Mexico.

The first matrix shown in [Table 2.5.2-205](#) is a version of the EPRI Incompleteness Region 2 matrix, modified to add additional years since 1984 (the last complete year in the 1988 EPRI earthquake catalog). The latest bin time of the Incompleteness Region 2 matrix (1975–1983) has detection probabilities of 1.00 for all magnitude bins. Therefore, given that detection probability would not be expected to decrease with time, additional time bins with detection probabilities of 1.00 for all magnitudes were appended to the Incompleteness Region 2.

The first matrix of detection probability shown in [Table 2.5.2-205](#) is appropriate for much of the on, or very near, onshore sites of seismic activity of the Gulf of Mexico. This matrix may be used for seismicity occurring through the year 2007.

In developing the detection probability of matrix appropriate for the Gulf of Mexico region, the modified Incompleteness Region 2 matrix in [Table 2.5.2-205](#) was qualitatively modified in consideration of the following constraints:

- For a given magnitude bin, detection probability for a given time bin would be expected to be the same or more than the detection probability of an adjacent earlier time bin. That is, the overall trend is for detection probabilities for a given magnitude interval to increase with time.
- For a given time bin, the probability of earthquake detection for a given magnitude bin would be the same or more than the detection probability for an adjacent smaller magnitude bin. That is, the overall trend is for detection probabilities for a given time interval to increase with magnitude.
- Given the lack of regional seismographic stations in the Gulf of Mexico, as well as the obvious lack of felt or damage reports in the Gulf, detection probabilities for the Gulf of Mexico are expected to be no higher for any magnitude and time bin than that corresponding to the nearest onshore location of lowest detection probabilities.
- It was assumed that after the advent of the World-Wide Standardized Seismograph Network in the mid-1960s most earthquakes of magnitude 5.5 and greater would be detectable and recorded ([Reference 250](#)).
- In general, global b-values tend to average about 0.8 to 1.2 (see Table 2 of the 2002 Engdahl and Villasenor study ([Reference 250](#)) and Table 4-7 of the 1994

Johnston et al. study ([Reference 268](#)) for stable continental regions). It was assumed that a value within this range is reasonable for the Gulf of Mexico.

The time intervals of the matrix of detection probabilities for Incompleteness Region 2 were subdivided to allow for refinement of the probabilities of detection for the Gulf of Mexico region—the second matrix shown in [Table 2.5.2-205](#). Following the elements of expert judgment noted above, the EPRI Incompleteness Region 2 matrix of detection probability was modified for the Gulf of Mexico region, as given in [Table 2.5.2-206](#). Using the detection probability matrix with the seismicity of the Gulf of Mexico region results in a reasonable test b-value of 0.84.

Near Atlantic

The Near Atlantic region may be considered to have reduced probabilities of detection for reasons similar to those for the Gulf of Mexico region, however, the Near Atlantic region is most proximal to the Incompleteness Region 13 (see [Figure 2.5.2-202](#)).

To estimate the probability of detection matrix for the Near Atlantic region, the reduction in probabilities developed for the Gulf of Mexico region as a fraction of the probabilities for Incompleteness Region 2 may be applied as a scaling factor to the probabilities of detection for Incompleteness Region 13, shown as the third matrix in [Table 2.5.2-205](#). The results of this scaling gives the same probability of detection matrix for the Near Atlantic region, as was developed for the Gulf of Mexico region, and considered for the Near Atlantic region because of the distribution of the unity [1.00] and zero [0.00] values in both of the probabilities of detection matrices for Incompleteness Regions 2 and 13.

Seismicity is actually too sparse within the Near Atlantic region to determine a test calculation of b-value to assess the probability of detection matrix for the Near Atlantic region.

Near Florida

For the Near Florida region, the appropriate probability of detection matrix would be transitional between those values in Florida, given by the matrix for the Incompleteness Region 13, and those developed for Near Atlantic region. Therefore, the probability of detection matrix for Near Florida region was developed as simply the average of the detection probabilities for Incompleteness Region 13 ([Table 2.5.2-205](#), third matrix) and Near Atlantic region ([Table 2.5.2-206](#)). These average values are listed in [Table 2.5.2-206](#).

Again, seismicity is too sparse within the Near Florida region to determine a test calculation of b-value to assess the probability of detection matrix for the Near Florida region.

PTN COL 2.5-2

2.5.2.2 Geologic Structures and EPRI Seismic Source Model for the Site Region

RG 1.208 provides guidance on methods acceptable to the NRC to satisfy the requirements of 10 CFR 100.23 for assessing the appropriate SSE ground motion levels for new nuclear power plants. RG 1.208 states that an acceptable starting point for this assessment at sites in the CEUS is the PSHA conducted by the EPRI in the 1980s (References 243 and 247). RG 1.208 further specifies that the adequacy of the EPRI hazard results must be evaluated in light of more recent data and evolving knowledge pertaining to seismic hazard evaluation in the CEUS. As described in Subsection 2.5.1, a comprehensive review of available geological, seismological, and geophysical data has been performed for the site region and adjoining areas.

Subsection 2.5.2.2 summarizes seismic source interpretations from the original EPRI PSHA study (References 243 and 247) and relevant post-EPRI source characterization studies. Modifications and updates to the original EPRI model as applied to the site are required for the following reasons:

- Recent earthquakes in the Gulf of Mexico and U.S. Gulf Coast region require updates to Mmax distributions and weights for the original EPRI model. Subsection 2.5.2.4.2 describes these Mmax updates.
- The original EPRI model (Reference 243) does not cover the entire 200-mile radius site region. As such, supplemental source zones are defined to cover the entire site region. Subsection 2.5.2.4.4.1 describes these supplemental source zones.
- New seismic source characterizations of seismic sources beyond the site region, including Cuba, the northern Caribbean region, and the Charleston seismic source, should be included. Subsections 2.5.2.4.4.2 and 2.5.2.4.4.3 describe the Charleston source characterization and the Cuba and northern Caribbean source characterization, respectively.

2.5.2.2.1 Summary of EPRI Seismic Sources

This subsection summarizes the seismic sources and parameters used in the original EPRI project (References 243 and 247). The description of seismic sources includes those sources located at least partially within 200 miles of Units 6 & 7 (i.e., the site region).

In the original EPRI project, six independent Earth Science Teams (ESTs) evaluated geological, geophysical, and seismological data to develop a model of seismic sources in the CEUS. These sources were used to model the occurrence of future earthquakes and evaluate earthquake hazards at nuclear power plant sites across the CEUS.

The six ESTs involved in the original EPRI project were Bechtel Group, Dames & Moore, Law Engineering, Rondout Associates, Weston Geophysical, and Woodward-Clyde Consultants. Each team produced a report (volumes 5 through 10 of Reference 247) providing detailed descriptions of how they identified and defined seismic sources. The results were implemented into a PSHA study (Reference 243). For the computation of hazard in the 1989 study, a few seismic source parameters were modified or simplified from the original parameters determined by the six ESTs. Reference 243 summarizes the parameters used in the final PSHA calculations, and this reference is the primary source for the seismicity parameters. Each EST provides more detailed descriptions of the rationale and methodology used in evaluating tectonic features and establishing the seismic sources (volumes 5 through 10 of Reference 247).

Figures 2.5.2-203 through 2.5.2-209 show the EPRI source zones located at least partially within the site region. These figures also show earthquakes from the Phase 1 seismicity update (see Subsection 2.5.2.1.2) plus non-MAIN EPRI catalog seismicity with $E_{mb} \geq 3.0$, to show the spatial relationships between seismicity and seismic sources.

The M_{max} , interdependencies, and probability of activity for each EST's seismic sources are presented in Table 2.5.2-207. This table presents the parameters assigned to each source. Table 2.5.2-207 also indicates whether new information has been identified that would lead to a revision of the source's geometry, M_{max} , or recurrence parameters.

The EPRI PSHA study expressed M_{max} values in terms of m_b , whereas most modern seismic hazard analyses describe M_{max} in terms of moment magnitude M_w . To provide a consistent comparison between magnitude scales,

Subsection 2.5.2 relates body-wave magnitude to moment magnitude using the arithmetic average of three equations, or their inversions, presented in Atkinson and Boore (**Reference 210**), Frankel et al. (**Reference 252**), and EPRI TR-102293 (**Reference 244**). The conversion relations are consistent for magnitudes ≥ 4.5 , but begin to show divergence at lower magnitudes. **Table 2.5.2-201** lists m_b and M_w equivalences developed from these relations over the range of interest for this study. Throughout this subsection, the values of M_{max} distributions assigned by the ESTs to seismic sources are presented for both magnitude scales (m_b and M_w) to give perspective on the maximum earthquakes that were considered possible in each seismic source. For example, EPRI m_b values of M_{max} are followed by the equivalent M_w value.

The following subsections describe the most significant EPRI sources for each EST with respect to the site. For all EPRI sources located within the site region, recent, post-EPRI-catalog earthquakes exceed the minimum M_{max} bound assigned by the ESTs, thereby requiring M_{max} updates for all EPRI sources within the site region. **Subsection 2.5.2.4.2** describes these M_{max} updates.

2.5.2.2.2 Sources Used for EPRI PSHA — Bechtel Group

Bechtel Group characterized only one seismic source within the site region, the Gulf Coast (BZ1) source zone. **Table 2.5.2-207** summarizes the source parameters for this and other EPRI-ESTs' source zones within the site region. **Figures 2.5.2-203** and **2.5.2-204** show the location and geometry of Bechtel Group's Gulf Coast (BZ1) seismic source zone.

Units 6 & 7 are located within Bechtel Group's Gulf Coast (BZ1) source zone. This background source extends from east Texas to the continental shelf east of Florida, including all of Louisiana and the southern portions of Mississippi, Alabama, and Georgia. The Bechtel Group assigned a maximum M_{max} value of m_b 6.6 (M_w 6.5) to this zone.

2.5.2.2.3 Sources Used for EPRI PSHA — Dames & Moore

Dames & Moore characterized only one seismic source within the site region, the Southern Coastal Margin (20) source zone. **Table 2.5.2-207** summarizes the source parameters for this and other EPRI-ESTs' source zones within the site region. **Figures 2.5.2-203** and **2.5.2-205** show the location and geometry of Dames & Moore's Southern Coastal Margin (20) seismic source zone.

The site is located within Dames & Moore's Southern Coastal Margin (20) source zone. This source roughly parallels the Paleozoic rifted continental margin from

Texas to Alabama and also includes most of Florida. This source represents the down-warping wedge of continental margin sediments that has been accumulating since the Cretaceous Period and is characterized by diffuse seismicity (Reference 247). The Dames & Moore team assigned a maximum M_{max} value of m_b 7.2 (M_w 7.5) to this zone, reflecting its assumption of the possibility for moderate to large earthquakes within this area.

2.5.2.2.4 Sources Used for EPRI PSHA — Law Engineering

Law Engineering characterized only one seismic source within the site region, the South Coastal Block (126) source zone. Table 2.5.2-207 summarizes the source parameters for this and other EPRI-ESTs' source zones within the site region. Figures 2.5.2-203 and 2.5.2-206 show the location and geometry of Law Engineering's South Coastal Block (126) seismic source zone.

Units 6 & 7 are located within Law Engineering's South Coastal Block (126) source zone. This source represents an area of low amplitude, broad wavelength magnetic anomalies extending from the Texas/Mexico border to the continental shelf east of Florida. Law Engineering interprets the northern portion of the zone from Texas to Alabama as the Paleozoic edge of the North American craton (Reference 247). The Law Engineering team assigned a maximum M_{max} value of m_b 4.9 (M_w 4.5) to this zone.

2.5.2.2.5 Sources Used for EPRI PSHA — Rondout Associates

Rondout Associates characterized two seismic sources within the site region. These two sources are:

- Appalachian Basement (49-05)
- Gulf Coast to Bahamas Fracture Zone (51)

Table 2.5.2-207 summarizes the source parameters for these two Rondout Associates sources zones, as well as other EPRI-ESTs' source zones within the site region. Figures 2.5.2-203 and 2.5.2-207 show the locations and geometries of the Rondout seismic sources 49-05.

Units 6 & 7 are located within the Gulf Coast to Bahamas Fracture Zone (51) source zone. This roughly coast-parallel background source extends from the Texas/Mexico border to southern Florida. Source zone 51 comprises Paleozoic crust that is separated from Appalachian crust of roughly the same age based on

Turkey Point Units 6 & 7
COL Application
Part 2 — FSAR

differing stress regimes (Reference 247). The Rondout Associates team assigned a maximum Mmax value of m_b 5.8 (M_w 5.4) to this zone.

At its nearest point, the Appalachian Basement (49-05) source zone is located about 70 miles northeast of Units 6 & 7. This source zone incorporates crust located east of the Precambrian cratonic edge and represents a complex accretionary terrane that may not have uniform seismic potential (Reference 247). The Rondout Associates team assigned a maximum Mmax value of m_b 5.8 (M_w 5.4) to this zone.

2.5.2.2.6 Sources Used for EPRI PSHA — Weston Geophysical

Weston Geophysical characterized only one seismic source within the site region, the Gulf Coast (107) source zone. Table 2.5.2-207 summarizes the source parameters for this and other EPRI-ESTs' source zones within the site region. Figures 2.5.2-203 and 2.5.2-208 show the location and geometry of Weston Geophysical's Gulf Coast (107) seismic source zone.

Units 6 & 7 are located within Weston Geophysical's Gulf Coast (107) source zone. This background source extends from eastern Texas to Florida, including all of Louisiana and the southern portions of Mississippi, Alabama, and Georgia. The Weston Geophysical team assigned a maximum Mmax value of m_b 6.0 (M_w 5.7) to this zone.

2.5.2.2.7 Sources Used for EPRI PSHA — Woodward-Clyde Consultants

The Woodward-Clyde Consultants team characterized only one seismic source within the site region, the Turkey Point Background (BG-35) source zone. Table 2.5.2-207 summarizes the source parameters for this and other EPRI-ESTs' source zones within the site region. Figures 2.5.2-203 and 2.5.2-209 show the location and geometry of Woodward-Clyde's Turkey Point Background (BG-35) seismic source zone.

The Turkey Point Background (BG-35) source is a large rectangle containing Units 6 & 7 and covering most of southern Florida and extending offshore to include parts of the Atlantic continental shelf, the Gulf Coast, and northern Cuba. This source is a background zone defined as a rectangular area centered on Units 6 & 7, and its geometry is not based on any geological, geophysical, or seismological features. The largest Mmax assigned by the Woodward-Clyde Consultants team to this zone is m_b 6.6 (M_w 6.5).

2.5.2.3 Correlation of Seismicity with Geologic Structures and EPRI Sources

The EPRI seismicity catalog covers earthquakes in the CEUS through 1984, as described in [Subsection 2.5.2.1](#). [Figures 2.5.2-203](#) through [2.5.2-209](#) show the distribution of earthquake epicenters from both the EPRI (pre-1985) and Phase 1 update earthquake catalog (through mid-February 2008) in comparison to the seismic sources identified by each of the EPRI ESTs.

Comparison of the additional events of the updated earthquake catalog to the EPRI earthquake catalog shows:

- There are no new earthquakes within the site region that can be associated with a known geologic structure.
- There are no unique clusters of seismicity that suggest a new seismic source not captured by the EPRI seismic source model.
- The updated seismicity catalog does not show a pattern of seismicity that requires revision to the geometry of any of the EPRI seismic sources. The updated catalog extends farther south than the original EPRI catalog to include seismicity in Cuba and the northern Caribbean region. [Subsection 2.5.2.4.3](#) describes the Cuba and northern Caribbean seismic source model.
- The updated catalog does not imply a significant change in seismicity parameters (rate of activity, b-value) for any of the EPRI seismic sources.
- The updated catalog does indicate that Mmax updates are required for all EPRI seismic sources located at least partially within the site region. [Subsection 2.5.2.4.3](#) describes these Mmax updates.

2.5.2.4 Probabilistic Seismic Hazard Analysis and Controlling Earthquakes

This subsection describes the PSHA conducted for the site. This subsection follows the procedures described in RG 1.208, as follows. [Subsections 2.5.2.4.1](#) and [2.5.2.4.2](#) address the potential significance of new information on seismic source characterization and ground motion characterization, respectively, as that new information relates to the 1989 EPRI seismic hazard model ([Reference 245](#)). [Subsection 2.5.2.4.3](#) describes the results of PSHA sensitivity analyses used to test the impact of the new information on the seismic hazard. As a result of these studies, an updated PSHA analysis was performed, as described in

Subsection 2.5.2.4.4. The results of this updated PSHA are used to UHRS and to identify controlling earthquakes (**Subsection 2.5.2.4.5**).

2.5.2.4.1 1989 EPRI Seismic Hazard Study

The starting point of the PSHA calculations for the site was the 1989 EPRI study (**Reference 245**). The 1989 EPRI study used expert opinion on alternative, competing models of earthquake occurrences (size, location, and rates of occurrence) and of ground motion amplitude and its variability, to weight alternative hypotheses. PSHA calculations are conducted for these alternative hypotheses. The result is a family of weighted seismic hazard curves from which mean and fractile seismic hazard can be derived.

There were no PSHA results published in the 1989 EPRI study (**Reference 245**) for Units 6 & 7. Therefore, as a starting point for calculations, the seismic hazard for the Crystal River site was replicated, because those hazard results were available from the 1989 EPRI study. The Crystal River site is on the west coast of Florida, near the northern end of the Florida peninsula, and is the closest site for which 1989 EPRI study results are available. The purpose of this replication was to use the same assumptions on seismic sources and ground motion equations, to calculate seismic hazard, and to compare results to the 1989 EPRI study.

Table 2.5.2-208 compares individual team and total annual frequencies of exceedance calculated in the 1989 EPRI study for the Crystal River site (labeled “EPRI-SOG”) to annual frequencies of exceedance calculated in the Units 6 & 7 study (labeled “2008”) for peak ground acceleration (PGA) amplitudes of 100, 250, and 500 cm/s². All results are for hard rock conditions. The “% diff” columns show the percent difference between the 1989 calculations and the current hazard calculations at the Crystal River site. Comparisons are shown for mean PGA hazard and for the 15th fractile, median, and 85th fractile hazard curves. Note that the minimum magnitude (M_{min}) for these hazard calculations was m_b = 5.0, which was the assumption made in the 1989 EPRI study. Observations for these comparisons are as follows:

- Bechtel team: comparison is good, with current results slightly higher than for 1989 EPRI study (**Reference 245**).
- Dames & Moore team: comparison is good except for 85th fractile hazards, with current results being +43 percent to –30 percent different from 1989 EPRI study. The cause of this difference for the 85th fractile hazard is not known.

Turkey Point Units 6 & 7
COL Application
Part 2 — FSAR

- Law Engineering: current results are well below 1989 EPRI study results. The host source (LAW-126) has Mmax values that are all below the value of Mmin = 5.0 used in the 1989 EPRI study, so it is reasonable that the current calculation shows very low hazard for the Law team (the host source contributes zero hazard in the current calculation).
- Rondout: comparison is good except for the 15 percent fractile, where the current results are much lower than the 1989 EPRI results. Rondout sources RND-51 and RND-C01 (the host sources) have a Mmax distribution that includes a value of 4.8 (weight 0.2), which is below Mmin = 5.0, so it is reasonable that the 15 percent fractile hazard would be very low for the Rondout team, as the current calculations show.
- Weston: comparison is good, with current results slightly higher than for the 1989 EPRI study.
- Woodward-Clyde: comparison is good except for the 15 percent fractile, where the current results are much lower than the 1989 EPRI results. Woodward-Clyde source WGC-B36 (the background host source) has a Mmax distribution that includes a value of 4.9 (weight 0.17), which is below Mmin = 5.0, so it is logical that the 15 percent fractile hazard would be very low for the Woodward-Clyde team, as the current calculations show.
- Total: comparison of mean hazard is good, with agreement being between 0 percent and 3 percent for PGA amplitudes of 100, 250, and 500 cm/s². The agreement for specific fractiles is not as good, for reasons discussed above, but this is less of a concern because (a) mean hazards are used to derive recommendations for design spectra, and (b) differences related to Mmax distributions are resolved since Mmax distributions for the EPRI team sources are updated as described below.

The conclusion from this comparison is that the overall mean seismic hazard from the 1989 EPRI study ([Reference 245](#)) can be replicated accurately, but unstated assumptions and different treatment of Mmax distributions below a value of 5.0 lead to somewhat different fractile hazards for individual team results. Given that mean hazards are used to derive recommendations for design spectra, the comparison is considered acceptable.

At the Units 6 & 7 site, updates to the inputs to PSHA lead to changes in the level of seismic hazard compared to what would have been calculated based on the 1989 EPRI assumptions ([Reference 245](#)). Seismic source characterization data

and ground motion assumptions that could affect the calculated level of seismic hazard include:

- Updates in the characterization of the rate of earthquake occurrence as a function of magnitude for one or more seismic sources.
- Updates in the characterization of the maximum magnitude for seismic sources.
- Extension of seismic sources to additional regions not covered in the EPRI 1989 study.
- Modeling of new seismic sources to the south, outside the original 1989 EPRI study region.
- Updates to models used for estimating strong ground shaking and its variability in the CEUS.

Possible changes to seismic hazard caused by changes in these areas are addressed in the following subsections.

2.5.2.4.2 Effect of Updated Earthquake Catalog

Subsection 2.5.2.1.1 describes the development of an updated earthquake catalog. This updated catalog involves the addition of earthquakes that have occurred after completion of the EPRI evaluation development (post-1984). The impact of the new catalog information was assessed by evaluating the effect of the new data on earthquake recurrence estimates for the Florida peninsula, as described below.

The 1989 EPRI study (**Reference 245**) defined completeness regions for the entire CEUS, within the boundaries of a study region that approximately followed the Atlantic and Gulf of Mexico coasts. In the Florida region only the Florida peninsula was defined to be within the boundaries of the EPRI study region because the earthquake catalog was thought to be incomplete in the Gulf of Mexico and in the Atlantic region east of Florida. **Figure 2.5.2-210** shows the boundary of the EPRI region and also shows the “Florida test region” used here to examine the effects of an updated earthquake catalog. Earthquake locations are shown for both the original EPRI earthquake catalog and for the updated catalog (south of latitude 35°N), as given in **Table 2.5.2-202**. The effect of the updated earthquake catalog on earthquake occurrence rates was assessed by computing earthquake recurrence parameters for the Florida test region shown in

Figure 2.5.2-210. The truncated exponential recurrence model was fit to the seismicity data using the EPRI EQPARAM program, which uses the maximum likelihood technique. Earthquake recurrence parameters were computed first using the original EPRI catalog and periods of completeness, and then using the updated catalog and extending the periods of completeness to 2007, assuming that the probability of detection for all magnitudes is unity for the time period 1985 to 2007. The resulting earthquake recurrence rates for the Florida test region are compared in **Figure 2.5.2-211**. This comparison shows that the updated earthquake catalog results in lower estimated earthquake recurrence rates.

On the basis of the comparison shown in **Figure 2.5.2-211**, it is concluded that the earthquake occurrence rate parameters developed in the 1989 EPRI evaluation (**Reference 245**) have not increased in the period 1985–2007. Therefore, on the basis of earthquake occurrences alone, the seismicity rates of all EPRI team sources were not updated. Note that the EPRI analysis assumed that the EPRI catalog was complete for all magnitudes during the period 1975–1984 (probability of detection is 1.0, see **Table 2.5.2-205**), so this was an extension of that assumption to cover the updated catalog period.

2.5.2.4.3 New Maximum Magnitude Information

The updated seismicity catalog described in **Subsection 2.5.2.1.2** indicates that increases in Mmax values are required for all source zones within the site region. Post-EPRI earthquakes in the updated seismicity catalog require Mmax increases because recent earthquakes have occurred in each site region source zone with magnitudes exceeding the original EPRI lower bound Mmax values (**Table 2.5.2-207**). **Subsection 2.5.2.4.3.1** describes these earthquakes, and **Subsection 2.5.2.4.3.2** and **Table 2.5.2-207** present rationale for, and updates of, the original EPRI source parameters.

With the exception of earthquakes in Cuba and the northern Caribbean region, the updated seismicity catalog does not indicate any post-EPRI seismicity patterns indicative of new seismic sources. Assessment of seismicity in Cuba and the northern Caribbean region was not included in the original EPRI study.

Subsection 2.5.2.4.4.3 presents details of the Cuba and northern Caribbean seismic source model.

2.5.2.4.3.1 Earthquakes Significant to EPRI Mmax Values

A total of four post-EPRI earthquakes have magnitudes greater than the lower bound Mmax value for the source zone within which they occurred. These new

data require revision to the Mmax distributions for all seven EPRI seismic source zones within the site region. The following subsections describe these four earthquakes. In the following discussion, magnitude estimates are presented in units of either body wave magnitude, m_b , or the “best estimate” of body wave magnitude, Emb. For the purposes of this subsection, m_b and Emb are considered equivalent.

2.5.2.4.3.1.1 September 10, 2006, Emb 5.90 Gulf of Mexico Earthquake

The September 10, 2006, earthquake occurred in the Gulf of Mexico, roughly equidistant from the Florida and Alabama coasts. The event was felt throughout the southeastern U.S. including Louisiana, Arkansas, Missouri, Alabama, Georgia, South Carolina, and Florida. Maximum felt intensities were MMI IV (Reference 330). Focal mechanisms indicate reverse faulting and hypocentral depth estimates indicate a source located beneath the Gulf of Mexico sedimentary section (Reference 330).

The updated seismicity catalog compiled for Units 6 & 7 assigns Emb 5.90 to the September 10, 2006, Gulf of Mexico earthquake (Figures 2.5.2-204 through 2.5.2-209). Based on preliminary data, however, previous studies assigned Emb 6.11 to this same earthquake. The Emb 6.11 estimate is conservatively adopted for the purpose of updating EPRI Mmax ranges. The difference in magnitude estimates for this event reflects the uncertainty in magnitude determination and the older and slightly larger estimate is used.

The magnitude of the September 10, 2006, earthquake exceeds the original EPRI Mmax lower bound magnitudes, and thereby provides the rationale for revising upward the Mmax distributions for the following sources (Table 2.5.2-207):

- Bechtel source BZ1 (Gulf Coast)
- Rondout Associates source 51 (Gulf Coast to Bahamas Fracture Zone)
- Weston Geophysical source 107 (Gulf Coast)

2.5.2.4.3.1.2 February 10, 2006, Emb 5.58 Gulf of Mexico Earthquake

The February 10, 2006, earthquake occurred in the Gulf of Mexico south of Louisiana. This Emb 5.58 event was felt in coastal Louisiana, Texas, and Florida with a maximum intensity of MMI III (Reference 291). The earthquake occurred along the Sigsbee escarpment offshore of Louisiana. Nettles (Reference 293) and Dellinger et al. (Reference 228) suggest that this event may be the result of a

Turkey Point Units 6 & 7
COL Application
Part 2 — FSAR

gravity-driven landslide. This interpretation is based on the lack of high-frequency energy in the waveforms, slow rise time, preliminary focal mechanism determinations, and the location of the event on the Sigsbee escarpment. The implication of the “landslide” interpretation is that large mass-sliding events along the Sigsbee escarpment may be detectable on local and regional seismic networks. However, no other earthquakes within the Gulf of Mexico have been attributed to this mechanism, and other independent researchers have not confirmed the landslide mechanism for the February 10, 2006, event.

There is a significant possibility that the February 10, 2006 earthquake was non-tectonic in origin. Because this is not a consensus conclusion within the seismological community, however, this event is conservatively assumed to be of tectonic origin and Mmax values are updated for source zones containing the event.

The magnitude of the February 10, 2006, earthquake exceeds the original EPRI Mmax lower bound magnitudes, and thereby provides the rationale for revising upward the Mmax distributions for the following sources ([Table 2.5.2-207](#)):

- Dames & Moore source 20 (Southern Coastal Margin)
- Law Engineering source 126 (South Coastal Block)

While this event also is located within Roundout Associates source 51 (Gulf Coast to Bahamas Fracture Zone) and Weston Geophysical source 107 (Gulf Coast) and has a larger magnitude than the lower bound Mmax value for both zones, updates to Roundout Associates source 51 and Weston Geophysical source 107 are based on the larger September 10, 2006, earthquake described above. The February 10, 2006, earthquake is located about 22 miles south of Law Engineering source 126 ([Figure 2.5.2-206](#)). This earthquake was poorly located by traditional land-based seismograph networks, and the epicentral location is uncertain. Therefore, it is conservatively assumed that the February 10, 2006, Emb 5.58 earthquake occurred within Law Engineering source 126 based on positional uncertainty and the lack of any known seismotectonic boundaries that would suggest a change in seismotectonic behavior across the southern source boundary.

2.5.2.4.3.1.3 October 24, 1997, Emb 4.96 Southwestern Alabama Earthquake

The October 24, 1997, Escambia County, Alabama earthquake occurred in southwestern Alabama. This Emb 4.96 event was felt throughout southwestern

Alabama and westernmost Florida with a maximum intensity of MMI VI to VII (Reference 259). This earthquake occurred within or at the perimeter of an active oil and gas extraction field, suggesting the possibility of a causal relationship between hydrocarbon recovery and the October 24, 1997, earthquake (Reference 259). Therefore, it is possible that this earthquake is non-tectonic in origin. Regardless, this event is conservatively assumed to be tectonic in origin, and Mmax values are updated for source zones containing the event as appropriate.

The magnitude of the October 24, 1997, earthquake exceeds the original EPRI Mmax lower bound magnitude, and thereby provides the rationale for revising upward the Mmax distributions for the following sources (Table 2.5.2-207):

- Rondout Associates source 49-05 (Appalachian Basement)
- Law Engineering source 126 (South Coastal Block)

However, as described in the preceding subsection, it is conservatively assumed that the poorly located and larger February 10, 2006, Emb 5.58 earthquake also occurred within Law Engineering source 126. Therefore, the Mmax distribution for Law Engineering source 126 is updated based on the February 10, 2006, earthquake.

2.5.2.4.3.1.4 January 23, 1880, Emb 6.09 West Cuba Earthquake

The largest earthquake in Woodward-Clyde seismic source BG-35 is the January 23, 1880, Emb 6.09 San Cristobal-Candelaria, Cuba earthquake in west Cuba (Figure 2.5.2-203). The magnitude of this earthquake exceeds the minimum Mmax value (m_b 5.8) defined by Woodward-Clyde for its source BG-35 (Table 2.5.2-207). However, as described in Subsection 2.5.2.4.4.3, the southern margin of Woodward-Clyde source BG-35 is truncated by the northern boundary of the new Caribbean seismic source model to avoid double-counting of earthquakes. As such, the January 23, 1880 west Cuba earthquake is located outside of the truncated Woodward-Clyde source and within the area modeled by the new Caribbean seismic source model. Therefore, the January 23, 1880, earthquake does not provide rationale for updating to the original EPRI Mmax distribution for Woodward-Clyde source BG-35.

The largest earthquake in the truncated Woodward-Clyde source is the June 2, 1990, Emb 4.09 earthquake, north of Cuba (Figure 2.5.2-209). Subsection 2.5.2.4.4.3 describes the geometry of the truncated Woodward-Clyde

source zone. Because this earthquake is smaller than the minimum value of the original EPRI Mmax distribution (m_b 5.8), no change to the original Mmax distribution is required for the truncated Woodward-Clyde seismic source.

2.5.2.4.3.2 EPRI Site Region Source Zone Mmax Revisions

The following subsections describe Mmax modifications to the original EPRI source zones within 200 miles of Units 6 & 7. Review of published literature does not indicate any new information that requires revision to the existing EPRI source zone geometries. Post-EPRI earthquakes in the updated seismicity catalog, however, require Mmax increases for five of the six ESTs because recent earthquakes have occurred in each site region source zone with magnitudes larger than the original EPRI lower bound Mmax values ([Table 2.5.2-207](#)).

Modifications to the original EPRI seismic source zones in the site region are limited to:

- Revising Mmax distributions based on updated seismicity.
- Truncating the southern extent of Woodward-Clyde source BG-35 to prevent overlap with the Cuba and northern Caribbean seismic source model developed. [Subsection 2.5.2.4.4.3](#) describes the Cuba and northern Caribbean source model.

Mmax distribution revisions follow the individual EST methodologies as described in the original EPRI team reports ([Reference 247](#)). These recommended changes are described in the subsections below.

2.5.2.4.3.2.1 Mmax Update — Bechtel Corporation

Source BZ1 (Gulf Coast) is the only Bechtel source within 200 miles of Units 6 & 7 ([Figure 2.5.2-204](#) and [Table 2.5.2-207](#)). The only post-EPRI information that requires revision to this source zone is the September 10, 2006, Emb 5.90 earthquake that occurred within the Gulf Coast source zone. As described in [Subsection 2.5.2.4.3.1.1](#), Emb 6.11 is conservatively adopted for this earthquake.

The original EPRI Mmax distribution for Bechtel source BZ1 (with weights in brackets) is: m_b 5.4 [0.1], 5.7 [0.4], 6.0 [0.4], and 6.6 [0.1] ([Table 2.5.2-207](#)) ([Reference 243](#)). Because the September 10, 2006, earthquake has a larger magnitude than the lower bound Mmax magnitude, the original EPRI Mmax distribution is updated.

Turkey Point Units 6 & 7
COL Application
Part 2 — FSAR

The updated Mmax distribution of 6.1 [0.10], 6.4 [0.40] and 6.6 [0.50] recommended here (Table 2.5.2-207) was determined from Bechtel's methodology of defining Mmax distributions, as described below (Reference 247):

- The lower bound magnitude of the distribution is defined as the greater of either the largest observed earthquake magnitude within the zone, or m_b 5.4.
- The next higher magnitude is 0.3 magnitude units greater than the minimum.
- The third magnitude is 0.6 magnitude units above the minimum.
- The fourth magnitude, and upper bound of the distribution, is m_b 6.6.
- The weightings on the four Mmax values are 0.1, 0.4, 0.4, and 0.1, assigned consecutively from the minimum Mmax value.
- If these guidelines result in an upper bound magnitude or magnitudes greater than m_b 6.6, then the upper Mmax distribution is truncated at m_b 6.6, and all weightings for magnitudes greater than or equal to 6.6 are summed and collapsed onto the magnitude 6.6 upper bound.

2.5.2.4.3.2.2 Mmax Update — Dames & Moore

Source 20 (Southern Coastal Margin) is the only Dames & Moore source within 200 miles of Units 6 & 7 (Figure 2.5.2-205 and Table 2.5.2-207). The only post-EPRI information that requires revision to this source zone is the February 10, 2006, Emb 5.58 earthquake that occurred within the southern boundary of the Southern Coastal Margin source zone.

The original EPRI Mmax distribution for Dames & Moore source 20 (with weights in brackets) is: m_b 5.3 [0.8] and 7.2 [0.2] (Table 2.5.2-207) (Reference 243). The February 10, 2006, earthquake was poorly recorded by traditional land-based seismograph networks. Despite the potential uncertainty in location, it is assumed that this event is correctly positioned within the source zone. Because the earthquake's Emb 5.58 magnitude is larger than the lower bound Mmax value, the original EPRI Mmax distribution is updated.

The Mmax distribution for Dames & Moore source 20 presented here results from increasing the lower-bound Mmax to match the magnitude of the observed Emb 5.58 earthquake (and rounding to the nearest tenth of a magnitude unit), while maintaining the same upper bound and weightings as the original EPRI Mmax distribution for the source zone. The updated Mmax values are (with weights in

brackets) m_b 5.6 [0.8] and 7.2 [0.2] (Table 2.5.2-207). The updated lower bound Mmax value for Dames & Moore source 20 is 0.1 magnitude unit greater than that defined for this source. This discrepancy is the result of slight differences in the magnitude estimates for the February 10, 2006, earthquake. The larger magnitude estimate (Emb 5.58) is conservatively retained for the February 10, 2006, earthquake.

Moreover, Dames & Moore did not prescribe any smoothing in determining seismicity parameters for their source 20 (Reference 243). The revised smoothing options shown in Table 2.5.2-207 are based on the range of smoothing options provided to the EPRI ESTs. The smoothing options vary between moderate to strong smoothing on a- and b-values, and all the options have a strong prior of 1.04 on b-value based on the Dames & Moore preference of that option (Reference 243).

2.5.2.4.3.2.3 Mmax Update — Law Engineering

Source 126 (South Coastal Block) is the only Law Engineering source within 200 miles of Units 6 & 7 (Figure 2.5.2-206 and Table 2.5.2-207). The only post-EPRI information that requires revisions to this source zone is the February 10, 2006, Emb 5.58 earthquake that occurred about 22 miles south of the South Coastal Block source zone. The February 10, 2006, earthquake was poorly recorded by traditional land-based seismograph networks and conservatively is assumed to have occurred within Law Engineering source 126.

The original EPRI Mmax distribution for Law Engineering source 126 (with weights in brackets) is: m_b 4.6 [0.9] and 4.9 [0.1] (Table 2.5.2-207) (Reference 243). Based on the inclusion of the earthquake within the source zone and the observation that the earthquake's Emb 5.58 magnitude is larger than the lower bound Mmax value, the original EPRI Mmax distribution for this source zone is revised.

The updated Mmax distribution of m_b 5.6 [0.90] and 5.7 [0.10] (Table 2.5.2-207) is determined using Law Engineering's methodology for developing Mmax distributions, as follows (Reference 247):

- The lower bound Mmax is the magnitude of the maximum observed earthquake in the zone.

Turkey Point Units 6 & 7
COL Application
Part 2 — FSAR

- The upper bound M_{max} magnitude defined by Law Engineering for regions with earthquakes occurring within 6.2 miles (10 kilometers) of the surface is m_b 5.7.

Weights for the original M_{max} distribution (0.9 on the lower bound M_{max} and 0.1 on the upper bound M_{max}) (References 243 and 247) are retained in the updated M_{max} distribution. The updated lower bound M_{max} value for Law Engineering source 126 is 0.1 magnitude unit greater than that defined for this source. This discrepancy is the result of slight differences in the magnitude estimates for the February 10, 2006, earthquake. The more recent and larger magnitude estimate (Emb 5.58) is conservatively retained for the February 10, 2006, earthquake.

2.5.2.4.3.2.4 M_{max} Update — Rondout Associates

Source 51 (Gulf Coast to Bahamas Fracture Zone) and source 49-05 (Appalachian Basement) are the only Rondout Associates source zones within 200 miles of Units 6 & 7 (Figure 2.5.2-207 and Table 2.5.2-207). Two sources of post-EPRI information require revisions to the M_{max} distributions of these source zones: (1) the October 24, 1997, Emb 4.96 earthquake that occurred within source 49-05, and (2) the September 10, 2006 Emb 5.90 earthquake that occurred within source 51. As described in Subsection 2.5.2.4.3.1.1, Emb 6.11 is conservatively adopted for the September 10, 2006, earthquake.

The original EPRI M_{max} distribution for sources 51 and 49-05 (with weights in brackets) is: m_b 4.8 [0.2], 5.5 [0.6], and 5.8 [0.2] (Table 2.5.2-207) (Reference 243). Because the October 24, 1997, and September 10, 2006, earthquakes have larger magnitudes than the lower bound M_{max} magnitude, the original EPRI M_{max} distributions for sources 51 and 49-05 are updated.

For Rondout Associates source 51, the updated M_{max} values of m_b 6.1 [0.3], 6.3 [0.55], and 6.5 [0.15] (Table 2.5.2-207) follow from reclassifying the source zone as one capable of producing moderate earthquakes instead of the original classification of the source zone as one only capable of producing smaller than moderate earthquakes (Reference 247). The original Rondout Associates M_{max} distribution for moderate earthquake source zones is m_b 5.2 [0.3], 6.3 [0.55], and 6.5 [0.15]. The updated M_{max} distribution follows this distribution with the exception of an increase in the lower bound of the distribution to m_b 6.1 to account for the observed September 10, 2006 earthquake within this zone.

For Rondout Associates source 49-05, the updated M_{max} values of m_b 5.0 [0.2], 5.5 [0.6], and 5.8 [0.2] (Table 2.5.2-207) result from increasing the lower M_{max}

bound to match the magnitude of the observed October 24, 1997, Emb 4.96 earthquake while maintaining the same upper bound and weightings of the original Mmax distribution for the source zone.

2.5.2.4.3.2.5 Mmax Update — Weston Geophysical Corporation

Source 107 (Gulf Coast Background) is the only Weston Geophysical source within 200 miles of Units 6 & 7 (Figure 2.5.2-208 and Table 2.5.2-207). The only post-EPRI information requiring revisions to any of these source zones is the September 10, 2006, Emb 5.90 earthquake that occurred within the Gulf Coast source zone. As described in Subsection 2.5.2.4.3.1.1, Emb 6.11 is conservatively adopted for this earthquake to be consistent with earlier studies.

The original EPRI Mmax distribution for Weston Geophysical source 107 (with weights in brackets) is: m_b 5.4 [0.71] and 6.0 [0.29] (Table 2.5.2-207) (Reference 243). Because the September 10, 2006, earthquake has a larger magnitude than the lower bound Mmax magnitude, the original EPRI Mmax distribution is updated.

Weston Geophysical's methodology for defining Mmax is based on developing discrete distributions for the probability of Mmax being a particular value (Reference 247). For source 107, these Mmax values and probabilities determined by the Weston Geophysical EST are: m_b 3.6 [0.04628], 4.2 [0.11982], 4.8 [0.27542], 5.4 [0.34415], 6.0 [0.16169], 6.6 [0.04461], and 7.2 [0.00553] (Reference 247). Following a conservative interpretation of Weston Geophysical's methodology, this discrete probability distribution is truncated at the magnitude that is closest to, yet greater than, the maximum observed earthquake within the source zone. For this study the distribution is truncated at 6.6 because the September 10, 2006, Emb 5.90 earthquake (for which Emb 6.11 is conservatively adopted) occurred within the source zone, and the next highest discrete magnitude in the distribution is 6.6. The truncated distribution is then renormalized so that the sum of all the probabilities is 1.0. The final Mmax values are the truncated distribution, and the weightings are the renormalized probabilities. For source 107, the updated Mmax distribution is: m_b 6.6 [0.89], 7.2 [0.11] (Table 2.5.2-207).

2.5.2.4.3.2.6 Mmax Update — Woodward-Clyde Consultants

Woodward-Clyde Consultants originally defined large background zones that cover the majority of the CEUS and a small set of source zones to represent tectonic features (Reference 247). These large background zones were simplified

in later stages of the EPRI project to individual, rectangular background zones centered on plant sites. Source BG-35 (Turkey Point Background) is a roughly 400 x 400 miles rectangle centered on Units 6 & 7 and extending southward into northern Cuba (Figure 2.5.2-203). The original EPRI Mmax distribution for source BG-35 is the same as those for the other Woodward-Clyde East Coast backgrounds: m_b 5.8 [0.33], 6.2 [0.34], 6.6 [0.33] (Table 2.5.2-207) (Reference 243).

To update Woodward-Clyde source BG-35, this source is truncated at the northern margin of the new Cuba and northern Caribbean seismic source model. Subsection 2.5.2.4.4.3 describes the new Cuba and northern Caribbean source model. Southward truncation of Woodward-Clyde source BG-35 is required to avoid double-counting of earthquakes in the northern portion of the new Cuba and northern Caribbean seismic source model.

The largest earthquake in the truncated Woodward-Clyde BG-35 source zone is the June 2, 1990, Emb 4.09 earthquake located off the north coast of Cuba (Figure 2.5.2-209 and Table 2.5.2-207). Because this earthquake is smaller than the minimum value of the original EPRI Mmax distribution (m_b 5.8), no change to the original Mmax distribution is required for the truncated Woodward-Clyde source.

2.5.2.4.4 New Seismic Source Characterizations

To complement the updated EPRI seismic source model described above, three new seismic source characterizations are included for analysis. These three new source characterizations are:

- Supplemental seismic source zones that fill the area of the site region beyond the area covered by the original EPRI source model (Subsection 2.5.2.4.4.1).
- New, post-EPRI characterization of the Charleston seismic source (Subsection 2.5.2.4.4.2).
- New, post-EPRI characterization of seismic sources located in Cuba and the northern Caribbean region (Subsection 2.5.2.4.4.3).

2.5.2.4.4.1 Supplemental Source Zones

In all but one case, the Woodward-Clyde Consultants team, the EPRI ESTs' source zones do not cover the entire 200-mile radius site region (Figure 2.5.2-203). In general, the EPRI Gulf Coast seismic source zones do not extend much

Turkey Point Units 6 & 7
COL Application
Part 2 — FSAR

beyond the site to either the south or east, thus leaving large portions of the site region without any seismic source zones. This subsection provides rationale for adding supplemental source zones to account for potential seismic sources within the remainder of the site region north of the northern border of the new Caribbean seismic source model (Subsection 2.5.2.4.4.3), consistent with current knowledge of the geologic, geophysical, and seismic characteristics of the crust in this region. The areas of the site region not covered by the original EPRI model are largely devoid of seismicity (Figures 2.5.2-203 through 2.5.2-209). Based on this observation, new supplemental sources within the site region are added to represent the extension of Gulf Coast seismic sources, instead of expanding the existing EPRI source zones to cover the site region. By simply expanding existing EPRI Gulf Coast source zones to offshore areas devoid of historical earthquake activity, the site hazard may be unduly decreased due to seismicity smoothing options detailed for these zones. Adding new source zones (with similar parameters to the updated EPRI Gulf Coast zones) instead, is a conservative approach, the details of which are described below. The combination of a Gulf Coast zone and a new supplemental source zone with similar parameters provides source zones covering the entire site region to account for future earthquakes.

In general, the EPRI ESTs provide minimal documentation describing the data and interpretations that define the southern and eastern boundaries of their Gulf Coast source zones (Reference 247). The eastern and southern boundaries of the Gulf Coast source zones are largely arbitrary and are not tied to any specific geologic, seismologic, or geophysical features. The southern boundary of five of the six original EPRI ESTs' Gulf Coast source zones appear to have been arbitrarily truncated at about 25°N latitude (Figure 2.5.2-203). The sixth team, Woodward-Clyde Consultants, defines its Turkey Point Background (BG-35) source as a rectangular area centered on Units 6 & 7 and is not based on any geological, geophysical, or seismological features.

The new supplemental source zones are based on the assumption that the entire site region is potentially seismogenic. The geometries of these supplemental zones, which were created by using the original EPRI Gulf Coast source zone geometries and filling in the remainder of the site region north of the northern boundary of the new Caribbean seismic source model, are shown in Figures 2.5.2-204 through 2.5.2-209. As shown in Table 2.5.2-209, this process results in five new source zones (one for each EPRI EST except Woodward-Clyde). A sixth, modified source is the result of truncating existing Woodward-Clyde source BG-35 by the northern boundary of the new Caribbean seismic

Turkey Point Units 6 & 7
COL Application
Part 2 — FSAR

source model. This truncated source is intended to replace the original EPRI Woodward-Clyde source BG-35. [Table 2.5.2-210](#) provides geographic coordinates of the corner points of the five supplemental source zones and the truncated Woodward-Clyde source.

The new supplemental source zones also are based on the assumption that the crust within the site region between southern Florida and the northern boundary of the new Caribbean seismic source model is similar and has similar earthquake potential. The following lines of evidence support crustal similarity within this area:

- Kanter's Plate 8 ([Reference 270](#)) shows crustal zone 216b (Gulf Coast) extending from southern Florida to northern Cuba coastline and comprising extended and transitional crust ([Figure 2.5.2-212](#)).
- Bally et al.'s Figure 1 ([Reference 212](#)) shows passive margin basins on continental and transitional crust mapped throughout Florida, offshore to at least continental shelf break, and south to northern coast of Cuba ([Figure 2.5.2-213](#)).
- Toiran ([Reference 327](#), p. 359) states, "Over most of its length, Cuba is the dividing line between extremely stable geologic conditions to the north and a complex one to the south . . . much of the north coast of Cuba belongs to the Florida-Bahama carbonate province."
- Pindell and Kennan's Figure 18 ([Reference 302](#)) plate reconstruction shows "stretched continental crust" extending from southern Florida to northern Cuba ([Figure 2.5.2-214](#)).
- Dunbar and Sawyer's Figures 1 and 4b ([Reference 239](#)) show the area in question as "extended continental crust" with β (extension parameter) = 1 to 4.5 ([Figure 2.5.2-215](#)).
- Sawyer et al.'s Figure 5 ([Reference 315](#)) shows the area in question as "thick transitional crust" ([Figure 2.5.2-216](#)).
- No internal patterns in seismicity. Most dramatic change occurs at northern Cuba coastline ([Figure 2.5.2-201](#)).

Implementation of this method involves the following:

Turkey Point Units 6 & 7
COL Application
Part 2 — FSAR

- No changes to the geometries of the original EPRI Gulf Coast source zones (except Woodward-Clyde seismic source BG-35, which is truncated at the northern boundary of new Caribbean seismic source model).
- Add five additional source zones (one for each EST except Woodward-Clyde) to fill in site region, truncated at the northern boundary of new Caribbean seismic source model (Figures 2.5.2-204 through 2.5.2-209, Tables 2.5.2-209 and 2.5.2-210).
- Reassess Mmax distributions and weights for original EPRI source zones within the site region based on the updated seismicity catalog, as described in Subsection 2.5.2.4.3.2.
- Assess Mmax distributions and weights for five new source zones based on the updated seismicity catalog. These five new source zones are largely devoid of historical seismicity (Table 2.5.2-209), thus Mmax distributions are conservatively based on Mmax estimates for their respective updated EPRI EST Gulf Coast zones (Table 2.5.2-207). Due to the similarity of the crust between the supplemental source zones and the original EPRI Gulf Coast source zones, the new zones reflect the same Mmax distributions as their updated Gulf Coast source zone counterpart for each EST.

Given the paucity of earthquakes in 1 x 1 degree cells offshore of Florida, the following steps were used to assign a- and b-values to the updated EPRI sources and new supplemental source zones:

- Average a- and b-values were calculated for peninsular Florida using the updated seismicity catalog and original completeness matrices (extended to 2007) and full smoothing.
- These average a- and b-values were used to represent seismicity in 1 x 1 degree cells for the five new supplemental source zones.
- These average a- and b-values also were used to represent seismicity in 1 x 1 degree cells in the updated EPRI team sources representing Gulf Coast seismicity outside of the original EPRI completeness regions. One x one degree cells more than 200 miles from Units 6 & 7 were not modeled.
- The original a- and b-values were used for the updated EPRI team sources, where they are defined.

2.5.2.4.4.2 Updated Charleston Seismic Source (UCSS) Model

Units 6 & 7 are located roughly 500 miles from Charleston, South Carolina (Figure 2.5.2-203). The original EPRI seismic source model (References 243 and 247) includes assessments of the Charleston seismic source. However, several studies that post-date the EPRI EST assessments demonstrate that the source parameters for geometry, Mmax, and recurrence of Mmax in the Charleston seismic source need to be updated to capture a more current understanding of both the 1886 Charleston earthquake and the seismic source that produced this earthquake. Therefore, this subsection presents an update of the Charleston seismic source.

The Updated Charleston Seismic Source (UCSS) model presented in this subsection was developed through use of a Senior Seismic Hazard Analysis Committee (SSHAC) Level 2 process (Reference 318) for the Vogtle site in Georgia. Subsections 2.5.2.4.4.2.1 through 2.5.2.4.4.2.3 describe the UCSS model.

2.5.2.4.4.2.1 UCSS Model Geometry

The UCSS model includes four mutually exclusive source zone geometries (A, B, B', and C; Figure 2.5.2-217). Table 2.5.2-211 presents the latitude and longitude coordinates that define these four source zones. The four geometries of the UCSS model are defined based on current understanding of geologic and tectonic features in the 1886 Charleston earthquake epicentral region: the 1886 Charleston earthquake shaking intensity; distribution of seismicity; and geographic distribution, age, and density of liquefaction features associated with both the 1886 and prehistoric earthquakes. These features strongly suggest that the majority of evidence for the Charleston source is concentrated in the Charleston area and is not widely distributed throughout South Carolina.

Geometry A — Charleston. Geometry A is about 100 x 50 kilometers, northeast-oriented area centered on the 1886 Charleston meizoseismal area (Figure 2.5.2-217). Geometry A is intended to represent a localized source area that generally confines the Charleston source to the 1886 meizoseismal area (i.e., a stationary source in time and space). Geometry A completely envelops the 1886 earthquake MMI X isoseismal (Reference 216), the majority of identified Charleston-area tectonic features and inferred fault intersections, and the majority of reported 1886 liquefaction features. Geometry A excludes the northern extension of the southern segment of the East Coast fault system because this system extends well north of the meizoseismal zone and is included in its own source geometry (Geometry C).

Turkey Point Units 6 & 7
COL Application
Part 2 — FSAR

Geometry A also excludes outlying liquefaction features because liquefaction occurs as a result of strong ground shaking that may extend well beyond the areal extent of the tectonic source. Geometry A also envelops instrumentally located earthquakes spatially associated with the Middleton Place-Summerville Seismic Zone (MPSSZ) (References 272, 324, and 325).

The preponderance of evidence strongly supports the conclusion that the seismic source for the 1886 Charleston earthquake is located in a relatively restricted area defined by Geometry A. Geometry A envelops the following:

- The meizoseismal area of the 1886 earthquake.
- The area containing the majority of local tectonic features (although many have large uncertainties associated with their existence and activity).
- The area of ongoing concentrated seismicity.
- The area of greatest density of 1886 liquefaction and prehistoric liquefaction.

These observations show that future earthquakes having magnitudes comparable to the Charleston earthquake of 1886 most likely would occur within the area defined by Geometry A. The UCSS model assigns a weight of 0.70 to Geometry A (Figure 2.5.2-218). To confine the rupture dimension to within the source area and to maintain a preferred northeast fault orientation, Geometry A is represented in the model by a series of closely spaced, northeast-trending faults parallel to the long axis of the zone.

Geometries B, B', and C. Whereas the preponderance of evidence supports the assessment that the 1886 Charleston meizoseismal area and Geometry A define the area where future events would most likely be centered, it is possible that the tectonic feature responsible for the 1886 earthquake either extends beyond or lies outside Geometry A. Therefore, the remaining three geometries (B, B', and C) are assessed to capture the uncertainty that future events may not be restricted to Geometry A. The distribution of liquefaction features along the entire coast of South Carolina and observations from the paleoliquefaction record that a few events were localized (moderate earthquakes to the northeast and southwest of Charleston), suggest that the Charleston source could extend well beyond Charleston proper. Geometries B and B' represent a larger source zone, while Geometry C represents the southern segment of the East Coast fault system as a possible source zone. The UCSS model assigns a weight of 0.20 to the combined geometries of B and B', and a weight of 0.10 to Geometry C. Geometry B' is a

Turkey Point Units 6 & 7
COL Application
Part 2 — FSAR

subset of B, and formally defines the onshore coastal area as a source that restricts earthquakes to the onshore region. Geometry B, which includes the onshore and offshore regions, and Geometry B' are mutually exclusive. The UCSS model assigns equal weights of 0.10 to Geometries B and B'.

Geometry B — Coastal and Offshore Zone. Geometry B is a coast-parallel, approximately 260 x 100 kilometers source area that (1) incorporates all of Geometry A, (2) is elongated to the northeast and southwest to capture other, more distant liquefaction features in coastal South Carolina (References 207, 208, and 323), and (3) extends to the southeast to include the offshore Helena Banks fault zone (Reference 213) (Figure 2.5.2-217). The elongation and orientation of Geometry B is roughly parallel to the regional structural grain as well as roughly parallel to the elongation of 1886 isoseismals. The mapped extent of paleoliquefaction features (References 207, 208, and 323) defines the northeastern and southwestern extents of Geometry B.

The location and timing of paleoliquefaction features in the Georgetown and Bluffton areas to the northeast and southwest of Charleston suggest to some researchers that the earthquake source may not be restricted to the Charleston area (References 207, 295, 296, and 323). Geometry B accounts for the possibility that there may be an elongated source or multiple sources along the South Carolina coast. Paleoliquefaction features in the Georgetown and Bluffton areas may be explained by an earthquake source both northeast and southwest of Charleston, as well as possibly offshore.

Geometry B extends southeast to include an offshore area and the Helena Banks fault zone. The Helena Banks fault zone is clearly shown by multiple seismic reflection profiles and has demonstrable late Miocene offset (Reference 213). Offshore earthquakes in 2002 (m_b 3.5 and 4.4) suggest a possible spatial association of seismicity with the mapped trace of the Helena Banks fault system. Whereas these two events in the vicinity of the Helena Banks fault system do not provide a positive correlation with seismicity or demonstrate recent fault activity, these small earthquakes are new data that post-date the EPRI studies.

The UCSS model assigns a low weight of 0.10 to Geometry B (Figure 2.5.2-218) because the preponderance of evidence indicates that the seismic source that produced the 1886 earthquake lies onshore in the Charleston meizoseismal area and not in the offshore region. To confine the rupture dimension to within the source area and to maintain a preferred northeast fault orientation, the UCSS model represents Geometry B as a series of closely spaced, northeast-trending faults parallel to the long axis of the zone.

Geometry B' — Coastal Zone. Geometry B' is a coast-parallel, approximately 260 x 50 kilometers source area that incorporates all of Geometry A, as well as the majority of reported paleoliquefaction features (References 207, 208, and 323). Unlike Geometry B, however, Geometry B' does not include the offshore Helena Banks fault zone (Figure 2.5.2-217).

The Helena Banks fault system is excluded from Geometry B' because the preponderance of data and evaluations support the assessment that the fault system is not active and because evidence strongly suggests that the 1886 Charleston earthquake occurred onshore in the 1886 meizoseismal area and not on an offshore fault. Whereas there is little uncertainty regarding the existence of the Helena Banks fault, there is a lack of evidence that this feature is still active. Isoseismal maps documenting shaking intensity in 1886 indicate an onshore meizoseismal area (Figure 2.5.2-218). An onshore source for the 1886 earthquake and prehistoric events is supported by the instrumentally recorded seismicity in the MPSSZ and the corresponding high-density cluster of 1886 and prehistoric liquefaction features.

Similar to Geometry B above, the UCSS model assigns a weight of 0.10 to Geometry B', reflecting the assessment that Geometry B' has a much lower probability of being the source zone for Charleston-type earthquakes than Geometry A (Figure 2.5.2-218). To confine the rupture dimension to within the source area and to maintain a preferred northeast fault orientation, the UCSS model represents Geometry B' as a series of closely spaced, northeast-trending faults parallel to the long axis of the zone.

Geometry C — East Coast Fault System - South. Geometry C is about 200 x 30 kilometers, north-northeast-oriented source area (Figure 2.5.2-217) enveloping the southern segment of the proposed East Coast fault system shown in Figure 3 of Marple and Talwani (Reference 278). The area of Geometry C is restricted to envelop the original depiction of the East Coast Fault System-South by Marple and Talwani (Reference 278).

The UCSS model assigns a low weight of 0.10 to Geometry C to reflect the assessment that Geometries B, B', and C all have equal, but relatively low, likelihoods of producing large-magnitude earthquakes (Figure 2.5.2-218). As with the other UCSS geometries, the UCSS model represents Geometry C as a series of parallel, vertical faults oriented northeast-southwest and parallel to the long axis of the narrow rectangular zone. The faults and extent of earthquake ruptures are confined within the rectangle depicting Geometry C.

UCSS Model Parameters. Based on studies by Bollinger et al. (References 214 and 215) and Bollinger (Reference 217), the UCSS model assumes a 20-kilometer-thick seismogenic crust. To model the occurrence of earthquakes in the characteristic part of the Charleston distribution ($M_w \geq 6.7$), the model uses a series of closely-spaced, vertical faults parallel to the long axis of each of the four source zones (A, B, B', and C). Faults and earthquake ruptures are limited to within each respective source zone and are not allowed to extend beyond the zone boundaries, and ruptures are constrained to occur within the depth range of 0 to 20 kilometers. The UCSS model assumes fault rupture areas have a width-to-length aspect ratio of 0.5, conditional on the assumed maximum fault width of 20 kilometers. To obtain Mmax earthquake rupture lengths from magnitude, the UCSS model uses the Wells and Coppersmith (Reference 334) empirical relationship between surface rupture length and magnitude for earthquakes of all slip types.

To maintain as much similarity as possible with the original EPRI model, the UCSS model treats earthquakes in the exponential part of the distribution ($M_w < 6.7$) as point sources uniformly distributed within the source area (full smoothing), with a constant depth fixed at 10 kilometers.

2.5.2.4.4.2.2 UCSS Model Mmax

Mmax estimates for the Charleston seismic source are based on published literature and previous source characterizations. Given the large uncertainties in working with the paleoliquefaction record and methods for estimating magnitudes from these data, the best representation of the Mmax for the Charleston seismic source should be based on estimates of the size of the 1886 earthquake.

Based on assessment of the currently available data and interpretations regarding the range of modern Mmax estimates, the UCSS model modifies the 2008 USGS hazard model magnitude distribution (Reference 300) to include a total of five discrete magnitude values, each separated by 0.2 M_w units (Figure 2.5.2-218). The UCSS Mmax distribution is based on recent studies, as summarized in Table 2.5.2-212. The UCSS Mmax distribution includes a discrete value of M_w 6.9 to represent the Bakun and Hopper (Reference 211) best estimate of the 1886 Charleston earthquake magnitude, as well as a lower value of M_w 6.7 to capture a low probability that the 1886 earthquake was smaller than the Bakun and Hopper (Reference 211) mean estimate of M_w 6.9. Bakun and Hopper (Reference 211) do not explicitly report a 1-sigma range in magnitude estimate of the 1886 earthquake, but do provide a 2-sigma range of M_w 6.4 to 7.2.

Turkey Point Units 6 & 7
COL Application
Part 2 — FSAR

The UCSS magnitudes and weights are as follows:

<u>M_w</u>	<u>Weight</u>	
6.7	0.10	
6.9	0.25	Bakun and Hopper (Reference 211) mean
7.1	0.30	
7.3	0.25	Johnston (Reference 267) mean
7.5	0.10	

This results in a weighted Mmax mean magnitude of M_w 7.1 for the UCSS, slightly lower than the mean magnitude of M_w 7.2 in the 2008 USGS model ([Reference 300](#)).

2.5.2.4.4.2.3 UCSS Model Recurrence of Mmax

In the 1989 EPRI study ([Reference 243](#)), the six EPRI ESTs use an exponential magnitude distribution to represent earthquake sizes for their Charleston sources. Parameters of the exponential magnitude distribution are estimated from historical seismicity in the respective source areas. This results in recurrence intervals for Mmax earthquakes (at the upper end of the exponential distribution) of several thousand years.

The UCSS model for earthquake recurrence is a composite model consisting of two distributions. The first is an exponential magnitude distribution used to estimate recurrence between the lower-bound magnitude used for hazard calculations and m_b 6.7. The parameters of this distribution are estimated from the earthquake catalog, as they were for the 1989 EPRI study. This is the standard procedure for smaller magnitudes and is the model used, for example, by the USGS 2002 national hazard maps ([Reference 251](#)). The second distribution treats Mmax earthquakes (M_w ≥ 6.7) according to a characteristic model, with discrete magnitudes and mean recurrence intervals estimated through analysis of geologic data, including paleoliquefaction studies. The term Mmax is used to describe the range of largest earthquakes in both the characteristic portion of the UCSS recurrence model and the EPRI exponential recurrence model.

This composite model achieves consistency between the occurrence of earthquakes with M_w < 6.7 and the earthquake catalog and between the occurrence of large earthquakes (M_w ≥ 6.7) with paleoliquefaction evidence. It is a

type of “characteristic earthquake” model, in which the recurrence rate of large events is higher than what would be estimated from an exponential distribution inferred from the historical seismic record.

Mmax Recurrence. This subsection describes how the UCSS model determines mean recurrence intervals for Mmax earthquakes. The UCSS model incorporates geologic data to characterize the recurrence intervals for Mmax earthquakes. As described earlier, identifying and dating paleoliquefaction features provides a basis for estimating the recurrence of large Charleston area earthquakes. Most of the available geologic data pertaining to the recurrence of large earthquakes in the Charleston area were published after 1990 and therefore were not available to the six EPRI ESTs. In the absence of geologic data, the six EPRI EST estimates of recurrence for large, Charleston-type earthquakes are based on a truncated exponential model using historical seismicity ([References 243 and 247](#)). The truncated exponential model also provides the relative frequency of all earthquakes greater than m_b 5.0 up to Mmax in the EPRI PSHA. The recurrence of Mmax earthquakes in the EPRI models is on the order of several thousand years, which is significantly greater than more recently published estimates of about 500 to 600 years, based on paleoliquefaction data ([Reference 323](#)).

Paleoliquefaction Data. Strong ground shaking during the 1886 Charleston earthquake produced extensive liquefaction, and liquefaction features from the 1886 event are preserved in geologic deposits at numerous locations in the South Carolina coastal region. Documentation of older liquefaction-related features in geologic deposits provides evidence for prior strong ground motions during prehistoric large earthquakes. Estimates of the recurrence of large earthquakes in the UCSS are based on dating paleoliquefaction features. Many potential sources of ambiguity and/or error are associated with dating and interpreting paleoliquefaction features. This assessment does not reevaluate field interpretations and data; rather, it reevaluates criteria used to define individual paleoearthquakes in the published literature. In particular, the UCSS reevaluates the paleoearthquake record interpreted by Talwani and Schaeffer ([Reference 323](#)) based on that study’s compilation of sites with paleoliquefaction features.

Talwani and Schaeffer ([Reference 323](#)) compile radiocarbon ages from paleoliquefaction features along the coast of South Carolina. These data include ages that provide contemporary, minimum, and maximum limiting ages for liquefaction events. Radiocarbon ages are corrected for past variability in atmospheric ^{14}C using well-established calibration curves and converted to “calibrated” (approximately calendar) ages. From their compilation of calibrated radiocarbon ages from various geographic locations, Talwani and Schaeffer

(Reference 323) correlate individual earthquake episodes. They identify an individual earthquake episode based on samples with a “contemporary” age constraint that have overlapping calibrated radiocarbon ages at approximately 1-sigma confidence interval. The estimated age of each earthquake is “calculated from the weighted averages of overlapping contemporary ages” (p. 6632). They define as many as eight events (named 1886, A, B, C, D, E, F, and G in order of increasing age) from the paleoliquefaction record, and offer two scenarios to explain the distribution and timing of paleoliquefaction features (Table 2.5.2-213).

The two scenario paleoearthquake records proposed by Talwani and Schaeffer (Reference 323) have different interpretations for the size and location of prehistoric events (Table 2.5.2-213). In their Scenario 1, the four prehistoric events, A, B, E, and G, that produced widespread liquefaction features similar to the large 1886 Charleston earthquake are interpreted to be large, 1886 Charleston-type events. Three events, C, D, and F, are defined by paleoliquefaction features that are more limited in geographic extent than other events and are interpreted to be smaller, moderate-magnitude events (approximately M_w 6). Events C and F are defined by features found north of Charleston in the Georgetown region, and Event D is defined by sites south of Charleston in the Bluffton area. In their Scenario 2, all events are interpreted as large, 1886 Charleston-type events. Furthermore, Events C and D are combined into a large Event C'. Talwani and Schaeffer (Reference 323) justify the grouping of the two events based on the observation that the calibrated radiocarbon ages that constrain the timing of Events C and D are indistinguishable at the 95 percent (2-sigma) confidence interval.

The length and completeness of the paleoearthquake record based on paleoliquefaction features is a source of epistemic uncertainty in the UCSS model (epistemic uncertainty is the result of inaccurate or incomplete information and can be reduced or eliminated given better models or additional observations, as opposed to aleatory uncertainty that results from randomness and cannot be reduced with more or better observations). The paleoliquefaction record along the South Carolina coast extends from 1886 to the mid-Holocene (Reference 323). The consensus of the scientists who have evaluated these data is that the paleoliquefaction record of earthquakes is complete only for approximately the most-recent 2000 years and that it is possible that liquefaction events are missing from the older portions of the record. The suggested incompleteness of the paleoseismic record is based on the argument that past fluctuations in sea level have produced time intervals of low water table conditions (and thus low liquefaction susceptibility), during which large earthquake events may not have

been recorded in the paleoliquefaction record ([Reference 323](#)). While this assertion may be true, it is possible that the paleoliquefaction record may be complete back to the mid-Holocene.

2-Sigma Analysis of Event Ages. The Talwani and Schaeffer ([Reference 323](#)) data compilation of liquefaction is the basis for analysis of the coastal South Carolina paleoliquefaction record performed in support of [Subsection 2.5.2](#). As described above, Talwani and Schaeffer ([Reference 323](#)) use calibrated radiocarbon ages with 1-sigma error bands to define the timing of past liquefaction episodes in coastal South Carolina. The standard in paleoseismology, however, is to use calibrated ages with 2-sigma (95.4 percent confidence interval) error bands ([Reference 261](#)). Likewise, in paleoliquefaction studies, to more accurately reflect the uncertainties in radiocarbon dating, Tuttle ([Reference 328](#)) advises the use of calibrated radiocarbon dates with 2-sigma error bands (as opposed to narrower 1-sigma error bands). Talwani and Schaeffer's ([Reference 323](#)) use of 1-sigma error bands may lead to over-interpretation of the paleoliquefaction record such that more episodes are interpreted than actually occurred. In recognition of this possibility, the conventional radiocarbon ages presented in Talwani and Schaeffer ([Reference 323](#)) are recalibrated and reported with 2-sigma error bands. The recalibration of individual radiocarbon samples and estimation of age ranges for paleoliquefaction events show broader age ranges with 2-sigma error bands that are used to obtain broader age ranges for paleoliquefaction events in the Charleston area.

Event ages based on overlapping 2-sigma ages of paleoliquefaction features are presented in [Table 2.5.2-213](#). Paleoearthquakes are distinguished based on grouping paleoliquefaction features that have contemporary radiocarbon samples with overlapping calibrated ages. Event ages are defined by selecting the age range common to each of the samples. For example, an event defined by overlapping 2-sigma sample ages of 100 to 200 calendar year before present and 50 to 150 calendar year before present has an event age of 100 to 150 calendar year before present. The UCSS model considers these "trimmed" ages to represent the approximately 95 percent confidence interval, with a "best estimate" event age as the midpoint of the approximately 95 percent age range.

The UCSS model 2-sigma analysis identifies six distinct paleoearthquakes in the data presented by Talwani and Schaeffer ([Reference 323](#)). As noted by that study, Events C and D are indistinguishable at the 95 percent confidence interval, and in the UCSS, those samples define Event C' ([Table 2.5.2-213](#)). Additionally, the UCSS 2-sigma analysis suggests that Talwani and Schaeffer ([Reference 323](#)) Events F and G are a single, large event, defined in the UCSS as F'. One

important difference between the UCSS result and that of Talwani and Schaeffer (Reference 323) is that the three Events C, D, and F in their Scenario 1, which are inferred to be smaller, moderate-magnitude events, are grouped into more regionally extensive Events C' and F' (Table 2.5.2-213). Therefore, in the UCSS, all earthquakes in the 2-sigma analysis are interpreted to represent large, Charleston-type events. The incorporation of large Events C' and F' into the UCSS model is, in effect, a conservative approach. In the effort to estimate the recurrence of Mmax events (M_w 6.7 to 7.5), moderate-magnitude (about M_w 6) earthquakes C and D would be eliminated from the record of large (Mmax) earthquakes in the UCSS model, thereby increasing the calculated Mmax recurrence interval and lowering the hazard without sufficient justification. For these reasons the UCSS model uses a single, large Event C' (instead of separate, smaller Events C and D) and a single, large Event F' (instead of separate, smaller Events F and G). Analysis suggests that there have been four large earthquakes in the most-recent, about 2000-year portion of the record (1886 and Events A, B, and C'). In the entire 5000-year paleoliquefaction record, there is evidence for six large, Charleston-type earthquakes (1886, A, B, C', E, F'; Table 2.5.2-213). Figure 2.5.2-217 shows the geographic distribution of liquefaction features associated with each event in the UCSS model. The distributions of paleoliquefaction sites for Events A, B, C', E, and F' are all very similar to the coastal extent of the liquefaction features from the 1886 earthquake.

Recurrence intervals developed from the earthquakes recorded by paleoliquefaction features assume that these features were produced by large Mmax events and that both the 2000-year and 5000-year records are complete. However, the UCSS model highlights at least two concerns regarding the use of the paleoliquefaction record to characterize the recurrence of past Mmax events. First, it is possible that multiple, moderate-sized earthquakes closely spaced in time produced the paleoliquefaction features associated with one or more of the pre-1886 events. If this is the case, then the calculated recurrence interval would yield artificially short recurrence for Mmax, because it is calculated using repeat times of both large (Mmax) events and smaller earthquakes. Limitations of radiocarbon dating and limitations in the stratigraphic record often preclude identifying individual events in the paleoseismologic record that are closely spaced in time (i.e., separated by only a few years to a few decades). Several seismic sources have demonstrated tightly clustered earthquake activity in space and time that are indistinguishable in the radiocarbon and paleoseismic record:

- New Madrid (December 1811, January 1812, and February 1812)

Turkey Point Units 6 & 7
COL Application
Part 2 — FSAR

- North Anatolian Fault (August 1999 and November 1999)
- San Andreas Fault (December 1812 and January 1857)

Therefore the UCSS acknowledges the distinct possibility that M_{max} occurs less frequently than what is calculated from the paleoliquefaction record.

A second concern is that the recurrence behavior of the M_{max} event may be highly variable through time. For example, the UCSS considers it unlikely that M_w 6.7 to 7.5 events have occurred on a Charleston source at an average repeat time of about 500 to 600 years (Reference 323) throughout the Holocene Epoch. Such a moment release rate would likely produce tectonic landforms with clear geomorphic expression, such as are present in regions of the world with comparably high rates of moderate to large earthquakes (for example, faults in the Eastern California shear zone with sub-millimeter per year slip rates and recurrence intervals on the order of about 5000 years have clear geomorphic expression [Reference 309]). Perhaps it is more likely that the Charleston source has a recurrence behavior that is highly variable through time, such that a sequence of events spaced about 500 years apart is followed by quiescent intervals of thousands of years or longer. This sort of variability in inter-event time may be represented by the entire mid-Holocene record, in which both short inter-event times (e.g., about 400 years between Events A and B) are included in a record with long inter-event times (e.g., about 1900 years between Events C' and E).

Recurrence of M_{max} . The UCSS model calculates two average recurrence intervals covering two different time intervals. The UCSS model represents these two recurrence intervals as separate branches on the logic tree (Figure 2.5.2-218). The first average recurrence interval is based on the four events that occurred within the past about 2000 years. This time period is considered to represent a complete portion of the paleoseismic record (Reference 323). These events include 1886, A, B, and C' (Table 2.5.2-213). The average recurrence interval calculated for the most recent portion of the paleoliquefaction record (four events over the past about 2000 years) is given 0.80 weight on the logic tree (Figure 2.5.2-218).

The second average recurrence interval is based on events that occurred within the past about 5000 years. This time period represents the entire paleoseismic record based on paleoliquefaction data (Reference 323). These events include 1886, A, B, C', E, and F' as listed in Table 2.5.2-213. Published literature and questioned researchers suggest that the older part of the record (older than about

Turkey Point Units 6 & 7
COL Application
Part 2 — FSAR

2000 years ago) may be incomplete. Whereas this assertion may be true, it is also possible that the older record, which exhibits longer inter-event times, is complete. The UCSS model assigns a weight of 0.20 to the average recurrence interval calculated for the 5000-year record (six events) (Figure 2.5.2-218). The 0.80 and 0.20 weighting of the 2000-year and 5000-year paleoliquefaction records, respectively, reflects incomplete knowledge of both the short- and long-term recurrence behavior of the Charleston source.

The mean recurrence intervals for the most recent 2000-year and 5000-year records represent the average time interval between earthquakes attributed to the Charleston seismic source. The mean recurrence intervals and their parametric uncertainties are calculated according to the methods outlined by Savage (Reference 313) and Cramer (Reference 227). The methods provide a description of mean recurrence interval, with a best estimate mean and an uncertainty described as a lognormal distribution with a median and parametric lognormal shape factor.

The lognormal distribution is one of several distributions, including the Weibull, Double Exponential, and Gaussian, among others, used to characterize earthquake recurrence (Reference 248). Ellsworth et al. (Reference 248) and Matthews et al. (Reference 280) propose a Brownian-passage time model to represent earthquake recurrence, arguing that it more closely simulates the physical process of strain build-up and release. This Brownian-passage time model is currently used to calculate earthquake probabilities in the greater San Francisco Bay region (Reference 337). Analyses show that the lognormal distribution is very similar to the Brownian-passage time model of earthquake recurrence for cases where the time elapsed since the most recent earthquake is less than the mean recurrence interval (References 225 and 248). This is the case for Charleston, where 120 years have elapsed since the 1886 earthquake and the mean recurrence interval determined over the past 2000 years is about 548 years. The UCSS model calculates average recurrence intervals using a lognormal distribution because its statistics are well-known (Reference 294) and numerous other studies use this method (References 227, 313, and 336).

The average interval between earthquakes is expressed as two continuous lognormal distributions. The average recurrence interval for the 2000-year record, based on the three most recent inter-event times (1886-A, A-B, B-C'), has a best estimate mean value of 548 years, an uncertainty distribution described by a median value of 531 years, a lognormal shape factor of 0.25. The average recurrence interval for the 5000-year record, based on five inter-event times (1886-A, A-B, B-C', C'-E, E-F'), has a best estimate mean value of 958 years, an

Turkey Point Units 6 & 7
COL Application
Part 2 — FSAR

uncertainty distribution described by a median value of 841 years, and a lognormal shape factor of 0.51. At one standard deviation, the average recurrence interval for the 2000-year record is between 409 and 690 years; for the 5000-year record, it is between 452 and 1564 years. Combining these mean values of 548 and 958 years with their respective logic tree weights of 0.8 and 0.2 results in a weighted mean of 630 years for Charleston Mmax recurrence.

The UCSS model uses mean recurrence values that are similar to those determined by earlier studies. Talwani and Schaeffer (Reference 323) consider two possible scenarios to explain the distribution in time and space of paleoliquefaction features. In their Scenario 1, large earthquakes have occurred with an average recurrence of 454 ± 21 years over about the past 2000 years; in their Scenario 2, large earthquakes have occurred with an average recurrence of 523 ± 100 years over the past 2000 years. Talwani and Schaeffer (Reference 323) state that, "In anticipation of additional data we suggest a recurrence rate [sic] between 500 and 600 years for M 7+ earthquakes at Charleston." For the 2000-year record, the 1-standard-deviation range of 409 to 690 years completely encompasses the range of average recurrence interval reported by Talwani and Schaeffer (Reference 323). The best-estimate mean recurrence interval value of 548 years is comparable to the midpoint of the Talwani and Schaeffer (Reference 323) best-estimate range of 500 to 600 years. The best estimate mean recurrence interval value from the 5000-year paleoseismic record of 958 years is outside the age ranges reported by Talwani and Schaeffer (Reference 323), although they did not determine an average recurrence interval based on the longer record.

The 2008 USGS updated seismic hazard maps for the conterminous United States use a mean recurrence value of 550 years for characteristic earthquakes in the Charleston region (Reference 300). This value is based on the above-quoted 500 to 600 year estimate from Talwani and Schaeffer (Reference 323). The USGS updated seismic hazard maps for the conterminous United States do not incorporate uncertainty in mean recurrence interval in their calculations.

For computation of seismic hazard, discrete values of activity rate (inverse of recurrence interval) are required as input to the PSHA code (Reference 224). To evaluate PSHA based on mean hazard, the mean recurrence interval and its uncertainty distribution should be converted to mean activity rate with associated uncertainty. The final discretized activity rates used to model the UCSS in the PSHA reflect a mean recurrence of 548 years and 958 years for the 2000-year and 5000-year branches of the logic tree, respectively. Lognormal uncertainty distributions in activity rate are obtained by the following steps:

Turkey Point Units 6 & 7
COL Application
Part 2 — FSAR

1. Invert the mean recurrence intervals to get mean activity rates.
2. Calculate median activity rates using the mean rates and lognormal shape factors of 0.25 and 0.51 established for the 2000-year and 5000-year records, respectively.
3. Determine the lognormal distributions based on the calculated median rate and shape factors.

The lognormal distributions of activity rate can then be discretized to obtain individual activity rates with corresponding weights.

2.5.2.4.4.3 Cuba and Northern Caribbean Source Model

This subsection describes the seismic source characterization of the Cuba and northern North America-Caribbean plate boundary region. The original EPRI study did not model this region, despite the presence of major active sources (Figures 2.5.2-219 and 2.5.2-220). In order to evaluate contributions to seismic hazards from all portions of the 200-mile site region, and contributions from more distant but potentially significant seismic sources, additional seismic sources in the Cuba and northern Caribbean region are required to supplement the updated EPRI source model. This seismic source characterization is intended for use at Units 6 & 7, and is not appropriate for use at sites within Cuba or the North America-Caribbean plate boundary region.

The seismic source characterization of Cuba and the northern North America-Caribbean plate boundary region was performed through the use of a Senior Seismic Hazard Analysis Committee (SSHAC) Level 2 process. This process involves input from recognized experts and a Technical Integrator (TI) committee to characterize specific seismic source parameters and associated parametric uncertainty and to develop an overall regional seismic source model that effectively captures the hazard contributed from each seismic source (Reference 318). A SSHAC Level 2 study is required to develop a seismic source model because there is no seismic source model approved by the NRC (e.g., EPRI) that covers the Cuba and northern North America-Caribbean plate boundary region. The SSHAC process has been approved by the NRC in RG 1.208 as an acceptable approach for developing a seismic source model outside the CEUS. A SSHAC Level 2 study is a satisfactory level of effort for the following two reasons:

Turkey Point Units 6 & 7
COL Application
Part 2 — FSAR

- Cuba and the North America-Caribbean plate boundary region are located at great distances from Units 6 & 7 (>140 to 760 miles).
- A significant amount of preexisting information is available in the region to synthesize and utilize as a basis for a defensible seismic source model for use in a PSHA.

A detailed discussion of the SSHAC Level 2 process is provided in [Subsection 2.5.2.4.4.3.1](#).

The northern boundary of the new Cuba and northern Caribbean seismic source model lies north of, and roughly parallel to, northern Cuba, partially within the site region. To avoid double-counting earthquakes between the new supplemental sources described in [Subsection 2.5.2.4.4.1](#) and the new Caribbean seismic sources, the supplemental sources have all been truncated southward by the northern boundary of the new Caribbean seismic source model ([Figures 2.5.2-204 through 2.5.2-209](#)).

2.5.2.4.4.3.1 Methodology and SSHAC Level 2 Process

A SSHAC Level 2 study was performed to incorporate current literature, data, and the understanding of experts into a new Caribbean seismic source model. SSHAC ([Reference 318](#)) outlines this methodology and provides guidance on incorporating uncertainty and the use of experts in PSHA studies. The intent of the SSHAC process is to represent the range of current understanding of seismic source parameters by the informed technical community. SSHAC ([Reference 318](#)) describes four levels of study (Levels 1 through 4), in increasing order of sophistication and effort. The choice of the level of a PSHA is driven by two factors: (1) the degree of uncertainty and contention associated with the particular project, and (2) the amount of resources available for the study ([Reference 318](#)). SSHAC ([Reference 318](#), Table 3-1) suggests that a Level 2 study is appropriate for issues with “significant uncertainty and diversity,” and for issues that are “controversial” and “complex.”

The SSHAC Level 2 process utilizes an individual, team, or company to act as the TI. For this study, the TI was a team of four William Lettis & Associates, Inc., personnel (Ross Hartleb, Stephen Thompson, Roland LaForge, and Scott Lindvall). In a SSHAC Level 2 study, the TI is responsible for reviewing data and literature and contacting experts who have developed interpretations or who have specific knowledge of the seismic sources. The TI interacts with experts to identify issues and interpretations, and to assess the range of informed expert opinion.

Turkey Point Units 6 & 7
COL Application
Part 2 — FSAR

This TI team (1) compiled and reviewed literature pertaining to the geology, tectonics, and seismicity of Cuba and the Northern Caribbean, (2) contacted scientists familiar with recent and ongoing research in the study region, and (3) integrated this information to develop a seismic source characterization of Cuba and the northern North America-Caribbean plate boundary region that captures the composite representation of the informed technical community. [Table 2.5.2-214](#) provides a tabulation of the experts contacted as part of the SSHAC Level 2 process.

The Technical Advisory Group (TAG) provided participatory review for this process. TAG members include:

- Dr. Robert Kennedy (RPK Structural Mechanics Consulting)
- Dr. William McCann (Earth Scientific Consultants)
- Mr. Donald Moore (Southern Nuclear)
- Dr. J. Carl Stepp (Earthquake Hazards Solutions)
- Dr. Robert Youngs (AMEC Geomatrix)

The experts listed in [Table 2.5.2-214](#) were provided with a standard questionnaire pertaining to key issues regarding seismic sources in Cuba and the northern Caribbean. This survey was not a formal process of expert interrogation to obtain from each expert all of the specific parameters and weights to be used in the model. Instead, the experts were allowed to speak to their own areas of expertise. It was then the TI's responsibility to combine these responses with data from the published literature to capture the range of expert opinion and judgment regarding parameters and weights to be used in the seismic source model.

The seismic source model presented herein represents a composite of the TI's assessment of the interpretations of informed expert opinion regarding seismic sources in Cuba and the northern Caribbean. The seismic source model parameters for geometry, Mmax, and recurrence of Mmax reflect the TI's assessment of the range of expert interpretations.

There are many earthquake catalogs that list historical and instrumental earthquakes within portions of the North America-Caribbean plate boundary region, but no single earthquake catalog includes sufficient coverage for assessing earthquake occurrence within this region. Data were compiled from regional and global catalogs into the Phase 2 seismicity catalog that covers the

region 100°W to 65°W, and 15°N and 24°N for all time through mid-March 2008 (Figure 2.5.2-221). Subsection 2.5.2.1.3 describes in detail the development of the Phase 2 seismicity catalog. The Phase 2 seismicity catalog, along with earthquake descriptions from the published literature, was used to constrain maximum magnitude estimates for seismic sources within the Cuba and northern North America-Caribbean plate boundary region.

2.5.2.4.4.3.2 Geologic, Tectonic, and Seismic Setting

This subsection provides overviews of the geologic, tectonic, and seismic settings of the Cuba and northern Caribbean plate boundary region. This region, which is defined as the area between about 70°W and 92°W longitude and 15°N and 24°N latitude, is geologically, tectonically, and seismically diverse. The region contains continental and oceanic crustal elements that record the breakup and disruption of Pangaea in latest Triassic time and eastward drift of the Caribbean plate with respect to North America starting in the Cretaceous Period (Reference 266). Present-day major plate boundary structures, namely left-lateral strike-slip and thrust or reverse faults, form a zone up to 150 miles wide and accommodate most of the relative plate motion and historical seismic moment release (References 230 and 285). Domains distant from active plate boundary structures are observed to have low strain rates and/or low rates of historical seismicity.

2.5.2.4.4.3.2.1 Geologic Setting

The Cuba and northern North America-Caribbean plate boundary region (Figure 2.5.2-219) includes ancient and modern geologic structures that have accommodated strike-slip and oblique-slip block motion, subduction, continental and ocean arc volcanism, and overthrusting and suturing (References 258, 301, and 302). The current plate boundary configuration has persisted since about 50 million years ago, with the following major features: (1) collision between the Caribbean plate and the Bahama platform/North American plate, (2) initiation and development of the mid-Cayman spreading center and Cayman trough, (3) development of major left-lateral faults east and west of the mid-Cayman spreading center, and (4) initiation and development of the Middle America subduction zone (References 301 and 326).

Prior to about 50 million years ago, the northern Caribbean-North American plate boundary was formed on structures north of the present-day Cayman trough. Attenuated North American-affinity rocks, volcanoclastic foreland strata, and ophiolitic assemblages in Cuba record overthrusting of North American crust in Paleocene time and cessation (suturing) in the Eocene along the Nortecubana

and subparallel faults (Reference 303) (Figure 2.5.2-219). The northwest-southeast trending Nortecubana fault and similar contractional structures within Cuba and the Greater Antilles thus represent the ancestral leading edge and northeastern boundaries of the Caribbean plate. The northwestern plate boundary juxtaposed rocks of the Caribbean plate with continental rocks of the Yucatan block on structures located from the northern tip of Cuba westward and southwestward to offshore of the eastern coast of the Yucatan peninsula. Accordingly, Johnston et al. (Reference 268) delineate the boundary between stable continental region and non-stable continental region crust to the north and south of this early Cenozoic plate boundary, respectively.

The northern plate boundary and the leading edge of the Caribbean plate has shifted south since the Paleocene, probably in a series of southward steps that involved formation and abandonment of left-lateral strike-slip faults (Reference 276, Figure 36). As collision of arc-related rocks at the leading edge of the plate against thicker crust of the Bahama platform continued, new, more favorably oriented strike-slip faults formed across the Yucatan basin and central and southern Cuba. In Middle Eocene to Oligocene time, collision ended in central Cuba contemporaneous with locking of the Nortecubana fault suture. The Cayman trough fault system and mid-Cayman spreading center nucleated as the overriding Caribbean plate rotated clockwise towards a more eastward direction. The formation of the new strike-slip faults created small microplates in the Yucatan basin that eventually transferred crust from the Caribbean to the North American plate as more of the leading edge of Cuba locked and sutured. This process of microplate formation and migration of the northern plate boundary to the south explains the major crustal faults identified on Cuba that can be grouped into: (1) west to northwest-trending sutures, and (2) east-northeast-trending transcurrent faults that cut the sutures (Reference 254) (Figure 2.5.2-220). The process of microplate formation and transfer of Caribbean crust to North America is continuing today with the Gonâve microplate situated east of the mid-Cayman spreading center (Reference 276) (Figure 2.5.2-219).

2.5.2.4.4.3.2.2 Tectonic Setting

The Caribbean plate is presently moving relative to the North America plate at a rate of about 18 to 20 millimeters/year along an ~075° azimuth (References 230, 231, and 274). In the Cuba and northern North America-Caribbean plate boundary region, the relative plate motion is accommodated by the mid-Cayman spreading center and several subvertical, left-lateral transform faults extending from offshore of the northern coast of Honduras eastward through the Cayman trough and through the islands of Jamaica and Hispaniola. The Cayman

spreading center itself is located southwest of the Cayman Islands and is characterized by a north-south-trending axis of spreading with an average rate of ~15 millimeters/year since about 25 to 30 Ma (Reference 311). The 60-mile-wide, 700-mile-long, and 3-mile-deep Cayman trough, a pull-apart basin formed at the transform-ridge-transform boundary, bounds the major plate boundary faults that accommodate left-lateral Caribbean-North American relative plate motion. The Cayman trough consists of thin, warm oceanic crust and highly attenuated continental crust (Reference 326). West of the Cayman trough, Caribbean-North American plate motion is accommodated offshore on the left-lateral Swan Islands fault (Figure 2.5.2-219). East of the Cayman trough, on Hispaniola, the orientation of the plate-bounding structures changes from plate-motion parallel to oblique, and motion is partitioned between strike-slip faults (e.g., Septentrional and Enriquillo faults), minor oblique-reverse faults, and subduction on low-angle thrust faults (e.g., Northern Hispaniola thrust fault) (References 234, 238, and 276). Farther east, at the longitude of Puerto Rico, south-dipping subduction of North American crust at the Puerto Rico trench and north-dipping subduction of Caribbean crust at the Muertos trough accommodate relative plate motion with a highly oblique sense of shear (Figure 2.5.2-219).

Major plate boundary faults accommodating Caribbean-North American relative plate motion in the Cuba and northern North America-Caribbean plate boundary region can be divided into faults west and east of the mid-Cayman spreading center (Figure 2.5.2-219). West of the spreading center, major plate boundary faults includes the Swan Islands fault located offshore the northern coast of Honduras and eastward to the southern end of the mid-Cayman spreading center (Reference 310).

East of the spreading center, major plate boundary faults extend eastward from the northern and southern limits of the spreading center axis. These subparallel faults and the spreading center axis bound the Gonâve microplate to the north, south, and west, respectively. Major faults east of the spreading center that form the northern boundary of the Gonâve microplate include the:

- Oriente fault, from the mid-Cayman spreading center to offshore the southern coast of Cuba (Reference 221)
- Septentrional fault, from the Windward Passage across northern Hispaniola to the Mona Passage (Reference 275)
- Northern Hispaniola fault, offshore the eastern tip of Cuba to offshore Puerto Rico (References 234 and 236)

Major faults east of the Mid-Cayman spreading center that form the southern margin of the Gonâve microplate include the:

- Walton fault, from the Cayman spreading center to offshore Jamaica (Reference 310)
- Duanvale fault and smaller faults in northern Jamaica (Reference 335)
- Plantain Garden fault and smaller faults in southern and eastern Jamaica (Reference 335)
- Enriquillo fault from offshore Jamaica to southern Hispaniola (Reference 271)
- Muertos trough, the subduction zone offshore southeastern Hispaniola and southern Puerto Rico (Reference 238)

The structures listed above are described in more detail in Subsection 2.5.2.4.4.3.2.5. Faults considered in the seismic source model are parameterized in Subsection 2.5.2.4.4.3.3.

2.5.2.4.4.3.2.3 Seismicity

As shown by the Phase 2 seismicity catalog for the study region, the distribution of small and large historical earthquakes in the Cuba and northern North America-Caribbean plate boundary region is highly nonuniform (Figure 2.5.2-221). In general, both small earthquakes measured since the mid-20th century and large earthquakes recorded over the last ~400 years are concentrated along the currently active boundary between the Caribbean and North America plates (References 281 and 285). Areas with higher rates of seismicity coincide with plate boundary faults, including the Swan Islands fault, the eastern part of the Oriente fault, the Septentrional and Northern Hispaniola faults, and the southern boundary of the Gonâve microplate between the eastern portion of the Walton fault and the end of the Enriquillo fault on Hispaniola. Other plate boundary faults, including the western portions of the Oriente and Walton faults and the mid-Cayman spreading center, are associated with lower rates of historical seismicity and moderate-magnitude earthquakes (Reference 331).

Other areas distant from major plate boundary faults but showing historical seismicity include (a) the area of extended continental crust between Jamaica, southern Cuba, and western Hispaniola; (b) the Nicaragua rise southwest of Jamaica; and (c) Cuba (References 254 and 255). Elsewhere away from plate

Turkey Point Units 6 & 7
COL Application
Part 2 — FSAR

boundary faults, including the Yucatan basin north of the Cayman trough and the Bahama platform north of Cuba and Hispaniola, the rates of seismicity are low.

Hypocenters and focal mechanisms of historical earthquakes provide information on fault geometry, crustal thickness, and fault kinematics throughout the Cuba and northern North America-Caribbean plate boundary region. The Cayman trough and western Hispaniola are characterized by shallow (crustal) seismicity with most focal mechanisms consistent with left-lateral strike slip on east-west striking vertical faults (References 281, 285, and 331). Shallow seismicity in Jamaica is associated with strike-slip, oblique, and reverse focal mechanisms accommodating left-lateral shear across east-west and west-northwest-striking faults (Reference 229). Seismicity along the Oriente fault changes along strike south of Cuba as focal mechanisms show strike-slip and oblique-normal movement near the Cabo Cruz basin and strike-slip to north-dipping reverse motion trends associated with the Santiago deformed belt (Reference 286). Shallow- to intermediate-depth seismicity defines south-dipping planes associated with the Northern Hispaniola fault and Puerto Rico trench, with shallow focal mechanisms consistent with underthrusting of North American crust beneath the Caribbean on gently dipping planes (Reference 236). A north-dipping zone of seismicity from shallow to intermediate crustal depths is associated with the Muertos trough (Reference 236).

The thickness of the seismogenic crust in the Cuba and northern North America-Caribbean plate boundary region is highly variable. Gravity data suggest the crust beneath the Cayman trough is about 2 to 6 kilometers thick (about 1 to 4 miles thick) up to 230 miles east of the mid-Cayman spreading center and about 5.5 kilometers thick (about 3.5 miles) up to 270 miles west of the spreading center (Reference 326). Crustal thicknesses reach values greater than 15 kilometers (9 miles) beyond about 300 miles from the spreading center. Calculated focal depths of intermediate to large earthquakes near the mid-Cayman spreading center are 8 to 12 kilometers (5 to 7.5 miles) (Reference 331), although these depths rely on simplified velocity models. Moderate to large events beneath and southwest of Jamaica commonly have focal depths between 15 and 25 kilometers (9 and 16 miles) and up to 30 kilometers (19 miles) (References 229 and 331). Thick seismogenic crust is also documented beneath southern Cuba, with abundant seismicity down to 30 kilometers (19 miles) depth and common earthquakes above 60 kilometers (37 miles) depth on the Santiago deformed belt (References 286 and 327).

2.5.2.4.4.3.2.4 Historically Significant Earthquakes

Large to great, damaging earthquakes have been recorded in the northern North America-Caribbean plate boundary region since the 16th century after the arrival of Europeans in the Greater Antilles (References 254, 281, and 282). Table 2.5.2-215 shows significant historical earthquakes of magnitude roughly greater than or equal to 6.75 in the region, and additional earthquakes within Cuba of MMI VIII or greater or magnitude 6.2 or greater. (Note: Earthquake literature commonly refers to 'magnitude' without specific reference to the magnitude type. In such referenced instances herein, unspecified type magnitude is symbolized by 'M', where the value may differ from that tabulated in Table 2.5.2-203.) Earthquakes of estimated magnitude greater than or equal to 8 have occurred on the Swan Islands fault (possibly in November 1539 and August 1856), on the Muertos trough (in October 1751), on the Septentrional fault (in May 1842), and on the Northern Hispaniola fault (in August 1946) (References 236 and 282). Every major active plate boundary fault in the northern North America-Caribbean plate boundary region has experienced at least one earthquake of estimated magnitude 7 or greater, and several faults have produced multiple ruptures and significant earthquakes. The mid-Cayman spreading center has produced at least three historical earthquakes of estimated magnitude between 6.0 and 6.5 (June 1925 M 6.2; December 1954 M 6.2; July 1962 M 6.1) (Reference 331), but no earthquakes of M_w 6.6 or larger have occurred on the spreading center or on the Oriente fault, Walton fault, or Swan Islands fault within 185 miles of the spreading center. The island of Cuba has experienced at least three significant earthquakes that nucleated below or near the island north of the active plate boundary: in 1551 (MMI VIII), January 1880 (MMI VIII and M 6.0-6.6), and February 1914 (M 6.2) (References 226 and 254). Six additional M 6.6 to M 7.1 events (in August 1578, February 1678, June 1766, August 1852, February 1932, and August 1947) probably occurred offshore southern Cuba, presumably on the Oriente fault and Santiago deformed belt (References 226, 254, and 331).

2.5.2.4.4.3.2.5 Regional Plate Boundary Elements

The tectonic elements within the Cuba and northern North America-Caribbean plate boundary region are potential sources of ground motion at Units 6 & 7. These tectonic elements are grouped below as specific faults, fault systems, or regions of similar or shared tectonic history and/or activity. This following discussion emphasizes tectonic elements that are either (a) capable of generating large to great earthquakes (i.e., $M \sim 7.5$ or greater) and/or (b) within the 200-mile site region. The discussion also provides justification for omitting other seismic

Turkey Point Units 6 & 7
COL Application
Part 2 — FSAR

sources in the Cuba and northern North America-Caribbean plate boundary region from consideration for seismic hazard to Units 6 & 7.

Cuba — The island of Cuba and areas directly offshore define a geologically diverse region that has undergone Cretaceous to early Cenozoic folding and Eocene to Holocene post-deformational sedimentation. The fold belt incorporates continental (platform and slope deposits) and oceanic (ophiolite and volcanic arc) crustal elements and syn-deformational strata that are cut by Cenozoic faults ([Reference 312](#)). Several faults onshore and directly offshore have been included in past seismic source characterizations of Cuba ([References 226](#) and [254](#)). Significant faults within Cuba include east-northeast-trending strike-slip faults and east-west- or west-northwest-trending sutures or former thrust faults that are commonly cut by the strike-slip faults ([Reference 254](#)) ([Figure 2.5.2-220](#)).

The current kinematics of crustal deformation and faulting in Cuba are poorly constrained. Geodetic data from the regional GPS network clearly show that the current plate boundary is mostly south of Cuba, coincident with the Oriente and Plantain Garden-Enriquillo fault systems that border the Gonâve microplate ([References 229](#) and [230](#)). The current orientation and rate of deformation across Cuba are unresolved, however, because few focal mechanism data exist for the island, few faults have adequate late Quaternary characterization, and the regional GPS geodetic network contains only one station in Cuba—at the southern end of the island at Guantanamo Bay (site SCUB). Site SCUB moves parallel to the Oriente fault zone at a rate of about 3 millimeters/year relative to North America. The direction of motion is consistent with elastic strain accumulation across the Oriente fault zone. There is no SCUB motion orthogonal to the Oriente fault zone, which implies that there is little or no north-south strain that accumulates between SCUB and the North America plate. Motion of two sites on the Cayman Islands south of Cuba (sites GCGT and CBSB) show low velocities (<2 millimeters/year) relative to fixed North America, and comparable motion vectors as sites in southern Florida. Thus, the geodetic data demonstrate that modern strain rates across Cuba relative to North America are less than 3 millimeters/year (the velocity of site SCUB), and are probably much lower given the likelihood that the eastward component of SCUB motion is dominantly an elastic response to coupling and strain accumulation on the adjacent Oriente fault.

Despite the recognition of several major crustal faults on Cuba, none has been adequately characterized for purposes of seismic hazard analysis for the Units 6 & 7 site. Several major strike-slip faults are visible from satellite photos and are associated with linear range fronts ([Reference 260](#)), and are possibly linked to large historical earthquakes (e.g., the 1880 MMI VIII earthquake on the

Pinar fault; the 1551 MMI VIII earthquake on the Cauto-Nipe fault zone) (Reference 254). However, none have been characterized with a late Quaternary slip rate, or have clear data to constrain timing or recurrence of large earthquakes (Reference 226). In addition, a paucity of detailed geologic maps of Cuba makes it difficult to assess geometries and potential segmentation of faults. In recognition of this, Garcia et al. (Reference 255) departed from their 2003 fault model to a regional zonation model in their updated PSHA of Cuba. Because of this lack of characterization, and the evidence from the geodetic data that all of Cuba is associated with low deformation rates compared to the plate boundary, Cuba and its direct offshore region is modeled as a single area source. The parameters for the Cuba area source are developed in Subsection 2.5.2.4.4.3.3.

Oriente Fault Zone — The Oriente fault is a left-lateral transform fault that forms the northern boundary of the Gonâve microplate and extends for more than 500 miles from the southeastern tip of Cuba westward to the northern tip of the mid-Cayman spreading center (Figure 2.5.2-219) (References 221, 285, 310, and 326). To the east, the Oriente fault connects to the Septentrional fault in the Windward Passage. The slip rate on the Oriente fault is determined by subtracting the ~7–11 millimeters/year rate of Gonâve-Caribbean relative motion measured in Jamaica (Reference 229) and Haiti from the entire 18–20 millimeters/year North America-Caribbean plate motion (Reference 230). This yields a slip rate on the Oriente fault between about 8 and 13 millimeters/year, with a best estimate of 11 millimeters/year.

The structural complexity and historical seismicity of the Oriente fault changes character along strike and forms the basis of a division into western and eastern sections (Figure 2.5.2-219). The western Oriente fault extends from the mid-Cayman spreading center to the southern tip of Cuba and the offshore Cabo Cruz basin. This section of the fault is characterized by a simple, linearly continuous expression on the seafloor trending almost exactly parallel to relative Caribbean-North America plate motion (References 221, 230, and 310). Seismicity on the western Oriente fault is less frequent than on other areas of the plate boundary, including on the eastern Oriente fault. Most seismicity has been localized on the Cabo Cruz pull-apart basin, which is associated with left-lateral strike-slip-normal oblique motion (References 286 and 331). The largest historical earthquakes on the western Oriente fault are the May 1992 M 6.8-7.0 event on the Cabo Cruz basin and the February 1917 M 7.0-7.1 event that occurred offshore the southern tip of Cuba (References 254, 282, and 331). A magnitude 6.2 event in 1962 on the western Oriente fault adjacent to the Cayman spreading center is the largest historical event west of the Cabo Cruz basin and shows pure left-lateral strike-slip

motion (Reference 331). It is unclear if the low seismicity rate on the western Oriente fault west of the Cabo Cruz basin indicates it is fully locked, or if it is mostly unlocked and sliding at a relatively uniform rate. As mentioned previously, the crust of the Cayman trough that constitutes the southern block of the Oriente fault is anomalously thin (2 to 6 kilometers or 1 to 4 miles) for distances up to 200 miles or more from the mid-Cayman spreading center (Reference 326), which probably limits the seismogenic thickness of the western Oriente fault. A low coupling of the western Oriente fault west of the Cabo Cruz basin would be consistent with oceanic transform faults worldwide, for which up to 95 percent of total slip is released aseismically (Reference 299).

The eastern Oriente fault extends along southern Cuba and is characterized by a zone that includes: (a) segmented, discontinuous, and probably vertical strike-slip faults and (b) more continuous, steeply north-dipping faults of the Santiago deformed belt south of the strike-slip faults (Reference 221). The eastern Oriente fault is characterized by more intense seismic activity than the western Oriente fault (Figures 2.5.2-219 and 2.5.2-221), with focal mechanisms indicating strike-slip, oblique, and reverse mechanisms (References 286 and 331). Seismicity depths reach 70 kilometers (45 miles) beneath southern Cuba associated with the Santiago deformed belt, indicating a thick seismogenic crust that contrasts with the thin crust of the western Oriente fault (Reference 286). The seismic moment release of historical large earthquakes is consistent with the ~11 millimeters/year slip rate on the Oriente fault determined by GPS (References 222 and 299), indicating that the plate interface there is fully locked (Reference 273).

For purpose of characterizing earthquake hazards to the Units 6 & 7 site in southern Florida, the Oriente fault zone is modeled as two sources coinciding with the western and eastern Oriente fault sections. Parameters including slip rate, rupture length and area, and maximum magnitude for each section are presented in Subsections 2.5.2.4.4.3.3.2 and 2.5.2.4.4.3.3.3.

Septentrional Fault — The Septentrional fault is a left-lateral strike-slip fault that extends for about 650 miles from the Windward Passage between Hispaniola and Cuba to the Mona Passage offshore north of Puerto Rico (Figure 2.5.2-219) (Reference 238). In the Windward Passage offshore northwest Hispaniola, the Septentrional fault merges westward with the Oriente fault (References 222 and 238). The offshore expression of the fault is linear and continuous and projects directly to the onshore portion of the fault in Hispaniola (Reference 222). Surface mapping of the Septentrional fault shows multiple parallel surface traces that are delineated by prominent scarps in alluvium, lineaments, and offset geomorphic features.

Turkey Point Units 6 & 7
COL Application
Part 2 — FSAR

Together with the gently south-dipping Northern Hispaniola fault (discussed below), the Septentrional fault represents a classic example of strain partitioning along an obliquely convergent margin (References 234 and 273). Slip rate estimates for the Septentrional fault vary, but indicate that the Septentrional fault accommodates a significant percentage of the total North America-Caribbean plate boundary strain. Using offset geomorphic features in Hispaniola dated by radiocarbon, Holocene slip rate estimates range from 13 ± 4 millimeters/year (Reference 275) to 9 ± 3 millimeters/year (Reference 304). Simple elastic strain models by Dixon et al. (Reference 233) using GPS data predict a slip rate of 8 ± 3 millimeters/year for the Septentrional fault. Based on assessment of previous studies, Mann (Reference 274) suggests a best estimate of 6 to 12 millimeters/year for slip on the central Septentrional fault.

Regions of strong shaking associated with historical earthquakes in 1564, 1783, 1842, 1887, and 1897 are spatially associated with the Septentrional fault, suggesting that at least some of these earthquakes likely occurred on this fault (Reference 275). McCann and Pennington (Reference 281) and McCann (Reference 282) suggest that the largest historical earthquakes associated with the Septentrional fault occurred in May 1842 ($M_w \sim 8.2$) and September 1887 ($M_w \sim 7.9$) in central and western Hispaniola (Table 2.5.2-215). Mann (Reference 274) suggests that the 1842 earthquake likely occurred on the Septentrional fault in the western Cibao Valley and along the northwestern coast of Haiti. Paleoseismic studies of the central Septentrional fault indicate the most recent surface-rupturing earthquake occurred between A.D. 1040 and 1230 and involved a minimum of about 4 meters of left-lateral strike-slip and 2.3 meters of normal slip (Reference 304). Tuttle et al. (Reference 329) describe liquefaction features in the Dominican Republic that they interpret as evidence for a cluster of two to four prehistoric earthquakes of M_w 7 to 8 that likely resulted from ruptures on the Septentrional fault circa A.D. 1200. The historical and paleoseismic evidence for repeated large magnitude earthquakes on the Septentrional fault and the general agreement between geologically and geodetically determined slip rates for this fault support a fully coupled fault model.

For the purpose of characterizing earthquake hazards to the Units 6 & 7 site, the Septentrional fault is modeled as one source extending from the Windward Passage eastward across Hispaniola. Parameters including slip rate, rupture length and area, and maximum magnitude are presented in [Subsection 2.5.2.4.4.3.3](#).

Northern Hispaniola Fault — The westward continuation of the Puerto Rico trench north of Hispaniola is known by various names, including the North Hispaniola

deformed belt (References 235, 236, and 238), the Northern Hispaniola fold-thrust belt (Reference 234), and the Northern Hispaniola fault (Reference 273). This subsection adopts the name Northern Hispaniola fault for this gently south-dipping thrust system (Figure 2.5.2-219). The Northern Hispaniola fault extends offshore for roughly 500 miles from a poorly defined westward termination east of Cuba, to an equally poorly defined location about north of the Mona Passage.

Together with the left-lateral strike-slip Septentrional fault in the overriding plate, the Northern Hispaniola fault represents a classic example of strain partitioning along an obliquely convergent margin (References 236 and 273). Of the 18–20 millimeters/year Caribbean-North America relative plate motion measured by GPS geodesy, Calais et al. (Reference 220) model a fault-normal elastic strain accumulation rate on the thrust system of 5.2 ± 2 millimeters/year.

The largest historical earthquake associated with the Northern Hispaniola fault is the August 4, 1946, surface-wave magnitude (M_S) 8.1 earthquake (References 236 and 281) (Table 2.5.2-215). The focal mechanism for this event indicates thrust motion and the dimensions of the aftershock zone suggest rupture on a shallowly south-dipping plane (Reference 236). In addition to the 1946 earthquake and its aftershocks, other noteworthy historical earthquakes on the Northern Hispaniola fault include the July 29, 1943 M_S 7.5 to 7.8; April 21, 1948, M_S 7.3; and May 31, 1953, M_S 7.0 events (References 234 and 236). The 1953 earthquake occurred directly west of the patch of the fault that ruptured in the 1946 event. The 1943 and 1948 earthquakes occurred east of the 1946 rupture and east of the region considered in this report.

Segmentation of the Northern Hispaniola fault is suggested by the association between crustal structure and the aftershock zones of the large historical events in 1946 and 1953. Dolan and Wald (Reference 236) note that the western boundary of the 1946 rupture coincides with a boundary in the overriding Bahama platform and a bend in the fault at about 70°W longitude. East of the 70°W boundary, the Northern Hispaniola fault is well imaged by microseismicity dipping beneath Hispaniola and the Mona Passage, suggesting that the fault accommodates subduction of North American crust at the plate margin (Figure 2.5.2-222). This eastern portion of the Northern Hispaniola fault produced historical M 7.5-8.1 earthquakes in 1943 and 1946. West of the 70°W boundary, the Northern Hispaniola fault is poorly expressed seismically, and possibly roots at the vertical Septentrional fault beneath western Hispaniola (Figure 2.5.2-222). The largest historical earthquake on the western section of the Northern Hispaniola fault is the May 1953 M 7.0 event.

Turkey Point Units 6 & 7
COL Application
Part 2 — FSAR

For purpose of characterizing earthquake hazards to the Units 6 & 7 site, the Northern Hispaniola is modeled fault as two distinct rupture segments. The western segment extends from offshore Cuba to the eastern end of the 1953 rupture area at approximately 70°W longitude (Figure 2.5.2-223). The eastern segment extends from the western end of the 1946 rupture area eastward to the Mona Passage and the eastern boundary of the study region. Parameters including slip rate, rupture length and area, and maximum magnitude are presented in Subsection 2.5.2.4.4.3.3.

Swan Islands Fault — The Swan Islands fault is a left-lateral oceanic transform fault that extends from the southern tip of the mid-Cayman spreading center westward for roughly 450 miles where it merges with the onshore Polochic-Motagua fault system of Central America (Figure 2.5.2-219). West of the mid-Cayman spreading center, the northern margin of the Cayman trough does not appear to accommodate significant lateral relative plate motion; essentially the entire 18–20 millimeters/year North America-Caribbean plate motion is accommodated on the Swan Islands fault (References 230 and 231).

Interpretation of high-resolution sea-floor bathymetry suggests the Swan Islands fault consists of several faults that locally form restraining and releasing geometries (References 277 and 310). West of the Swan Islands, the Swan Islands fault is expressed on the sea floor as a relatively continuous lineament. The thickened crust associated with the emergent Swan Islands is associated with a roughly 20-mile-wide right step-over that forms a restraining geometry and a probable segmentation point for rupture propagation. Surrounding and east of the Swan Islands, the fault consists of one or more sections of about 60 to 120 miles in length to the eastern termination at the mid-Cayman trough. Here, the crust of the mid-Cayman trough that bounds the fault to the north is about 5.5 kilometers (3.5 miles) thick based on gravity (Reference 326).

McCann and Pennington (Reference 281) and McCann (Reference 282) note a large earthquake that occurred in August 1856 off the northern coast of Honduras that may have ruptured the western portion of the Swan Islands fault. The estimated magnitude for this event is about M 8.3 (Reference 282), based on descriptions of the event summarized by Osiecki (Reference 297) (Table 2.5.2-215). Earlier accounts of a similar great event off the northern Honduran coast suggest the possibility of a prior M ~8 event on the western Swan Islands fault in 1539 (Reference 282). The probability of at least one great historical earthquake on the western Swan Islands fault suggests the fault is fully coupled. The eastern section of the fault between the Swan Islands and the mid-Cayman spreading center is not associated with large historical earthquakes.

Turkey Point Units 6 & 7
COL Application
Part 2 — FSAR

For purpose of characterizing earthquake hazards to the Units 6 & 7 site, the Swan Islands fault is modeled as two rupture segments. The western segment extends from offshore Honduras to the Swan Islands. The eastern segment extends from the Swan Islands to the mid-Cayman spreading center. Parameters including slip rate, rupture length and area, and maximum magnitude are presented in [Subsections 2.5.2.4.4.3.3.7](#) and [2.5.2.4.4.3.3.8](#).

Walton-Plantain Garden-Enriquillo Fault System — The Walton, Plantain Garden, and Enriquillo faults are left-lateral strike-slip faults that collectively form the southern margin of the Cayman trough and Gonâve microplate from west to east ([Figure 2.5.2-219](#)). The Walton fault extends for about 185 miles eastward from the southern end of the mid-Cayman spreading center to northwestern Jamaica ([Reference 310](#)). Slip is transferred from the Walton fault across the island of Jamaica through a broad restraining bend that includes the east-west striking Duanvale, Rio Minho-Crawle River, South Coast, and Plantain Garden faults ([Reference 229](#)). The Plantain Garden fault continues eastward and connects with the Enriquillo fault offshore southwestern Haiti. The Plantain Garden-Enriquillo fault system extends for about 375 miles from southeastern Jamaica to south-central Hispaniola and terminates eastward in southern Dominican Republic east of Lake Enriquillo ([Reference 276](#)). There, slip apparently is transferred in a complex manner onto the Muertos trough.

Estimates of slip rate on the Walton-Plantain Garden-Enriquillo fault system are determined from GPS geodetic networks on Jamaica ([Reference 229](#)) and on Haiti and the Dominican Republic ([Reference 220](#)). DeMets and Wiggins-Grandison ([Reference 229](#)) present a preferred slip rate estimate for the Walton-Plantain Garden-Enriquillo fault system of 8 ± 1 millimeters/year at Jamaica, although they acknowledge an upper bound of 13 ± 1 millimeters/year. Gonâve-Caribbean plate motion is permissible if additional elastic strain energy is stored offshore. Calais reports a slip rate on the Enriquillo fault system of about 7 ± 3 millimeters/year determined through Haiti. Because it is likely that the slip rate along the entire Gonâve-Caribbean plate boundary is more or less constant, the lower rate of ~ 8 millimeters/year by DeMets and Wiggins-Grandison ([Reference 229](#)) is preferred as the best estimate slip rate for the fault system.

The Walton-Plantain Garden-Enriquillo fault system can be divided into its western portion, the Walton-Duanvale fault (extending from the Cayman spreading center to northern Jamaica), and its eastern portion, the Plantain Garden-Enriquillo fault (extending from southern Jamaica to southern Hispaniola) ([Figure 2.5.2-219](#)). The boundary between the two “segments” of the fault system is the island of Jamaica, which represents thickened crust near the tip of the

Turkey Point Units 6 & 7
COL Application
Part 2 — FSAR

Nicaragua rise where a restraining bend occurs between the Walton and Plantain Garden faults. Because many of the remaining faults within Jamaica are limited in length, it is concluded that they are not capable of generating earthquakes larger than $M\sim 7-7\frac{1}{4}$ and thus are not considered to be separate seismic sources for estimating ground motions in southern Florida. The major earthquakes that have occurred on or near Jamaica can be attributed to either the Walton-Duanvale fault zone or the Plantain Garden-Enriquillo fault. Additionally, the western and eastern division of the fault system is justified based on similarities in fault segment continuity and historical earthquake activity. The Walton fault consists of several, discontinuous faults offshore ([Reference 310](#)), whereas the Plantain Garden-Enriquillo fault forms a relatively continuous structure onshore and offshore, with a possible rupture termination point near the western tip of Haiti.

The largest historical earthquakes on the Walton-Duanvale fault zone impacted northern Jamaica in January 1907 ($M\sim 6.5-7.0$) and March 1957 ($M\sim 6.6-6.9$) ([Table 2.5.2-215](#)). No earthquakes of magnitude greater than 6.5 have occurred farther west on the Walton fault, near the thin crust of the Cayman trough near the mid-Cayman spreading center. Large earthquakes have occurred historically on the Plantain Garden-Enriquillo fault, including the destructive June 7, 1692, MMI X ($M\sim 7.5$) Port Royal earthquake on the Plantain Garden fault ([Reference 229](#) and [Reference 282](#)). The Enriquillo fault ruptured in large events in September 1751 ($M\sim 7.5$) near Port-au-Prince, Haiti and again in June 1770 ($M\sim 7.5$) farther west ([Reference 282](#)). Other large earthquakes on the Plantain Garden-Enriquillo fault system occurred in 1615, 1673, 1751, 1761, 1770, 1812, 1860, and 1941 ([References 236](#) and [281](#)), and support a model whereby the Plantain Garden-Enriquillo fault is fully coupled.

For purpose of characterizing earthquake hazards to the Units 6 & 7 site, the southern boundary of the Gonâve microplate is modeled as two rupture segments. The western segment is the Walton-Duanvale fault zone. The eastern segment is the Plantain Garden-Enriquillo fault. Although additional segmentation points are probably defensible within both of these fault sources, the faults are drawn instead as longer sources but restrict the maximum earthquake on each fault to only a portion of its total length. Parameters including slip rate, rupture length and area, and maximum magnitude are presented in [Subsection 2.5.2.4.4.3.3](#).

Muertos Trough — The Muertos trough is a 300-mile-long linear feature defined prominently in the bathymetry offshore the southern Dominican Republic and Puerto Rico ([Figure 2.5.2-219](#)) and a prominent north-dipping trend in seismicity ([Reference 236](#)). The structure accommodates underthrusting of the Caribbean

plate beneath the Puerto Rico microplate that is situated between the Muertos trough and the Puerto Rico-Northern Hispaniola subduction zone. The Muertos trough ruptured in October 1751 in a great earthquake with an estimated magnitude M 8.0 (References 236 and 282). Despite its potential for generating large to great earthquakes in the region, it is not included as a seismic source for evaluating ground motions at the Units 6 & 7 site. The omission of the Muertos trough is justified because (a) it is located roughly 850 miles from Units 6 & 7 site and (b) seismic sources capable of generating similar M 8+ great earthquakes with similar or greater frequency are located closer to Units 6 & 7 (e.g., Northern Hispaniola and Septentrional faults).

Other Tectonic Elements — Other tectonic elements in northern North America-Caribbean plate boundary region that are associated with seismicity and/or Cenozoic tectonics include: (1) the Nicaragua rise and Hess escarpment, (2) the Beata ridge, (3) the northern boundary of the Cayman trough west of the mid-Cayman spreading center, and (4) the Yucatan basin and the ancestral plate boundary zone/escarpment separating the Yucatan basin from the Maya block/Yucatan peninsula. All these features are probably capable of earthquakes of magnitude M ~7, similar to the April 1941 M 7 earthquake on the Nicaragua rise southwest of Jamaica (References 282 and 331). However, all these features are distant from southern Florida (all greater than 200 miles, some greater than 400 miles), all have low strain rates compared to the plate boundary faults (e.g., Reference 230), and all have comparable or lesser magnitude potential than plate boundary faults or source areas (i.e., Cuba) that are closer to Units 6 & 7. On this basis, these other tectonic elements are not considered in the characterization of potentially significant sources of ground motion at the Units 6 & 7 site.

2.5.2.4.4.3.3 Seismic Source Characterization

Seismic sources for Cuba and the North America-Caribbean plate boundary region are separated into two categories: a single area source (for the island of Cuba) and nine line sources (for major plate boundary faults) (Figure 2.5.2-224). The area source zone is characterized with a maximum magnitude (M_{max}) earthquake distribution determined by historical seismicity, published values, fault lengths, and our assessment of the range of informed technical opinion. An exponential recurrence model describes M_{max} earthquake behavior for the area source, with calculated recurrence parameters (a- and b-values) based on observed seismicity.

For Cuba, which is partially inside the 200-mile site region, a simple model is preferred because of the lack of knowledge about fault behavior and slip rates for

Turkey Point Units 6 & 7
COL Application
Part 2 — FSAR

Cuban faults. For the North America-Caribbean plate boundary faults, simplicity is acceptable because of the distances (>420 miles) from Units 6 & 7 to the sources. Thus, simple models that consider only the largest earthquakes that may be generated, and their recurrence are most important for evaluating sensitivity of these sources to the ground-motion hazards at the site.

Major faults along the northern North America-Caribbean plate boundary are represented in the source model by line sources. Earthquake activity is modeled based on fault slip rate, effective seismic coupling (the fraction of slip rate accommodated during large, main-shock earthquakes), and Mmax. Mmax, in turn, is determined based on estimates of fault source geometry (fault length, fault width, and fault area) and published empirical relations between earthquake magnitude and fault area or earthquake magnitude and fault length.

The line sources are characterized by fault slip rate, effective seismic coupling (the fraction or ratio of slip rate accommodated during large, main-shock earthquakes), and Mmax, with logic trees containing values and weights that integrate findings in published literature and the informed opinions of our panel experts. The rupture model assumes pure characteristic behavior. Because the attenuation model selected does not require inputs of fault depth, dip direction, and slip type, those parameters are not reviewed here. In most cases, fault slip rate is determined from published geodetic rates using network GPS geodetic data. Seismic coupling ratios are estimated based on historical seismicity rates, published modeling experiments, analogs with similar tectonic environments, and judgment. For the two modeled thrust fault sources with non-vertical dips, earthquakes are assumed to occur on the fault's surface trace. This is a conservative modeling decision because the two thrust fault sources (the western and eastern portions of the Northern Hispaniola fault) dip to the south. By constraining earthquake locations to the surface traces of these two thrust faults, source-to-site distances are minimized. Mmax is determined based on consideration of historical seismicity and empirical moment-area and moment-length scaling relationships. Fault length and fault area are defined either by the total source length or, where a single source can arguably be divided into several rupture segments, the length of the longest rupture segment. For all fault sources in the model regardless of slip type, consideration is given to:

- The empirical rupture area-magnitude relation of Wells and Coppersmith ([Reference 334](#)) for all slip types.
- The empirical rupture area-magnitude relation of Wyss ([Reference 339](#)).

Turkey Point Units 6 & 7
COL Application
Part 2 — FSAR

- The rupture length-magnitude relation of Wells and Coppersmith (Reference 334) for all slip types.

For strike-slip fault sources in the model, additional consideration is given to the empirical rupture area-magnitude relations of:

- Hanks and Bakun (Reference 262)
- Working Group on California Earthquake Predictions (WGCEP) (Reference 337)

For subduction zone fault sources in the model (i.e., western and eastern portions of the Northern Hispaniola fault), additional consideration is given to:

- The empirical rupture area-magnitude relation of Abe (References 201 and 202).
- The empirical rupture area-magnitude relation of Geomatrix (Reference 257).
- The empirical rupture length-magnitude relation of Geomatrix (Reference 257).

Table 2.5.2-216 presents a summary of these empirical relations. The range of results from the various empirical relations guided selection of the final magnitudes and weights on the logic trees. Table 2.5.2-217 presents a summary of source parameters for the ten seismic sources in the model. Geographic coordinates of the area source and line sources are presented in Tables 2.5.2-218 and 2.5.2-219, respectively.

The seismic source model presented in this subsection is relatively simple with respect to source geometries and earthquake occurrence (only Mmax earthquakes are considered). This reflects the intention of the source model to capture the contribution to ground motions at the site due to large-magnitude earthquakes on distant sources.

2.5.2.4.4.3.3.1 Cuba

The single area source representing Cuba (Figure 2.5.2-224) encompasses the major tectonic elements on the island and the majority of the historical seismicity. The northern and eastern boundary of the source zone is drawn near the base of the submarine escarpment that marks the location of the Nortecubana fault suture and the geologic boundary between the relatively undeformed North American

Turkey Point Units 6 & 7
COL Application
Part 2 — FSAR

crust of the Bahama platform and the highly attenuated crust of the former leading edge of the plate boundary zone. A buffer zone of 12.5 miles from the base of the escarpment toward the north and east was added to the area source. This buffer was added to account for poorly located earthquakes that probably occurred within the Cuba island arc region and/or a zone of fractured and faulted crust beyond the suture zone that formed during early Cenozoic subduction. The western boundary of the Cuba area source is based on bathymetry and the locations and density of historical seismicity. This boundary approximately follows the boundary between the Yucatan basin and the continental shelf surrounding Cuba. The southern boundary of the Cuba source zone coincides with the southern boundary of Cuba and the steep submarine escarpment that borders the Oriente fault. At closest approach, the Cuba area source is located about 140 miles from the site.

Table 2.5.2-217 summarizes source parameters for the Cuba area source zone. The distribution of Mmax shows equal weight to branches with $M_w = 7.0$ and $M_w = 7.25$. This magnitude distribution is larger than the maximum instrumented earthquake in the catalog (February 1914 $M_w \sim 6.3$) and larger than the maximum historical earthquake (January 1880 $M_w \sim 6.1$) (**Table 2.5.2-215**). Our Mmax distribution is consistent with a recently published source model for Cuba (**Reference 254**) that shows a Mmax upper limit of $M_S 7.0$ for intraplate Cuba sources. The Garcia et al. (**Reference 254**) study is based on previous source characterizations of Cuba's historical seismicity, and assessment of fault capability. Garcia et al.'s study (**Reference 255**) assigns $M_S 6.5$ to their intraplate Cuba zone. The $M_w 7$ to 7.25 range of Mmax for Cuba presented herein is consistent with rupture lengths of about 50 to 80 kilometers and rupture thicknesses of about 12 to 18 kilometers. These rupture dimensions are reasonably conservative given the lengths of major crustal faults in Cuba such as the Pinar, Nortecubana, and Cauto-Nipe faults (**Reference 226**) and estimates of Cuban crustal thickness (**Reference 327**).

The island of Cuba is represented in the model as an area source zone, with catalog seismicity representing earthquake activity. Earthquake rates within the area source are determined from an analysis of completeness and an evaluation of earthquake magnitude-frequency for the source zone, and a Gutenberg-Richter relation is tested and represented by the parameters a-value and b-value. Maximum magnitude values for Cuba are based on previous Cuba source models, historical seismicity, published literature, and an assessment of fault capability.

2.5.2.4.4.3.3.2 Oriente Fault — Western

At closest approach, the western Oriente fault source is located about 420 miles from Units 6 & 7 (Figure 2.5.2-224). Table 2.5.2-217 summarizes source parameters for this fault source. The slip rate distribution [and weights] for the western Oriente fault is 8 [0.1], 11 [0.7], and 13 [0.2] millimeters/year based on the GPS results of DeMets et al. (Reference 230) and DeMets and Wiggins-Grandison (Reference 229). The significant weight (0.4) given to seismic coupling ratios less than 1.0 is based on the thin, warm crust of the Cayman trough that typifies the south side of the fault for most of its length (Reference 326), low seismic coupling ratios noted globally for oceanic transform faults (Reference 299), and the lack of large earthquakes historically (Table 2.5.2-215). Higher weights on low seismic coupling ratios are judged to be under-conservative for purposes of evaluating ground motions at the site.

The Mmax distribution [and weights] for the western Oriente fault is M_w 7.5 [0.3], 7.7 [0.4], and 8.0 [0.3] (Table 2.5.2-217). These values are based on rupture dimensions 300 to 490 kilometers long and 6 to 10 kilometers wide. Values higher than M_w 8.0 are obtained using empirical magnitude-rupture length relations for lengths greater than about 300 kilometers. However, these higher values are rejected given the recognition that longer rupture lengths involve very warm and thin crust near the mid-Cayman spreading center. The Mmax distribution exceeds the historical maximum magnitude earthquakes recorded near the eastern portion of this source in 1917 (M_w 7.2) and 1992 (M_w 6.8) (Subsection 2.5.2.1.3).

2.5.2.4.4.3.3.3 Oriente Fault — Eastern

At closest approach, the eastern Oriente fault source is located about 445 miles from Units 6 & 7 (Figure 2.5.2-224). Table 2.5.2-217 summarizes source parameters for this fault source. The slip rate distribution and weighting for the eastern Oriente fault are identical to the western Oriente fault source. The seismic coupling ratio on the eastern Oriente fault is assigned a value of 1.0 given the repeated large earthquakes on the fault historically (Table 2.5.2-215).

The Mmax distribution [and weights] for the eastern Oriente fault is M_w 7.5 [0.2], 7.7 [0.6], and 7.9 [0.2] (Table 2.5.2-217). These values are based on rupture dimensions about 140 to 200 kilometers long (from mapped segments on the Oriente fault and Santiago deformed belt in Reference 222) and 15 to about 40 kilometers wide. Values higher than M_w 7.9 are obtained using the empirical strike-slip magnitude-area relations of Hanks and Bakun (Reference 262) and WGCEP (Reference 338) for rupture widths greater than about 20 kilometers.

These higher values are not used given the recognition that rupture dimensions involving widths greater than 20 kilometers would likely occur on the Santiago deformed belt with a strong reverse-oblique component, and this style of faulting is not captured in the strike-slip empirical databases. Instead, empirical values for the “all slip type” relation of Wells and Coppersmith (Reference 334) that yields an upper limit of M_w 7.9 are preferred for the larger rupture dimensions. The M_{max} distribution exceeds the historical maximum magnitude earthquake of M_w 7.53 in June 1766 (Table 2.5.2-215).

2.5.2.4.4.3.3.4 Septentrional Fault

At closest approach, the Septentrional fault source is located about 545 miles from Units 6 & 7 (Figure 2.5.2-224). Table 2.5.2-217 summarizes source parameters for this fault source. The slip rate distribution [and weights] for the Septentrional fault is 6 [0.2], 9 [0.6], and 12 [0.2] millimeters/year based on the geologic slip rate of Prentice et al. (Reference 304) and GPS-based results of Manaker et al. (Reference 273). The seismic coupling ratio on the Septentrional fault is assigned a value of 1.0 given the repeated large to great earthquakes on the fault historically (Table 2.5.2-215).

The M_{max} distribution [and weights] for the Septentrional fault is M_w 8.0 [0.5] and 8.25 [0.5] (Table 2.5.2-217). These values are based on the magnitude estimates of the historical 1842 rupture (Table 2.5.2-215). Equal weight is given to the lower magnitude estimate for this earthquake partially based on recognizing that strike-slip earthquakes greater than magnitude M_w 7.9 to 8.0 are exceedingly rare in the instrumental record globally. These values are consistent with rupture dimensions of about 350 kilometers long and 15 to 18 kilometers wide.

2.5.2.4.4.3.3.5 Northern Hispaniola Fault — Western

At closest approach, the western Northern Hispaniola fault source is located about 550 miles from Units 6 & 7 (Figure 2.5.2-224). Table 2.5.2-217 summarizes source parameters for this fault source. The slip rate distribution [and weights] is 4 [0.2], 6 [0.7], 8 [0.1] millimeters/year based on the GPS results of Calais et al. (Reference 220) and Manaker et al. (Reference 273). The source is modeled with a seismic coupling ratio of 1.0 based on goodness-of-fit with elastic block and fault modeling (Reference 273).

The M_{max} distribution [and weights] for the western portion of the Northern Hispaniola fault is M_w 7.8 [0.2], 8.0 [0.6], and 8.3 [0.2] (Table 2.5.2-217). These values are based on rupture dimensions of 200 to 350 kilometers long and 30 to

60 kilometers wide (assumed locking depth of 12 to 20 kilometers and fault dip of 20° to 25°). The Mmax distribution exceeds the historical maximum magnitude earthquake of M_w 6.93 in May 1953 recorded at the eastern end of this source (Table 2.5.2-215). Earthquakes on the south-dipping western Northern Hispaniola fault conservatively are assumed to occur on the fault's surface trace.

2.5.2.4.4.3.3.6 Northern Hispaniola Fault — Eastern

At closest approach, the eastern Northern Hispaniola fault source is located about 760 miles from Units 6 & 7 (Figure 2.5.2-224). Table 2.5.2-217 summarizes source parameters for this fault source. The slip rate distribution and weighting for the eastern fault source are identical to the western fault source. Similarly, the seismic coupling ratio on the eastern portion of the Northern Hispaniola fault is 1.0 given the modeling results of Manaker et al. (Reference 273) and the historical great earthquake on the fault in August 1946 (Table 2.5.2-215).

The Mmax distribution (and weights) for the eastern Northern Hispaniola fault is M_w 8.0 [0.2], 8.3 [0.6], and 8.6 [0.2] (Table 2.5.2-217). These values are based on the 1946 M_w 7.90 historical event and rupture dimensions about 200 to 400 kilometers long and 50 to about 100 kilometers wide (assumed locking depths of 20 to 35 kilometers and fault dip of 20° to 25°). Earthquakes on the south-dipping eastern Northern Hispaniola fault conservatively are assumed to occur on the fault's surface trace.

2.5.2.4.4.3.3.7 Swan Islands Fault — Western

At closest approach, the western Swan Islands fault source is located 620 miles from Units 6 & 7 (Figure 2.5.2-224). Table 2.5.2-217 summarizes source parameters for this fault source. The slip rate distribution [and weights] is 18 [0.2], 19 [0.6], and 20 [0.2] millimeters/year based on the GPS-derived relative plate motion rate of DeMets et al. (Reference 230). The seismic coupling ratio on the western Swan Islands fault is assigned a value of 1.0 given the possible repeated great earthquakes on the fault historically (Table 2.5.2-215).

The Mmax distribution [and weights] for the western Swan Islands fault is M_w 7.8 [0.2], 8.0 [0.7], and 8.3 [0.1] (Table 2.5.2-217). These values are based on the magnitude estimate of the historical 1856 earthquake (Table 2.5.2-215). These values are consistent with rupture dimensions of about 350 to 500 kilometers long and 10 to 15 kilometers wide. The low weight assigned to the historical estimate of M 8.3 is based on recognizing that strike-slip earthquakes greater than magnitude M_w 7.9 to 8.0 are exceedingly rare in the instrumental record globally, and that

only the largest rupture dimensions considered for the western Swan Islands fault source results in an empirical estimate of M_w 8.3.

2.5.2.4.4.3.3.8 Swan Islands Fault — Eastern

At closest approach, the eastern Swan Islands fault source is located 540 miles from Units 6 & 7 (Figure 2.5.2-224). Table 2.5.2-217 summarizes source parameters for this fault source. The slip rate distribution and weighting are identical to the western Swan Islands fault source. The significant weight of 0.4 to seismic coupling ratios less than 1.0 is based on the thin, warm crust of the Cayman trough that typifies the north side of the fault source for most of its length (Reference 326), low seismic coupling ratios noted globally for oceanic transform faults (Reference 299), and the lack of large earthquakes historically (Table 2.5.2-215). Placing higher weights on low seismic coupling ratios was judged to be under-conservative for purposes of evaluating ground motions at the site.

The M_{max} distribution [and weights] for the eastern Swan Islands fault is M_w 7.2 [0.4], 7.5 [0.5], and 7.7 [0.1] (Table 2.5.2-217). These values are based on rupture dimensions of 130 to 200 kilometers long (from mapping by Reference 310) and 8 to 15 kilometers wide. The low weight on the highest magnitude reflects the recognition that a rupture length of 200 kilometers would at least partially involve very warm and thin crust near the mid-Cayman spreading center, and thus a 15 kilometer wide average fault rupture is unlikely. No historical earthquakes greater than or equal to M_w 6.75 are recorded near this source (Table 2.5.2-215) (Reference 331).

2.5.2.4.4.3.3.9 Walton-Duanvale Fault

At closest approach, the Walton-Duanvale fault source is located 490 miles from Units 6 & 7 (Figure 2.5.2-224). Table 2.5.2-217 summarizes source parameters for this fault source. The slip rate distribution [and weights] is 6 [0.2], 8 [0.6], 10 [0.2] millimeters/year based on the GPS data of DeMets and Wiggins-Grandison (Reference 299). The weight of 0.3 for a seismic coupling ratio less than 1.0 is based on the thin, warm crust of the Cayman trough that typifies the north side of the fault for much of its length (Reference 326), low seismic coupling ratios noted globally for oceanic transform faults (Reference 299), and the lack of large earthquakes historically (Table 2.5.2-215). Placing higher weights on low seismic coupling ratios was judged to be under-conservative for purposes of evaluating ground motions at the site.

Turkey Point Units 6 & 7
COL Application
Part 2 — FSAR

The Mmax distribution [and weights] for the Walton-Duanvale fault source is M_w 7.3 [0.3], 7.6 [0.6], and 7.8 [0.1] (Table 2.5.2-217). These values are based on rupture dimensions of 140 to 215 kilometers long and 6 to 10 kilometers wide. The Mmax distribution exceeds the historical maximum magnitude earthquakes of about M_w 6.6 in January 1907 and March 1957 recorded near the eastern portion of this source (Table 2.5.2-215).

2.5.2.4.4.3.3.10 Plantain Garden-Enriquillo Fault

At closest approach, the western Plantain Garden-Enriquillo fault source is located 560 miles from Units 6 & 7 (Figure 2.5.2-224). Table 2.5.2-217 summarizes source parameters for this fault source. The slip rate distribution and weighting are identical to the Walton-Duanvale fault source. The seismic coupling ratio on the Plantain Garden-Enriquillo fault source is assigned a value of 1.0 given the repeated large earthquakes on the fault historically (Table 2.5.2-215) and the goodness-of-fit with elastic block and fault modeling (Reference 273).

The Mmax distribution [and weights] for the Plantain Garden-Enriquillo fault is M_w 7.5 [0.2], 7.7 [0.6] and 7.9 [0.2] (Table 2.5.2-217). These values are based on rupture dimensions of about 120 to 250 kilometers long (from mapping by Reference 276) and 15 to about 18 kilometers wide. The Mmax distribution is comparable to the upper estimates of historical earthquakes attributed to this source, including the June 1692 M_w 7.78, the October 1751 M_w 7.28, and the June 1770 M 7.53 events (Table 2.5.2-215).

2.5.2.4.4.4 Implementation Notes on Incorporation of New Seismic Source Parameterization into PSHA

Subsection 2.5.2.2 reviews new geological, geophysical, and seismological information related to seismic source characterization. New seismic sources (or extensions of existing seismic sources) were developed as follows:

Gulf of Mexico and Atlantic: Seismicity was added in degree cells offshore of the Florida peninsula (west in the Gulf of Mexico and east in the Atlantic), using seismicity rates smoothed over the Florida peninsula (see Figure 2.5.2-210) using the updated earthquake catalog through mid-February 2008. The completeness of earthquake catalogs offshore is problematic, and it is conservative to assume that rates of activity offshore are identical to average rates onshore. The degree cells for which seismicity was added are discussed in Subsection 2.5.2.2.

Caribbean South of Florida: Seismicity was added in degree cells south of Florida, because latitude 25°N was the southern-most extent of the EPRI completeness

regions (see [Figure 2.5.2-210](#)). As for the Gulf of Mexico and Atlantic, the seismicity in these degree cells was assigned the same rate as calculated for the Florida peninsula, using the updated earthquake catalog through mid-February 2008. The supplemental source for each EPRI team was given a geometry that completely filled the region between that team's Florida source and the Cuba area source (described below).

Cuba Area Source: This source represents earthquake occurrences on the island of Cuba and slightly offshore. Parameters of this source are described in [Subsection 2.5.2.2](#).

Caribbean Faults: Nine faults were identified in the Caribbean, and the geometries and parameters of these faults are described in [Subsection 2.5.2.2](#).

Charleston Seismic Source: An updated model for the Charleston seismic zone was adopted that reflects current scientific evidence on recurrence rates for large magnitude earthquakes in the Charleston, South Carolina region, and on the magnitudes of those earthquakes. This Charleston source was used rather than the EPRI team sources for Charleston because it reflects current thinking on both recurrence rates and magnitude values. The Charleston source is summarized in [Subsection 2.5.2.2](#).

2.5.2.4.5 New Ground Motion Models

2.5.2.4.5.1 Central and Eastern United States

Since the 1989 EPRI study ([Reference 245](#)), ground motion models for the CEUS have been evaluated, and alternative models have been published. An EPRI project was conducted to summarize these studies regarding CEUS ground motions, and results were published in 2004 EPRI report ([Reference 242](#)). These updated equations estimate median spectral acceleration and its uncertainty as a function of earthquake magnitude and distance. Epistemic uncertainty is modeled using multiple ground motion equations with weights, and multiple estimate of aleatory uncertainty, also with weights. Different sets of equations are recommended for seismic sources that represent rifted vs. non-rifted regions of the earth's crust. Equations are available for hard rock site conditions at spectral frequencies of 100 Hz (which is equivalent to peak ground acceleration, PGA), 25 Hz, 10 Hz, 5 Hz, 2.5 Hz, 1 Hz, and 0.5 Hz. All ground motion estimates are for spectral acceleration with 5 percent of critical damping.

Aleatory uncertainties published in the 2004 EPRI ([Reference 242](#)) model were reexamined by Abrahamson and Bommer ([Reference 203](#)) because it was

thought that the 2004 EPRI aleatory uncertainties were probably too large, resulting in over-estimates of seismic hazard. The Abrahamson and Bommer (Reference 203) study recommends a revised set of aleatory uncertainties and weights that can be used to replace the original 2004 EPRI (Reference 242) estimates of aleatory uncertainty.

In summary, the ground motion model used in the seismic hazard calculations for CEUS seismic sources consisted of the median equations from 2004 EPRI (Reference 242) combined with the updated aleatory uncertainties of the Abrahamson and Bommer study (Reference 203).

2.5.2.4.5.2 Cuba and the Caribbean

The use of the additional seismic sources developed for the Caribbean region in the PSHA requires the assignment of applicable ground motion attenuation models. Although the Caribbean region is relatively active seismically, the lack of a large dataset of empirical strong ground motion recordings, especially for larger magnitude earthquakes, has prevented the development of an empirical ground motion attenuation relationship for the region. The 2004 EPRI (Reference 242) attenuation relationship was not used in the analysis because of the observed geologic and tectonic differences between the CEUS and Caribbean regions.

Motazedian and Atkinson (Reference 287) have analyzed a dataset of approximately 300 earthquakes that were recorded by stations in Puerto Rico to develop a set of regional attenuation and source parameters. This dataset spans the magnitude range of 3–5.5 and, based on this limited upper magnitude, it cannot be used directly to develop an empirical attenuation model for earthquakes with magnitudes as large as magnitude 8+ as is needed in the PSHA.

Region specific attenuation models were developed by taking the empirically determined regional attenuation and source parameters from the Motazedian and Atkinson (Reference 287) study and using a stochastic ground motion simulation program (Reference 218). Ground motions were estimated for the seven spectral frequencies on hard rock site conditions for earthquakes with magnitudes between 4.75 and 8.75. The simulations spanned the distance range of 150–2000 kilometers.

The stress parameter and anelastic attenuation models were varied in the stochastic ground motion simulation analysis to account for the expected uncertainty in ground motions for this region. In addition, three separate source models were used in the analysis: single corner with constant stress parameter,

Turkey Point Units 6 & 7
COL Application
Part 2 — FSAR

single corner with magnitude dependent stress parameter, and double corner source model based on the analysis of CEUS data. These three source models are part of the larger set of source models that are included in the 2004 EPRI (Reference 242) ground motion models. A simple linear regression was performed on the simulation dataset to develop the Caribbean regional attenuation models for use in the PSHA. A more standard nonlinear attenuation functional form and regression was not required based on the large minimum distance of 150 kilometers for the attenuation models. An aleatory sigma value of 0.645 (in natural log units) was selected from the Motazedian and Atkinson (Reference 287) study and assigned to each Caribbean attenuation model for use in the PSHA independent of frequency. To capture the epistemic uncertainty in ground motion models in the hazard analysis, the suite of attenuation models based on the simulated data using the different source models were included along with model dependent weights. The weights for these new attenuation models were assigned based on the family class weights used in the 2004 EPRI ground motion model study and the family class source model (Reference 242).

Finally, a sensitivity analysis was performed examining the effect of adopting alternative attenuation relationships for use in the PSHA. These alternative relationships considered the use of a double corner source model based on the analysis of WUS data rather than CEUS data and the Gulf Coast region Q model rather than the Puerto Rico region specific Q model from Motazedian and Atkinson (Reference 287). Both alternatives could be argued to as well reflect region-specific attenuation parameters as the ones chosen. It was found that adoption of these alternatives would lead to lower ground motion values and a smaller range of results among the suite of attenuation curves than the results using the suite of attenuation models adopted to develop PSHA results for this study. The adopted suite of attenuation relationships is expected, therefore, to lead to a more conservative estimate of PSHA than would result from adoption of the alternative attenuation model.

2.5.2.4.6 Updated Probabilistic Seismic Hazard Analysis and Deaggregation for Rock

A PSHA for the site was conducted using as inputs the following:

- EPRI team sources with extended regions in the Gulf of Mexico and Atlantic
- Supplemental sources between Florida peninsula and Cuba
- Cuba area source

Turkey Point Units 6 & 7
COL Application
Part 2 — FSAR

- Caribbean faults
- Updated Charleston source
- Updated ground motion model for the CEUS
- New ground motion model for Caribbean faults and Cuba source

The first calculation was made for hard rock conditions, which is consistent with the 2004 EPRI ground motion model ([Reference 242](#)).

A PSHA consists of calculating annual frequencies of exceeding various ground motion amplitudes for all possible earthquakes that are hypothesized in a region. The seismic sources specify the rates of occurrence of earthquakes as a function of magnitude and location, and the ground motion model estimates the distribution of ground motions at the site for each event. Multiple weighted hypotheses on seismic sources characteristics, including rates of occurrence and magnitude distribution, and ground motions (characterized by the median ground motion amplitude and its uncertainty) result in multiple weighted seismic hazard curves. From this family of weighted curves, the mean and fractile seismic hazard can be determined. The calculation is made separately for each of the six EPRI teams, and the seismic hazard distribution for the teams is combined, weighting each team equally. This combination gives the overall mean and distribution of seismic hazard at the site.

[Figures 2.5.2-225](#) through [2.5.2-231](#) show mean and fractile (5th, 16th, median, 84th, and 95th) seismic hazard curves for hard rock from this calculation for the spectral frequencies of 100, 25, 10, 5, 2.5, 1, and 0.5 Hz, respectively.

[Table 2.5.2-220](#) documents the digital fractile and mean seismic hazard curves for the seven spectral frequencies. [Table 2.5.2-221](#) documents the UHRS values for this calculation. [Figure 2.5.2-232](#) plots the mean and median UHRS for 1E-04, 1E-05, and 1E-06 annual frequencies of exceedance.

As a sensitivity check, the potential contribution of the New Madrid seismic source to seismic hazard was examined for 1 Hz spectral acceleration. It was determined that the New Madrid seismic source's mean hazard was less than 0.1 percent of the mean hazard from other sources, so the New Madrid seismic source was not included in the overall hazard calculations. Also, the potential contribution of small earthquakes (smaller than the characteristic earthquakes, that is up to m_b 6.8) in the Charleston seismic source was examined for 1 Hz spectral acceleration. It was determined that these earthquakes (which are modeled with an exponential

Turkey Point Units 6 & 7
COL Application
Part 2 — FSAR

magnitude distribution) contributed a mean hazard that was less than 0.1 percent of the mean hazard from other sources. As a result, the smaller magnitude earthquakes were not included in the overall hazard calculations.

The rock hazard was deaggregated to identify the magnitudes and distances appropriate to represent rock spectral shapes for site response calculations. This deaggregation procedure followed the guidelines of RG 1.208. Specifically, the mean contributions to seismic hazard for 1 Hz and 2.5 Hz spectral accelerations (low frequencies, or LF) were deaggregated by magnitude and distance for the mean 1E-04 ground motion amplitude at 1 Hz and at 2.5 Hz, and these deaggregations were combined (contributions for each magnitude and distance bin were averaged). [Figure 2.5.2-233](#) shows this combined deaggregation. Similar deaggregations of the mean hazard were performed for 5 and 10 Hz spectral accelerations (high frequencies, or HF), and the combined deaggregation is shown in [Figure 2.5.2-234](#). Deaggregations of the HF and LF mean hazard for 1E-05 and 1E-06 ground motions are shown in [Figures 2.5.2-235 through 2.5.2-238](#). [Table 2.5.2-222](#) shows the percent contributions for various magnitude and distance bins for the six deaggregations, and [Table 2.5.2-223](#) summarizes the mean magnitudes and distances resulting from these deaggregations, for all contributions to hazard and for contributions with distances exceeding 100 kilometers. For the HF controlling earthquakes, the magnitudes and distances from all distances are used (the light grey shaded cells in [Table 2.5.2-223](#)). For the LF controlling earthquakes, the magnitudes and distances from distances greater than 100 kilometers are used (the dark grey shaded cells in [Table 2.5.2-223](#)), because the contribution to hazard for distances greater than 100 kilometers is more than 5 percent of the total hazard. This follows the guidelines in RG 1.208. For [Figures 2.5.2-233 through 2.5.2-238](#) and [Tables 2.5.2-222 and 2.5.2-223](#), deaggregation results are given in terms of moment magnitude.

The deaggregation plots in [Figures 2.5.2-233 through 2.5.2-238](#) indicate that local earthquakes are a contributor to seismic hazard at the site for high frequencies, but that distant sources also make an important contribution. Distant sources contribute because the seismicity rate of local earthquakes in the Florida peninsula is very low. For LF, distant sources have the major contribution to seismic hazard, with the Cuba area source, Caribbean faults, and Charleston source contributing most of the hazard.

Smooth rock UHRS were developed from the UHRS amplitudes in [Table 2.5.2-221](#), using controlling earthquake M and R values shown in [Table 2.5.2-223](#) and using the hard rock spectral shapes for CEUS earthquake ground motions recommended in NUREG/CR-6728 ([Reference 308](#)). Separate spectral shapes

were developed for HF and LF. In creating these spectral shapes, the single-corner and double-corner models recommended in NUREG/CR-6728 were weighted equally. In order to reflect accurately the UHRS values calculated by the PSHA as shown in [Table 2.5.2-221](#), the HF spectral shape was anchored to the UHRS values from [Table 2.5.2-221](#) at 100 Hz, 25 Hz, 10 Hz, and 5 Hz. In between these frequencies, the spectrum was interpolated using shapes anchored to the next higher and lower frequency and using weights on the two shapes equal to the inverse logarithmic difference between the intermediate frequency and the next higher or lower frequency. Below 5 Hz, the HF shape was extrapolated from 5 Hz. For the LF spectral shape a similar procedure was used except that the LF spectral shape was anchored to the UHRS values at all seven frequencies for which UHRS values are available from [Table 2.5.2-221](#) (100 Hz, 25 Hz, 10 Hz, 5 Hz, 2.5 Hz, 1 Hz, and 0.5 Hz). The reason that the LF spectral shape was anchored to all seven frequencies, including the HF, was that, if this anchoring were not done, the LF spectrum would exceed the HF spectrum at high frequencies, which would not be realistic. The UHRS at all frequencies accounts for all earthquakes, small and large, close and distant, and the UHRS amplitudes should not be exceeded by spectra representing the controlling earthquakes.

For frequencies below 0.5 Hz, the spectral shapes for both the HF and LF spectra were extrapolated from the value at 0.5 Hz assuming a constant spectral velocity (i.e., spectral accelerations were assumed to scale linearly with frequency) down to 0.125 Hz (8 seconds). From 0.125 Hz to 0.1 Hz, spectral accelerations were assumed to scale as (frequency)². This follows the recommendation of Building Seismic Safety Council ([Reference 219](#)) for long periods.

[Figures 2.5.2-239](#) through [2.5.2-241](#) show the horizontal HF and LF spectra calculated in this way for 1E-04, 1E-05, and 1E-06 annual frequencies of exceedance, respectively. As mentioned previously, these spectra were appropriately anchored to accurately reflect the rock UHRS amplitudes in [Table 2.5.2-221](#) that were calculated for the seven spectral frequencies at which PSHA calculations were done.

2.5.2.5 Seismic Wave Transmission Characteristics of the Site

The UHRS described in the previous subsection are defined on hard rock characterized with shear-wave velocity (V_S) = 9200 feet per second (fps), which is located at about 10,000 feet (3050 meters) below the ground surface. This subsection describes the development of the site amplification factors that result from the transmission of the seismic waves through the thick soil column. The effect is modeled by randomized soil columns, extending from the finished

Turkey Point Units 6 & 7
COL Application
Part 2 — FSAR

ground surface (including structural fill) to randomized hard rock depths varying between 7400 feet (2256 meters) and 11,400 feet (3476 meters), and an adjustment to the soil damping within the soil column to represent the anelastic attenuation of ground motion by the entire soil column (the “kappa” value).

The development of the site amplification factors is performed in the following steps:

1. Develop a model of the base case soil column, using site-specific geotechnical and geophysical data to a depth of about 636 feet (194 meters), augmented to a depth of about 12,000 feet (3658 meters) with deep velocity profiles taken from industry, as described in [Subsection 2.5.2.5.1](#). The model for the upper 636 feet (194 meters) is based on mean shear-wave velocities measured at the site, except for the upper 30.5 feet (9.3 meters) of structural fill. Strain-dependent in situ soil shear modulus and damping are selected from generic curves based on Resonant Column Torsional Shear (RCTS) results (see [Subsection 2.5.4.7](#)). The deeper soil layers are assumed to behave linearly. This model provides the base case representation of the dynamic subsurface properties for Units 6 & 7.
2. Calculate strain-independent (linear-elastic) material damping values for the deep soil strata (between 636 feet and the top of hard rock), which experience small levels of strain during the earthquake to ensure that the site model accurately accounts for the dissipation of energy in this depth interval. This is done by constraining the damping within these deeper strata to replicate an estimate of the kappa for the site.
3. Generate a set of 60 artificial “randomized” soil profiles by using a base soil column and developing a probabilistic model that includes the uncertainties in the above soil properties, location of layer and hard rock boundaries, correlation between the velocities in adjacent layers and the overall dissipation of energy in the site.
4. Use the 1E-04 and 1E-05 annual-frequency-of-exceedance smooth LF and HF hard rock spectra of [Subsection 2.5.2.4](#) for input into the base of the randomized soil columns, calculate dynamic response of the site for each of the 60 artificial profiles by using an equivalent-linear site-response formulation together with Random Vibration Theory (RVT), and calculate the mean site response. Time histories for the site response analysis are not required for the frequency-domain RVT approach to site response

Turkey Point Units 6 & 7
COL Application
Part 2 — FSAR

analysis. This step is repeated for each of the four input motions (1E-04 and 1E-05 annual frequencies, HF and LF smooth spectra). Note that the GMRS horizon is defined at elevation (El.) –35 feet. To calculate the site response at GMRS horizon, two consecutive site response analyses are conducted. In the first analysis, the randomized profiles with full soil column height up to finished grade at El. +25.5 feet are analyzed. In the second analysis, the strain-compatible properties of the soil columns, provided by the first analysis, are used without iteration, the layers above the GMRS horizon are omitted, and the amplification factors at El. –35 feet (corresponding to zero depth in this case) are calculated.

These steps are described in the following subsections. The resulting site-specific amplification factors are used with the hard rock spectra of [Subsection 2.5.2.4](#) to develop the GMRS in [Subsection 2.5.2.6](#).

2.5.2.5.1 Base Case Soil Column and Uncertainties

Development of a base case soil column is described in detail in [Subsection 2.5.4](#). Summaries of the low strain shear-wave velocity, material damping, and strain-dependent properties of the base case soil strata are provided below in this subsection. These parameters serve as input for the generation of randomized profiles and for site response analyses.

The site is a limestone and sand site covered with a 5-foot thick layer of muck (refer to [Subsection 2.5.4](#)). The existing upper approximately 611 feet (186 meters) of the site soils were investigated using test borings, Cone Penetration Testing (CPT), test pits, and geophysical methods. The soil layers and approximate thicknesses encountered at the boring and CPT locations consist of, in descending order:

- Five feet of muck, consisting of peat and silt (during construction, structural fill is designed to replace the five feet of muck)
- Miami Limestone (25 feet)
- Key Largo Limestone (20 feet)
- Fort Thompson Formation (70 feet)
- Tamiami Formation (100 feet)
- Upper Hawthorn sand (230 feet)

Turkey Point Units 6 & 7
COL Application
Part 2 — FSAR

- Lower Hawthorn Group consisting of limestone, mudstone, dolomite, dolosilt, shells, quartz sand, clay, and mixtures of these materials

The GMRS, at El. -35 feet, is located near the top of the Key Largo Limestone, below the Miami Limestone.

The Primary-Secondary (P-S) suspension measurements and CPT results provided shear and compression wave velocities of the soil and rock at 1.6 feet (0.5 meters) intervals. These data were used to develop mean shear-wave profile for the upper 611 feet (186 meters) of in situ soil. Note that the estimated mean shear-wave velocity values of 650 feet/second at the ground surface to 1100 feet/second at a depth of 30.5 feet were assigned to the structural fill layer (uppermost 30.5 feet, 9.3 meters) (refer to [Subsection 2.5.4](#)). Due to the uncertainty in this estimate, a coefficient of variation of 0.5 was used to provide upper and lower bounds. These values are based on an assumed unit weight of 130 pounds per cubic foot (pcf) and a normalized Standard Penetration Test (SPT) resistance of $N_1 = 30$ for the fill. Unit weights for the upper 636 feet (194 meters) soil and rock, i.e. including fill, are in the range of 120 pcf to 130 pcf.

Information on subsurface conditions for depths exceeding 636 feet (194 meters) below top of fill were sought from available industry resources (refer to [Subsection 2.5.4](#)). A total of eight deep sonic logs of compression wave velocity were located within about a 115-mile radius of Units 6 & 7: six were obtained in digitized format at 0.5 feet (0.15 meters) intervals, and two were digitized manually at 10 feet (3 meters) intervals. The compression wave velocities were converted to shear-wave velocities using values of Poisson ratios based on near surface measurements taken at the site and values published by the U.S. Army Corps of Engineers (see [Subsection 2.5.4](#)). In this manner, shear-wave velocity data at varying depths ranging from 500 feet to 11,920 feet were determined. Unit weights of the deep soils (below approximately 636 feet [194 meters]) were assumed to be 130 pcf.

As described in [Subsection 2.5.4.7](#), Resonant Column Torsional Shear (RCTS) testing was conducted on seven samples obtained from the Tamiami Formation sands. These results were matched to the closest fitting generic EPRI material shear modulus and damping degradation curves for sandy soils ([Reference 244](#)). The remaining materials consist of hard limestones which are treated as elastic materials with 1 percent damping. Analyses for the development of site-specific amplification factors was therefore conducted using measured wave velocity profiles combined with shear modulus and damping degradation curves for the sands and elastic properties for the limestone. Generic EPRI curves

(Reference 244) were adopted to describe the strain dependencies of shear modulus and damping for the sands occurring between depths of about 120 feet (37 meters) and 450 feet (137 meters). Above the GMRS elevation, the 30.5 foot (9.3 meter) thick fill layer is derived from crushed limestone during construction. EPRI shear modulus and damping degradation curves for gravel (Reference 317) are used to model the fill layers, as shown in Subsection 2.5.4.7.

Damping values were developed for the linear deep layers to maintain the total kappa (κ) for the site as described below. Low-strain kappa value, a near surface damping parameter for modeling site-dependent effects, is used as a measure of the total dissipation of energy of the site during the small strain events. The site kappa value is directly related to damping of the soil layers and scattering of the waves at layer interface boundaries. The kappa representing soil layer damping is additive for all layers. The following expression shows the relationship between kappa (κ_i) and the damping coefficient, (ζ_i) of the soil layer (i):

$$\kappa_i = \frac{2H_i \zeta_i}{V_{S_i}} \quad \text{Equation 2.5.2-11}$$

where, H_i is the thickness and V_{S_i} is the shear-wave velocity of the soil layer (i).

Total kappa value of the site associated with material damping equals the sum of the κ_i values of all soil layers included in the model:

$$\kappa = \sum_i \kappa_i \quad \text{Equation 2.5.2-12}$$

Total kappa is directly evaluated from recordings of earthquakes (Reference 209), of which there are too few in the site vicinity to obtain an explicit site-specific estimate of kappa. Therefore, when total kappa is not available from near or applicable earthquake recordings, an alternative is to estimate total kappa directly using the correlation with average rock shear-wave velocity, V_S , from Reference 241:

$$\log(\kappa) = 2.2189 - 1.0930 \times \log(V_S [ft / sec]) \quad \text{Equation 2.5.2-13}$$

Based on review of Reference 241, the average shear-wave velocity to use with Equation 2.5.2-13 appears to be representative of the uppermost approximate 100 feet of rock. The average velocity of the Key Largo Limestone and Fort Thompson Formation (which totals about 86 feet thick) is used for this analysis.

The average shear-wave velocity of the 86 feet of Key Largo Limestone and Fort Thompson Formation was calculated to be 4239 fps, which, using Equation 2.5.2-13, corresponds to a total kappa of 0.018 second. By inspection

Turkey Point Units 6 & 7
COL Application
Part 2 — FSAR

of [Figure 2.5.2-242](#), the shear-wave velocities determined in the upper 1000 feet of rock vary between about 4000 fps and 5000 fps, which correspond to total kappa values of 0.019 second and 0.015 second, respectively. Therefore, a total kappa value of 0.018 second can be used for the soil/rock column with a standard deviation of 0.4 natural log units.

A kappa value of 0.006 second is assumed to apply to the CEUS crystalline basement and below ([Reference 244](#)), leaving a total soil kappa value of 0.012 second for the damping of the full depth of the soil column.

[Reference 244](#) recommends a standard deviation of 0.4 natural log units to be appropriate for total kappa values of sites within the eastern United States. This is consistent with [Reference 241](#) in considering ± 50 percent variation about the base case value of kappa for Mississippi embayment sites.

Therefore, a base case kappa value of 0.012 second is used for the Units 6 & 7 site model with a standard deviation of 0.4 natural log units.

The following procedure is used to assign the damping to the models of the soil at depths below 636 feet (194 meters) in order to match the assigned kappa value:

1. From Equations 2.5.2-11 and 2.5.2-12, kappa associated with material damping is calculated for the top approximately 600 feet (183 meters) of soil strata, i.e. excluding top fill, by using small strain damping for each soil layer.
2. The kappa value of the top approximately 600 feet (183 meters) of soil is deducted from the total kappa value, and a constant damping value is assigned to deep soil layers. The process of the randomization of soil velocity profiles introduces additional scattering of upward propagating shear waves (S-waves) in such a manner that the median response of all randomized profiles is lower than the response obtained from the analyses of the median profile. These scattering effects are accounted for by decreasing the damping value of the deep soil layers in the randomized profiles, and therefore reduce total kappa for the site. In this case, however, because damping in the deep layers was very small (median of 0.3 percent), no additional reduction was applied.
3. The damping of each deep soil layer is randomized with consideration given to the mean and variation of the total kappa.

The input motion for soil amplification analysis was specified at the bottom of the soil profile, below which the halfspace was modeled with shear-wave velocity of 9200 fps and a damping ratio of 1 percent.

As described in [Subsection 2.5.2.5.2](#), the soil properties for each layer were randomized to account for the inherent natural variability of soil deposits, as well as the (epistemic) uncertainty associated with the choice of curves for variation of shear modulus and damping with strain level. Therefore, the actual site response analysis comprised a range of soil properties for each layer, and in particular, a range of initial small strain shear modulus and degradation curves. Because of different properties in each of the randomized profiles, the site response analysis generated a range of results, as reported in [Subsection 2.5.2.5.3](#).

2.5.2.5.2 Site Properties Representing Uncertainties and Correlations

To account for variations in shear-wave velocity across the site, 60 randomized profiles were generated using the stochastic model discussed in [Reference 319](#), with some modifications to account for conditions at the Turkey Point Units 6 & 7 site. These randomized profiles represent the truncated soil column from the top of bedrock with shear-wave velocity of 9200 fps to the ground surface. This model uses as inputs the following quantities:

1. A shear-wave velocity profile which is equal to the base-case soil profile described above.
2. The standard deviation of $\ln(V_S)$ (the natural logarithm of the shear-wave velocity) as a function of depth, which was developed using available site and regional data.
3. The correlation coefficient between $\ln(V_S)$ in adjacent layers, which is taken from generic studies, using the inter-layer correlation model for category U.S. Geological Survey “A” soils ([Reference 319](#)), with modifications to some of the parameters to increase the correlation in order to reduce the number of V_S reversals.
4. The probabilistic characterization of layer thickness consists of a function that describes the rate of layer boundaries as a function of depth. This study used a form of this function, taken from [Reference 319](#), but modified to allow for sharp changes and discontinuities in the adopted base-case velocity profile, especially near the surface.

5. The profiles of the median and plus/minus one standard deviation of the shear-wave velocity profile are shown in [Figure 2.5.2-243](#). The variation was used in the randomization of the shear-wave velocity profile.
6. For each artificial profile, bedrock is defined to occur at the depth where the randomization algorithm calculates a V_S that exceeds 9200 fps (excluding depths shallower than 7000 feet).
7. Median values of shear stiffness (G/G_{MAX}) and damping for each geologic unit are described in [Subsection 2.5.4](#). Uncertainties in the strain-dependent properties for each soil unit are characterized using the values in [Reference 320](#). [Figures 2.5.2-244](#) and [2.5.2-245](#) illustrate the shear stiffness and damping curves generated for natural soils found at less than 150 foot depth, described in [Subsection 2.5.4](#).

[Figure 2.5.2-246](#) illustrates the 60 V_S profiles generated, using the median, logarithmic standard deviation, and correlation model described above. The same figure compares the median of these 60 V_S profiles (randomized median) to the input median V_S profile described in the previous subsection, indicating good agreement. At depths greater than 7000 feet, the randomized median appears lower than the input median because, when a random V_S profile exceeds 9200 fps, the profile is truncated at that depth. The randomized median curve in [Figure 2.5.2-246](#) does not include these truncated profiles but shows the median of only the remaining profiles (with $V_S < 9200$ fps) at each depth. Therefore, it is reasonable that the median of these filtered profiles (with $V_S < 9200$ fps) is lower than the overall median at deep locations in the profile.

This set of 60 profiles, consisting of V_S versus depth, depth to bedrock, stiffness, and damping, are used to calculate and quantify site response and its uncertainty, as described in the following subsections.

2.5.2.5.3 Site Response Analyses

The site response analysis performed for the site uses Random Vibration Theory (RVT) ([References 232](#) and [306](#)) with the following assumptions:

- Vertically-propagating shear waves are the dominant contributor to site response.
- An equivalent-linear formulation of soil nonlinearity is appropriate for the characterization of site response.

These are the same assumptions that are implemented in the SHAKE program ([Reference 263](#)) and that constitute standard practice for site-response calculations. In this respect, RVT and SHAKE solve the same problem, but RVT works with ground-motion response spectra and their power spectral density (and its relation to peak values), while SHAKE works with individual time histories and their Fourier spectra.

The RVT site-response analysis requires the following additional parameters:

- Strong-motion duration. The RVT methodology requires this parameter, but results are not very sensitive to it. These are calculated from the mean magnitudes from the deaggregation. Table 2.3.1 in [Reference 206](#) provides strong motion duration values as a function of magnitude. Accordingly, strong motion durations were assigned for each of the cases considered (1E-04 and 1E-05 annual frequencies, HF and LF smooth spectra) and are presented in [Table 2.5.2-224](#).
- Effective strain ratio. A value of 0.65 is used. Effective strain ratio is defined as the ratio between the peak acceleration of earthquake time history and the equivalent harmonic wave going through the soil layers ([Reference 316](#)).

As discussed earlier, the GMRS horizon is defined at El. -35 feet. To calculate the site response at GMRS horizon, two consecutive site response analyses are conducted. In the first analysis, the full soil column height up to finished grade at El. +25.5 feet is analyzed. In the second analysis, the strain-compatible properties of the soil column, provided by the first analysis, are used without iteration after omitting the layers above the GMRS horizon, and the amplification factors at El. -35 feet (corresponding to zero depth in this case) are calculated.

[Figure 2.5.2-247](#) show with thick red line the logarithmic mean (median) of site amplification factor at GMRS horizon from the analysis of the 60 modified random profiles with the 1E-04 LF input motion. Amplifications are largest at low frequencies (below 6.0 Hz) and de-amplification occurs at high frequencies because of soil damping. The maximum strains in the soil column are low for this motion, and this is shown in [Figure 2.5.2-248](#), which plot the maximum strains versus depth that are calculated for the 60 profiles and their logarithmic mean (in red thick line). The median of maximum strains does not exceed 0.020 percent. The maximum strain calculated from the analyses of all 60 profiles is 0.070 percent in the structural fill layers. The maximum strains in the deep soil layer at depths below 636 feet (194 meters) are very small and do not exceed a value of 0.005 percent.

Figures 2.5.2-249 and 2.5.2-250 show similar plots of amplification factors and maximum strains obtained from the analyses with 1E-04 HF motion. The maximum strain results show that the soil column exhibits a lower level of straining under this earthquake with maximum strains being less than 0.04 percent.

Figures 2.5.2-251 through 2.5.2-254 show comparable plots of amplification factors and maximum strains from the analyses performed with the 1E-05 input motion, both LF and HF. For this higher motion, larger maximum strains are observed, but the maximum median does not exceed 0.045 percent. From all of 1E-05 analyses, a maximum strain of 0.23 percent is calculated at the top structural fill layers. The maximum strain in the deep soil layers, below 636 feet (194 meters), is very small, less than 0.01 percent.

Comparison of the profiles of median maximum strains in Figure 2.5.2-255, for the full soil column and the upper 800 feet, respectively, clearly indicates that response of the site under the LF motions is stronger than under HF motions. Figure 2.5.2-256 show the median profiles for the strain-compatible damping resulting from the four input rock motions as well as the low-strain damping, for the full soil column and the upper 800 feet, respectively. Damping is a measure of energy dissipation in the soil profile during the shaking. Corresponding to the strains, a maximum damping value of 5 percent for depths above 636 feet (194 meters) of soil are calculated for the analyses with the 1E-05 LF motion. The strain compatible damping calculated for 1E-04 LF motion is small and does not exceed 3 percent.

A comparison of the envelopes of median soil amplification factors at GMRS horizon for LF and HF 1E-04 and 1E-05 input motions is shown in Figure 2.5.2-257. The amplifications at 1E-04 level of input motion are larger due to LF input motion than the ones due to HF input motion. De-amplification occurs at higher frequencies and is smaller for the LF input motion, followed by amplification of the peak ground acceleration starting from 1 at about 80 Hz to about 1.3 at 100 Hz. The amplification due to 1E-05 level of input motion is smaller than for the 1E-04 level of input motion, at frequencies larger than 3 Hz, due to the higher strain levels and nonlinearity in the soil column. At these higher frequencies, amplification factors for the LF and HF 1E-05 motions are very close.

The corresponding numerical values of the soil amplification factors are tabulated in Tables 2.5.2-225 and 2.5.2-226. These tables show values for just 38 frequencies, but site amplification factors and site spectra were calculated for 301 frequencies between 0.1 and 100 Hz.

PTN COL 2.5-2
PTN COL 2.5-3

2.5.2.6 Ground Motion Response Spectra

2.5.2.6.1 Horizontal Spectra

With the site-specific amplification calculations described in the previous subsection, the site ground motion response spectra (GMRS) were determined as follows. [Figure 2.5.2-258](#) shows the 1E-04 and 1E-05 horizontal HF and LF site spectra, plotted on a linear spectral acceleration scale. These HF and LF 1E-04 and 1E-05 horizontal site spectra were enveloped and smoothed to remove small frequency-to-frequency variations, using smoothing function that averaged over spectral accelerations at adjacent frequencies. [Figure 2.5.2-259](#) shows the smoothed, enveloped spectra calculated in this way, plotted on a linear spectral acceleration scale.

The horizontal GMRS was calculated at each frequency using the following equations:

$$A_R = SA(10^{-5})/SA(10^{-4}) \quad \text{Equation 2.5.2-14}$$

$$DF = 0.6 \times A_R^{0.8} \quad \text{Equation 2.5.2-15}$$

$$GMRS = \max[SA(10^{-4}) \times \max(1.0, DF), 0.45 \times SA(10^{-5})] \quad \text{Equation 2.5.2-16}$$

where, $SA(10^{-4})$ is the spectral acceleration for the 1E-04 envelope spectrum at each spectral frequency (and similarly for 1E-05), and GMRS is the Ground Motion Response Spectrum at that spectral frequency. These equations follow the procedure in RG 1.208 to determine the GMRS from the 1E-04 and 1E-05 spectra.

[Figure 2.5.2-260](#) shows the GMRS calculated with the above equations at each spectral frequency, and shows the 1E-04 and 1E-05 horizontal spectra, plotted on a logarithmic spectral acceleration scale. At low spectral frequencies (2 Hz and below), the hazard curves are steep, so A_R in Equation 2.5.2-14 above is low, and the GMRS from Equation 2.5.2-16 is equal to the 1E-04 UHRS.

[Tables 2.5.2-225](#) and [2.5.2-226](#) document the 1E-04 and 1E-05 spectra, respectively, including the rock spectra, site amplification factors, and site spectra.

The method described above corresponds to Approach 2A in Risk Engineering, Inc. ([Reference 308](#)). Thus hazard curves were not generated for the GMRS

elevation; only the 1E-04, 1E-05, and 1E-06 site spectra were generated at the GMRS elevation. [Table 2.5.2-227](#) documents the 1E-04 and 1E-05 spectral amplitudes, the calculation of A_R and DF from Equations 2.5.2-14 and 2.5.2-15, and the GMRS calculated according to Equation 2.5.2-16. [Table 2.5.2-228](#) documents the 1E-04, 1E-05, and 1E-06 site spectra, with smoothing for the 1E-06 spectrum conducted with the same function as described above for the 1E-04 and 1E-05 spectra.

2.5.2.6.2 Vertical Spectra

To calculate vertical spectra, V:H ratios from RG 1.60 were adopted. The V:H ratios were applied to the 1E-04 and 1E-05 horizontal spectra to calculate 1E-04 and 1E-05 vertical spectra, and Equations 2.5.2-14 through 2.5.2-16 were applied to the 1E-04 and 1E-05 vertical spectral accelerations to calculate a vertical GMRS. The resulting vertical 1E-04 and 1E-05 spectra and GMRS are plotted in [Figure 2.5.2-261](#).

[Table 2.5.2-229](#) documents the V:H ratios, the 1E-04 and 1E-05 vertical spectra, values of A_R and DF from Equations 2.5.2-14 and 2.5.2-15, and the calculated vertical GMRS from Equation 2.5.2-16.

2.5.2.7 References

201. Abe, K., "Complements to 'Magnitudes of Large Shallow Earthquakes from 1904 to 1980'," *Physics of the Earth and Planetary Interiors*, v. 34, no. 1-2, pp. 17–23, 1984.
202. Abe, K., "Magnitudes of Large Shallow Earthquakes from 1904 to 1980," *Physics of the Earth and Planetary Interiors*, v. 27, no. 1, pp. 72–92, 1981.
203. Abrahamson, N.A., and Bommer, J., *Program on Technology Innovation: Truncation of the Lognormal Distribution and Value of the Standard Deviation for Ground Motion Models in the Central and Eastern United States*, Technical Report 1014381, Electric Power Research Institute, August 2006.
204. Advanced National Seismic System (ANSS), *ANSS/CNSS Worldwide Earthquake Catalog*. Available at <http://www.ncedc.org/anss/catalog-search.html>, accessed February 14, 2008.
205. Alvarez, L., Chuy, T., García, J., Moreno, B., Alvarez, H., Blanco, M., Expósito, O., González, O., Fernández, A.I., *An earthquake Catalogue of*

Turkey Point Units 6 & 7
COL Application
Part 2 — FSAR

Cuba and Neighboring Areas, internal report from the United Nations Educational, Scientific and Cultural Organization, International Atomic Energy Agency, and The Abdus Salam International Centre for Theoretical Physics, Trieste, Italy, January 1999.

206. American Society of Civil Engineers, *Seismic Analysis of Safety-Related Nuclear Structures and Commentary*, ASCE 4-98, 2000.
207. Amick, D., Gelinas, R., Maurath, G., Cannon, R., Moore, D., Billington, E., and Kempinen, H., *Paleoliquefaction Features along the Atlantic Seaboard*, U.S. Nuclear Regulatory Commission Report, NUREG/CR-5613, 1990.
208. Amick, D., Maurath, G., and Gelinas, R., "Characteristics of Seismically Induced Liquefaction Sites and Features Located in the Vicinity of the 1886 Charleston, South Carolina Earthquake," *Seismological Research Letters*, v. 61, no. 2, pp. 117–130, 1990.
209. Anderson, J.G., and Hough, S.E., "A Model for the Shape of the Fourier Amplitude Spectrum of Acceleration at High Frequencies," *Bulletin of the Seismological Society of America*, v. 74, 1969–1993, 1984.
210. Atkinson, G.M., and Boore, D.M., "Ground-Motion Relations for Eastern North America," *Bulletin of the Seismological Society of America*, v. 85, no. 1, pp. 17–30, 1995.
211. Bakun, W.H., and Hopper, M.G., "Magnitudes and Locations of the 1811–1812 New Madrid, Missouri, and the 1886 Charleston, South Carolina, Earthquakes," *Bulletin of the Seismological Society of America*, v. 94, no. 1, pp. 64–75, 2004.
212. Bally, A.W., Scotese, C.R., and Ross, M.I., "Simplified Tectonic Map of North America," *The Geology of North America*, v. A, *An Overview*, The Geological Society of America, 1989.
213. Behrendt, J.C., and Yuan, A., "The Helena Banks Strike-Slip (?) Fault Zone in the Charleston, South Carolina Earthquake Area: Results from a Marine, High-Resolution, Multichannel, Seismic-Reflection Survey," *Geological Society of America Bulletin*, v. 98, pp. 591–601, 1987.

Turkey Point Units 6 & 7
COL Application
Part 2 — FSAR

214. Bollinger, G.A., Chapman, M.C., Sibol, M.S., and Costain, J.K., "An Analysis of Earthquake Focal Depths in the Southeastern U.S.," *Geophysical Research Letters*, v. 12, no. 11, pp. 785–788, 1985.
215. Bollinger, G.A., Johnston, A.C., Talwani, P., Long, L.T., Shedlock, K.M., Sibol, M.S., and Chapman, M.C., "Seismicity of the Southeastern United States; 1698–1986," *Neotectonics of North America*, Decade Map Volume to Accompany the Neotectonic Maps, ed. D.B. Slemmons, E.R. Engdahl, M.D. Zoback, and D.B. Blackwell, Geological Society of America, 1991.
216. Bollinger, G.A., *Reinterpretation of the Intensity Data for the 1886 Charleston, South Carolina, Earthquake: in Studies Related to the Charleston, South Carolina, Earthquake of 1886 — A Preliminary Report*, Professional Paper 1028, U.S. Geological Survey, pp. 17–32, 1977.
217. Bollinger, G.A., *Specification of Source Zones, Recurrence Rates, Focal Depths, and Maximum Magnitudes for Earthquakes Affecting the Savannah River Site in South Carolina*, U.S. Geological Survey Bulletin 2017, 1992.
218. Boore, D.M., *SMSIM — Fortran Programs for Simulating Ground Motions from Earthquakes Version 2.3 — A Revision of OFR 96-80-A*, Open File Report 00-509, U.S. Geological Survey, 2005.
219. Building Seismic Safety Council (BSSC), *NEHRP Recommended Provisions and Commentary for Seismic Regulations for New Buildings and Other Structures*, 2003 Edition (FEMA 450), p. 752, 2004.
220. Calais, E., Mazabraud, Y., Mercier de Lepinay, B., and Mann, P., "Strain Partitioning and Fault Slip Rates in the Northeastern Caribbean from GPS Measurements," *Geophysical Research Letters*, v. 29, pp. 1856–1859, 2002.
221. Calais, E., Perrot, J., and Mercier de Lepinay, B., "From Transpression to Transtension along the Northern Caribbean Plate Boundary off Cuba: Implications for the Recent Motion of the Caribbean Plate," *Tectonophysics*, v. 186, pp. 329–350, 1991.
222. Calais, E., and Mercier de Lepinay, B., "Strike-slip Tectonics and Seismicity along the Northern Caribbean Plate Boundary from Cuba to Hispaniola," *Active Strike Slip and Collisional Tectonics of the Northern*

Turkey Point Units 6 & 7
COL Application
Part 2 — FSAR

Caribbean Plate Boundary Zone, J.F. Dolan and P. Mann (eds.), Special Paper 326, pp. 125–141, Geological Society of America, 1998.

223. Chapman, M.C. and Talwani, P., *Seismic Hazard Mapping for Bridge and Highway Design in South Carolina*, South Carolina Department of Transportation Report, 2002.
224. Cornell, C.A., “Engineering Seismic Risk Analysis,” *Bulletin of the Seismological Society of America*, v. 58, no. 5, pp. 1583–1606, 1968.
225. Cornell, C.A., and Winterstein, S.R., “Temporal and Magnitude Dependence in Earthquake Recurrence Models,” *Bulletin of the Seismological Society of America*, v. 79, pp. 1522–1537, 1988.
226. Cotilla Rodriguez, M.O., Franzke, H.J., and Cordoba Barba, D., “Seismicity and Seismoactive Faults of Cuba,” *Russian Geology and Geophysics*, v. 48, pp. 505–522, 2007.
227. Cramer, C.H., “A Seismic Hazard Uncertainty Analysis for the New Madrid Seismic Zone,” *Engineering Geology*, v. 62, pp. 251–266, 2001.
228. Dellinger, J.A., Dewey, J.W., Blum, J., and Nettles, M., “Relocating and Characterizing the 10 Feb 2006 “Green Canyon” Gulf of Mexico Earthquake Using Oil-Industry Data,” *Eos, Transactions of the American Geophysical Union*, v. 88, no. 52, Fall Meeting Supplement, Abstract S13F-01, 2007.
229. DeMets, C., and Wiggins-Grandison, M., “Deformation of Jamaica and Motion of the Gonave Microplate from GPS and Seismic Data,” *Geophysical Journal International*, v. 168, pp. 362–378, 2007.
230. DeMets, C., Jansma, P.E., Mattioli, G.S., Dixon, T.H., Farina, F., Bilham, R., Calais, E., and Mann, P., “GPS Geodetic Constraints on Caribbean-North America Plate Motion,” *Geophysical Research Letters*, v. 27, pp. 437–440, 2000.
231. DeMets, C., Mattioli, G., Jansma, P., Rogers, R.D., Tenorio, C., and Turner, H.L., “Present Motion and Deformation of the Caribbean Plate: Constraints from new GPS Geodetic Measurements from Honduras and Nicaragua,” *Geologic and Tectonic Development of the Caribbean Plate in Northern*

Turkey Point Units 6 & 7
COL Application
Part 2 — FSAR

Central America, P. Mann (ed.), Special Paper 428, pp. 21–36, Geological Society of America, 2007.

232. Der Kiureghian, A., “Structural Response to Stationary Excitation,” *Journal of the Engineering Mechanics Division ASCE*, v. 106, no. EM6, December, pp. 1195–1213, 1980.
233. Dixon, T., Farina, F., DeMets, C., Jansma, P., Mann, P., and Calais, E., “Relative Motion Between the Caribbean and North American Plates and Associated Boundary Zone Deformation Based on a Decade of GPS Observations,” *Journal of Geophysical Research*, v. 103, pp. 15, 157-15,182, 1998.
234. Dolan, J.F., and Bowman, D.D., “Tectonic and Seismologic Setting of the 22 September 2003, Puerto Plata, Dominican Republic Earthquake: Implications for Earthquake Hazard in Northern Hispaniola,” *Seismological Research Letters*, v. 75, no. 5, 2004.
235. Dolan, J.F., and Wald, D.J., “Comment on “The 1946 Hispaniola earthquake and the tectonics of the North America-Caribbean plate boundary zone, northeastern Hispaniola” by R.M. Russo and A. Villasenor,” *Journal of Geophysical Research*, v. 102, no. B1, pp. 785–792, 1997.
236. Dolan, J.F., and Wald, D.J., “The 1943–1953 North-Central Caribbean Earthquakes: Active Tectonic Setting, Seismic Hazards, and Implications for Caribbean-North America Plate Motions,” *Active Strike Slip and Collisional Tectonics of the Northern Caribbean Plate Boundary Zone*, J.F. Dolan and P. Mann (eds.), Special Paper 326, pp. 143–169, Geological Society of America, 1998.
237. Deleted
238. Dolan, J.F., Mullins, H.T., and Wald, D.J., “Active Tectonics of the North-Central Caribbean: Oblique Collision, Strain Partitioning, and Opposing Subducted Slabs,” *Active Strike Slip and Collisional Tectonics of the Northern Caribbean Plate Boundary Zone*, J.F. Dolan and P. Mann (eds.), Special Paper 326, pp. 1–61, Geological Society of America, 1998.

Turkey Point Units 6 & 7
COL Application
Part 2 — FSAR

239. Dunbar, J.A., and Sawyer, D.S., "Implications of Continental Crust Extension for Plate Reconstruction: an Example from the Gulf of Mexico," *Tectonics*, v. 6, no. 6, pp. 739–755, 1987.
240. Ekstrom, G., and Dziewonski, A.M., "Evidence of Bias in Estimations of Earthquakes Size," *Nature*, v. 332, pp. 319–323, 1988.
241. Electric Power Research Institute (EPRI) and U.S. Department of Energy, *Program on Technology Innovation: Assessment of a Performance-Based Approach for Determining Seismic Ground Motions for New Plant Sites*, v. 2, *Seismic Hazard Results at 28 Sites*, Final Report, Report TR-1012045, August 2005.
242. Electric Power Research Institute (EPRI), *CEUS Ground Motion Project Final Report*, Report TR-1009684, December 2004.
243. Electric Power Research Institute (EPRI), *EQHAZARD Primer*, prepared by Risk Engineering for Seismicity Owners Group and Electric Power Research Institute, Report NP-6452-D, June 1989.
244. Electric Power Research Institute (EPRI), *Guidelines for Determining Design Basis Ground Motions*, Report TR-102293, Project 3302, Final Report, November 1993.
245. Electric Power Research Institute (EPRI), *Probabilistic Seismic Hazard Evaluation at Nuclear Plant Sites in the Central and Eastern United States*, Resolution of the Charleston Earthquake Issue, Report NP-6395-D, 1989.
246. Electric Power Research Institute (EPRI), *Seismic Hazard Methodology for the Central and Eastern United States*, v. 1, part 2, *Methodology* (rev. 1), Report NP-4726-A, Rev. 1, 1988.
247. Electric Power Research Institute (EPRI), *Seismic Hazard Methodology for the Central and Eastern United States*, v. 5–10, *Tectonic Interpretations*, Report NP-4726, July 1986.
248. Ellsworth, W.L., Matthews, M.V., Nadeau, R.M., Nishenko, S.P., Reasenber, P.A., and Simpson, R.W., *A Physically-Based Earthquake Recurrence Model for Estimation of Long-Term Earthquake Probabilities*, Report 99-522, p. 22, U.S. Geological Survey Open-File, 1999.

Turkey Point Units 6 & 7
COL Application
Part 2 — FSAR

249. Engdahl, E.R., Hilst, R.V.D., and Buland, R., "Global Teleseismic Earthquake Relocation with Improved Travel Times and Procedures for Depth Procedures," *Bulletin of the Seismological Society of America*, v. 88, no. 3, pp. 722–743, 1998.
250. Engdahl, E.H., and A. Villasenor, "Global Seismicity: 1900–1999," *International Handbook of Earthquake & Engineering Seismology*, International Association of Seismology and Physics of the Earth's Interior, Academic Press, pp. 665–690, 2002.
251. Frankel, A.D., Petersen, M.D., Mueller, C.S., Haller, K.M., Wheeler, R.L., Leyendecker, E.V., Wesson, R.L., Harmsen, S.C., Cramer, C.H., Perkins, D.M., and Rukstales, K.S., *Documentation for the 2002 Update of the National Seismic Hazard Maps*, Open-File Report 02-420, U.S. Geological Survey, 2002.
252. Frankel, A., Mueller, C., Barnhard, T., Perkins, D., Leyendecker, E.V., Dickman, N., Hanson, S., and Hopper, M., *National Seismic-Hazard Maps; Documentation*, Open-File Report 96-532, p. 110, U.S. Geological Survey, 1996.
253. Frohlich, C., and Davis, S.D., *Texas Earthquakes*, pp. 240–255, 2002.
254. Garcia, J., Slejko, D., Alvarez, L., Peruzza, L., and Rebez, A., "Seismic Hazard Maps for Cuba and Surrounding Areas," *Bulletin of the Seismological Society of America*, v. 93, no. 6, pp. 2563–2590, 2003.
255. Garcia, J., Slejko, D., Rebez, A., Santulin, M., and Alvarez, L., "Seismic Hazard Map for Cuba and Adjacent Areas Using the Spatially Smoothed Seismicity Approach," *Journal of Earthquake Engineering*, v. 12, pp. 173–196. 2008.
256. Gardner, J.K., and Knopoff, L., "Is the Sequence of Earthquakes in Southern California, with Aftershocks Removed, Poissonian?" *Bulletin of Seismological Society of America*, v. 64, pp.1363–1367, 1974.
257. AMEC Geomatrix, *Seismic Design Mapping, State of Oregon*, Final report prepared for the Oregon Department of Transportation, Salem, OR, 1995.
258. Giunta, G., Beccaluva, L., and Siena, F., "Caribbean Plate Margin Evolution: Constraints and Current Problems," *Caribbean Plate Tectonics*,

Turkey Point Units 6 & 7
COL Application
Part 2 — FSAR

Stratigraphic, Magmatic, Metamorphic, and Tectonic Events, *Geologica Acta*, M.A. Iturralde-Vinent and E.G. Lidiak (eds.) v. 4, no. 1-2, pp. 265–278, 2006.

259. Gomberg, J., and Wolf, L., “Possible Cause for an Improbable Earthquake: the 1997 Mw 4.9 Southern Alabama Earthquake and Hydrocarbon Recovery,” *Geology*, v. 27, no. 4, pp. 367–370, 1999.
260. Gordon, M.B., Mann, P., Caceres, D., and Flores, R., “Cenozoic Tectonic History of the North America-Caribbean Plate Boundary in Western Cuba,” *Journal of Geophysical Research*, v. 102, no. B5, pp. 10,055–10,082, 1997.
261. Grant, L.B., and Sieh, K., “Paleoseismic Evidence of Clustered Earthquakes on the San Andreas Fault in the Carrizo Plain, California,” *Journal of Geophysical Research*, v. 99, n. B4, pp. 6819–6841, 1994.
262. Hanks, T.C., and Bakun, W.H., “A Bilinear Source-Scaling Model for M-log A Observations of Continental Earthquakes,” *Bulletin of the Seismological Society of America*, v. 92, no. 5, pp. 1841–1846, 2002.
263. Idriss, I.M., and Sun, J.I., *SHAKE91: A Computer Program for Conducting Equivalent Linear Seismic Response Analyses of Horizontally Layered Soil Deposits*, Department of Civil and Environmental Engineering, Center for Geotechnical Modeling, University of California, 1992.
264. Incorporated Research Institutions for Seismology (IRIS), *Event Search*. Available at <http://www.iris.edu/quakes/eventsrch.htm>, accessed February 14, 2008.
265. International Seismological Centre (ISC), *Bulletin*, United Kingdom. Available at <http://www.isc.ac.uk>, accessed February 28, 2008.
266. Iturralde-Vinent, M.A., and Lidiak, E.G., “Caribbean Tectonic, Magmatic, Metamorphic, and Stratigraphic Events — Implications for Plate Tectonics,” *Geologica Acta*, v. 4, no. 1-2, pp. 1–5, 2006.
267. Johnston, A.C., “Seismic Moment Assessment of Earthquakes in Stable Continental Regions — III. New Madrid 1811–1812, Charleston 1886 and Lisbon 1755,” *Geophysical Journal International*, v. 126, pp. 314–344, 1996.

Turkey Point Units 6 & 7
COL Application
Part 2 — FSAR

268. Johnston, A.C., Coppersmith, K.J., Kanter, L.R., and Cornell, C.A., *The Earthquakes of Stable Continental Regions*, v. 1, *Assessment of Large Earthquake Potential*, Final Report, TR-102261-V1, Electric Power Research Institute (EPRI), 1994.
269. Kanamori, H., "The Energy Release in Great Earthquakes," *Journal of Geophysical Research*, v. 82, no. 20, pp. 2981–2987, 1977.
270. Kanter, L.R., "Tectonic Interpretation of Stable Continental Crust," *The Earthquakes of Stable Continental Regions*, v. 1, *Assessment of Large Earthquake Potential*, Electric Power Research Institute (EPRI), pp. 2.1–2.98, 1994.
271. Leroy, S., Mercier de Lepinay, B., Mauffret, A., and Pubellier, M., "Structural and Tectonic Evolution of the Eastern Cayman Trough (Caribbean Sea) from Seismic Reflection Data," *AAPG Bulletin*, v. 80, no. 2, pp. 222–247, American Association of Petroleum Geologists, 1996.
272. Madabhushi, S., and Talwani, P., "Fault Plane Solutions and Relocations of Recent Earthquakes in Middleton Place-Summerville Seismic Zone near Charleston, South Carolina," *Bulletin of the Seismological Society of America*, v. 83, no. 5, pp. 1442–1466, 1993.
273. Manaker, D.M., Calais, E., Freed, A.M., Ali, S.T., Przybylski, P., Mattioli, G., and Jansma, P., "Interseismic Plate Coupling and Strain Partitioning in the Northeastern Caribbean," *Geophysical Journal International*, in press 2008.
274. Mann, P., "Earthquakes Shakes the "Big Bend" Region of North America-Caribbean Boundary Zone," *Eos, Transactions, American Geophysical Union*, v. 85, no. 8, pp. 77–83, 2004.
275. Mann, P., Prentice, C.S., Burr, G., Pena, L.R., and Taylor, F.W., "Tectonic Geomorphology and Paleoseismology of the Septentrional Fault System, Dominican Republic," *Active Strike Slip and Collisional Tectonics of the Northern Caribbean Plate Boundary Zone*, J.F. Dolan and P. Mann (eds.), Special Paper 326, pp. 63–123, Geological Society of America, 1998.
276. Mann, P., Taylor, F.W., Edwards, R.L., Ku, T.H., "Actively Evolving Microplate Formation by Oblique Collision and Sideways Motion Along

Turkey Point Units 6 & 7
COL Application
Part 2 — FSAR

Strike-Slip Faults: and Example from the Northeastern Caribbean Plate Margin,” *Tectonophysics*, v. 246, pp. 1–69, 1995.

277. Mann, P., Tyburski, S.A., and Rosencrantz, E., “Neogene Development of the Swan Islands Restraining Bend Complex, Caribbean Sea,” *Geology*, v. 19, pp. 823–826, 1991.
278. Marple, R.T., and Talwani, P., “Evidence for a Buried Fault System in the Coastal Plain of the Carolinas and Virginia—Implications for Neotectonics in the Southeastern United States,” *Geological Society of America Bulletin*, v. 112, no. 2, pp. 200–220, 2000.
279. Martin, J.R., and Clough, G.W., “Seismic parameters from liquefaction evidence,” *Journal of Geotechnical Engineering*, v. 120, no. 8, pp. 1345–1361, 1994.
280. Matthews, M.V., Ellsworth, W.L., and Reasenber, P.A., “A Brownian Model for Recurrent Earthquakes,” *Bulletin of the Seismological Society of America*, v. 92, pp. 2233–2250, 2002.
281. McCann, W.R., and Pennington, W.D., “Seismicity, Large Earthquakes, and the Margin of the Caribbean Plate,” *The Geology of North America*, v. H, *The Caribbean Region*, G. Dengo and J.E. Case (eds.), The Geological Society of America, pp. 291–306, 1990.
282. McCann, W.R., “Estimating The Threat of Tsunamigenic Earthquakes and Earthquake Induced Landslide Tsunami the Caribbean,” *Caribbean Tsunami Hazard, Proceedings of the National Science Foundation Caribbean Tsunami Workshop*, A. Mercado-Irizarry and P. Liu (eds.), World Scientific Publishing Co., Singapore, pp. 43–65, 2006.
283. McCann, W.R., personal communication, 2008.
284. Middle America Seismograph Consortium (MIDAS), *MIDAS Catalog*. Available at <http://midas.uprm.edu>, accessed January 22, 2008.
285. Molnar, P., and Sykes, L.R., “Tectonics of the Caribbean and Middle America Regions from Focal Mechanisms and Seismicity,” *Geological Society of America Bulletin*, v. 80, pp. 1639–1684, 1969.
286. Moreno, B., Grandison, M., and Atakan, K., “Crustal Velocity Model along the Southern Cuban Margin: Implications for the Tectonic Regime at an

Turkey Point Units 6 & 7
COL Application
Part 2 — FSAR

Active Plate Boundary,” *Geophysical Journal International*, v. 151, pp. 632–645, 2002.

287. Motazedian, D., and Atkinson, G., *Ground-Motion relations for Puerto Rico*, Geological Soc. America, Special Paper 385, pp. 61–80, 2005.
288. National Earthquake Information Center (NEIC), “Eastern, Central, and Mountain States of the United States, 1350–1986 (SRA),” *Earthquake Search*. Available at http://neic.usgs.gov/neis/epic/epic_rect.html, accessed February 14, 2008.
289. National Earthquake Information Center (NEIC), “NEIC Mexico, Central America and Caribbean, 1900–1979 (MCAC),” *Earthquake Search*. Available at http://neic.usgs.gov/neis/epic/epic_rect.html, accessed February 14, 2008.
290. National Earthquake Information Center (NEIC), *Information Regarding Technical and Scientific Information on the September 10, 2006 Earthquake in the Gulf of Mexico*. Available at <http://earthquake.usgs.gov/eqcenter/equinthenews/2006/usslav/#scitech>, accessed September 13, 2006.
291. National Earthquake Information Center (NEIC), PDE-W Earthquake Summary for 10 February 2006 041717 event, U.S. Geological Survey. Available at <http://neic.usgs.gov/cgi-bin/epic/epic.cgi?SEARCHMETHOD=2&CLAT=0.0&CLON=0.0&CRAD=0.0&FILEFORMAT=1&SEARCHRANGE=HH&SLAT2=28&SLAT1=27&SLON2=-90&SLON1=-91&SUBMIT=Submit+Search&SYEAR=&SMONTH=&SDAY=&EYEAR=&EMONTH=&EDAY=&LMAG=&UMAG=&NDEP1=&NDEP2=&IO1=&IO2>, accessed on August 23, 2007.
292. National Earthquake Information Center (NEIC), *Preliminary Determination of Epicenter (PDE)*. Available at http://neic.usgs.gov/neis/epic/code_catalog.html, accessed February 14, 2008.
293. Nettles, M., “Analysis of the 10 February 2006 Gulf of Mexico Earthquake from Global and Regional Seismic Data,” *2007 Offshore Technology Conference: Houston, Texas*, p. OTC 19099, 2007.
294. NIST/SEMATECH, *E-Handbook of Statistical Methods*. Available at <http://www.itl.nist.gov/div898/handbook/>, accessed 11 January 2006.

Turkey Point Units 6 & 7
COL Application
Part 2 — FSAR

295. Obermeier, S.F., Weems, R.E., Jacobson, R.B., and Gohn, G.S., "Liquefaction Evidence for Repeated Holocene Earthquakes in the Coastal Region of South Carolina," *Annals of the New York Academy of Sciences*, v. 558, pp. 183–195, 1989.
296. Obermeier, S., "Liquefaction-Induced Features," *Paleoseismology*, ed. J. McCalpin, Academic Press, San Diego, 1996.
297. Osiecki, P.S., "Estimated Intensities and Probable Tectonic Sources of Historic (pre-1898) Honduran Earthquakes," *Bulletin of the Seismological Society of America*, v. 71, no. 3, pp. 865–881, 1981.
298. Perez, O.J., "Revised World Seismicity Catalog (1950–1997) for Strong ($M_s \geq 6$) Shallow ($H \leq 70$ Km) Earthquakes," *Bulletin of the Seismological Society of America*, v. 89, no. 2, pp. 335–341, 1999.
299. Perrot, J., Calais, E., and Mercier de Lepinay, B., "Tectonic and Kinematic Regime along the Northern Caribbean Plate Boundary: New Insights from Broad-Band Modeling of the May 25, 1992, $M_s = 6.9$ Cabo Cruz, Cuba, Earthquake," *Pure and Applied Geophysics*, v. 149, pp. 475–487, 1997.
300. Petersen, M.D., Frankel, A.D., Harmsen, S.C., Mueller, C.S., Haller, K.M., Wheeler, R.L., Wesson, R.L., Zeng, Y., Boyd, O.S., Perkins, D.M., Luco, N., Field, E.H., Wills, C.J., and Rukstales, K.S., *Documentation for the 2008 Update of the National Seismic Hazard Maps*, Open-File Report 2008-1128, U.S. Geological Survey, 2008.
301. Pindell, J.L., and Barrett, S.F., "Geologic Evolution of the Caribbean: a Plate Tectonic Perspective," *The Geology of North America*, v. H, *The Caribbean Region*, G. Dengo and J.E. Case (eds.), Geological Society of America, Boulder, CO, pp. 405–432, 1990.
302. Pindell, J., and Kennan, L., "Kinematic Evolution of the Gulf of Mexico and Caribbean," *GCSSEPM Foundation 21st Annual Research Conference Transactions, Petroleum Systems of Deep-Water Basins*, pp. 193–220, 2001.
303. Pindell, J., Kennan, L., Stanek, K.P., Maresch, W.V., and Draper, G., "Foundations of Gulf of Mexico and Caribbean Evolution: Eight Controversies Resolved in M.A. Iturralde-Vinent and E.G. Lidiak (eds.)

Turkey Point Units 6 & 7
COL Application
Part 2 — FSAR

Caribbean Plate Tectonics, Stratigraphic, Magmatic, Metamorphic, and Tectonic Events,” *Geologica Acta*, v. 4, no. 1-2, pp. 303–341, 2006.

304. Prentice, C.S., Mann, P., Pea, L.R., and Burr, G., “Slip Rate and Earthquake Recurrence Along the Central Septentrional Fault, North American-Caribbean Plate Boundary, Dominican Republic,” *Journal of Geophysical Research*, v. 108, 2003.
305. Puerto Rico Seismic Network (PRSN), *On-line Puerto Rico Seismic Network*. Available at <http://temblor.uprm.edu/cgi-bin/new-search.cgi>, accessed February 8, 2008.
306. Rathje, E., and Ozbey, C.M., “Site-Specific Validation of Random Vibration Theory-Based Seismic Site Response Analysis,” *Journal of Geotechnical and Geoenvironmental Engineering*, v. 132, no. 7, July, pp. 911–922, 2006.
307. Rinehart, W., Ganse, R., and Teik, P., National Geophysical Data Center (NGDC); Arnold, E., and Stover, C., U.S. Geological Survey (USGS), and Smith, R.H., (CIRES), National Earthquake Information Center (NEIC), *Seismicity of Middle America, National Geophysical Data Center and National Earthquake Information Service*, U.S. Geological Survey, 1982. Available at http://neic.usgs.gov/neis/epic/code_catalog.html, accessed February 15, 2008.
308. Risk Engineering, Inc., *Technical Basis for Revision of Regulatory Guidance on Design Ground Motions: Hazard- and Risk-Consistent Ground Motion Spectra Guidelines*, NUREG/CR-6728, U.S. Nuclear Regulatory Commission, Washington, D.C., 2001.
309. Rockwell, T.K., Lindvall, S., Herzberg, M., Murbach, D., Dawson, T., and Berger, G., “Paleoseismology of the Johnson Valley, Kickapoo, and Homestead Valley Faults: Clustering of Earthquakes in the Eastern California Shear Zone,” *Bulletin of the Seismological Society of America*, v. 90, no. 5, pp. 1200–1236, 2000.
310. Rosencrantz, E., and Mann, P., “SeaMARC II Mapping of Transform Faults in the Cayman Trough, Caribbean Sea,” *Geology*, v. 19, pp. 690–693, 1991.

Turkey Point Units 6 & 7
COL Application
Part 2 — FSAR

311. Rosencrantz, E., Ross, M.I., and Sclater, J.G., "Age and Spreading History of the Cayman Trough as Determined from Depth, Heat Flow, And Magnetic Anomalies," *Journal of Geophysical Research*, v. 93, pp. 2141–2157, 1988.
312. Saura, E., Verges, J., Brown, D., Lukito, P., Soriano, S., Torrescusa, S., Garcia, R., Sanchez, J.R., Sosa, C., and Tenreyo, R., "Structural and Tectonic Evolution of Western Cuba Fold and Thrust Belt," *Tectonics*, v. 27, pp. 1–22, 2008.
313. Savage, J.C., "Criticism of Some Forecasts of the National Earthquake Evaluation Council," *Bulletin of the Seismological Society of America*, v. 81, n. 3, pp. 862–881, 1991.
314. Savage, M.K., and Depolo, M., "Foreshock Probabilities in the Western Great-Basin Eastern Sierra Nevada," *Bulletin of Seismological Society of America*, v. 83, pp.1910–1938, 1993.
315. Sawyer, D.S., Buffler, R.T., and Pilger, R.H., Jr., "The Crust Under the Gulf of Mexico Basin," *The Geology of North America*, v. J, *The Gulf of Mexico Basin*, The Geological Society of America, pp. 53–72, 1991.
316. Schnabel, S., and Seed, H. B., *Shake — A Computer Program for Earthquake Response Analysis of Horizontally Layered Sites*, Report No. 72-12, Earthquake Engineering Research Center (EERC), December 1972.
317. Seed, H.B., Wong, R.T., Idriss, I.M., and Tokimatsu, K., "Moduli and Damping Factors for Dynamic Analysis of Cohesionless Soils," *Journal of Soil Mechanics and Foundations Division*, vol. SM11, no. 112, pp. 1016-1032, ASCE, 1986.
318. Senior Seismic Hazard Analysis Committee (SSHAC), *Recommendations for Probabilistic Seismic Hazard Analysis- Guidance on Uncertainty and Use of Experts*, Prepared by SSHAC, NUREG/CR-6372, 1997.
319. Silva, W.J., Abrahamson, N., Toro, G., and Costantino, C., "Probabilistic Models of Site Velocity Profiles for Generic and Site-Specific Ground Motion Amplification Studies," (appendix), *Description and Validation of the Stochastic Ground Motion Model*, Associated Universities, Inc., Upton,

Turkey Point Units 6 & 7
COL Application
Part 2 — FSAR

New York, 1996. Report submitted to Brookhaven National Laboratory, contract No. 770573.

320. Silva, W.J., Abrahamson, N., Toro, G., and Costantino, C., "Recommendations for Uncertainty Estimates in Shear Modulus Reduction and Hysteretic Damping Relationships," (appendix), *Description and Validation of the Stochastic Ground Motion Model*, 1996.
321. Deleted
322. Deleted
323. Talwani, P., and Schaeffer, W.T., "Recurrence Rates of Large Earthquakes in the South Carolina Coastal Plain Based on Paleoliquefaction Data," *Journal of Geophysical Research*, v. 106, no. B4, pp. 6621–6642, 2001.
324. Tarr, A.C., Talwani, P., Rhea, S., Carver, D., and Amick, D., "Results of Recent South Carolina Seismological Studies," *Bulletin of the Seismological Society of America*, v. 71, no. 6, pp. 1883–1902, 1981.
325. Tarr, A.C., and Rhea, B.S., "Seismicity Near Charleston, South Carolina, March 1973 to December 1979," *Studies Related to the Charleston, South Carolina Earthquake of 1886 Tectonics and Seismicity*, Professional Paper 1313:R1-R17, U.S. Geological Survey, 1983.
326. Ten Brink, U., Coleman, D.F., and Dillon, W.P., "The Nature of the Crust under Cayman Rough from Gravity," *Marine and Petroleum Geology*, v. 19, pp. 971–987, 2002.
327. Toiran, B.M., "The Crustal Structure of Cuba Derived from Receiver Function Analysis," *Journal of Seismology*, v. 7, pp. 359–375, 2003.
328. Tuttle, M.P., "The Use of Liquefaction Features in Paleoseismology: Lessons Learned in the New Madrid Seismic Zone, Central United States," *Journal of Seismology*, v. 5, pp. 361–380, 2001.
329. Tuttle, M.P., Prentice, C.S., Dyer-Williams, K., Pena, L.R., and Burr, G., "Late Holocene Liquefaction Features in the Dominican Republic: a Powerful Tool for Earthquake Hazard Assessment in the Northeast Caribbean," *Bulletin of the Seismological Society of America*, v. 93, no. 1, pp. 27–46, 2003.

Turkey Point Units 6 & 7
COL Application
Part 2 — FSAR

330. U.S. Geological Survey, *Preliminary Earthquake Report Magnitude 6.0 — Gulf of Mexico*, 2006 September 10 14:56:07 UTC. Available at <http://earthquake.usgs.gov/eqcenter/eqinthenews/2006/usslav/index.php>, accessed on May 4, 2007.
331. van Dusen, S.R., and Doser, D., "Faulting Processes of Historic (1917–1962) M6.0 Earthquakes along the North-Central Caribbean Margin," *Pure and Applied Geophysics*, v. 157, pp. 719–736, 2000.
332. Villasenor, A. and Engdahl, E.R., "Systematic Relocation of Early Instrumental Seismicity: Earthquakes in the International Seismological Summary for 1960–1963," *Bulletin of the Seismological Society of America*, v. 97, no. 6, pp. 1820–1832, December 2007.
333. Villasenor, A., Bergman, E.A., Boyd, T.M., Engdahl, E.R., Frazier, D.W., Harden, M.M., Orth, J.L., Parkes, R.L., and Shedlock, K.M., "Toward a Comprehensive Catalog of Global Historical Seismicity," *Eos, Transactions, American Geophysical Union*, v. 78, no. 50, 1997.
334. Wells, D.L., and Coppersmith, K.J., "New Empirical Relationships Among Magnitude, Rupture Length, Rupture Width, Rupture Area, and Surface Displacement," *Bulletin Seismological Society of America*, v. 84, no. 4, pp. 974–1002, 1994.
335. Wiggins-Grandison, M.D., and Atakan, K., "Seismotectonics of Jamaica," *Geophysical Journal International*, v. 160, pp. 573–580, 2005.
336. Working Group on California Earthquake Probabilities (WGCEP), "Seismic Hazards in Southern California: Probable earthquakes, 1994 to 2024," *Bulletin of the Seismological Society of America*, v. 85, pp. 379–439, 1995.
337. Working Group on California Earthquake Probabilities (WGCEP), *Earthquake Probabilities in the San Francisco Bay Region: 2002–2031*, Open-File Report 03-2134, U.S. Geological Survey, 2003.
338. Wyssession, M., Wilson, J., Bartko, L., and Sakata, R., "Intraplate Seismicity in the Atlantic Ocean Basin: a Teleseismic Catalog," *Bulletin of Seismological Society of America*, v. 85, no. 3, pp. 755–774, June 1995.
339. Wyss, M., "Estimating Maximum Expectable Magnitude of Earthquakes from Fault Dimensions," *Geology*, v. 7, no. 7, pp. 366–340, 1979.

Turkey Point Units 6 & 7
COL Application
Part 2 — FSAR

340. National Earthquake Information Center (NEIC), "Significant U.S. Earthquakes, 1568–1989 (USHIS)," *Earthquake Search*. Available at http://neic.usgs.gov/neis/epic/epic_rect.html, accessed February 14, 2008.
341. Chapman, M., Virginia Tech Department of Geosciences, personal communication, February 11, 2008.
-

Turkey Point Units 6 & 7
COL Application
Part 2 — FSAR

PTN COL 2.5-2

Table 2.5.2-201
Conversion between Body-Wave (m_b) and Moment (M_w) Magnitudes^(a)

Convert	To	Convert	To
m_b	M_w	M_w	m_b
4.00	3.77	4.00	4.28
4.10	3.84	4.10	4.41
4.20	3.92	4.20	4.54
4.30	4.00	4.30	4.66
4.40	4.08	4.40	4.78
4.50	4.16	4.50	4.90
4.60	4.24	4.60	5.01
4.70	4.33	4.70	5.12
4.80	4.42	4.80	5.23
4.90	4.50	4.90	5.33
5.00	4.59	5.00	5.43
5.10	4.69	5.10	5.52
5.20	4.78	5.20	5.61
5.30	4.88	5.30	5.70
5.40	4.97	5.40	5.78
5.50	5.08	5.50	5.87
5.60	5.19	5.60	5.95
5.70	5.31	5.70	6.03
5.80	5.42	5.80	6.11
5.90	5.54	5.90	6.18
6.00	5.66	6.00	6.26
6.10	5.79	6.10	6.33
6.20	5.92	6.20	6.40
6.30	6.06	6.30	6.47
6.40	6.20	6.40	6.53
6.50	6.34	6.50	6.60
6.60	6.49	6.60	6.66
6.70	6.65	6.70	6.73
6.80	6.82	6.80	6.79
6.90	6.98	6.90	6.85
7.00	7.16	7.00	6.91
7.10	7.33	7.10	6.97
7.20	7.51	7.20	7.03
7.30	7.69	7.30	7.09
7.40	7.87	7.40	7.15
7.50	8.04	7.50	7.20
—	—	7.60	7.26
—	—	7.70	7.32
—	—	7.80	7.37
—	—	7.90	7.43
—	—	8.00	7.49

(a) Average of relations given by [References 210, 244, and 252](#).

Turkey Point Units 6 & 7
COL Application
Part 2 — FSAR

PTN COL 2.5-2

Table 2.5.2-202 (Sheet 1 of 25)
Seismicity Catalog for the Phase 1 Investigation Region [22°N to 35°N, 100°W to 65°W] for which the Events are Rmb Magnitude Greater than or Equal to 3.0 or Intensity [Int] Greater than or Equal to IV(4)

Catalog Reference ^(a)	Year	Month	Day	Hour	Min	Sec	Lat	Lon	Depth (km)	Int	Emb	Smb	Rmb	Epicenter (km) ^(b)
SEUSN	1698	3	5	0	0	00.00	32.900	-80.000	0	3	2.70	0.56	3.06	828
SEUSN	1699	12	25	19	0	00.00	34.900	-90.300	0	4	3.10	0.56	3.46	1421
SEUSN	1754	5	19	16	0	00.00	32.900	-80.000	0	3	2.70	0.56	3.06	828
SEUSN	1755	11	0	0	0	00.00	33.400	-79.300	0	3	2.70	0.56	3.06	888
SEUSN	1757	2	7	0	0	00.00	32.900	-80.000	0	3	2.70	0.56	3.06	828
CUBA	1762	11	13	0	0	00.00	22.980	-82.370	10	—	3.97	0.56	4.33	339
CUBA	1777	7	7	9	29	00.00	22.830	-82.030	10	—	4.41	0.56	4.77	333
EPRIm	1780	2	6	0	0	00.00	30.400	-87.200	0	6	4.30	0.55	4.65	869
EPRIm	1799	4	4	0	0	00.00	32.900	-80.000	0	5	3.70	0.56	4.06	828
CUBA	1810	0	0	0	0	00.00	23.130	-82.400	10	—	3.97	0.56	4.33	328
CUBA	1812	0	0	0	0	00.00	23.050	-81.580	10	—	3.97	0.56	4.33	290
EPRIm	1820	9	3	8	30	00.00	33.400	-79.300	0	4	3.11	0.56	3.47	888
CUBA	1824	0	0	0	0	00.00	22.810	-80.080	10	—	3.97	0.56	4.33	289
SEUSN	1843	2	7	15	0	00.00	32.900	-80.000	0	3	2.70	0.56	3.06	828
CUBA	1843	2	21	0	0	00.00	23.130	-82.400	10	—	4.41	0.56	4.77	328
CUBA	1843	3	5	0	0	00.00	23.050	-81.580	10	—	3.53	0.56	3.89	290
SEUSN	1843	4	11	0	0	00.00	34.200	-80.600	0	3	2.70	0.56	3.06	972
CUBA	1846	10	10	0	0	00.00	23.000	-82.080	10	—	3.75	0.56	4.11	320
FD02	1847	2	14	2	0	00.00	29.600	-98.000	0	5	3.60	0.56	3.96	>1609
CUBA	1849	0	0	0	0	00.00	22.710	-83.060	15	—	4.12	0.56	4.48	407
CUBA	1849	8	30	0	0	00.00	22.150	-80.450	10	—	3.97	0.56	4.33	361
CUBA	1852	0	0	0	0	00.00	23.050	-81.580	10	—	4.41	0.56	4.77	290
CUBA	1852	7	7	14	59	00.00	22.420	-79.970	10	—	3.97	0.56	4.33	333
EPRIm	1853	5	20	0	0	00.00	34.000	-81.200	0	6	4.30	0.55	4.65	953
CUBA	1854	9	9	0	0	00.00	23.050	-81.580	10	—	4.41	0.56	4.77	290
CUBA	1857	7	7	0	0	00.00	22.810	-80.080	10	—	3.75	0.56	4.11	289
EPRIm	1857	12	19	14	4	00.00	32.900	-80.000	0	5	3.70	0.56	4.06	828

Turkey Point Units 6 & 7
COL Application
Part 2 — FSAR

PTN COL 2.5-2

Table 2.5.2-202 (Sheet 2 of 25)
Seismicity Catalog for the Phase 1 Investigation Region [22°N to 35°N, 100°W to 65°W] for which the Events are Rmb Magnitude Greater than or Equal to 3.0 or Intensity [Int] Greater than or Equal to IV(4)

Catalog Reference ^(a)	Year	Month	Day	Hour	Min	Sec	Lat	Lon	Depth (km)	Int	Emb	Smb	Rmb	Epicenter (km) ^(b)
CUBA	1858	3	7	12	29	00.00	22.480	-79.550	10	—	4.26	0.56	4.62	334
CUBA	1858	8	14	6	29	00.00	22.480	-79.550	10	—	4.26	0.56	4.62	334
CUBA	1859	8	15	2	59	00.00	22.480	-79.550	10	—	3.97	0.56	4.33	334
CUBA	1859	10	4	0	0	00.00	23.130	-82.400	10	—	3.97	0.56	4.33	328
EPRIm	1860	1	19	23	0	00.00	32.900	-80.000	0	5	3.70	0.56	4.06	828
SEUSN	1860	10	0	0	0	00.00	32.900	-80.000	0	3	2.70	0.56	3.06	828
SEUSN	1860	10	22	0	0	00.00	34.200	-82.400	0	3	2.70	0.56	3.06	992
SEUSN	1860	12	19	0	0	00.00	32.900	-80.000	0	3	2.70	0.56	3.06	828
CUBA	1861	5	27	13	59	00.00	22.810	-80.080	10	—	3.75	0.56	4.11	289
CUBA	1861	6	27	0	0	00.00	22.810	-80.080	10	—	4.48	0.56	4.84	289
CUBA	1862	0	0	0	0	00.00	23.130	-82.400	10	—	3.53	0.56	3.89	328
CUBA	1862	8	0	0	0	00.00	23.130	-82.400	10	—	3.53	0.56	3.89	328
CUBA	1868	3	25	0	0	00.00	23.130	-82.400	10	—	4.41	0.56	4.77	328
CUBA	1868	5	1	0	0	00.00	22.360	-79.580	10	—	3.97	0.56	4.33	346
EPRIm	1869	0	0	0	0	00.00	32.900	-80.000	0	4	3.11	0.56	3.47	828
EPRIm	1871	4	16	5	0	00.00	34.300	-78.000	0	5	3.70	0.56	4.06	1008
CUBA	1872	0	0	0	0	00.00	22.910	-81.860	10	—	3.53	0.56	3.89	317
CUBA	1872	0	0	0	0	00.00	22.710	-83.060	15	—	3.68	0.56	4.04	407
CUBA	1872	6	0	0	0	00.00	22.510	-79.470	10	—	4.77	0.56	5.13	333
EPRIm	1872	6	17	20	0	00.00	33.100	-83.300	0	5	3.70	0.56	4.06	896
EPRIm	1873	5	1	4	30	00.00	30.200	-97.700	0	4	2.81	0.56	3.17	>1609
CUBA	1873	8	12	3	29	00.00	22.480	-79.550	10	—	4.99	0.56	5.35	334
SEUSN	1875	7	28	23	5	00.00	33.100	-83.300	0	3	2.70	0.56	3.06	896
EPRIm	1875	11	2	2	55	00.00	33.800	-82.500	0	6	4.30	0.55	4.65	950
SEUSN	1876	10	0	0	0	00.00	32.900	-80.000	0	3	2.70	0.56	3.06	828
EPRIm	1876	12	12	0	0	00.00	32.900	-80.000	0	4	3.11	0.56	3.47	828
EPRIm	1879	1	13	4	45	00.00	29.500	-82.000	0	6	4.30	0.55	4.65	479
CUBA	1879	9	21	0	0	00.00	22.710	-83.060	15	—	4.12	0.56	4.48	407
SEUSN	1879	10	27	1	0	00.00	34.400	-81.100	0	3	2.70	0.56	3.06	997

Turkey Point Units 6 & 7
COL Application
Part 2 — FSAR

PTN COL 2.5-2

Table 2.5.2-202 (Sheet 3 of 25)
Seismicity Catalog for the Phase 1 Investigation Region [22°N to 35°N, 100°W to 65°W] for which the Events are Rmb Magnitude Greater than or Equal to 3.0 or Intensity [Int] Greater than or Equal to IV(4)

Catalog Reference ^(a)	Year	Month	Day	Hour	Min	Sec	Lat	Lon	Depth (km)	Int	Emb	Smb	Rmb	Epicenter (km) ^(b)
CUBA	1880	1	23	4	39	00.00	22.700	-83.000	15	—	6.09	0.56	6.45	404
CUBA	1880	6	12	1	29	00.00	22.420	-79.630	10	—	3.97	0.56	4.33	339
EPRIm	1882	1	8	22	10	00.00	34.600	-76.500	0	4	3.11	0.56	3.47	1081
EPRIm	1882	10	22	22	15	00.00	33.600	-95.600	0	8	5.39	0.28	5.48	>1609
EPRIm	1884	1	18	13	0	00.00	34.300	-78.000	0	5	3.70	0.56	4.06	1008
SEUSN	1884	3	31	10	0	00.00	33.100	-83.300	0	3	2.70	0.56	3.06	896
EPRIm	1885	10	17	22	30	00.00	33.000	-83.000	0	4	3.11	0.56	3.47	877
CUBA	1886	0	0	0	0	00.00	22.810	-80.080	10	—	3.97	0.56	4.33	289
EPRIm	1886	2	5	1	0	00.00	32.800	-88.000	0	5	3.70	0.56	4.06	1104
CUBA	1886	8	31	22	20	00.00	22.940	-80.010	15	—	4.48	0.56	4.84	276
EPRIm	1886	9	1	0	0	00.00	30.400	-81.700	0	4	3.11	0.56	3.47	565
EPRIm	1886	9	1	2	51	00.00	32.900	-80.000	0	X ^(c)	6.75	0.20	6.80	828
CUBA	1886	9	3	0	0	00.00	22.940	-80.010	15	—	4.19	0.56	4.55	276
CUBA	1887	0	0	0	0	00.00	22.900	-83.330	20	—	4.77	0.56	5.13	411
SEUSN	1887	1	5	17	57	00.00	30.150	-97.060	0	5	3.60	0.56	3.96	>1609
SEUSN	1887	1	31	22	14	00.00	30.530	-96.300	0	4	3.10	0.56	3.46	>1609
CUBA	1889	4	12	2	19	00.00	22.810	-80.080	10	—	3.97	0.56	4.33	289
EPRIm	1891	1	8	6	0	00.00	31.700	-95.200	0	7	3.70	0.30	3.80	1606
EPRIm	1891	10	13	5	55	00.00	32.900	-80.000	0	4	3.11	0.56	3.47	828
EPRIm	1893	6	21	7	7	00.00	30.400	-81.700	0	4	3.11	0.56	3.47	565
EPRIm	1893	7	5	8	10	00.00	32.900	-80.000	0	4	3.11	0.56	3.47	828
CUBA	1894	7	29	0	0	00.00	22.020	-75.840	15	—	4.19	0.56	4.55	590
EPRIm	1895	10	6	6	25	00.00	32.900	-80.000	0	4	3.11	0.56	3.47	828
CUBA	1896	0	0	0	0	00.00	22.750	-83.560	20	—	4.77	0.56	5.13	440
CUBA	1896	4	25	0	0	00.00	22.510	-79.470	10	—	4.55	0.56	4.92	333
SEUSN	1897	5	9	0	0	00.00	33.900	-81.600	0	3	2.70	0.56	3.06	946
EPRIm	1898	1	27	1	35	00.00	34.600	-90.600	0	4	3.11	0.56	3.47	1417
EPRIm	1899	3	10	5	45	00.00	32.900	-80.000	0	4	3.11	0.56	3.47	828
CUBA	1899	9	16	0	0	00.00	22.710	-83.060	15	—	4.12	0.56	4.48	407

Turkey Point Units 6 & 7
COL Application
Part 2 — FSAR

PTN COL 2.5-2

Table 2.5.2-202 (Sheet 4 of 25)
Seismicity Catalog for the Phase 1 Investigation Region [22°N to 35°N, 100°W to 65°W] for which the Events are Rmb Magnitude Greater than or Equal to 3.0 or Intensity [Int] Greater than or Equal to IV(4)

Catalog Reference ^(a)	Year	Month	Day	Hour	Min	Sec	Lat	Lon	Depth (km)	Int	Emb	Smb	Rmb	Epicenter (km) ^(b)
SEUSN	1899	11	4	0	0	00.00	34.300	-82.800	0	3	2.70	0.56	3.06	1011
EPRIm	1899	12	4	12	48	00.00	32.900	-80.000	0	4	3.11	0.56	3.47	828
SEUSN	1899	12	19	0	0	00.00	34.300	-81.400	0	3	2.70	0.56	3.06	988
EPRIm	1900	10	31	16	15	00.00	30.400	-81.700	0	5	3.70	0.56	4.06	565
EPRIm	1901	12	2	0	26	00.00	32.900	-80.000	0	4	3.11	0.56	3.47	828
SEUSN	1902	6	10	0	0	00.00	34.200	-81.700	0	3	2.70	0.56	3.06	981
FD02	1902	10	9	19	0	00.00	30.100	-97.600	0	5	3.90	0.56	4.26	>1609
CUBA	1903	0	0	0	0	00.00	22.680	-81.110	18	—	4.70	0.56	5.06	312
EPRIm	1903	1	24	1	0	00.00	32.900	-80.000	0	4	3.11	0.56	3.47	828
SEUSN	1903	1	24	1	15	00.00	32.100	-81.100	0	6	4.10	0.56	4.46	742
CUBA	1905	0	0	0	0	00.00	22.750	-83.700	20	—	4.26	0.56	4.62	450
EPRIm	1905	2	3	0	0	00.00	30.500	-91.100	0	5	3.70	0.56	4.06	1194
SEUSN	1905	9	4	9	0	00.00	27.500	-82.600	0	3	2.70	0.56	3.06	321
CUBA	1905	10	12	0	0	00.00	23.050	-82.010	10	—	3.97	0.56	4.33	312
CUBA	1906	0	0	0	0	00.00	22.650	-83.200	15	—	3.53	0.56	3.89	421
CUBA	1906	1	15	0	0	00.00	22.600	-80.330	10	—	4.04	0.56	4.40	311
CUBA	1906	5	6	20	29	00.00	22.710	-83.060	15	—	3.68	0.56	4.04	407
CUBA	1906	5	8	0	0	00.00	22.710	-83.060	15	—	3.68	0.56	4.04	407
CUBA	1906	5	26	20	29	00.00	22.710	-83.060	15	—	3.68	0.56	4.04	407
CUBA	1906	6	5	5	59	00.00	22.880	-80.380	10	—	4.48	0.56	4.84	280
CUBA	1906	10	0	0	0	00.00	22.200	-84.090	20	—	4.12	0.56	4.48	521
CUBA	1907	2	19	0	0	00.00	23.130	-82.400	10	—	4.41	0.56	4.77	328
CUBA	1907	4	15	0	0	00.00	23.130	-82.400	10	—	3.97	0.56	4.33	328
EPRIm	1907	4	19	8	30	00.00	32.900	-80.000	0	5	3.70	0.56	4.06	828
CUBA	1908	1	0	0	0	00.00	22.480	-79.550	10	—	3.82	0.56	4.19	334
EPRIm	1909	10	8	10	0	00.00	34.900	-85.000	0	4	3.11	0.56	3.47	1142
CUBA	1910	0	0	0	0	00.00	22.630	-83.370	15	—	3.90	0.56	4.26	435
FD02	1910	5	8	17	18	00.00	30.100	-96.000	0	4	3.80	0.56	4.16	>1609
EPRIm	1911	3	31	16	57	00.00	34.000	-91.800	0	7	4.10	0.30	4.20	1458

Turkey Point Units 6 & 7
COL Application
Part 2 — FSAR

PTN COL 2.5-2

Table 2.5.2-202 (Sheet 5 of 25)
Seismicity Catalog for the Phase 1 Investigation Region [22°N to 35°N, 100°W to 65°W] for which the Events are Rmb Magnitude Greater than or Equal to 3.0 or Intensity [Int] Greater than or Equal to IV(4)

Catalog Reference ^(a)	Year	Month	Day	Hour	Min	Sec	Lat	Lon	Depth (km)	Int	Emb	Smb	Rmb	Epicenter (km) ^(b)
EPRIm	1911	3	31	18	10	00.00	33.800	-92.200	0	4	3.70	0.30	3.80	1474
CUBA	1912	5	6	0	0	00.00	22.510	-79.690	10	—	3.97	0.56	4.33	328
EPRIm	1912	6	12	10	30	00.00	32.900	-80.000	0	7	4.90	0.56	5.26	828
EPRIm	1912	6	20	0	0	00.00	32.000	-81.000	0	5	3.70	0.56	4.06	730
EPRIm	1912	10	23	1	15	00.00	32.700	-83.500	0	4	3.11	0.56	3.47	861
CUBA	1913	0	0	0	0	00.00	22.340	-84.390	0	—	4.26	0.56	4.62	533
CUBA	1913	0	0	0	0	00.00	22.150	-80.450	10	—	3.97	0.56	4.33	361
EPRIm	1913	1	1	18	28	00.00	34.700	-81.700	0	8	4.94	0.30	5.04	1036
EPRIm	1913	3	13	5	0	00.00	34.500	-85.000	0	4	3.11	0.56	3.47	1101
CUBA	1914	0	0	0	0	00.00	22.150	-80.450	10	—	4.26	0.56	4.62	361
EPRIm	1914	3	5	20	5	00.00	33.500	-83.500	0	6	4.30	0.55	4.65	945
EPRIm	1914	3	7	1	20	00.00	34.200	-79.800	0	4	3.11	0.56	3.47	973
CUBA	1914	5	27	6	59	00.00	22.710	-82.280	10	—	3.97	0.56	4.33	358
CUBA	1914	5	28	3	29	00.00	22.710	-82.280	10	—	4.41	0.56	4.77	358
EPRIm	1914	12	30	1	0	00.00	30.500	-95.900	0	4	3.40	0.30	3.50	>1609
EPRIm	1916	3	2	5	2	00.00	34.500	-82.700	0	4	3.11	0.56	3.47	1031
EPRIm	1916	10	18	22	3	40.00	33.500	-86.200	0	7	4.90	0.56	5.26	1059
EPRIm	1917	6	30	1	23	00.00	32.700	-87.500	0	5	3.70	0.56	4.06	1063
EPRIm	1918	10	4	9	21	00.00	35.000	-91.100	0	4	4.30	0.30	4.40	1482
CUBA	1920	0	0	0	0	00.00	22.510	-79.710	10	—	3.82	0.56	4.19	327
CUBA	1921	9	23	0	0	00.00	22.910	-82.610	10	—	3.97	0.56	4.33	360
EPRIm	1923	3	27	8	0	00.00	34.600	-89.700	0	4	3.80	0.30	3.90	1358
SEUSN	1923	10	28	16	15	00.00	34.900	-88.100	0	3	2.90	0.56	3.26	1288
EPRIm	1923	12	31	20	6	00.00	34.800	-82.500	0	4	3.11	0.56	3.47	1060
EPRIm	1924	10	20	8	30	00.00	35.000	-82.600	0	5	3.70	0.56	4.06	1084
CUBA	1925	0	0	0	0	00.00	22.350	-83.500	10	—	3.97	0.56	4.33	466
CUBA	1926	0	0	0	0	00.00	22.600	-80.330	10	—	4.04	0.56	4.40	311
CUBA	1927	1	0	0	0	00.00	22.770	-81.020	18	—	4.34	0.56	4.70	301
EPRIm	1927	6	16	12	0	00.00	34.700	-86.000	0	5	3.70	0.30	3.80	1163

Turkey Point Units 6 & 7
COL Application
Part 2 — FSAR

PTN COL 2.5-2

Table 2.5.2-202 (Sheet 6 of 25)
Seismicity Catalog for the Phase 1 Investigation Region [22°N to 35°N, 100°W to 65°W] for which the Events are Rmb Magnitude Greater than or Equal to 3.0 or Intensity [Int] Greater than or Equal to IV(4)

Catalog Reference ^(a)	Year	Month	Day	Hour	Min	Sec	Lat	Lon	Depth (km)	Int	Emb	Smb	Rmb	Epicenter (km) ^(b)
EPRIm	1927	10	8	12	56	00.00	35.000	-85.300	0	5	3.70	0.56	4.06	1164
EPRIm	1927	11	13	16	21	00.00	32.300	-90.200	0	4	3.80	0.30	3.90	1224
EPRIm	1927	11	23	0	50	00.00	33.900	-78.000	0	4	3.11	0.56	3.47	965
EPRIm	1927	12	15	4	30	00.00	28.900	-89.400	0	4	3.80	0.30	3.90	973
SEUSN	1928	5	23	10	15	00.00	30.800	-83.300	0	3	2.70	0.56	3.06	661
CUBA	1928	6	5	0	0	00.00	22.770	-81.020	18	—	3.90	0.56	4.26	301
CUBA	1929	0	0	0	0	00.00	22.290	-84.290	20	—	3.82	0.56	4.19	529
EPRIm	1929	1	3	12	5	00.00	33.900	-80.300	0	4	3.11	0.56	3.47	938
SEUSN	1929	6	13	14	44	00.00	30.700	-88.000	0	3	2.90	0.56	3.26	950
EPRIm	1929	7	28	17	0	00.00	28.900	-89.400	0	4	3.80	0.30	3.90	973
EPRIm	1929	10	28	2	15	00.00	34.300	-82.400	0	4	3.11	0.56	3.47	1003
EPRIm	1930	7	19	18	53	00.00	25.800	-81.400	0	5	3.70	0.56	4.06	114
EPRIm	1930	10	19	12	12	00.00	30.100	-91.000	0	6	4.20	0.30	4.30	1167
EPRIm	1930	11	16	12	30	00.00	34.300	-92.800	0	5	3.20	0.30	3.30	1552
EPRIm	1930	12	10	0	2	00.00	34.300	-82.400	0	4	3.11	0.56	3.47	1003
EPRIm	1930	12	26	3	0	00.00	34.500	-80.300	0	4	3.11	0.56	3.47	1005
CUBA	1931	0	0	0	0	00.00	22.230	-79.330	10	—	3.97	0.56	4.33	366
EPRIm	1931	5	5	12	18	00.00	33.700	-86.600	0	6	4.30	0.55	4.65	1098
CUBA	1931	8	12	18	0	00.00	22.810	-80.080	10	—	3.97	0.56	4.33	289
ISSv	1931	8	16	8	6	18.00	28.800	-65.200	0	—	5.76	0.10	5.77	1538
EPRIm	1931	12	17	3	36	00.00	34.100	-89.800	0	6	4.60	0.30	4.70	1325
CUBA	1932	0	0	0	0	00.00	22.980	-80.590	10	—	3.75	0.56	4.11	270
CUBA	1932	0	0	0	0	00.00	23.130	-82.400	10	—	3.97	0.56	4.33	328
EPRIm	1932	4	9	10	15	00.00	31.700	-96.400	0	6	3.50	0.30	3.60	>1609
CUBA	1933	0	0	0	0	00.00	22.050	-79.460	10	—	3.97	0.56	4.33	382
EPRIm	1933	6	9	11	30	00.00	33.300	-83.500	0	4	3.11	0.56	3.47	924
EPRIm	1933	12	23	9	40	00.00	32.900	-80.000	0	5	3.70	0.56	4.06	828
CUBA	1934	0	0	0	0	00.00	22.660	-80.190	10	—	3.97	0.56	4.33	305
EPRIm	1934	4	11	17	40	00.00	33.900	-95.500	0	5	3.80	0.30	3.90	>1609

Turkey Point Units 6 & 7
COL Application
Part 2 — FSAR

PTN COL 2.5-2

Table 2.5.2-202 (Sheet 7 of 25)
Seismicity Catalog for the Phase 1 Investigation Region [22°N to 35°N, 100°W to 65°W] for which the Events are Rmb Magnitude Greater than or Equal to 3.0 or Intensity [Int] Greater than or Equal to IV(4)

Catalog Reference ^(a)	Year	Month	Day	Hour	Min	Sec	Lat	Lon	Depth (km)	Int	Emb	Smb	Rmb	Epicenter (km) ^(b)
EPRIm	1935	11	14	3	10	00.00	29.600	-81.700	0	4	3.11	0.56	3.47	480
CUBA	1936	0	19	15	30	00.00	22.340	-79.340	15	—	4.26	0.56	4.62	354
EPRIm	1936	3	14	17	20	00.00	34.000	-95.200	0	5	3.50	0.30	3.60	>1609
CUBA	1936	12	19	15	30	00.00	22.340	-79.340	15	—	4.26	0.56	4.62	354
CUBA	1937	1	1	16	0	00.00	22.290	-79.200	10	—	3.97	0.56	4.33	364
CUBA	1937	1	8	0	0	00.00	22.330	-79.260	10	—	3.97	0.56	4.33	358
CUBA	1937	4	17	0	0	00.00	22.710	-83.060	15	—	3.68	0.56	4.04	407
CUBA	1937	5	14	0	0	00.00	22.780	-80.080	10	—	4.34	0.56	4.70	293
CUBA	1937	5	20	15	35	00.00	22.710	-83.060	15	—	4.99	0.56	5.35	407
CUBA	1937	12	20	15	35	00.00	22.710	-83.060	15	—	4.99	0.56	5.35	407
CUBA	1937	12	21	16	30	00.00	22.710	-83.060	15	—	4.12	0.56	4.48	407
CUBA	1938	1	0	0	0	00.00	22.300	-79.730	10	—	3.82	0.56	4.19	350
EPRIm	1938	4	26	5	42	00.00	34.200	-93.500	0	4	3.11	0.56	3.47	1598
SEUSN	1938	6	24	9	0	00.00	34.700	-86.600	0	—	3.00	0.10	3.01	1191
CUBA	1938	6	30	0	0	00.00	22.510	-79.470	10	—	3.75	0.56	4.11	333
CUBA	1938	7	29	0	0	00.00	22.480	-79.550	10	—	3.75	0.56	4.11	334
CUBA	1938	10	0	0	0	00.00	22.300	-79.730	10	—	3.82	0.56	4.19	350
CUBA	1938	11	0	0	0	00.00	22.310	-79.240	10	—	3.97	0.56	4.33	361
CUBA	1939	1	1	14	0	00.00	22.310	-79.240	10	—	3.82	0.56	4.19	361
CUBA	1939	1	13	9	20	00.00	22.510	-79.470	10	—	4.48	0.56	4.84	333
CUBA	1939	1	13	9	30	00.00	22.420	-79.350	10	—	4.04	0.56	4.40	346
CUBA	1939	1	13	9	35	00.00	22.310	-79.240	10	—	3.75	0.56	4.11	361
CUBA	1939	2	15	0	0	00.00	22.310	-79.240	10	—	3.97	0.56	4.33	361
CUBA	1939	2	15	16	45	00.00	22.600	-83.300	15	—	3.68	0.56	4.04	432
ISSv	1939	3	5	15	12	09.00	23.100	-69.400	160	—	5.80	0.10	5.81	1133
CUBA	1939	5	0	0	0	00.00	22.510	-79.470	10	—	3.97	0.56	4.33	333
EPRIm	1939	5	5	2	45	00.00	33.700	-85.800	0	5	3.70	0.56	4.06	1057
EPRIm	1939	6	1	7	30	00.00	35.000	-96.400	0	4	4.30	0.30	4.40	>1609
EPRIm	1939	6	19	21	43	12.00	34.100	-92.600	0	5	4.30	0.30	4.40	1524

Turkey Point Units 6 & 7
COL Application
Part 2 — FSAR

PTN COL 2.5-2

Table 2.5.2-202 (Sheet 8 of 25)
Seismicity Catalog for the Phase 1 Investigation Region [22°N to 35°N, 100°W to 65°W] for which the Events are Rmb Magnitude Greater than or Equal to 3.0 or Intensity [Int] Greater than or Equal to IV(4)

Catalog Reference ^(a)	Year	Month	Day	Hour	Min	Sec	Lat	Lon	Depth (km)	Int	Emb	Smb	Rmb	Epicenter (km) ^(b)
EPRIm	1939	6	24	10	27	00.00	34.700	-86.600	0	4	3.40	0.30	3.50	1191
CUBA	1939	8	15	3	50	00.00	22.720	-75.550	10	—	3.75	0.56	4.11	568
ISSv	1939	8	15	3	52	31.00	22.500	-79.000	0	—	5.80	0.10	5.81	349
EPRIm	1940	10	19	5	54	00.00	34.700	-85.100	0	4	3.40	0.30	3.50	1125
EPRIm	1940	12	2	16	16	00.00	33.000	-94.000	0	4	3.11	0.56	3.47	1567
CUBA	1941	0	0	0	0	00.00	22.080	-78.500	10	—	3.97	0.56	4.33	413
CUBA	1941	0	0	0	0	00.00	23.130	-82.400	10	—	3.97	0.56	4.33	328
CUBA	1941	4	24	20	30	00.00	22.810	-80.080	10	—	3.97	0.56	4.33	289
CUBA	1941	4	25	2	15	00.00	22.850	-80.100	15	—	4.12	0.56	4.48	285
EPRIm	1941	6	28	18	30	00.00	32.300	-90.800	0	4	2.81	0.56	3.17	1270
CUBA	1942	0	0	0	0	00.00	22.410	-83.720	15	—	4.12	0.56	4.48	477
EPRIm	1942	1	19	0	0	00.00	26.500	-81.000	0	4	3.11	0.56	3.47	136
CUBA	1942	3	9	18	10	00.00	22.940	-80.010	15	—	4.19	0.56	4.55	276
CUBA	1942	4	11	5	40	00.00	22.480	-79.550	10	—	3.97	0.56	4.33	334
CUBA	1942	6	4	6	0	00.00	22.810	-80.080	10	—	3.75	0.56	4.11	289
CUBA	1942	8	0	0	0	00.00	22.340	-80.560	10	—	4.26	0.56	4.62	341
CUBA	1942	8	18	0	0	00.00	23.130	-82.400	10	—	3.97	0.56	4.33	328
CUBA	1942	12	18	0	0	00.00	23.130	-82.400	10	—	3.97	0.56	4.33	328
CUBA	1943	0	0	0	0	00.00	22.810	-80.080	10	—	3.82	0.56	4.19	289
CUBA	1943	1	1	0	0	00.00	22.810	-80.080	10	—	3.82	0.56	4.19	289
CUBA	1943	7	0	0	0	00.00	22.210	-79.240	10	—	3.82	0.56	4.19	371
CUBA	1943	7	31	2	0	00.00	22.150	-79.970	10	—	3.97	0.56	4.33	363
CUBA	1943	7	31	3	15	00.00	22.110	-79.720	10	—	3.75	0.56	4.11	370
CUBA	1943	12	0	0	0	00.00	22.210	-79.240	10	—	3.82	0.56	4.19	371
EPRIm	1943	12	28	10	25	00.00	33.000	-80.200	0	4	3.11	0.56	3.47	838
CUBA	1944	0	0	0	0	00.00	22.060	-79.400	10	—	4.04	0.56	4.40	383
CUBA	1944	1	0	0	0	00.00	22.350	-79.230	10	—	3.97	0.56	4.33	357
CUBA	1944	1	1	3	0	00.00	22.330	-79.260	10	—	4.48	0.56	4.84	358
CUBA	1944	1	1	19	0	00.00	22.800	-80.100	10	—	4.04	0.56	4.40	290

Turkey Point Units 6 & 7
COL Application
Part 2 — FSAR

PTN COL 2.5-2

Table 2.5.2-202 (Sheet 9 of 25)
Seismicity Catalog for the Phase 1 Investigation Region [22°N to 35°N, 100°W to 65°W] for which the Events are Rmb Magnitude Greater than or Equal to 3.0 or Intensity [Int] Greater than or Equal to IV(4)

Catalog Reference ^(a)	Year	Month	Day	Hour	Min	Sec	Lat	Lon	Depth (km)	Int	Emb	Smb	Rmb	Epicenter (km) ^(b)
CUBA	1944	10	12	15	0	00.00	22.710	-83.060	15	—	4.63	0.56	4.99	407
CUBA	1945	0	0	0	0	00.00	22.680	-79.710	10	—	3.97	0.56	4.33	309
EPRIm	1945	6	14	3	25	00.00	35.000	-84.500	0	5	3.90	0.30	4.00	1134
EPRIm	1945	7	26	10	32	16.40	33.750	-81.380	5	4	4.30	0.30	4.40	927
SEUSN	1945	12	22	15	25	00.00	25.800	-80.000	0	3	2.70	0.56	3.06	053
CUBA	1946	0	0	0	0	00.00	22.000	-79.360	10	—	4.04	0.56	4.40	390
CUBA	1946	0	0	0	0	00.00	22.600	-83.310	15	—	4.12	0.56	4.48	433
CUBA	1947	5	9	0	0	00.00	22.660	-76.030	10	—	4.04	0.56	4.40	531
CUBA	1947	9	0	0	0	00.00	22.030	-78.300	10	—	3.97	0.56	4.33	427
EPRIm	1947	9	20	21	30	00.00	31.900	-92.600	0	4	3.40	0.56	3.76	1392
EPRIm	1947	11	2	4	30	00.00	32.900	-80.000	0	4	3.11	0.56	3.47	828
EPRIm	1947	12	27	19	0	00.00	35.000	-85.300	0	4	3.11	0.56	3.47	1164
CUBA	1948	9	0	0	0	00.00	22.810	-80.080	10	—	3.97	0.56	4.33	289
EPRIm	1948	11	8	17	44	00.00	26.500	-82.200	0	4	3.11	0.56	3.47	221
EPRIm	1949	2	2	10	52	00.00	32.900	-80.000	0	4	3.11	0.56	3.47	828
EPRIm	1949	7	9	18	44	43.00	32.250	-70.750	0	—	5.61	0.20	5.66	1199
CUBA	1950	0	0	0	0	00.00	22.800	-80.280	10	—	3.97	0.56	4.33	289
CUBA	1950	1	1	0	0	00.00	22.800	-80.280	10	—	3.97	0.56	4.33	289
EPRIm	1950	3	20	13	24	00.00	33.500	-97.100	0	4	3.11	0.56	3.47	>1609
CUBA	1951	1	12	11	0	00.00	22.480	-79.550	10	—	3.97	0.56	4.33	334
EPRIm	1951	3	4	2	55	00.00	32.900	-80.000	0	4	3.11	0.56	3.47	828
EPRIm	1951	12	30	7	55	00.00	32.900	-80.000	0	4	3.11	0.56	3.47	828
CUBA	1952	2	3	6	30	00.00	22.790	-80.160	10	—	4.26	0.56	4.62	291
CUBA	1952	2	3	16	30	00.00	22.880	-80.280	15	—	4.63	0.56	4.99	280
SEUSN	1952	2	6	15	12	00.00	33.500	-86.900	0	4	3.30	0.56	3.66	1096
CUBA	1952	3	10	14	0	00.00	22.110	-78.630	15	—	4.63	0.56	4.99	404
EPRIm	1952	10	17	15	48	00.00	30.100	-93.700	0	4	3.11	0.56	3.47	1409
EPRIm	1952	11	18	20	12	00.00	30.600	-84.600	0	4	3.11	0.56	3.47	708
EPRIm	1952	11	19	0	0	00.00	32.900	-80.000	0	5	3.70	0.56	4.06	828

Turkey Point Units 6 & 7
COL Application
Part 2 — FSAR

PTN COL 2.5-2

Table 2.5.2-202 (Sheet 10 of 25)
Seismicity Catalog for the Phase 1 Investigation Region [22°N to 35°N, 100°W to 65°W] for which the Events are Rmb Magnitude Greater than or Equal to 3.0 or Intensity [Int] Greater than or Equal to IV(4)

Catalog Reference ^(a)	Year	Month	Day	Hour	Min	Sec	Lat	Lon	Depth (km)	Int	Emb	Smb	Rmb	Epicenter (km) ^(b)
CUBA	1953	0	0	0	0	00.00	22.410	-83.720	15	—	4.12	0.56	4.48	477
CUBA	1953	0	0	0	0	00.00	22.980	-80.590	10	—	3.82	0.56	4.19	270
CUBA	1953	1	1	11	20	00.00	22.150	-78.600	15	—	4.85	0.56	5.21	401
CUBA	1953	1	1	15	0	00.00	22.980	-80.590	10	—	3.82	0.56	4.19	270
CUBA	1953	1	2	15	0	00.00	22.800	-80.020	10	—	3.97	0.56	4.33	291
EPRIm	1953	3	26	0	0	00.00	28.600	-81.400	0	4	3.11	0.56	3.47	366
CUBA	1953	5	16	0	0	00.00	23.030	-82.130	10	—	4.48	0.56	4.84	320
EPRIm	1953	6	6	17	40	00.00	34.700	-96.700	0	4	3.11	0.56	3.47	>1609
CUBA	1954	0	0	0	0	00.00	22.500	-79.600	10	—	4.04	0.56	4.40	331
CUBA	1954	1	1	0	0	00.00	22.500	-79.600	10	—	4.04	0.56	4.40	331
EPRIm	1954	4	11	0	0	00.00	35.000	-96.400	0	4	3.11	0.56	3.47	>1609
EPRIm	1955	2	1	14	45	00.00	30.400	-89.100	0	5	4.30	0.30	4.40	1020
CUBA	1956	0	0	0	0	00.00	22.810	-80.080	10	—	3.75	0.56	4.11	289
EPRIm	1956	1	5	8	0	00.00	34.300	-82.400	0	4	3.11	0.56	3.47	1003
EPRIm	1956	1	8	0	35	00.00	29.300	-94.800	0	4	3.11	0.56	3.47	1487
EPRIm	1956	4	2	16	3	18.00	34.200	-95.600	0	5	3.70	0.30	3.80	>1609
EPRIm	1956	9	27	14	15	00.00	31.900	-88.400	0	4	3.11	0.56	3.47	1063
EPRIm	1957	3	19	16	37	38.00	32.600	-94.700	0	5	4.20	0.30	4.30	1604
EPRIm	1957	4	23	9	23	39.00	33.770	-86.720	5	6	4.11	0.20	4.16	1111
CUBA	1957	9	11	23	30	00.00	22.180	-83.650	10	—	4.63	0.56	4.99	491
EPRIm	1957	11	24	20	6	17.00	35.000	-83.500	0	6	3.90	0.30	4.00	1104
CUBA	1958	0	0	0	0	00.00	22.710	-83.060	15	—	4.12	0.56	4.48	407
EPRIm	1958	3	5	11	53	43.00	34.200	-77.800	0	5	3.70	0.56	4.06	1002
SEUSN	1958	4	8	17	0	00.00	31.500	-83.500	0	3	2.70	0.56	3.06	739
EPRIm	1958	10	20	6	16	00.00	34.500	-82.700	0	5	3.70	0.56	4.06	1031
EPRIm	1958	11	6	23	8	00.00	29.900	-90.100	0	4	3.11	0.56	3.47	1079
EPRIm	1958	11	19	18	15	00.00	30.500	-91.200	0	5	3.20	0.30	3.30	1203
EPRIm	1959	6	15	12	45	00.00	34.700	-96.700	0	5	3.90	0.30	4.00	>1609
FD02	1959	6	17	16	27	07.00	34.500	-98.500	0	—	4.70	0.10	4.71	>1609

Turkey Point Units 6 & 7
COL Application
Part 2 — FSAR

PTN COL 2.5-2

Table 2.5.2-202 (Sheet 11 of 25)
Seismicity Catalog for the Phase 1 Investigation Region [22°N to 35°N, 100°W to 65°W] for which the Events are Rmb Magnitude Greater than or Equal to 3.0 or Intensity [Int] Greater than or Equal to IV(4)

Catalog Reference ^(a)	Year	Month	Day	Hour	Min	Sec	Lat	Lon	Depth (km)	Int	Emb	Smb	Rmb	Epicenter (km) ^(b)
EPRIm	1959	8	3	6	8	36.80	33.050	-80.130	1	6	4.31	0.20	4.36	844
EPRIm	1959	8	12	18	6	01.40	34.790	-86.560	5	6	3.71	0.20	3.76	1198
EPRIm	1959	10	15	15	45	00.00	29.800	-93.100	0	4	3.70	0.30	3.80	1344
EPRIm	1959	10	27	2	7	28.00	34.500	-80.200	0	6	4.30	0.55	4.65	1005
CUBA	1960	0	0	0	0	00.00	22.080	-78.340	10	—	3.97	0.56	4.33	420
EPRIm	1960	5	4	16	31	32.00	34.200	-92.000	0	4	3.11	0.56	3.47	1486
CUBA	1960	5	25	15	30	00.00	22.580	-79.480	15	—	4.63	0.56	4.99	325
CUBA	1960	7	0	0	0	00.00	22.480	-79.550	10	—	3.97	0.56	4.33	334
CUBA	1960	7	18	13	35	00.00	22.480	-79.550	10	—	3.75	0.56	4.11	334
USN	1960	7	28	3	37	30.00	32.800	-82.700	0	5	3.70	0.56	4.07	847
CUBA	1960	12	0	0	0	00.00	22.480	-79.550	10	—	3.97	0.56	4.33	334
CUBA	1961	0	0	0	0	00.00	22.330	-79.260	10	—	3.97	0.56	4.33	358
CUBA	1961	1	0	0	0	00.00	22.980	-80.590	10	—	3.97	0.56	4.33	270
EPRIm	1961	1	11	1	40	00.00	34.900	-95.500	0	5	3.70	0.30	3.80	>1609
EPRIm	1961	4	26	7	5	00.00	34.600	-95.000	0	3	3.70	0.30	3.80	>1609
EPRIm	1961	4	27	7	30	00.00	34.900	-95.300	0	5	4.00	0.30	4.10	>1609
STO	1962	8	10	20	47	19.00	34.800	-97.400	0	—	3.25	0.41	3.45	>1609
STO	1962	9	7	22	53	44.00	34.700	-98.400	0	—	3.25	0.41	3.45	>1609
STO	1962	10	23	17	55	58.00	35.000	-98.500	0	—	3.01	0.41	3.20	>1609
CUBA	1963	1	0	0	0	00.00	22.480	-79.550	10	—	3.97	0.56	4.33	334
STO	1963	2	2	16	57	39.00	34.700	-98.200	0	—	2.93	0.41	3.12	>1609
EPRIm	1963	2	7	21	18	36.00	34.400	-92.100	0	—	3.31	0.20	3.36	1507
EPRIm	1963	4	11	17	45	00.00	34.900	-82.400	0	4	3.11	0.56	3.47	1069
STO	1963	5	7	20	3	29.00	34.300	-96.400	0	—	3.09	0.41	3.28	>1609
CUBA	1963	8	26	0	0	00.00	22.480	-79.550	10	—	3.75	0.56	4.11	334
SEUSN	1963	10	8	6	1	43.40	33.900	-82.500	0	—	3.20	0.10	3.21	961
EPRIm	1963	11	5	22	45	03.40	27.490	-92.580	15	—	4.71	0.20	4.76	1236
EPRIm	1964	2	18	9	31	10.40	34.670	-85.390	1	5	4.18	0.10	4.19	1134
EPRIm	1964	3	13	1	20	17.50	33.190	-83.310	1	5	4.38	0.10	4.39	906

Turkey Point Units 6 & 7
COL Application
Part 2 — FSAR

PTN COL 2.5-2

Table 2.5.2-202 (Sheet 12 of 25)
Seismicity Catalog for the Phase 1 Investigation Region [22°N to 35°N, 100°W to 65°W] for which the Events are Rmb Magnitude Greater than or Equal to 3.0 or Intensity [Int] Greater than or Equal to IV(4)

Catalog Reference ^(a)	Year	Month	Day	Hour	Min	Sec	Lat	Lon	Depth (km)	Int	Emb	Smb	Rmb	Epicenter (km) ^(b)
CUBA	1964	3	27	0	0	00.00	22.070	-81.040	10	—	4.41	0.56	4.77	377
EPRIm	1964	4	20	19	4	44.10	33.840	-81.100	3	5	3.48	0.10	3.49	935
EPRIm	1964	4	24	7	33	51.90	31.420	-93.810	5	4	3.58	0.10	3.59	1472
EPRIm	1964	6	3	9	37	00.00	31.000	-94.000	0	4	2.81	0.56	3.17	1470
PDEnp	1965	3	29	13	10	22.30	33.900	-65.000	10	—	4.20	0.10	4.21	>1609
EPRIm	1965	9	9	14	42	20.00	34.700	-81.200	0	—	3.82	0.41	4.01	1031
SEUSN	1965	11	8	12	58	01.00	33.200	-83.200	0	—	3.30	0.10	3.31	904
CUBA	1966	0	0	0	0	00.00	22.640	-80.280	10	—	3.90	0.56	4.26	307
CUBA	1966	1	1	0	0	00.00	22.640	-80.280	10	—	3.90	0.56	4.26	307
SEUSN	1966	2	13	6	29	43.00	33.600	-87.000	0	—	3.50	0.10	3.51	1111
CUBA	1966	7	29	0	0	00.00	22.310	-79.240	10	—	3.97	0.56	4.33	361
CUBA	1966	7	29	15	0	00.00	22.310	-79.240	10	—	3.75	0.56	4.11	361
ISC	1966	12	15	8	16	00.00	23.130	-69.010	32	—	5.70	0.10	5.71	1171
PEREZ	1967	2	4	14	8	50.00	24.000	-65.700	1	—	6.55	0.10	6.56	1480
ISC	1967	3	13	0	58	48.10	24.290	-65.390	280	—	4.60	0.10	4.61	1507
ISC	1967	3	21	20	41	27.00	24.000	-97.000	33	—	3.90	0.10	3.91	>1609
EPRIm	1967	6	4	16	14	12.60	33.550	-90.840	6	6	4.28	0.10	4.29	1356
ISC	1967	6	20	3	57	18.00	22.000	-96.000	33	—	4.00	0.10	4.01	>1609
ISC	1967	10	4	2	45	45.00	27.000	-94.000	33	—	3.20	0.10	3.21	1369
EPRIm	1967	10	23	9	4	02.50	32.800	-80.220	19	5	3.78	0.10	3.79	816
CUBA	1968	1	1	0	0	00.00	22.980	-80.590	10	—	3.97	0.56	4.33	270
EPRIm	1968	1	4	22	30	00.00	34.850	-95.550	0	4	3.11	0.56	3.47	>1609
EPRIm	1968	7	12	1	12	00.00	32.800	-79.700	0	4	3.11	0.56	3.47	818
EPRIm	1968	9	22	21	41	18.20	34.110	-81.480	1	4	3.68	0.10	3.69	968
EPRIm	1968	10	14	14	42	54.00	34.000	-96.800	0	6	3.48	0.10	3.49	>1609
EPRIm	1968	11	25	20	0	00.00	34.100	-77.900	0	4	3.11	0.56	3.47	989
EPRIm	1969	1	1	23	35	38.70	34.990	-92.690	7	6	4.38	0.10	4.39	1591
EPRIm	1969	4	13	6	27	51.00	34.200	-96.300	0	—	3.48	0.10	3.49	>1609
CUBA	1969	5	0	0	0	00.00	22.140	-78.980	10	—	3.97	0.56	4.33	387

Turkey Point Units 6 & 7
COL Application
Part 2 — FSAR

PTN COL 2.5-2

Table 2.5.2-202 (Sheet 13 of 25)
Seismicity Catalog for the Phase 1 Investigation Region [22°N to 35°N, 100°W to 65°W] for which the Events are Rmb Magnitude Greater than or Equal to 3.0 or Intensity [Int] Greater than or Equal to IV(4)

Catalog Reference ^(a)	Year	Month	Day	Hour	Min	Sec	Lat	Lon	Depth (km)	Int	Emb	Smb	Rmb	Epicenter (km) ^(b)
EPRIm	1969	5	18	0	0	00.00	33.950	-82.580	0	—	3.50	0.41	3.69	968
CUBA	1969	6	0	0	0	00.00	22.180	-78.980	10	—	3.97	0.56	4.33	383
CUBA	1969	6	1	3	0	00.00	22.140	-78.980	10	—	3.97	0.56	4.33	387
CUBA	1969	12	0	0	0	00.00	22.180	-78.980	10	—	3.97	0.56	4.33	383
EPRIm	1970	2	3	0	0	00.00	31.000	-97.000	0	4	3.11	0.56	3.47	>1609
CUBA	1970	4	27	11	55	00.00	23.050	-81.580	10	—	3.97	0.56	4.33	290
CUBA	1970	7	24	0	0	00.00	22.900	-83.160	20	—	3.90	0.56	4.26	399
CUBA	1970	10	16	13	7	22.00	23.100	-82.900	10	—	4.34	0.56	4.70	364
EPRIm	1971	3	14	17	27	54.60	33.180	-87.840	12	3	3.88	0.10	3.89	1125
EPRIm	1971	3	15	14	53	22.00	32.800	-88.300	0	—	3.48	0.10	3.49	1124
EPRIm	1971	5	19	12	54	03.60	33.360	-80.660	1	4	4.08	0.10	4.09	879
EPRIm	1971	7	13	11	42	26.00	34.800	-83.000	0	5	3.78	0.10	3.79	1070
EPRIm	1972	8	14	15	5	19.00	33.200	-81.400	0	3	3.14	0.33	3.27	866
CUBA	1973	0	0	0	0	00.00	22.660	-83.580	20	—	3.75	0.56	4.11	448
CUBA	1973	1	1	0	0	00.00	22.660	-83.580	20	—	3.75	0.56	4.11	448
EPRIm	1973	1	8	9	11	37.00	33.800	-90.600	0	3	3.48	0.10	3.49	1357
CUBA	1973	8	11	0	38	35.00	22.600	-74.000	0	—	4.82	0.41	5.01	712
EPRIm	1973	10	27	6	21	02.00	28.480	-80.650	5	5	3.48	0.10	3.49	338
EPRIm	1973	12	25	2	46	00.00	29.000	-98.300	0	4	3.11	0.56	3.47	>1609
CUBA	1974	0	0	0	0	00.00	22.700	-81.200	18	—	4.19	0.56	4.55	313
EPRIm	1974	2	15	22	32	38.20	34.040	-92.980	17	3	3.48	0.10	3.49	1548
EPRIm	1974	8	2	8	52	11.10	33.910	-82.530	4	6	4.28	0.10	4.29	963
ISC c	1974	9	13	17	29	57.80	23.782	-96.428	0	—	3.60	0.10	3.61	>1609
EPRIm	1974	11	5	3	0	00.00	33.730	-82.220	0	3	3.68	0.10	3.69	937
EPRIm	1974	11	22	5	25	56.70	32.920	-80.160	6	6	4.28	0.10	4.29	829
SEUSN	1974	12	9	18	40	00.00	34.200	-77.200	0	3	2.70	0.56	3.06	1018
CUBA	1975	0	0	0	0	00.00	22.700	-79.690	10	—	3.97	0.56	4.33	307
EPRIm	1975	4	1	21	9	00.00	33.200	-83.200	0	—	3.82	0.41	4.01	904
EPRIm	1975	6	24	11	11	36.60	33.700	-87.840	4	4	3.78	0.10	3.79	1168

Turkey Point Units 6 & 7
COL Application
Part 2 — FSAR

PTN COL 2.5-2

Table 2.5.2-202 (Sheet 14 of 25)
Seismicity Catalog for the Phase 1 Investigation Region [22°N to 35°N, 100°W to 65°W] for which the Events are Rmb Magnitude Greater than or Equal to 3.0 or Intensity [Int] Greater than or Equal to IV(4)

Catalog Reference ^(a)	Year	Month	Day	Hour	Min	Sec	Lat	Lon	Depth (km)	Int	Emb	Smb	Rmb	Epicenter (km) ^(b)
EPRIm	1975	8	29	4	22	52.10	33.660	-86.590	4	6	3.48	0.10	3.49	1094
PDE	1975	10	12	2	58	11.20	34.816	-97.406	20	—	3.20	0.10	3.21	>1609
EPRIm	1975	10	18	4	31	00.00	34.900	-83.000	0	4	3.11	0.56	3.47	1081
EPRIm	1975	11	7	23	39	31.70	33.310	-87.330	4	—	3.48	0.10	3.49	1104
EPRIm	1975	11	29	14	29	44.90	34.680	-97.420	14	4	3.48	0.10	3.49	>1609
EPRIm	1975	12	4	11	57	00.00	29.200	-81.000	0	4	3.29	0.33	3.42	422
CUBA	1976	0	0	0	0	00.00	22.550	-79.720	10	—	3.75	0.56	4.11	323
EPRIm	1976	2	4	19	53	53.00	34.970	-84.700	14	6	3.58	0.10	3.59	1138
CUBA	1976	3	9	16	5	00.00	22.650	-83.010	15	—	3.68	0.56	4.04	408
CUBA	1976	3	10	15	40	00.00	22.650	-83.010	15	—	3.68	0.56	4.04	408
CUBA	1976	3	15	18	50	00.00	22.650	-83.010	15	—	3.68	0.56	4.04	408
CUBA	1976	10	20	8	15	00.00	22.300	-79.450	10	—	3.97	0.56	4.33	356
CUBA	1976	11	0	0	0	00.00	22.000	-79.370	5	—	3.90	0.56	4.26	390
CUBA	1976	11	1	0	0	00.00	22.000	-79.370	5	—	3.90	0.56	4.26	390
EPRIm	1976	12	27	6	57	15.20	32.060	-82.500	14	5	3.68	0.10	3.69	763
CUBA	1977	0	0	0	0	00.00	22.680	-80.150	10	—	3.75	0.56	4.11	303
EPRIm	1977	3	30	8	27	47.80	32.950	-80.180	8	5	4.17	0.27	4.25	832
EPRIm	1977	5	4	2	0	24.30	31.960	-88.440	0	5	3.58	0.10	3.59	1070
EPRIm	1977	6	2	23	29	10.60	34.560	-94.170	10	6	3.58	0.10	3.59	>1609
ISC	1977	9	27	20	56	03.70	33.880	-97.480	5	—	3.00	0.10	3.01	>1609
CUBA	1977	10	7	5	36	55.00	22.350	-76.100	0	—	4.26	0.41	4.45	546
SLU	1977	11	4	11	21	06.80	34.010	-89.220	2	—	3.40	0.10	3.41	1280
CUBA	1978	0	0	0	0	00.00	23.050	-81.580	10	—	3.53	0.56	3.89	290
CUBA	1978	0	0	0	0	00.00	22.240	-83.580	10	—	3.97	0.56	4.33	481
CUBA	1978	1	1	0	0	00.00	23.050	-81.580	10	—	3.53	0.56	3.89	290
CUBA	1978	1	1	10	0	00.00	22.240	-83.580	10	—	3.97	0.56	4.33	481
SEUSN	1978	1	12	21	10	00.00	28.100	-81.600	0	4	3.30	0.56	3.66	321
EPRIm	1978	3	24	0	42	36.30	29.800	-67.400	20	—	6.08	0.10	6.09	1359
SLU	1978	4	11	8	51	02.43	34.693	-95.681	5	—	3.00	0.10	3.01	>1609

Turkey Point Units 6 & 7
COL Application
Part 2 — FSAR

PTN COL 2.5-2

Table 2.5.2-202 (Sheet 15 of 25)
Seismicity Catalog for the Phase 1 Investigation Region [22°N to 35°N, 100°W to 65°W] for which the Events are Rmb Magnitude Greater than or Equal to 3.0 or Intensity [Int] Greater than or Equal to IV(4)

Catalog Reference ^(a)	Year	Month	Day	Hour	Min	Sec	Lat	Lon	Depth (km)	Int	Emb	Smb	Rmb	Epicenter (km) ^(b)
SLU	1978	4	20	8	13	04.00	34.586	-96.293	5	—	3.00	0.10	3.01	>1609
CUBA	1978	5	31	16	2	00.00	23.500	-82.100	0	—	3.77	0.41	3.96	277
PDE	1978	6	9	23	15	19.10	32.094	-88.580	10	—	3.30	0.10	3.31	1089
EPRIm	1978	7	24	8	6	16.90	26.380	-88.720	15	—	4.88	0.10	4.89	842
SEUSN	1978	11	6	23	0	00.00	30.200	-82.650	0	4	3.30	0.56	3.66	574
EPRIm	1978	12	11	2	6	50.10	31.910	-88.470	3	5	3.48	0.10	3.49	1068
CUBA	1979	0	0	0	0	00.00	22.640	-79.750	10	—	3.97	0.56	4.33	312
SEUSN	1979	2	27	8	25	00.00	34.200	-92.000	0	4	3.10	0.10	3.11	1486
SLU	1979	7	13	7	48	13.44	34.033	-95.087	5	—	3.00	0.10	3.01	>1609
DNA	1979	8	7	19	32	17.20	34.333	-81.358	3	—	3.00	0.10	3.01	992
SEUSN	1979	8	13	5	19	25.20	33.900	-82.540	23	—	3.97	0.30	4.08	962
DNA	1979	8	26	1	31	45.00	34.916	-82.956	1	—	3.70	0.10	3.71	1082
DNA	1979	10	8	23	20	11.00	34.306	-81.344	1	—	3.01	0.41	3.20	989
CUBA	1979	11	19	6	0	00.00	22.480	-79.550	10	—	3.97	0.56	4.33	334
EPRIm	1980	1	10	19	16	23.50	24.130	-85.710	15	—	3.88	0.10	3.89	559
DNA	1980	4	24	6	16	57.20	34.329	-81.324	3	—	2.97	0.30	3.08	991
ISC	1980	7	18	1	34	44.10	34.000	-97.350	5	—	3.00	0.10	3.01	>1609
STO	1980	7	25	15	30	12.50	33.940	-87.440	0	—	3.10	0.10	3.11	1166
DNA	1980	7	29	1	10	22.70	34.351	-81.364	1	—	3.16	0.30	3.26	994
EPRIm	1980	9	1	5	44	42.20	32.980	-80.190	7	4	3.29	0.33	3.42	836
SLU	1980	9	7	1	50	14.23	34.953	-97.258	5	—	3.48	0.10	3.49	>1609
CUBA	1980	10	18	0	0	00.00	22.600	-83.710	20	—	3.68	0.56	4.04	462
CUBA	1980	10	24	0	0	00.00	22.600	-83.710	20	—	3.68	0.56	4.04	462
SLU	1980	12	4	23	48	43.22	33.942	-97.352	5	1	3.60	0.10	3.61	>1609
CUBA	1981	0	0	0	0	00.00	22.900	-83.160	20	—	3.75	0.56	4.11	399
CUBA	1981	1	1	0	0	00.00	22.900	-83.160	20	—	3.75	0.56	4.11	399
SEUSN	1981	2	13	2	15	00.00	30.000	-91.800	0	4	3.10	0.56	3.46	1233
CUBA	1981	6	9	23	3	00.00	22.280	-83.840	15	—	3.90	0.56	4.26	496
CUBA	1981	6	11	18	35	00.00	22.200	-83.480	10	—	4.41	0.56	4.77	477

Turkey Point Units 6 & 7
COL Application
Part 2 — FSAR

PTN COL 2.5-2

Table 2.5.2-202 (Sheet 16 of 25)
Seismicity Catalog for the Phase 1 Investigation Region [22°N to 35°N, 100°W to 65°W] for which the Events are Rmb Magnitude Greater than or Equal to 3.0 or Intensity [Int] Greater than or Equal to IV(4)

Catalog Reference ^(a)	Year	Month	Day	Hour	Min	Sec	Lat	Lon	Depth (km)	Int	Emb	Smb	Rmb	Epicenter (km) ^(b)
SLU	1981	7	9	22	47	11.09	34.955	-97.651	5	—	3.72	0.10	3.73	>1609
EPRIm	1981	7	11	21	9	21.84	34.850	-97.730	5	5	3.48	0.10	3.49	>1609
SLU	1981	9	17	19	31	00.45	34.481	-96.823	5	—	3.72	0.10	3.73	>1609
CUBA	1981	9	30	0	54	00.00	22.350	-83.570	10	—	3.97	0.56	4.33	471
SLU	1981	11	6	19	28	25.31	34.676	-96.682	5	—	3.54	0.10	3.55	>1609
CUBA	1981	11	11	20	30	00.00	22.160	-84.100	15	—	4.55	0.56	4.92	525
CUBA	1982	0	0	0	0	00.00	22.660	-83.960	20	—	4.26	0.56	4.62	477
SLU	1982	1	12	23	40	25.00	34.742	-97.406	5	—	3.00	0.10	3.01	>1609
SEUSN	1982	1	28	4	52	51.90	32.982	-81.393	7	—	3.40	0.10	3.41	842
CUBA	1982	2	22	17	4	20.00	22.300	-83.200	0	—	3.28	0.41	3.47	450
CUBA	1982	2	26	18	23	47.00	22.300	-83.400	0	—	3.28	0.41	3.47	464
SLU	1982	3	15	21	39	10.98	34.832	-97.608	5	—	3.72	0.10	3.73	>1609
SLU	1982	3	18	9	51	52.95	34.175	-97.608	5	—	3.48	0.10	3.49	>1609
TEIC	1982	4	13	9	25	09.30	34.251	-81.260	12	—	3.17	0.41	3.37	982
SLU	1982	7	9	3	38	11.35	34.963	-97.432	5	—	3.54	0.10	3.55	>1609
SEUSN	1982	7	16	14	16	02.90	34.320	-81.550	2	3	3.06	0.27	3.15	992
SLU	1982	8	22	1	1	02.42	34.840	-96.936	5	—	3.72	0.10	3.73	>1609
TEIC	1982	9	2	21	52	05.30	34.917	-82.891	8	—	3.09	0.41	3.28	1080
CUBA	1982	11	0	0	0	00.00	22.590	-81.240	20	—	3.75	0.56	4.11	326
CUBA	1982	11	16	20	20	17.00	22.610	-81.230	30	—	5.36	0.56	5.72	323
EPRIm	1983	1	26	14	7	44.70	32.850	-83.560	0	—	3.48	0.10	3.49	879
SLU	1983	3	28	9	32	24.86	34.635	-96.561	5	—	3.60	0.10	3.61	>1609
EPRIm	1983	10	16	19	40	50.80	30.240	-93.390	5	3	3.78	0.10	3.79	1386
CUBA	1983	11	1	17	9	20.00	23.300	-82.800	0	—	3.24	0.41	3.43	342
EPRIm	1983	11	6	9	2	19.80	32.940	-80.160	10	5	3.51	0.27	3.59	831
CUBA	1983	11	30	17	15	13.00	22.200	-77.830	5	—	3.64	0.30	3.74	437
SLU	1983	12	9	20	52	11.04	33.227	-92.739	4	—	3.00	0.10	3.01	1479
CUBA	1984	0	0	0	0	00.00	22.510	-79.470	0	—	3.61	0.56	3.97	333
CUBA	1984	1	1	0	0	00.00	22.600	-83.710	20	—	3.82	0.56	4.19	462

Turkey Point Units 6 & 7
COL Application
Part 2 — FSAR

PTN COL 2.5-2

Table 2.5.2-202 (Sheet 17 of 25)
Seismicity Catalog for the Phase 1 Investigation Region [22°N to 35°N, 100°W to 65°W] for which the Events are Rmb Magnitude Greater than or Equal to 3.0 or Intensity [Int] Greater than or Equal to IV(4)

Catalog Reference ^(a)	Year	Month	Day	Hour	Min	Sec	Lat	Lon	Depth (km)	Int	Emb	Smb	Rmb	Epicenter (km) ^(b)
CUBA	1984	1	16	18	41	27.00	22.300	-83.800	0	—	3.49	0.41	3.68	492
CUBA	1984	1	17	20	55	00.00	23.400	-83.700	0	—	3.20	0.41	3.40	406
ANSS	1984	1	23	0	11	59.38	26.716	-87.339	5	—	2.85	0.41	3.04	712
TEIme	1984	1	23	1	15	09.40	26.716	-87.339	5	—	2.85	0.41	3.04	712
NAOme	1984	4	9	23	8	20.00	22.600	-80.300	33	—	4.50	0.10	4.51	311
CUBA	1984	4	17	20	23	04.00	23.200	-83.600	0	—	3.17	0.41	3.36	411
CUBA	1984	4	19	19	54	39.00	23.100	-82.400	0	—	3.20	0.41	3.40	330
CUBA	1984	5	16	2	50	37.00	22.930	-80.500	15	—	4.19	0.56	4.55	275
EPRIm	1984	8	9	2	42	35.81	34.620	-86.300	8	—	3.15	0.30	3.25	1169
CUBA	1984	8	20	18	37	26.00	22.500	-79.740	10	—	3.53	0.30	3.64	328
SLU	1984	9	25	1	53	26.26	34.018	-89.835	5	—	3.00	0.10	3.01	1321
EPRIm	1984	10	9	11	54	26.97	34.750	-85.200	12	6	4.18	0.10	4.19	1134
CUBA	1984	11	7	7	42	22.00	22.510	-79.470	0	—	3.61	0.56	3.97	333
SLU	1984	11	16	11	50	04.51	34.641	-97.487	5	—	3.60	0.10	3.61	>1609
CUBA	1984	11	16	13	34	11.00	23.010	-79.320	27	—	3.68	0.30	3.78	285
CUBA	1984	11	22	18	35	56.00	22.960	-79.640	20	—	3.97	0.30	4.07	280
CUBA	1985	1	21	10	45	33.00	22.390	-83.550	0	—	3.17	0.41	3.36	467
CUBA	1985	2	0	0	0	00.00	22.600	-83.710	20	—	4.12	0.56	4.48	462
CUBA	1985	2	21	20	22	25.00	23.250	-83.400	0	—	3.93	0.30	4.04	391
CUBA	1985	2	28	12	52	21.00	22.070	-83.760	0	—	3.49	0.41	3.68	507
ISC	1985	5	6	2	11	13.60	34.875	-97.572	5	5	2.30	0.10	2.31	>1609
CUBA	1985	5	17	11	50	26.00	22.310	-83.180	0	—	3.49	0.41	3.68	448
CUBA	1985	5	17	11	53	20.00	22.330	-83.360	0	—	3.49	0.41	3.68	459
CUBA	1985	9	13	10	2	49.00	24.070	-76.970	0	—	3.59	0.30	3.69	370
CUBA	1985	9	13	17	49	45.00	23.360	-82.830	0	—	3.31	0.41	3.51	339
FD02	1985	9	18	15	54	04.00	33.470	-97.040	0	5	3.30	0.10	3.31	>1609
CUBA	1985	9	21	18	34	20.00	22.560	-83.880	0	—	3.24	0.41	3.43	478
CUBA	1986	0	0	0	0	00.00	22.480	-84.240	20	—	4.26	0.56	4.62	512
TEIC	1986	2	13	1	35	00.00	34.793	-82.938	1	—	3.25	0.41	3.45	1068

Turkey Point Units 6 & 7
COL Application
Part 2 — FSAR

PTN COL 2.5-2

Table 2.5.2-202 (Sheet 18 of 25)
Seismicity Catalog for the Phase 1 Investigation Region [22°N to 35°N, 100°W to 65°W] for which the Events are Rmb Magnitude Greater than or Equal to 3.0 or Intensity [Int] Greater than or Equal to IV(4)

Catalog Reference ^(a)	Year	Month	Day	Hour	Min	Sec	Lat	Lon	Depth (km)	Int	Emb	Smb	Rmb	Epicenter (km) ^(b)
SLU	1986	2	13	11	35	47.05	34.816	-82.944	4	—	3.00	0.10	3.01	1071
SEUSN	1986	3	13	2	29	31.40	33.229	-83.226	5	4	3.30	0.27	3.38	908
PDE	1986	5	7	2	27	00.46	33.233	-87.361	1	—	4.50	0.10	4.51	1100
SLU	1986	5	12	4	18	48.31	30.902	-89.159	10	—	3.60	0.10	3.61	1054
SEUSN	1986	7	11	14	26	14.80	34.937	-84.987	13	6	3.80	0.10	3.81	1145
SEUSN	1986	9	17	9	33	49.50	32.931	-80.159	6	4	3.30	0.27	3.38	830
CUBA	1986	10	8	4	51	46.00	22.220	-78.700	0	—	3.90	0.56	4.26	390
PDE	1986	11	7	13	53	18.50	34.671	-70.896	10	—	4.00	0.10	4.01	1369
TEIC	1986	12	11	14	5	50.00	34.889	-82.887	9	—	2.93	0.41	3.12	1077
TEIC	1986	12	11	14	7	11.00	34.898	-82.880	9	—	3.09	0.41	3.28	1078
CUBA	1986	12	25	6	13	20.00	22.230	-79.030	0	—	3.24	0.30	3.34	376
CUBA	1986	12	30	8	16	27.00	22.350	-79.330	0	—	3.39	0.30	3.49	354
CUBA	1987	2	2	0	0	00.00	22.600	-83.710	20	—	3.68	0.56	4.04	462
NENG	1987	2	8	18	25	37.09	29.697	-67.634	12	—	4.70	0.10	4.71	1334
ISCwy	1987	2	21	2	17	52.40	29.560	-66.960	18	—	4.20	0.10	4.21	1392
SEUSN	1987	3	16	13	9	26.80	34.560	-80.948	3	—	3.06	0.30	3.17	1014
CUBA	1987	3	29	22	24	12.00	22.170	-77.930	5	—	3.14	0.30	3.24	433
PDE	1987	6	1	17	44	33.20	34.615	-97.380	5	4	2.90	0.10	2.91	>1609
TEIC	1987	12	12	3	53	28.00	34.154	-82.714	9	—	3.33	0.41	3.53	994
TEIC	1987	12	24	22	46	44.20	34.154	-82.723	6	—	3.09	0.41	3.28	994
CUBA	1988	1	4	10	33	30.00	22.320	-78.940	20	—	3.99	0.30	4.09	370
SEUSN	1988	1	23	1	57	16.40	32.935	-80.157	7	5	3.50	0.27	3.58	831
PRSN	1988	3	3	13	52	05.64	22.280	-70.270	5	—	4.10	0.23	4.16	1077
PRSN	1988	4	28	6	46	27.22	22.030	-67.510	25	—	3.80	0.23	3.86	1353
PRSN	1988	5	5	17	39	20.20	29.420	-71.660	54	—	5.40	0.23	5.46	961
PRSN	1988	5	9	0	31	29.37	22.320	-69.600	25	—	4.10	0.23	4.16	1140
CUBA	1988	6	0	0	0	00.00	22.650	-83.010	15	—	3.68	0.56	4.04	408
CUBA	1988	6	1	0	0	00.00	22.650	-83.010	15	—	3.68	0.56	4.04	408
PRSN	1988	8	15	5	46	56.00	23.850	-69.250	104	—	4.10	0.23	4.16	1129

Turkey Point Units 6 & 7
COL Application
Part 2 — FSAR

PTN COL 2.5-2

Table 2.5.2-202 (Sheet 19 of 25)
Seismicity Catalog for the Phase 1 Investigation Region [22°N to 35°N, 100°W to 65°W] for which the Events are Rmb Magnitude Greater than or Equal to 3.0 or Intensity [Int] Greater than or Equal to IV(4)

Catalog Reference ^(a)	Year	Month	Day	Hour	Min	Sec	Lat	Lon	Depth (km)	Int	Emb	Smb	Rmb	Epicenter (km) ^(b)
PRSN	1988	12	20	7	24	27.76	22.090	-70.710	25	—	4.10	0.23	4.16	1042
PRSN	1988	12	21	19	18	37.07	22.560	-69.460	25	—	4.50	0.23	4.56	1145
SLU	1988	12	25	15	57	57.53	34.197	-92.718	15	—	3.42	0.41	3.61	1539
TAC c	1989	1	29	4	57	40.50	22.780	-99.470	20	—	4.52	0.10	4.53	>1609
SLU	1989	2	28	17	31	50.68	33.399	-87.118	0	—	3.50	0.10	3.51	1100
PRSN	1989	5	25	23	12	09.08	22.690	-67.170	25	—	3.80	0.23	3.86	1365
SEUSN	1989	6	2	5	4	34.00	32.934	-80.166	5	4	3.30	0.27	3.38	831
PDE	1989	8	13	20	16	02.90	33.632	-87.086	0	—	3.40	0.10	3.41	1118
SEUSN	1989	8	20	0	3	18.30	34.803	-87.596	6	6	3.90	0.10	3.91	1252
SLU	1989	11	26	22	41	09.90	34.763	-91.086	5	—	3.00	0.10	3.01	1463
CUBA	1990	3	14	11	56	37.00	22.180	-70.500	70	—	5.21	0.10	5.22	1059
CUBA	1990	6	2	23	54	18.00	23.420	-79.480	17	—	4.09	0.30	4.19	237
SEUSN	1990	6	23	20	44	02.10	33.720	-87.946	6	—	3.06	0.30	3.17	1176
CUBA	1990	7	19	12	36	03.00	22.470	-78.470	5	—	3.19	0.30	3.29	376
TEIC	1990	7	28	7	53	33.00	34.600	-93.376	4	—	3.01	0.41	3.20	>1609
TEIC	1990	8	23	8	23	11.00	34.036	-82.503	14	—	2.93	0.41	3.12	976
SEUSN	1990	9	2	4	35	40.20	33.758	-87.928	0	—	3.16	0.30	3.26	1179
PDE	1990	9	16	21	13	32.40	34.800	-95.530	5	4	2.50	0.10	2.51	>1609
TEIC	1990	9	19	5	36	56.00	34.838	-83.002	5	—	3.09	0.41	3.28	1074
TEIC	1990	9	19	8	14	04.00	34.868	-83.016	16	—	2.85	0.41	3.04	1078
SEUSN	1990	11	13	15	22	13.00	32.947	-80.136	3	5	3.50	0.10	3.51	832
PDE	1990	11	15	11	44	41.40	34.760	-97.590	5	5	3.90	0.10	3.91	>1609
TEIC	1991	1	15	8	48	22.50	33.204	-83.205	12	—	3.25	0.41	3.45	904
TEIC	1991	1	16	15	26	39.40	33.171	-83.264	22	—	2.85	0.41	3.04	903
TEIC	1991	1	27	2	20	34.90	33.230	-83.247	20	—	3.17	0.41	3.37	908
TEIC	1991	2	7	4	3	14.30	33.195	-83.183	8	—	3.17	0.41	3.37	903
TEIC	1991	2	11	15	36	44.40	34.108	-90.599	12	—	2.85	0.41	3.04	1380
SEUSN	1991	6	2	6	5	34.90	32.980	-80.214	5	5	3.50	0.27	3.58	836
PRSN	1991	7	3	14	39	24.42	22.160	-65.580	20	—	5.70	0.23	5.76	1538

Turkey Point Units 6 & 7
COL Application
Part 2 — FSAR

PTN COL 2.5-2

Table 2.5.2-202 (Sheet 20 of 25)
Seismicity Catalog for the Phase 1 Investigation Region [22°N to 35°N, 100°W to 65°W] for which the Events are Rmb Magnitude Greater than or Equal to 3.0 or Intensity [Int] Greater than or Equal to IV(4)

Catalog Reference ^(a)	Year	Month	Day	Hour	Min	Sec	Lat	Lon	Depth (km)	Int	Emb	Smb	Rmb	Epicenter (km) ^(b)
NENG	1991	7	9	6	53	36.00	23.217	-65.569	9	—	6.11	0.10	6.12	1509
CUBA	1991	9	26	8	27	35.00	22.500	-75.200	20	—	3.66	0.41	3.86	611
SEUSN	1991	10	30	14	54	12.60	34.904	-84.713	8	—	3.06	0.30	3.17	1132
TEIC	1991	11	17	21	11	31.70	34.987	-82.956	8	—	3.01	0.41	3.20	1089
SEUSN	1992	1	3	4	21	23.90	33.981	-82.421	3	5	3.50	0.27	3.58	969
ISC	1992	1	4	3	19	06.70	24.371	-65.279	10	—	4.20	0.10	4.21	1516
PDE	1992	2	22	4	21	34.65	26.356	-78.888	10	—	3.20	0.10	3.21	177
PDE	1992	3	31	14	59	39.64	26.019	-85.731	5	—	3.80	0.10	3.81	543
PDE	1992	7	30	14	40	55.87	24.705	-99.779	10	—	4.30	0.10	4.31	>1609
PDE	1992	8	10	20	3	04.20	34.982	-97.453	5	4	2.88	0.27	2.97	>1609
SEUSN	1992	8	21	16	31	56.10	32.985	-80.163	6	6	4.10	0.10	4.11	837
SEUSN	1992	9	11	16	34	11.70	33.171	-87.501	6	—	2.97	0.30	3.08	1103
CUBA	1992	9	25	0	51	43.00	22.650	-79.400	15	—	4.28	0.30	4.39	320
CUBA	1992	9	25	3	15	57.00	22.690	-79.300	15	—	3.54	0.30	3.64	319
TEIC	1992	9	27	17	2	25.70	27.225	-88.711	10	—	3.80	0.10	3.81	855
PDE	1992	11	30	8	33	01.48	23.251	-98.199	10	—	4.61	0.30	4.71	>1609
PDE	1992	12	6	5	39	22.15	31.442	-66.108	10	—	3.90	0.10	3.91	1538
PDE	1992	12	17	7	18	04.27	34.744	-97.581	5	4	3.60	0.10	3.61	>1609
PRSN	1993	1	3	6	8	10.98	22.150	-67.960	54	—	5.70	0.23	5.76	1305
PDE	1993	7	16	10	54	32.86	31.747	-88.341	5	6	3.70	0.10	3.71	1047
SEUSN	1993	8	8	9	24	32.40	33.597	-81.591	8	5	3.20	0.10	3.21	913
PDE	1993	8	23	12	5	43.40	22.405	-99.347	33	—	4.00	0.10	4.01	>1609
ISC	1993	10	20	8	37	14.10	22.137	-99.051	10	—	4.00	0.10	4.01	>1609
PDE	1994	3	26	21	33	35.25	28.913	-66.146	10	—	4.70	0.10	4.71	1451
SEUSN	1994	4	5	22	22	00.40	34.969	-85.491	24	5	3.20	0.10	3.21	1168
ISC	1994	4	16	7	20	20.00	34.660	-97.710	5	—	3.17	0.23	3.23	>1609
SEUSN	1994	5	4	9	12	03.40	34.222	-87.195	19	4	3.00	0.10	3.01	1178
PDE	1994	6	10	23	34	02.92	33.013	-92.671	5	3	3.20	0.10	3.21	1460
PDE	1994	6	30	1	8	24.22	27.911	-90.177	10	—	4.20	0.10	4.21	1013

Turkey Point Units 6 & 7
COL Application
Part 2 — FSAR

PTN COL 2.5-2

Table 2.5.2-202 (Sheet 21 of 25)
Seismicity Catalog for the Phase 1 Investigation Region [22°N to 35°N, 100°W to 65°W] for which the Events are Rmb Magnitude Greater than or Equal to 3.0 or Intensity [Int] Greater than or Equal to IV(4)

Catalog Reference ^(a)	Year	Month	Day	Hour	Min	Sec	Lat	Lon	Depth (km)	Int	Emb	Smb	Rmb	Epicenter (km) ^(b)
PRSN	1994	10	14	22	26	23.54	22.980	-66.720	25	—	3.90	0.23	3.96	1401
PRSN	1994	11	4	6	0	41.77	22.610	-67.270	50	—	3.90	0.23	3.96	1357
PDE	1995	1	4	1	46	14.09	29.450	-96.950	5	4	2.70	0.10	2.71	>1609
PDE	1995	1	18	15	51	39.42	34.774	-97.596	5	5	4.20	0.10	4.21	>1609
CUBA	1995	1	18	20	45	07.00	22.320	-71.930	20	—	4.58	0.30	4.69	917
CUBA	1995	3	9	18	29	13.00	22.900	-82.210	3	—	3.24	0.30	3.34	337
SEUSN	1995	4	17	13	46	00.00	32.997	-80.171	8	6	3.90	0.10	3.91	838
PRSN	1995	5	1	7	30	46.77	22.230	-72.160	25	—	4.20	0.23	4.26	900
SEUSN	1995	5	28	15	28	37.00	33.191	-87.827	1	F ^(c)	3.40	0.10	3.41	1125
PDE	1995	6	1	4	49	29.32	34.287	-96.732	5	5	3.00	0.10	3.01	>1609
NENG	1995	7	2	3	35	11.33	30.974	-65.234	2	—	4.71	0.10	4.72	1598
SEUSN	1995	7	15	1	3	28.40	33.478	-87.665	1	—	3.30	0.10	3.31	1139
PRSN	1995	9	12	15	15	03.04	22.170	-66.140	25	—	3.80	0.23	3.86	1482
PRSN	1996	3	17	5	59	09.10	22.280	-66.820	25	—	3.60	0.23	3.66	1412
PDE	1996	3	25	14	15	50.55	32.131	-88.671	5	—	3.50	0.10	3.51	1099
PDE	1996	4	11	21	54	57.63	34.969	-91.162	5	5	3.30	0.10	3.31	1483
PDE	1996	8	8	22	25	11.03	22.110	-80.184	10	—	3.80	0.10	3.81	366
PDE	1996	8	11	18	17	49.88	33.577	-90.874	10	—	3.50	0.10	3.51	1361
PDE	1996	12	22	20	13	53.55	32.224	-65.447	10	—	4.40	0.10	4.41	>1609
PDE	1997	3	16	19	7	27.95	34.209	-93.435	5	4	3.40	0.10	3.41	1594
PDE	1997	4	18	14	57	35.39	25.782	-86.552	33	—	3.90	0.10	3.91	623
SEUSN	1997	5	4	3	39	12.80	30.934	-87.494	0	4	3.10	0.10	3.11	928
SEUSN	1997	5	19	19	45	35.80	34.622	-85.353	2	4	2.90	0.10	2.91	1128
FD02	1997	5	31	3	26	41.00	33.200	-96.100	0	4	3.40	0.10	3.41	>1609
PDE	1997	7	1	21	12	20.59	33.136	-67.854	10	—	3.60	0.10	3.61	1479
SEUSN	1997	7	19	17	6	34.40	34.953	-84.811	2	4	3.50	0.10	3.51	1140
PDE	1997	9	6	23	38	00.91	34.660	-96.435	5	5	4.50	0.10	4.51	>1609
NENG	1997	10	24	8	35	18.75	31.123	-87.272	2	—	4.96	0.10	4.97	925
ISC	1997	12	6	11	11	23.60	34.895	-95.968	5	—	3.01	0.10	3.02	>1609

Turkey Point Units 6 & 7
COL Application
Part 2 — FSAR

PTN COL 2.5-2

Table 2.5.2-202 (Sheet 22 of 25)
Seismicity Catalog for the Phase 1 Investigation Region [22°N to 35°N, 100°W to 65°W] for which the Events are Rmb Magnitude Greater than or Equal to 3.0 or Intensity [Int] Greater than or Equal to IV(4)

Catalog Reference ^(a)	Year	Month	Day	Hour	Min	Sec	Lat	Lon	Depth (km)	Int	Emb	Smb	Rmb	Epicenter (km) ^(b)
PDE	1997	12	12	8	42	20.25	33.466	-87.306	1	—	4.00	0.10	4.01	1116
PRSN	1998	3	30	7	15	36.26	22.960	-66.360	25	—	3.90	0.23	3.96	1437
SEUSN	1998	4	13	9	56	15.60	34.471	-80.603	6	5	3.90	0.10	3.91	1002
FD02	1998	4	28	14	13	02.00	34.780	-98.420	0	—	4.20	0.10	4.21	>1609
SEUSN	1998	6	24	15	20	04.70	32.760	-87.759	2	—	3.40	0.10	3.41	1085
NENG	1998	6	30	20	19	15.68	22.351	-69.892	14	—	4.80	0.10	4.81	1110
PDE	1998	7	6	6	54	03.79	25.016	-93.633	10	—	3.40	0.10	3.41	1333
PDE	1998	7	7	18	44	44.46	34.719	-97.589	5	—	3.20	0.10	3.21	>1609
ISC	1998	8	14	17	5	11.80	27.744	-99.864	0	—	3.90	0.10	3.91	>1609
PRSN	1998	12	14	3	10	38.19	22.650	-70.240	25	—	3.90	0.23	3.96	1066
PDE	1999	1	18	7	0	53.47	33.405	-87.255	1	—	4.80	0.10	4.81	1108
SEUSN	1999	3	29	14	49	37.80	33.064	-80.140	10	3	2.97	0.27	3.06	845
ISC	1999	5	28	11	36	48.90	22.117	-75.228	33	—	4.63	0.10	4.64	633
MIDAS	1999	9	10	17	16	28.68	29.906	-70.976	56	—	4.96	0.10	4.97	1043
PDE	1999	11	28	11	0	09.30	33.416	-87.253	1	—	3.80	0.10	3.81	1109
ISC	2000	1	14	10	39	34.90	34.674	-95.095	18	—	3.09	0.23	3.15	>1609
SEUSN	2000	1	18	22	19	32.20	32.920	-83.465	19	5	3.50	0.10	3.51	883
SEUSN	2000	5	28	11	32	06.30	33.708	-87.811	0	3	3.00	0.10	3.01	1167
PDE	2000	9	20	6	24	59.00	24.622	-99.933	33	—	4.24	0.30	4.35	>1609
PDE	2000	12	9	6	46	09.12	28.027	-90.171	10	—	4.96	0.10	4.97	1015
PDE	2001	3	3	10	46	13.00	33.190	-92.660	5	—	3.00	0.10	3.01	1470
PDE	2001	3	16	4	39	07.68	28.361	-89.029	10	—	3.60	0.10	3.61	918
SEUSN	2001	3	21	23	35	34.90	34.847	-85.438	0	3	3.16	0.27	3.24	1154
ISC	2001	6	3	14	58	12.30	29.890	-79.480	0	—	3.30	0.10	3.31	500
PDE	2001	6	11	18	27	54.25	30.226	-79.885	10	—	3.30	0.10	3.31	532
PDE	2001	8	4	1	13	25.38	34.292	-93.213	5	3	3.10	0.10	3.11	1582
SEUSN	2001	12	8	1	8	22.40	34.710	-86.231	0	5	3.90	0.10	3.91	1175
NENG	2002	1	12	8	26	53.23	28.126	-69.615	5	—	5.60	0.10	5.61	1101
PDE	2002	2	8	16	7	13.60	34.727	-98.361	5	5	3.80	0.10	3.81	>1609

Turkey Point Units 6 & 7
COL Application
Part 2 — FSAR

PTN COL 2.5-2

Table 2.5.2-202 (Sheet 23 of 25)
Seismicity Catalog for the Phase 1 Investigation Region [22°N to 35°N, 100°W to 65°W] for which the Events are Rmb Magnitude Greater than or Equal to 3.0 or Intensity [Int] Greater than or Equal to IV(4)

Catalog Reference ^(a)	Year	Month	Day	Hour	Min	Sec	Lat	Lon	Depth (km)	Int	Emb	Smb	Rmb	Epicenter (km) ^(b)
SEUSN	2002	5	21	20	35	31.90	32.456	-88.221	27	3	2.97	0.27	3.06	1092
PDE	2002	5	27	0	28	16.99	27.117	-94.442	10	—	3.80	0.10	3.81	1414
PDE	2002	5	31	9	57	10.02	34.025	-97.619	5	3	3.30	0.10	3.31	>1609
SEUSN	2002	7	26	21	7	03.00	33.060	-80.195	10	—	2.97	0.30	3.08	845
PDE	2002	9	19	14	44	36.15	27.822	-89.135	10	—	3.70	0.10	3.71	911
PDE	2002	10	20	2	18	13.00	34.274	-96.079	5	5	3.40	0.10	3.41	>1609
PDE	2002	10	26	20	5	55.93	34.029	-90.683	5	—	3.10	0.10	3.11	1380
PDE	2002	11	8	13	29	03.19	32.422	-79.950	3	—	3.50	0.10	3.51	775
NENG	2002	11	11	23	39	29.62	32.456	-79.927	6	—	4.20	0.10	4.21	778
PDE	2002	11	21	11	17	22.61	22.947	-70.252	10	—	3.90	0.10	3.91	1055
PDE	2003	3	18	6	4	24.21	33.689	-82.888	5	4	3.50	0.10	3.51	948
PDE	2003	4	13	4	52	53.92	26.087	-86.085	10	—	3.20	0.10	3.21	579
SEUSN	2003	4	29	8	59	38.10	34.445	-85.620	9	6	4.60	0.10	4.61	1121
SEUSN	2003	5	5	10	53	49.90	33.055	-80.190	11	—	3.06	0.30	3.17	844
ISC	2003	6	22	20	47	40.90	23.016	-65.416	10	—	3.70	0.10	3.71	1530
PDE	2003	7	13	20	15	16.96	32.335	-82.144	5	3	3.60	0.10	3.61	784
SEUSN	2003	9	30	2	28	04.50	31.022	-87.462	12	—	2.97	0.30	3.08	931
NENG	2003	10	10	14	48	17.25	23.142	-84.932	15	—	4.30	0.10	4.31	528
SEUSN	2003	12	22	23	50	26.00	32.924	-80.157	5	—	2.97	0.30	3.08	830
SEUSN	2004	3	20	10	40	34.80	33.267	-86.955	0	3	2.97	0.27	3.06	1079
PDE	2004	4	6	19	1	02.70	25.172	-99.532	37	—	4.33	0.30	4.44	>1609
SEUSN	2004	5	9	8	56	10.40	33.231	-86.960	5	3	3.30	0.10	3.31	1076
PDE	2004	6	8	0	15	09.99	34.233	-97.254	5	4	3.50	0.10	3.51	>1609
ISC	2004	6	18	19	20	56.40	27.027	-86.997	10	—	3.50	0.10	3.51	685
SEUSN	2004	7	20	9	13	14.40	32.972	-80.248	10	—	3.06	0.30	3.17	835
ISC	2004	8	7	18	13	42.10	23.001	-70.239	0	—	3.68	0.10	3.69	1054
SEUSN	2004	8	19	23	51	49.40	33.203	-86.968	5	3	3.50	0.10	3.51	1074
NENG	2004	9	18	7	7	47.57	23.119	-67.594	5	—	5.70	0.10	5.71	1311
NENG	2004	11	7	11	20	22.19	32.700	-87.888	8	—	4.59	0.10	4.60	1088

Turkey Point Units 6 & 7
COL Application
Part 2 — FSAR

PTN COL 2.5-2

Table 2.5.2-202 (Sheet 24 of 25)
Seismicity Catalog for the Phase 1 Investigation Region [22°N to 35°N, 100°W to 65°W] for which the Events are Rmb Magnitude Greater than or Equal to 3.0 or Intensity [Int] Greater than or Equal to IV(4)

Catalog Reference ^(a)	Year	Month	Day	Hour	Min	Sec	Lat	Lon	Depth (km)	Int	Emb	Smb	Rmb	Epicenter (km) ^(b)
PDE	2004	11	22	23	42	13.45	34.864	-97.672	5	—	3.00	0.10	3.01	>1609
PRSN	2005	1	11	8	9	38.09	22.803	-66.947	25	—	4.20	0.23	4.26	1384
PDE	2005	3	22	8	11	50.51	31.836	-88.060	5	4	3.30	0.10	3.31	1034
ISC	2005	3	30	2	22	57.70	22.572	-94.790	0	—	4.00	0.10	4.01	1496
PDE	2005	4	22	5	17	04.09	34.179	-95.192	5	5	3.00	0.10	3.01	>1609
ISC	2005	8	10	1	18	35.70	22.119	-98.731	25	—	4.10	0.10	4.11	>1609
PRSN	2005	9	2	21	12	00.87	22.833	-70.272	25	—	4.60	0.23	4.66	1056
PDE	2005	9	19	2	29	52.54	23.950	-66.442	15	—	4.52	0.30	4.62	1407
PDE	2005	12	20	0	52	20.51	30.258	-90.708	5	4	3.00	0.10	3.01	1149
PDE	2006	2	10	4	14	22.20	27.828	-90.210	5	3	5.58	0.10	5.59	1014
ISC	2006	2	18	15	59	56.70	22.426	-80.966	0	—	3.00	0.10	3.01	336
ISC	2006	4	3	2	30	13.00	22.455	-99.889	16	—	4.10	0.10	4.11	>1609
PDE	2006	4	5	18	46	23.14	34.069	-97.314	5	—	3.00	0.10	3.01	>1609
PRSN	2006	5	7	20	46	45.01	22.334	-66.804	126	—	4.20	0.23	4.26	1412
ISC	2006	6	19	5	31	54.10	23.111	-75.594	25	—	3.40	0.10	3.41	542
ISC	2006	9	8	12	24	06.80	23.605	-71.845	25	—	3.60	0.10	3.61	879
NENG	2006	9	10	14	56	07.75	26.258	-86.630	14	—	5.90	0.10	5.91	635
ISC	2006	9	15	8	39	33.20	22.196	-79.886	0	—	3.20	0.10	3.21	359
ISC	2006	9	20	20	53	33.20	22.966	-75.623	0	—	3.90	0.10	3.91	548
PDE	2006	9	22	11	22	00.28	34.551	-79.583	5	—	3.40	0.10	3.41	1014
PDE	2006	9	25	5	44	25.09	34.746	-79.876	5	4	3.70	0.10	3.71	1034
PDE	2006	10	6	22	13	16.78	34.122	-97.625	5	4	3.50	0.10	3.51	>1609
ISC	2006	11	5	14	1	41.60	22.628	-67.065	126	—	4.80	0.10	4.81	1377
ISC	2006	12	17	17	24	54.20	22.434	-76.982	0	—	3.10	0.10	3.11	473
ISC	2007	3	6	7	3	06.70	22.028	-71.023	20	—	4.20	0.10	4.21	1016
ISC	2007	4	26	22	13	50.10	22.692	-75.015	25	—	3.00	0.10	3.01	616
PDE	2007	5	4	16	16	28.18	33.797	-87.299	5	—	3.00	0.10	3.01	1145
PDE	2007	5	16	13	22	21.42	33.300	-92.587	5	4	3.00	0.10	3.01	1471
ISC	2007	5	23	19	9	14.40	22.049	-96.387	10	—	5.40	0.10	5.41	>1609

Turkey Point Units 6 & 7
COL Application
Part 2 — FSAR

PTN COL 2.5-2

Table 2.5.2-202 (Sheet 25 of 25)
Seismicity Catalog for the Phase 1 Investigation Region [22°N to 35°N, 100°W to 65°W] for which the Events are Rmb Magnitude Greater than or Equal to 3.0 or Intensity [Int] Greater than or Equal to IV(4)

Catalog Reference ^(a)	Year	Month	Day	Hour	Min	Sec	Lat	Lon	Depth (km)	Int	Emb	Smb	Rmb	Epicenter (km) ^(b)
ISC	2007	6	1	4	49	19.10	22.738	-71.141	0	—	4.00	0.10	4.01	976
ISC	2007	8	22	6	19	23.00	22.236	-71.628	25	—	4.90	0.23	4.96	949
PDE-W	2007	12	27	20	51	57.49	27.679	-71.076	10	—	4.60	0.10	4.61	951

- (a) "EPRIm" are the "MAIN" events from the EPRI catalog.
 "****c" are constituent catalogs from IPGH catalog
 "****wy" are constituent catalogs from Wysession et al. catalog ([Reference 338](#))
 "****me" are constituent catalogs from the Mexico Composite Catalog
 "****np" are constituent catalogs from National Geophysical Data Center catalog
- (b) Distance to epicenter ">1609" is greater than 1000 miles.
- (c) "X" indicates modified Mercalli Intensity of {Roman numeral} 10; "F" indicates the earthquake was felt.

Turkey Point Units 6 & 7
COL Application
Part 2 — FSAR

PTN COL 2.5-2

Table 2.5.2-203 (Sheet 1 of 9)
Seismicity Catalog for the Phase 2 Investigation Region [15°N to 24°N, 100°W to 65°W] for which the Events are M_w Magnitude Greater than or Equal to 6.0

Catalog Reference ^(a)	Year	Month	Day	Hr	Min	Sec	Lat	Lon	Depth (km)	Int	M _w	Epicenter (km) ^(b)
CUBA	1502	0	0	0	0	0.00	18.400	-69.900	30	—	6.21	1324
FELD	1539	11	24	0	0	0.00	16.750	-86.750	5	X ^(c)	7.69	1166
CUBA	1562	12	3	1	0	0.00	19.600	-70.800	30	—	7.23	1168
CUBA	1578	8	0	0	0	0.00	19.900	-76.000	30	—	6.78	753
PM c	1591	3	14	0	0	0.00	16.000	-92.500	0	8	7.00	>1609
CUBA	1667	0	0	0	0	0.00	17.800	-77.000	30	—	6.78	909
CUBA	1673	5	9	11	30	0.00	18.400	-70.300	30	—	7.53	1291
CUBA	1678	2	11	14	59	0.00	19.900	-76.000	30	8 ^(d)	6.78	753
CUBA	1684	0	0	0	0	0.00	18.400	-70.300	30	—	7.53	1291
NOAA	1691	0	0	0	0	0.00	18.300	-70.400	33	—	7.73	1289
CUBA	1692	6 ^(e)	7 ^(e)	0	0	0.00	18.200	-77.000	33	X ^{(c),(e)}	7.78	868
NOAA	1697	2	25	0	0	0.00	16.700	-99.200	0	—	7.83	>1609
CUBA	1701	11	9	0	0	0.00	18.700	-72.800	30	—	6.21	1072
SUARc	1711	8	15	0	0	0.00	19.000	-98.000	0	9	6.80	>1609
WHE c	1714	5	5	0	0	0.00	15.450	-92.200	10	7	6.23	>1609
WHE c	1728	0	0	0	0	0.00	15.755	-90.400	5	7	6.23	1496
WHE c	1741	2	15	0	0	0.00	15.750	-90.420	10	8	7.00	1497
W&C c	1743	5	30	0	0	0.00	16.750	-92.750	33	8	8.19	1603
WHE c	1750	3	8	0	0	0.00	15.450	-91.480	10	7	6.57	1600
CUBA	1751	9	16	3	29	0.00	18.600	-72.300	30	—	6.83	1117
CUBA	1751	10	18	20	0	0.00	18.400	-70.600	30	—	7.28	1266
NOAA	1754	9	1	0	0	0.00	16.700	-99.200	0	—	7.83	>1609
SAL c	1757	12	14	0	0	0.00	20.000	-75.833	10	—	6.23	755
CUBA	1760	7	11	0	0	0.00	19.900	-76.000	30	—	6.78	753
CUBA	1761	10	28	20	29	0.00	18.400	-69.900	30	—	6.21	1324
CUBA	1761	11	21	13	0	0.00	18.400	-70.800	30	—	6.64	1250
W&C c	1765	10	24	0	0	0.00	15.000	-91.916	0	8	7.59	>1609

Turkey Point Units 6 & 7
COL Application
Part 2 — FSAR

PTN COL 2.5-2

Table 2.5.2-203 (Sheet 2 of 9)
Seismicity Catalog for the Phase 2 Investigation Region [15°N to 24°N, 100°W to 65°W] for which the Events are
M_w Magnitude Greater than or Equal to 6.0

Catalog Reference ^(a)	Year	Month	Day	Hr	Min	Sec	Lat	Lon	Depth (km)	Int	M _w	Epicenter (km) ^(b)
CUBA	1766	6	12	5	14	0.00	19.900	-76.100	30	g ^(f)	7.53	747
CUBA	1770	6	4	0	15	0.00	18.600	-72.600	70	—	7.53	1095
SUARc	1776	4	21	0	0	0.00	16.800	100.000	0	9	7.70	>1609
CUBA	1783	2	11	0	0	0.00	19.700	-70.800	30	—	6.13	1162
SAL c	1784	7	29	0	0	0.00	19.780	-72.280	33	8	6.75	1033
NOAA	1785	0	0	0	0	0.00	16.700	-99.200	0	—	7.83	>1609
WHE c	1785	1	6	0	0	0.00	15.500	-89.700	5	9	7.40	1468
NOAA	1787	0	0	0	0	0.00	19.000	-66.000	33	—	8.03	>1609
SUARc	1787	3	28	0	0	0.00	16.000	-97.000	0	X ^(c)	8.40	>1609
CUBA	1793	4	0	0	0	0.00	18.400	-69.900	30	—	6.21	1324
WHE c	1795	12	29	0	0	0.00	15.375	-91.450	5	7	6.23	1604
SAL c	1798	5	28	0	0	0.00	18.800	-72.300	33	6	6.23	1102
WHE c	1798	7	2	0	0	0.00	15.080	-90.070	10	7	6.23	1529
W&C c	1804	0	0	0	0	0.00	16.500	-92.666	0	7	6.80	>1609
CUBA	1812	11	11	10	0	0.00	17.800	-77.000	20	—	6.13	909
NOAA	1816	7	22	0	0	0.00	15.500	-91.500	33	—	7.63	1598
SUARc	1820	5	4	0	0	0.00	16.500	-99.000	0	9	7.80	>1609
WHE c	1820	6	6	0	0	0.00	15.065	-90.320	5	7	6.23	1548
KSS c	1820	10	19	0	0	0.00	15.600	-88.050	10	8	6.44	1351
WHE c	1821	5	6	0	0	0.00	15.005	-91.165	15	8	6.37	>1609
SAL c	1826	9	18	9	8	0.00	19.500	-76.000	33	8	7.00	790
SAL c	1830	4	14	11	30	0.00	18.500	-72.300	10	7	6.57	1125
SUARc	1837	11	23	0	0	0.00	16.000	-98.000	0	—	7.70	>1609
CUBA	1842	5	7	22	15	0.00	19.800	-72.200	60	g ^(d)	8.23	1038
CUBA	1842	7	7	0	0	0.00	19.900	-76.000	30	—	6.13	753
CARIB	1844	4	16	13	20	0.00	18.300	-66.800	0	8	6.40	1599
SUARc	1845	8	7	0	0	0.00	16.800	100.000	0	X ^(c)	8.30	>1609
PM c	1851	5	17	0	0	0.00	15.083	-91.830	0	8	6.40	>1609
CUBA	1852	7	7	12	25	0.00	19.700	-79.700	30	g ^(f)	7.53	635

Turkey Point Units 6 & 7
COL Application
Part 2 — FSAR

PTN COL 2.5-2

Table 2.5.2-203 (Sheet 3 of 9)
Seismicity Catalog for the Phase 2 Investigation Region [15°N to 24°N, 100°W to 65°W] for which the Events are
M_w Magnitude Greater than or Equal to 6.0

Catalog Reference ^(a)	Year	Month	Day	Hr	Min	Sec	Lat	Lon	Depth (km)	Int	M _w	Epicenter (km) ^(b)
CUBA	1852	8	20	14	5	0.00	19.750	-75.320	30	—	7.33	809
CUBA	1852	11	26	8	44	0.00	19.900	-76.200	30	—	6.55	741
KSS c	1853	8	26	0	0	0.00	15.860	-86.265	0	7	6.03	1224
ROJ c	1856	5	5	0	0	0.00	16.400	-88.100	10	5	6.10	1282
KSS c	1856	8	4	22	47	0.00	16.750	-86.750	5	χ ^(c)	7.69	1166
SAL c	1856	8	28	18	0	0.00	18.500	-65.000	33	6	6.40	>1609
CUBA	1858	1	28	10	14	0.00	19.900	-76.000	30	—	6.55	753
CUBA	1860	4	9	3	30	0.00	18.600	-73.200	50	—	6.73	1051
SAL c	1860	10	23	0	0	0.00	18.500	-67.500	33	7	6.57	1525
SUARc	1864	10	3	0	0	0.00	19.000	-97.000	0	9	7.40	>1609
SAL c	1865	8	30	0	0	0.00	18.000	-66.500	33	6	6.07	>1609
SAL c	1867	11	12	5	0	0.00	19.000	-76.250	10	6	6.40	823
SAL c	1867	11	18	20	0	0.00	18.500	-65.000	33	8	7.50	>1609
SAL c	1870	9	11	0	0	0.00	19.000	-77.000	10	6	6.23	787
SAL c	1874	8	26	11	15	0.00	19.000	-66.000	50	6	6.40	>1609
SAL c	1875	12	9	0	0	0.00	19.000	-67.000	50	7	6.40	1541
CUBA	1880	1	23	4	39	0.00	22.700	-83.000	15	g ^(f)	6.13	404
SAL c	1880	12	30	0	0	0.00	18.250	-76.500	10	6	6.07	885
KSS c	1881	4	23	0	0	0.00	16.550	-87.500	10	8	6.44	1230
SAL c	1882	0	0	0	0	0.00	18.500	-70.000	33	6	6.23	1309
SUARc	1882	7	19	0	0	0.00	18.000	-98.000	0	9	6.70	>1609
CUBA	1887	9	23	11	55	0.00	19.400	-73.400	60	g ^(d)	7.93	973
NOAA	1897	6	5	0	0	0.00	17.000	-96.300	0	—	7.03	>1609
CUBA	1897	12	29	11	32	0.00	20.100	-71.200	50	—	7.03	1102
NOAA	1899	1	24	23	43	0.00	17.000	-98.000	60	—	8.42	>1609
AMB c	1899	3	25	14	27	0.00	16.800	-92.800	35	—	6.26	1604
GUT c	1899	6	14	0	0	0.00	18.000	-77.000	0	—	7.80	888
CHA c	1902	1	16	0	0	0.00	17.620	-99.720	0	—	7.00	>1609
EV02	1902	2	17	0	31	0.00	20.000	-70.000	0	—	6.93	1214

Turkey Point Units 6 & 7
COL Application
Part 2 — FSAR

PTN COL 2.5-2

Table 2.5.2-203 (Sheet 4 of 9)
Seismicity Catalog for the Phase 2 Investigation Region [15°N to 24°N, 100°W to 65°W] for which the Events are
M_w Magnitude Greater than or Equal to 6.0

Catalog Reference ^(a)	Year	Month	Day	Hr	Min	Sec	Lat	Lon	Depth (km)	Int	M _w	Epicenter (km) ^(b)
EV02	1902	9	23	20	18	0.00	16.000	-93.000	0	—	7.80	>1609
EV02	1903	1	14	1	47	0.00	15.000	-98.000	0	—	7.40	>1609
GUT c	1903	8	16	0	0	0.00	20.000	-72.000	0	—	6.44	1041
MACRc	1906	6	22	0	0	0.00	19.500	-76.000	10	7	6.57	790
CUBA	1907	1	14	20	29	0.00	18.400	-76.800	20	—	6.64	856
EV02	1907	4	15	6	8	6.00	17.000	100.000	0	—	7.90	>1609
EV02	1908	3	26	23	3	30.00	18.000	-99.000	80	—	7.73	>1609
EV02	1910	1	1	11	2	0.00	16.500	-84.000	60	—	7.10	1057
CHA c	1911	2	3	0	0	0.00	18.200	-96.360	80	—	7.19	>1609
EV02	1911	10	6	10	16	12.00	19.000	-70.500	0	—	6.83	1233
CUBA	1912	4	9	8	32	29.00	19.000	-85.000	0	—	7.69	855
EV02	1912	6	12	12	43	42.00	17.000	-89.000	0	—	6.83	1292
EV02	1912	11	19	13	55	0.00	19.000	100.000	80	—	6.93	>1609
EV02	1912	12	9	8	32	24.00	15.500	-93.000	0	—	7.10	>1609
CUBA	1914	2	28	5	19	0.00	21.300	-76.200	50	—	6.29	619
ISSv	1914	3	30	0	41	11.00	19.000	-96.000	0	—	7.23	>1609
ISC	1914	8	3	11	25	30.00	18.500	-76.500	35	—	6.13	1136
CUBA	1914	8	25	5	19	0.00	19.530	-76.370	30	—	6.73	766
ISSv	1915	10	11	19	32	50.00	18.000	-69.500	0	—	6.83	1385
EV02	1916	6	2	13	59	24.00	17.500	-95.000	150	—	7.03	>1609
ISSv	1916	11	21	6	25	24.00	18.000	100.000	0	—	6.80	>1609
ISSv	1916	11	30	3	17	50.00	19.000	-70.000	0	—	7.00	1275
ISSv	1917	2	20	19	29	32.00	19.000	-80.000	0	6 ^(d)	7.20	710
ISSv	1918	10	11	14	14	25.00	18.500	-68.000	0	—	7.30	1480
AMB c	1918	10	19	3	22	45.00	15.000	-91.000	35	—	6.24	1602
ISSv	1920	1	4	4	21	58.00	18.200	-97.500	0	—	7.83	>1609
ISSv	1920	4	19	21	6	25.00	18.400	-94.300	0	—	6.83	>1609
ISSv	1921	2	4	8	22	35.00	16.500	-89.500	0	—	7.43	1369
ISSv	1922	12	18	12	34	48.00	18.500	-68.000	0	—	6.29	1480

Turkey Point Units 6 & 7
COL Application
Part 2 — FSAR

PTN COL 2.5-2

Table 2.5.2-203 (Sheet 5 of 9)
Seismicity Catalog for the Phase 2 Investigation Region [15°N to 24°N, 100°W to 65°W] for which the Events are
M_w Magnitude Greater than or Equal to 6.0

Catalog Reference ^(a)	Year	Month	Day	Hr	Min	Sec	Lat	Lon	Depth (km)	Int	M _w	Epicenter (km) ^(b)
ISSv	1923	11	3	8	37	40.00	19.000	-74.000	95	—	6.13	962
ISSv	1925	6	14	22	28	6.00	17.500	-83.000	0	—	6.55	917
ISSv	1925	12	10	14	14	42.00	15.500	-92.500	0	—	7.00	>1609
ISSv	1928	3	22	4	16	50.00	16.000	-96.000	0	—	7.50	>1609
ISSv	1928	4	17	3	25	12.00	17.500	-94.500	0	—	7.73	>1609
ISSv	1928	6	17	3	19	19.00	16.200	-97.200	0	—	7.70	>1609
ISSv	1929	8	17	23	40	36.00	16.300	-99.000	0	—	6.17	>1609
ISSv	1931	1	15	1	50	49.00	16.400	-96.300	0	—	7.80	>1609
ISSv	1931	7	17	9	13	50.00	16.200	-97.200	0	—	6.29	>1609
ISSv	1931	9	26	19	50	33.00	15.000	-91.500	0	—	6.13	>1609
ISSv	1932	2	3	6	16	3.00	19.700	-75.500	0	—	6.83	802
ISSv	1932	6	6	11	50	0.00	19.600	-76.500	0	—	6.13	753
ISSv	1934	1	28	19	10	10.00	16.900	-99.600	0	—	6.83	>1609
ISC	1934	7	27	2	25	45.00	16.000	-92.500	50	—	6.29	>1609
ISC	1934	12	3	2	38	29.00	15.000	-88.750	35	—	6.29	1449
ISSv	1937	5	28	15	35	51.00	17.100	-93.400	95	—	6.55	>1609
ISSv	1937	7	26	3	47	3.00	18.500	-95.700	0	—	7.23	>1609
ISSv	1937	12	23	13	17	54.00	16.300	-98.600	0	—	7.40	>1609
ISC	1938	6	28	19	17	42.00	18.000	100.000	110	—	6.55	>1609
ISSv	1939	6	12	4	5	9.00	20.500	-66.000	0	—	6.29	1559
ISC	1939	9	28	14	58	27.00	15.500	-91.500	110	—	6.29	1598
ISSv	1941	4	7	23	29	17.00	17.500	-78.400	0	—	7.03	897
ISSv	1941	6	27	17	11	37.00	17.100	-93.400	160	—	6.29	>1609
ISSv	1942	10	28	10	44	39.00	15.000	-96.100	0	—	6.29	>1609
ISSv	1942	11	12	4	55	25.00	16.500	-94.400	0	—	6.83	>1609
ISSv	1943	7	29	3	2	14.00	19.100	-67.100	0	—	7.60	1526
EV02	1943	9	23	15	0	44.00	15.000	-91.500	110	—	6.83	>1609
EV02	1944	6	28	7	58	54.00	15.000	-92.500	0	—	7.13	>1609
ISSv	1945	10	11	16	53	2.00	18.300	-97.600	95	—	6.55	>1609

Turkey Point Units 6 & 7
COL Application
Part 2 — FSAR

PTN COL 2.5-2

Table 2.5.2-203 (Sheet 6 of 9)
Seismicity Catalog for the Phase 2 Investigation Region [15°N to 24°N, 100°W to 65°W] for which the Events are
M_w Magnitude Greater than or Equal to 6.0

Catalog Reference ^(a)	Year	Month	Day	Hr	Min	Sec	Lat	Lon	Depth (km)	Int	M _w	Epicenter (km) ^(b)
ISSv	1946	3	25	8	47	39.00	19.700	-74.700	0	—	6.13	855
ISSv	1946	5	15	22	10	34.00	15.500	-96.700	0	—	6.17	>1609
ISSv	1946	6	7	4	13	22.00	16.900	-94.200	95	—	6.93	>1609
ISSv	1946	8	4	17	51	4.00	18.900	-68.900	0	—	7.90	1377
ISSv	1946	8	8	13	28	28.00	19.600	-69.400	0	—	7.50	1290
ISSv	1947	8	7	0	40	20.00	19.900	-75.300	0	—	6.83	798
ISSv	1948	1	6	17	25	48.00	16.000	-98.400	0	—	7.03	>1609
ISSv	1948	8	11	10	36	18.00	17.700	-95.200	65	—	6.83	>1609
ISSv	1949	12	22	9	30	47.00	15.900	-93.000	65	—	6.57	>1609
ISSv	1950	8	3	6	14	55.00	18.100	-99.900	95	—	6.18	>1609
PDEnp	1950	10	23	17	5	25.00	15.000	-91.500	0	—	7.53	>1609
ISSv	1950	12	14	14	15	43.00	16.300	-98.600	0	—	7.30	>1609
ISSv	1951	12	12	1	37	40.00	16.500	-96.900	160	—	7.03	>1609
ISSv	1952	1	31	20	16	49.00	15.000	-93.800	95	—	6.34	>1609
ISSv	1952	5	14	21	11	35.00	16.500	-86.500	0	—	6.10	1175
ISSv	1952	10	28	4	29	52.00	18.300	-73.300	0	—	7.03	1069
ISSv	1953	5	31	19	58	39.00	19.400	-70.400	33	—	6.93	1215
PEREZ	1953	12	1	15	18	33.00	16.400	-98.850	0	—	6.70	>1609
ISC	1954	1	28	22	14	52.00	16.530	-99.720	0	—	6.04	>1609
ISSv	1954	5	13	14	46	39.00	16.900	-95.900	65	—	6.60	>1609
ISSv	1954	12	10	13	0	27.00	17.800	-81.800	0	—	6.37	855
ISSv	1955	9	26	8	28	31.00	15.900	-92.200	225	—	6.93	>1609
ISSv	1956	7	9	9	56	12.00	20.000	-72.950	40	—	6.93	963
ISSv	1956	11	9	13	6	15.00	17.450	-94.080	130	—	6.48	>1609
ISSv	1957	3	2	0	27	36.00	18.300	-78.150	0	—	6.61	818
ISSv	1957	4	10	5	12	7.00	15.530	-98.040	0	—	6.70	>1609
ISSv	1957	5	15	2	11	9.00	16.750	-93.510	125	—	6.03	>1609
ISSv	1957	7	28	8	40	7.00	17.070	-99.150	0	—	7.80	>1609
ISSv	1957	9	12	0	28	3.00	16.990	-85.600	0	—	6.04	1079

Turkey Point Units 6 & 7
COL Application
Part 2 — FSAR

PTN COL 2.5-2

Table 2.5.2-203 (Sheet 7 of 9)
Seismicity Catalog for the Phase 2 Investigation Region [15°N to 24°N, 100°W to 65°W] for which the Events are
M_w Magnitude Greater than or Equal to 6.0

Catalog Reference ^(a)	Year	Month	Day	Hr	Min	Sec	Lat	Lon	Depth (km)	Int	M _w	Epicenter (km) ^(b)
ISSv	1959	1	27	0	20	24.00	18.080	-68.660	90	—	6.04	1450
ISSv	1959	2	20	18	16	20.00	15.940	-90.590	48	7	6.57	1494
ISSv	1959	4	12	9	54	56.00	17.070	-95.040	124	—	6.40	>1609
PEREZ	1959	4	28	11	9	46.00	15.830	-92.830	0	—	6.34	>1609
ISSv	1959	5	24	19	17	40.00	17.610	-97.170	63	—	6.37	>1609
ISSv	1959	8	26	8	25	31.00	18.260	-94.430	0	—	6.93	>1609
ISC	1961	10	12	13	53	28.00	18.800	-65.000	50	—	6.37	>1609
ISSv	1961	11	16	8	19	49.00	18.500	-69.260	78	—	6.13	1371
PEREZ	1961	12	4	7	36	22.00	18.200	-69.100	0	—	6.34	1404
ISSv	1962	1	8	1	0	19.00	18.480	-70.400	0	—	6.73	1277
ISSv	1962	4	20	5	47	52.00	20.500	-72.140	0	—	6.73	997
ISSv	1962	4	22	4	45	26.00	15.470	-93.080	113	—	6.13	>1609
ISSv	1962	5	11	14	11	55.00	17.260	-99.630	37	—	7.30	>1609
ISSv	1962	5	20	15	1	15.00	20.630	-65.800	0	—	6.52	1573
ISSv	1962	7	24	21	8	22.00	15.420	-92.490	134	—	6.06	>1609
ISSv	1962	7	25	4	37	42.00	18.900	-81.410	0	—	6.29	728
EV02	1965	4	3	11	29	12.66	16.024	-97.861	30	—	6.29	>1609
NENG	1965	8	23	19	46	1.63	16.176	-95.847	10	—	6.73	>1609
CUBA	1965	10	16	9	30	0.00	18.500	-77.900	10	—	6.13	804
PDEnp	1965	12	9	6	7	47.70	17.300	100.000	54	—	6.04	>1609
PEREZ	1967	2	4	14	8	50.00	24.000	-65.700	1	—	6.43	1480
NENG	1968	8	2	14	6	46.18	16.493	-97.771	49	—	6.37	>1609
W&C c	1970	4	29	0	0	0.00	15.000	-92.333	56	—	7.09	>1609
NENG	1971	6	11	12	56	6.75	17.983	-69.809	59	—	6.04	1360
NENG	1972	9	16	9	14	35.88	15.187	-96.263	32	—	6.04	>1609
NENG	1973	8	28	9	50	41.02	18.233	-96.608	80	—	6.73	>1609
NENG	1976	2	4	9	1	46.20	15.296	-89.145	12	—	7.50	1448
NENG	1977	8	20	3	51	56.50	16.720	-86.638	31	—	6.40	1162
NENG	1978	3	19	1	39	11.37	16.932	-99.782	11	—	6.60	>1609

Turkey Point Units 6 & 7
COL Application
Part 2 — FSAR

PTN COL 2.5-2

Table 2.5.2-203 (Sheet 8 of 9)
Seismicity Catalog for the Phase 2 Investigation Region [15°N to 24°N, 100°W to 65°W] for which the Events are
M_w Magnitude Greater than or Equal to 6.0

Catalog Reference ^(a)	Year	Month	Day	Hr	Min	Sec	Lat	Lon	Depth (km)	Int	M _w	Epicenter (km) ^(b)
NENG	1978	11	29	19	52	50.15	16.011	-96.603	24	—	7.80	>1609
NENG	1979	3	23	19	32	32.73	17.963	-69.077	81	—	6.70	1422
NENG	1979	6	22	6	30	56.37	17.008	-94.623	113	—	6.90	>1609
NENG	1979	10	1	14	14	12.04	15.762	-92.198	164	—	6.20	>1609
NENG	1980	8	9	5	45	10.49	15.912	-88.490	16	—	6.50	1350
NENG	1980	10	24	14	53	35.55	18.175	-98.235	64	—	7.20	>1609
NENG	1981	9	14	12	44	31.00	18.260	-68.919	169	—	6.10	1416
NENG	1982	4	10	16	25	37.53	17.502	-83.427	19	—	6.30	931
NENG	1982	6	7	6	52	33.45	16.407	-98.294	8	—	6.90	>1609
NENG	1983	1	24	8	17	40.21	16.131	-95.238	48	—	6.80	>1609
NENG	1983	9	15	10	39	4.02	16.088	-93.179	118	—	6.30	>1609
NENG	1984	6	24	11	17	16.32	17.981	-69.371	45	—	6.70	1397
NENG	1984	7	2	4	50	44.25	16.753	-98.493	34	—	6.20	>1609
NENG	1985	9	15	7	57	55.31	17.940	-97.185	68	—	6.00	>1609
NENG	1986	7	5	22	9	34.27	15.488	-92.523	72	—	6.00	>1609
NENG	1987	3	12	12	18	13.86	15.545	-94.618	45	—	6.10	>1609
NENG	1987	7	15	7	16	14.62	17.508	-97.153	64	—	6.20	>1609
NENG	1988	11	3	19	42	20.70	19.000	-67.329	40	—	6.00	1511
NENG	1989	4	25	14	29	2.07	16.779	-99.275	19	—	6.90	>1609
NENG	1989	9	16	23	20	54.80	16.463	-93.661	113	—	6.10	>1609
NENG	1992	5	25	16	55	5.82	19.618	-77.883	23	7 ^(f)	6.80	688
PRSN	1992	11	20	22	13	21.00	19.060	-71.660	47	—	6.37	1134
NENG	1993	5	15	3	12	35.09	16.725	-98.325	25	—	6.10	>1609
NENG	1993	9	30	18	27	50.98	15.176	-94.851	19	—	6.50	>1609
NENG	1993	10	24	7	52	17.07	16.753	-98.758	21	—	6.60	>1609
NENG	1994	3	14	20	51	25.80	15.943	-92.403	164	—	6.90	>1609
NENG	1995	6	27	10	10	0.41	18.794	-81.767	15	—	6.00	746
NENG	1995	9	14	14	4	33.23	16.849	-98.608	23	—	7.40	>1609
NENG	1995	10	21	2	38	58.25	16.836	-93.465	159	—	7.20	>1609

Turkey Point Units 6 & 7
COL Application
Part 2 — FSAR

PTN COL 2.5-2

Table 2.5.2-203 (Sheet 9 of 9)
Seismicity Catalog for the Phase 2 Investigation Region [15°N to 24°N, 100°W to 65°W] for which the Events are
M_w Magnitude Greater than or Equal to 6.0

Catalog Reference ^(a)	Year	Month	Day	Hr	Min	Sec	Lat	Lon	Depth (km)	Int	M _w	Epicenter (km) ^(b)
NENG	1997	7	19	14	22	7.07	16.203	-98.154	15	—	6.70	>1609
NENG	1998	2	3	3	2	0.63	15.900	-96.245	24	—	6.30	>1609
NENG	1998	6	7	23	20	14.04	15.966	-93.741	75	—	6.30	>1609
NENG	1999	6	15	20	42	6.60	18.381	-97.445	63	—	7.00	>1609
NENG	1999	7	11	14	14	18.97	15.791	-88.285	15	—	6.70	1348
NENG	1999	9	30	16	31	14.81	16.055	-96.905	40	—	7.50	>1609
NENG	1999	12	1	19	23	8.62	17.667	-82.370	15	—	6.30	882
NENG	2000	3	12	22	21	31.62	15.141	-92.411	53	—	6.30	>1609
ISC	2000	12	4	4	42	15.40	15.014	-93.833	36	—	6.13	>1609
NENG	2001	11	28	14	32	34.62	15.683	-93.118	84	—	6.40	>1609
NENG	2003	9	22	4	45	38.67	19.766	-70.693	14	—	6.40	1167
NENG	2004	12	14	23	20	13.77	18.939	-81.384	13	—	6.80	724
NENG	2005	3	17	13	37	36.93	15.183	-91.360	194	—	6.20	>1609
NENG	2007	2	4	20	56	58.82	19.326	-78.521	10	—	6.20	698
NENG	2007	7	6	1	9	18.50	16.493	-93.638	113	—	6.10	>1609
PDE-W	2008	2	12	12	50	18.49	16.360	-94.300	83	—	6.40	>1609

- (a) "****c" are constituent catalogs from IPGH catalog
"****np" are constituent catalogs from National Geophysical Data Center catalog
- (b) Distance to epicenter ">1609" is greater than 1000 miles.
- (c) "X" indicates modified Mercalli Intensity of {Roman numeral} 10.
- (d) McCann ([Reference 282](#)).
- (e) DeMets and Wiggins-Grandison ([Reference 229](#)).
- (f) Garcia et al. ([Reference 254](#)).
- Additional Reference: "FELD" from McCann ([Reference 283](#)).

Turkey Point Units 6 & 7
COL Application
Part 2 — FSAR

PTN COL 2.5-2

Table 2.5.2-204
Seismicity Events Recommended for Recurrence Analysis within the Gulf of Mexico

Earthquakes in the Gulf of Mexico: MAIN [or equivalent] Events, Rmb \geq 3.0 or Int \geq IV(4)													
Source Catalog ^(a)	Year	Month	Day	Hour	Minute	Second	Lat	Lon	Depth (km)	Int	Emb	Smb	Rmb
EPRI _m	1927	12	15	4	30	0.00	28.900	-89.400	0	4	3.80	0.30	3.90
EPRI _m	1929	7	28	17	0	0.00	28.900	-89.400	0	4	3.80	0.30	3.90
EPRI _m	1958	11	6	23	8	0.00	29.900	-90.100	0	4	3.11	0.56	3.47
EPRI _m	1963	11	5	22	45	3.40	27.490	-92.580	15	—	4.71	0.20	4.76
ISC	1967	3	21	20	41	27.00	24.000	-97.000	33	—	3.90	0.10	3.91
ISC	1967	10	4	2	45	45.00	27.000	-94.000	33	—	3.20	0.10	3.21
ISC c	1974	9	13	17	29	57.80	23.782	-96.428	0	—	3.60	0.10	3.61
EPRI _m	1978	7	24	8	6	16.90	26.380	-88.720	15	—	4.88	0.10	4.89
EPRI _m	1980	1	10	19	16	23.50	24.130	-85.710	15	—	3.88	0.10	3.89
ANSS	1984	1	23	0	11	59.38	26.716	-87.339	5	—	2.85	0.41	3.04
TEI _{me}	1984	1	23	1	15	9.40	26.716	-87.339	5	—	2.85	0.41	3.04
PDE	1992	3	31	14	59	39.64	26.019	-85.731	5	—	3.80	0.10	3.81
TEIC	1992	9	27	17	2	25.70	27.225	-88.711	10	—	3.80	0.10	3.81
PDE	1992	11	30	8	33	1.48	23.251	-98.199	10	—	4.61	0.30	4.71
PDE	1994	6	30	1	8	24.22	27.911	-90.177	10	—	4.20	0.10	4.21
PDE	1997	4	18	14	57	35.39	25.782	-86.552	33	—	3.90	0.10	3.91
PDE	1998	7	6	6	54	3.79	25.016	-93.633	10	—	3.40	0.10	3.41
PDE	2000	12	9	6	46	9.12	28.027	-90.171	10	—	4.96	0.10	4.97
PDE	2001	3	16	4	39	7.68	28.361	-89.029	10	—	3.60	0.10	3.61
PDE	2002	5	27	0	28	16.99	27.117	-94.442	10	—	3.80	0.10	3.81
PDE	2002	9	19	14	44	36.15	27.822	-89.135	10	—	3.70	0.10	3.71
PDE	2003	4	13	4	52	53.92	26.087	-86.085	10	—	3.20	0.10	3.21
NENG	2003	10	10	14	48	17.25	23.142	-84.932	15	—	4.30	0.10	4.31
ISC	2004	6	18	19	20	56.40	27.027	-86.997	10	—	3.50	0.10	3.51
PDE	2006	2	10	4	14	22.20	27.828	-90.210	5	3	5.58	0.10	5.59
NENG	2006	9	10	14	56	7.75	26.258	-86.630	14	—	5.90	0.10	5.91

(a) "EPRI_m" are the "MAIN" events from the EPRI catalog.
 "****c" are constituent catalogs from IPGH catalog.
 "****me" are constituent catalogs from the Mexico Composite Catalog.

Turkey Point Units 6 & 7
COL Application
Part 2 — FSAR

PTN COL 2.5-2

Table 2.5.2-205 (Sheet 1 of 2)
Region 2 Matrix of Detection Probabilities; Modified to Extend the Matrix to Year 2007

Detection Probability Matrix: EPRI (Reference 243) Incompleteness Region 2 [Modified]								
Magnitude Intervals	Year Intervals							Total Years
	1625–1779	1780–1859	1860–1909	1910–1949	1950–1974	1975–1084	1985–2007	
	155 years	80 years	50 years	40 years	25 years	10 years	23 years	
3.3–3.89	0.00	0.00	0.10	0.51	0.63	1.00	1.00	74.2
3.9–4.49	0.00	0.00	0.15	0.90	1.00	1.00	1.00	101.5
4.5–5.09	0.00	0.00	0.24	0.98	1.00	1.00	1.00	109.2
5.1–5.69	0.00	0.00	0.24	0.98	1.00	1.00	1.00	109.2
5.7–6.29	0.00	0.00	0.70	1.00	1.00	1.00	1.00	133.0
6.3–7.5	0.00	0.01	1.00	1.00	1.00	1.00	1.00	148.8

Detection Probability Matrix: EPRI (Reference 243) Incompleteness Region 2 [Modified]												
Magnitude Intervals	Year Intervals										Total Years	
	1625–1779	1780–1859	1860–1899	1900–1924	1925–1949	1950–1959	1960–1964	1965–1969	1970–1974	1975–1979		1980–2007
	155 years	80 years	40 years	25 years	25 years	10 years	5 years	5 years	5 years	5 years	28 years	
3.3–3.89	0.00	0.00	0.10	0.31	0.51	0.55	0.60	0.65	0.80	1.00	1.00	73.1
3.9–4.49	0.00	0.00	0.15	0.53	0.90	0.99	1.00	1.00	1.00	1.00	1.00	99.5
4.5–5.09	0.00	0.00	0.24	0.61	0.98	0.99	1.00	1.00	1.00	1.00	1.00	107.3
5.1–5.69	0.00	0.00	0.24	0.61	0.98	0.99	1.00	1.00	1.00	1.00	1.00	107.3
5.7–6.29	0.00	0.00	0.70	0.85	1.00	1.00	1.00	1.00	1.00	1.00	1.00	132.3
6.3–7.5	0.00	0.01	1.00	1.00	1.00	1.00	1.00	1.00	1.00	1.00	1.00	148.8

Turkey Point Units 6 & 7
COL Application
Part 2 — FSAR

PTN COL 2.5-2

Table 2.5.2-205 (Sheet 2 of 2)
Region 2 Matrix of Detection Probabilities; Modified to Extend the Matrix to Year 2007

Detection Probability Matrix: EPRI (Reference 243) Incompleteness Region 13 [Modified]												
	Year Intervals											
	1625– 1779	1780– 1859	1860– 1899	1900– 1924	1925– 1949	1950– 1959	1960– 1964	1965– 1969	1970– 1974	1975– 1979	1980– 2007	
Magnitude Intervals	155 years	80 years	40 years	25 years	25 years	10 years	5 years	5 years	5 years	5 years	28 years	Total Years
3.3–3.89	0.00	0.00	0.24	0.48	0.71	0.80	0.88	0.93	0.98	1.00	1.00	94.2
3.9–4.49	0.00	0.00	0.24	0.51	0.77	0.90	0.97	0.98	0.99	1.00	1.00	98.2
4.5–5.09	0.00	0.00	0.30	0.61	0.92	0.97	0.99	1.00	1.00	1.00	1.00	107.9
5.1–5.69	0.00	0.03	0.69	0.84	0.99	0.99	1.00	1.00	1.00	1.00	1.00	133.7
5.7–6.29	0.11	0.54	0.98	0.99	1.00	1.00	1.00	1.00	1.00	1.00	1.00	207.2
6.3–7.5	0.51	0.90	1.00	1.00	1.00	1.00	1.00	1.00	1.00	1.00	1.00	299.1

Turkey Point Units 6 & 7
COL Application
Part 2 — FSAR

PTN COL 2.5-2

Table 2.5.2-206
Matrix of Detection Probabilities for the Gulf of Mexico

Detection Probability Matrix: Gulf of Mexico and Near Atlantic												
	Year Intervals											
	1625– 1779	1780– 1859	1860– 1899	1900– 1924	1925– 1949	1950– 1959	1960– 1964	1965– 1969	1970– 1974	1975– 1979	1980– 2007	
Magnitude Intervals	155 years	80 years	40 years	25 years	25 years	10 years	5 years	5 years	5 years	5 years	28 years	Total Years
3.3–3.89	0.00	0.00	0.00	0.00	0.00	0.00	0.00	0.00	0.00	0.00	0.30	8.4
3.9–4.49	0.00	0.00	0.00	0.00	0.00	0.00	0.00	0.00	0.00	0.50	0.60	19.3
4.5–5.09	0.00	0.00	0.00	0.00	0.00	0.00	0.00	0.50	0.70	0.70	0.90	34.7
5.1–5.69	0.00	0.00	0.00	0.00	0.00	0.00	0.70	0.90	1.00	1.00	1.00	46.0
5.7–6.29	0.00	0.00	0.00	0.00	0.70	0.90	1.00	1.00	1.00	1.00	1.00	74.5
6.3–7.5	0.00	0.00	0.00	0.30	0.90	1.00	1.00	1.00	1.00	1.00	1.00	88.0

Detection Probability Matrix: Near Florida												
	Year Intervals											
	1625– 1779	1780– 1859	1860– 1899	1900– 1924	1925– 1949	1950– 1959	1960– 1964	1965– 1969	1970– 1974	1975– 1979	1980– 2007	
Magnitude Intervals	155 years	80 years	40 years	25 years	25 years	10 years	5 years	5 years	5 years	5 years	28 years	Total Years
3.3–3.89	0.00	0.00	0.12	0.24	0.36	0.40	0.44	0.47	0.49	0.50	0.65	51.3
3.9–4.49	0.00	0.00	0.12	0.25	0.39	0.45	0.49	0.49	0.50	0.75	0.80	58.7
4.5–5.09	0.00	0.00	0.15	0.31	0.46	0.49	0.50	0.75	0.85	0.85	0.95	71.3
5.1–5.69	0.00	0.02	0.35	0.42	0.50	0.50	0.85	0.95	1.00	1.00	1.00	89.8
5.7–6.29	0.06	0.27	0.49	0.50	0.85	0.95	1.00	1.00	1.00	1.00	1.00	140.9
6.3–7.5	0.26	0.45	0.50	0.65	0.95	1.00	1.00	1.00	1.00	1.00	1.00	193.5

Turkey Point Units 6 & 7
COL Application
Part 2 — FSAR

PTN COL 2.5-2

Table 2.5.2-207 (Sheet 1 of 2)
Summary of EPRI Seismic Sources within the Site Region

Source	Description	Pa ^(a)	Mmax (m _b) and Weights ^(b)	Smoothing Options and Weights ^(c)	Interdependencies ^(d)	Largest Earthquake in Catalog (Emb)		New Data to Suggest Change in Source?		
						EPRI catalog (1627–1984)	Phase 1 Updated Catalog (1698–2007)	Geom. ^(e)	Mmax ^(f)	RI ^(g)
Bechtel Group										
BZ1	Gulf Coast	1.00	5.4 [0.10] 5.7 [0.40] 6.0 [0.40] 6.6 [0.10]	1 [0.33] 2 [0.34] 3 [0.33]	Background P _B =1.00	4.9	5.9	No	Yes	No
Dames & Moore										
20	So. Coastal Marg.	1.00	5.3 [0.80] 7.2 [0.20]	1 [0.75] 2 [0.25]	None	4.6	5.6	No	Yes	No
Law Engineering										
126	South Coastal Block	1.00	4.6 [0.90] 4.9 [0.10]	1a [1.00]	Background P _B =0.49	4.4	5.0	No	Yes	No
Rondout Associates										
49-05	Appalachian Basement	1.00	4.8 [0.20] 5.5 [0.60] 5.8 [0.20]	2 [1.00]	Background P _B =1.00	4.4	5.0	No	Yes	No
51	Gulf Coast to Bahamas Fract. Zone	1.00	4.8 [0.20] 5.5 [0.60] 5.8 [0.20]	3 [1.00]	Background P _B =1.00	4.9	5.9	No	Yes	No
Weston Geophysical										
107	Gulf Coast	1.00	5.4 [0.71] 6.0 [0.29]	1a [0.20] 2a [0.80]	Background P _B =1.00	4.9	5.9	No	Yes	No
Woodward-Clyde Consultants										
BG-35	Turkey Point Background	N/A	5.8 [0.33] 6.2 [0.34] 6.6 [0.33]	1 [0.25] 6 [0.25] 7 [0.25] 8 [0.25]	N/A	3.7	6.1	No	Yes	No

Turkey Point Units 6 & 7
COL Application
Part 2 — FSAR

PTN COL 2.5-2

Table 2.5.2-207 (Sheet 2 of 2)
Summary of EPRI Seismic Sources within the Site Region

- (a) P_a = Probability of activity (Reference 243)
- (b) Maximum Magnitude (M_{max}) and weights (Reference 243)
- (c) Smoothing options are defined as follows (Reference 243):
- Bechtel
1 = constant a-value, constant b-value (no prior); 2 = low smoothing on a-value, high smoothing on b-value (no prior); 3 = low smoothing on a-value, low smoothing on b-value (no prior)
Weights on magnitude intervals are all 1.0
- Dames & Moore
1 = no smoothing on a-value, no smoothing on b-value (strong prior of 1.04); 2 = no smoothing on a-value, no smoothing on b-value (weak prior of 1.04)
Weights on magnitude units are [0.1, 0.2, 0.4, 1.0, 1.0, 1.0, 1.0]
- Law Engineering
1a = high smoothing on a-value, constant b-value (strong prior of 1.05)
Weights on magnitude units are [0.0, 1.0, 1.0, 1.0, 1.0, 1.0, 1.0]
- Rondout Associates
3 = low smoothing on a-value, constant b-value (strong prior of 1.0)
- Weston Geophysical
1a = constant a-value, constant b-value (medium prior of 1.04); 2a = medium smoothing on a-value, medium smoothing on b-value (medium prior of 1.0)
- Woodward-Clyde Consultants
1 = low smoothing on a-value, high smoothing on b-value (no prior); 6 = low smoothing on a-value, high smoothing on b-value (moderate prior of 1.0);
7 = low smoothing on a-value, high smoothing on b-value (moderate prior of 0.9); 8 = low smoothing on a-value, high smoothing on b-value (moderate prior of 0.8)
Weights on magnitude intervals are all 1.0
- (d) P_B = the fraction of area of the background that is active (Reference 243)
- (e) No, unless (1) new geometry proposed in literature or (2) new seismicity pattern.
- (f) No, unless (1) new data suggest M_{max} exceeds or differs significantly from the EPRI M_{max} distribution or (2) exceeded by historical seismicity
- (g) RI = recurrence interval; assumed no change if no new paleoseismic data or rate of seismicity has not significantly changed
- N/A = Not Applicable

Turkey Point Units 6 & 7
COL Application
Part 2 — FSAR

PTN COL 2.5-2

Table 2.5.2-208 (Sheet 1 of 2)
Mean and Fractile Seismic Hazard Data for Crystal River Site from
EPRI-SOG Study and Units 6 & 7 Study

PGA		Bechtel			Dames & More			Law Engineering		
Ampl. cm/s ²	Hazard	EPRI-SOG	Units 6 & 7 Study	% diff	EPRI-SOG	Units 6 & 7 Study	% diff	EPRI-SOG	Units 6 & 7 Study	% diff
100	mean	1.47E-05	1.48E-05	0%	1.57E-05	1.58E-05	1%	2.23E-07	8.72E-08	-61%
	0.15	6.70E-06	6.46E-06	-4%	3.93E-06	3.98E-06	1%	1.49E-10	3.39E-29	-100%
	0.5	1.25E-05	1.29E-05	3%	8.84E-06	9.12E-06	3%	1.53E-07	3.89E-29	-100%
	0.85	2.25E-05	2.24E-05	0%	1.74E-05	2.48E-05	43%	2.38E-07	5.25E-09	-98%
250	mean	1.83E-06	1.86E-06	1%	2.08E-06	2.11E-06	1%	1.08E-08	9.18E-10	-92%
	0.15	7.77E-07	8.13E-07	5%	3.11E-07	3.09E-07	-1%	1.49E-10	3.39E-29	-100%
	0.5	1.50E-06	1.62E-06	8%	8.35E-07	8.71E-07	4%	1.18E-08	3.89E-29	-100%
	0.85	2.93E-06	3.02E-06	3%	6.06E-06	4.27E-06	-30%	1.61E-08	6.46E-12	-100%
500	mean	1.82E-07	1.90E-07	4%	2.99E-07	3.06E-07	2%	3.80E-10	7.52E-12	-98%
	0.15	4.64E-08	5.13E-08	11%	1.24E-08	1.29E-08	4%	1.49E-10	3.39E-29	-100%
	0.5	1.20E-07	1.45E-07	20%	4.52E-08	5.13E-08	13%	5.74E-10	3.89E-29	-100%
	0.85	3.67E-07	3.55E-07	-3%	1.08E-06	7.85E-07	-27%	6.74E-10	6.46E-15	-100%

Turkey Point Units 6 & 7
COL Application
Part 2 — FSAR

PTN COL 2.5-2

Table 2.5.2-208 (Sheet 2 of 2)
Mean and Fractile Seismic Hazard Data for Crystal River Site from
EPRI-SOG Study and Units 6 & 7 Study

PGA		Rondout			Weston			Woodward-Clyde			Total		
Ampl. cm/s ²	Hazard	EPRI-SOG	Units 6 & 7 Study	% diff	EPRI-SOG	Units 6 & 7 Study	% diff	EPRI-SOG	Units 6 & 7 Study	% diff	EPRI-SOG	Units 6 & 7 Study	% diff
100	mean	1.48E-05	1.48E-05	0%	2.47E-05	2.48E-05	0%	2.59E-05	2.60E-05	0%	1.60E-05	1.60E-05	0%
	0.15	5.27E-07	1.05E-08	-98%	7.94E-06	7.94E-06	0%	6.78E-07	4.96E-08	-93%	5.37E-06	5.37E-10	-100%
	0.5	1.55E-05	1.59E-05	3%	1.78E-05	1.82E-05	2%	1.65E-05	1.70E-05	3%	1.52E-05	1.20E-05	-21%
	0.85	2.71E-05	2.75E-05	1%	3.79E-05	3.89E-05	3%	4.97E-05	5.13E-05	3%	3.06E-05	3.06E-05	0%
250	mean	1.61E-06	1.63E-06	1%	2.79E-06	2.83E-06	1%	3.58E-06	3.62E-06	1%	1.98E-06	2.01E-06	2%
	0.15	2.60E-08	1.12E-11	-100%	6.72E-07	6.61E-07	-2%	4.44E-08	2.09E-11	-100%	5.40E-07	8.32E-14	-100%
	0.5	1.67E-06	1.74E-06	4%	1.79E-06	1.86E-06	4%	1.89E-06	2.00E-06	6%	1.67E-06	1.23E-06	-26%
	0.85	2.69E-06	2.82E-06	5%	5.17E-06	5.25E-06	2%	6.98E-06	6.92E-06	-1%	3.76E-06	3.35E-06	-11%
500	mean	1.19E-07	1.24E-07	4%	2.36E-07	2.46E-07	4%	4.52E-07	4.65E-07	3%	2.15E-07	2.22E-07	3%
	0.15	1.24E-09	9.12E-15	-100%	2.98E-08	2.95E-08	-1%	1.79E-09	4.42E-15	-100%	2.78E-08	1.64E-23	-100%
	0.5	1.11E-07	1.26E-07	14%	1.06E-07	1.18E-07	11%	1.40E-07	1.55E-07	11%	1.06E-07	7.76E-08	-27%
	0.85	1.81E-07	2.27E-07	25%	5.37E-07	5.75E-07	7%	8.74E-07	8.71E-07	0%	4.69E-07	3.67E-07	-22%

PGA = Peak ground acceleration

% diff = Percent difference between the 1989 calculations and the current hazard calculations at the Crystal River site

Turkey Point Units 6 & 7
COL Application
Part 2 — FSAR

PTN COL 2.5-2

Table 2.5.2-209
Summary of Supplemental Sources and Truncated Woodward-Clyde Source

EPRI EST	New Source Area (km ²) ^(a)	New Source Total Earthquakes ^(b)	New Source Max Recorded Event (Emb) ^(b)	Mmax (m _b) and Weights
Bechtel	136,769	1	4.09	6.1 [0.10] 6.4 [0.40] 6.6 [0.50]
Dames & Moore	139,208	2	4.09	5.6 [0.80] 7.2 [0.20]
Law Engineering	97,273	1	4.09	5.6 [0.90] 5.7 [0.10]
Rondout Associates	103,436	1	4.09	6.1 [0.30] 6.3 [0.55] 6.5 [0.15]
Weston Geophysical	171,264	2	4.09	6.6 [0.89] 7.2 [0.11]
Woodward-Clyde ^(c) (truncated)	349,569	8	4.09	5.8 [0.33] 6.2 [0.34] 6.6 [0.33]

(a) Area calculated using North America Albers equal area conic projection.

(b) From updated seismicity catalog.

(c) Not a "supplemental" zone; Woodward-Clyde source BG-35 geometry is truncated by the northern boundary of new Caribbean seismic source model.

EST = Earth Science Team

Turkey Point Units 6 & 7
COL Application
Part 2 — FSAR

PTN COL 2.5-2

Table 2.5.2-210 (Sheet 1 of 2)
Geographic Coordinates of Supplemental Sources and Truncated Woodward-Clyde Source

Bechtel Group		Dames & Moore		Law Engineering		Rondout Associates		Weston Geophysical		Woodward-Clyde Consultants ^(a)	
Latitude	Longitude	Latitude	Longitude	Latitude	Longitude	Latitude	Longitude	Latitude	Longitude	Latitude	Longitude
27.512	-78.336	25.440	-83.228	25.026	-77.0478	26.630	-77.711	28.317	-80.311	26.006	-77.500
27.033	-77.927	26.133	-83.129	24.853	-77.495	26.531	-77.659	28.263	-79.768	25.420	-77.439
26.531	-77.659	25.030	-82.570	24.309	-77.662	25.986	-77.494	28.098	-79.223	24.840	-77.500
25.986	-77.494	25.000	-80.000	23.811	-77.930	25.420	-77.439	27.829	-78.721	22.400	-77.499
25.420	-77.439	25.020	-79.290	23.372	-78.292	24.853	-77.495	27.470	-78.285	22.400	-77.613
24.853	-77.495	25.620	-78.940	23.012	-78.733	24.309	-77.662	27.033	-77.927	22.760	-78.456
24.309	-77.662	27.100	-78.870	22.911	-78.923	23.811	-77.930	26.531	-77.659	22.911	-78.923
23.811	-77.930	28.032	-79.101	23.421	-80.497	23.372	-78.292	25.986	-77.494	23.421	-80.497
23.372	-78.292	27.829	-78.721	23.505	-81.043	23.012	-78.733	25.420	-77.439	23.505	-81.043
23.012	-78.733	27.470	-78.285	23.506	-82.095	22.911	-78.923	24.853	-77.495	23.506	-82.095
22.911	-78.923	27.033	-77.927	23.456	-82.445	23.421	-80.497	24.309	-77.662	23.456	-82.445
23.421	-80.497	26.531	-77.659	23.828	-82.748	23.505	-81.043	23.811	-77.930	23.304	-83.500
23.505	-81.043	25.986	-77.494	24.332	-83.014	23.506	-82.095	23.372	-78.292	28.400	-83.500
23.506	-82.095	25.420	-77.439	24.873	-83.175	23.456	-82.445	23.012	-78.733	28.400	-77.500
23.456	-82.445	24.853	-77.495	25.008	-83.188	23.828	-82.748	22.911	-78.923	26.006	-77.500
23.828	-82.748	24.309	-77.662	25.000	-79.999	24.332	-83.014	23.421	-80.497	—	—
24.332	-83.014	23.811	-77.930	25.026	-77.478	24.873	-83.175	23.505	-81.043	—	—
24.873	-83.175	23.372	-78.292	25.026	-77.478	25.000	-83.187	23.506	-82.095	—	—
25.182	-83.204	23.012	-78.733	—	—	25.000	-80.000	23.456	-82.445	—	—
25.150	-81.710	22.911	-78.923	—	—	25.030	-78.230	23.828	-82.748	—	—
25.070	-80.210	23.421	-80.497	—	—	25.160	-78.110	24.332	-83.014	—	—
25.440	-79.470	23.505	-81.043	—	—	25.520	-77.900	24.873	-83.175	—	—
26.240	-78.780	23.506	-82.095	—	—	25.980	-77.770	25.003	-83.187	—	—
27.150	-78.410	23.456	-82.445	—	—	26.630	-77.711	25.000	-80.000	—	—
27.512	-78.336	23.828	-82.748	—	—	—	—	26.620	-79.900	—	—

Turkey Point Units 6 & 7
COL Application
Part 2 — FSAR

PTN COL 2.5-2

Table 2.5.2-210 (Sheet 2 of 2)
Geographic Coordinates of Supplemental Sources and Truncated Woodward-Clyde Source

Bechtel Group		Dames & Moore		Law Engineering		Rondout Associates		Weston Geophysical		Woodward-Clyde Consultants ^(a)	
Latitude	Longitude	Latitude	Longitude	Latitude	Longitude	Latitude	Longitude	Latitude	Longitude	Latitude	Longitude
—	—	24.332	-83.014	—	—	—	—	28.317	-80.311	—	—
—	—	24.873	-83.175	—	—	—	—	—	—	—	—
—	—	25.440	-83.228	—	—	—	—	—	—	—	—

(a) Not a “supplemental” zone; Woodward-Clyde source BG-35 geometry is truncated by the northern boundary of new Caribbean seismic source model.
Note: Coordinates in decimal degrees.

Turkey Point Units 6 & 7
COL Application
Part 2 — FSAR

PTN COL 2.5-2

Table 2.5.2-211
Geographic Coordinates of Updated Charleston Seismic Source (UCSS)
Model Sources

UCSS Source	Longitude	Latitude
A	-80.707	32.811
A	-79.840	33.354
A	-79.527	32.997
A	-80.392	32.455
B	-81.216	32.485
B	-78.965	33.891
B	-78.3432	33.168
B	-80.587	31.775
B'	-78.965	33.891
B'	-78.654	33.531
B'	-80.900	32.131
B'	-81.216	32.485
C	-80.397	32.687
C	-79.776	34.425
C	-79.483	34.351
C	-80.109	32.614

Note: Coordinates in decimal degrees.

Turkey Point Units 6 & 7
COL Application
Part 2 — FSAR

PTN COL 2.5-2

Table 2.5.2-212
Comparison of Post-EPRI Magnitude Estimates for the 1886
Charleston Earthquake

Study	Magnitude Estimation Method	Reported Magnitude Estimate	Assigned Weights	Mean Magnitude (M_w)
Johnston et al. (Reference 268)	Worldwide survey of passive-margin, extended-crust earthquakes	$M_w 7.56 \pm 0.35^{(a)}$	—	7.56
Martin and Clough (Reference 279)	Geotechnical assessment of 1886 liquefaction data	$M_w 7-7.5$	—	7.25
Johnston (Reference 267)	Isoseismal area regression, accounting for eastern North America anelastic attenuation	$M_w 7.3 \pm 0.26$	—	7.3
Chapman and Talwani (Reference 223) (SCDOT)	Consideration of available magnitude estimates	$M_w 7.1$ $M_w 7.3$ $M_w 7.5$	0.2 0.6 0.2	7.3
Bakun and Hopper (Reference 211)	Isoseismal area regression, including empirical site corrections	$M_I 6.4-7.2^{(b)}$	—	6.9 ^(c)
Petersen et al. (Reference 300) (USGS)	Consideration of available magnitude estimates	$M_w 6.8$ $M_w 7.1$ $M_w 7.3$ $M_w 7.5$	0.20 0.20 0.45 0.15	7.2

(a) Estimate from Johnston et al. (Reference 268), Chapter 3.

(b) 95 percent confidence interval estimate; M_I (intensity magnitude) is considered equivalent to M_w (moment magnitude) (Reference 211).

(c) Bakun and Hopper's preferred estimate (Reference 211).

Turkey Point Units 6 & 7
COL Application
Part 2 — FSAR

PTN COL 2.5-2

Table 2.5.2-213
Comparison of Talwani and Schaeffer and UCSS Age Constraints on Charleston-Area Paleoliquefaction Events

Liquefaction Event	Event Age (YBP) ^(b)	Talwani and Schaeffer (Reference 223) ^(a)				This Study Event Age (YBP) ^{(b)(d)}
		Scenario 1		Scenario 2		
		Source	M ^(c)	Source	M ^(c)	
1886 A.D.	64	Charleston	7.3	Charleston	7.3	64
A	546 ± 17	Charleston	7+	Charleston	7+	600 ± 70
B	1,021 ± 30	Charleston	7+	Charleston	7+	1,025 ± 25
C	1,648 ± 74	Northern (Georgetown)	6+	—	—	—
C'	1,683 ± 70	—	—	Charleston	7+	1,695 ± 175
D	1,966 ± 212	Southern (Bluffton)	6+	—	—	—
E	3,548 ± 66	Charleston	7+	Charleston	7+	3,585 ± 115
F	5,038 ± 166	Northern (Georgetown)	6+	Charleston	7+	—
F'	—	—	—	—	—	5,075 ± 215
G	5,800 ± 500	Charleston	7+	Charleston	7+	—

- (a) YBP = years before present, relative to 1950 A.D.
(b) Modified after Talwani and Schaeffer's (Reference 223) Table 2.
(c) Unspecified magnitude type.
(d) Event ages based upon our recalibration of radiocarbon ages to 2-sigma using OxCal 3.8, from data presented in Talwani and Schaeffer's (Reference 223) Table 2.

Turkey Point Units 6 & 7
COL Application
Part 2 — FSAR

PTN COL 2.5-2

Table 2.5.2-214
List of Experts Contacted as part of Cuba and Northern Caribbean Source
Model SSHAC Level 2 Process

Name	Affiliation	Response
Prof. Gail Atkinson	Carleton University, Ottawa, Canada	<i>[declined, lack of expertise]</i>
Prof. Eric Calais	Purdue University	Detailed response; email and telephone
Prof. Charles DeMets	University Wisconsin	Detailed response; email and telephone
Prof. James Dolan	University of Southern California	Detailed response; email and in-person
Dr. Art Frankel	U.S. Geological Survey	<i>[declined, conflict]</i>
Dr. Julio Garcia	National Institute of Oceanography and Experimental Geophysics (OGS), Trieste, Italy	Detailed response; email
Prof. Paul Mann	University of Texas	Detailed response; email
Dr. William McCann	Earth Scientific Consultants; TAG member	Detailed response; email, telephone, and in-person
Dr. James Pindell	Tectonic Analysis, Ltd.; Rice U.	<i>[declined, lack of expertise]</i>
Dr. Uri ten Brink	U.S. Geological Survey	<i>[declined, conflict]</i>
Dr. Marticia Tuttle	M. Tuttle & Associates	<i>[declined, conflict]</i>
Prof. Margaret Wiggins-Grandison	University of West Indies, Mona, Jamaica	Detailed response; email

SSHAC = Senior Seismic Hazard Analysis Committee

Turkey Point Units 6 & 7
COL Application
Part 2 — FSAR

PTN COL 2.5-2

Table 2.5.2-215
Significant Earthquakes in the Cuba and Northern Caribbean Region, 1500 to 2008

Date	Location	Seismic Source	MMI	M, high	M, low	M _w
November 1539	Western Caribbean Sea	Swan Islands fault — Western	X ^(a)	~8 ^(b)		7.69
1551	SE Cuba	Cuba	VIII ^(c)			5.98
August 1578	Cuba	Cuba		6.75 ^(c)		6.78
February 1678	SE Cuba	Oriente fault — Eastern	VIII ^(b)	7.0 ^(b)		6.78
June 1692	S Jamaica	Plantain Garden-Enriquillo fault	X ^(d)	7.5 ^(b)		7.78
October 1751	SW of Dominican Republic	Plantain Garden-Enriquillo fault		8.0 ^(b)		7.28
September 1751	Haiti, near Port-au-Prince	Plantain Garden-Enriquillo fault		7.5 ^(b)		6.83
June 1766	SE Cuba	Oriente fault — Eastern	IX ^(c)	7.5 ^(c)	7.0 ^(b)	7.53
June 1770	Haiti, west of Port-au-Prince	Plantain Garden-Enriquillo fault		7.5 ^(b)		7.53
November 1812	SE Jamaica	Plantain Garden-Enriquillo fault		6.8 ^(b)		6.13
May 1842	Offshore Haiti to Dominican Republic	Septentrional fault	IX ^(b)	8.2 ^(e)	8.0 ^(b)	8.23
August 1852	Offshore Santiago de Cuba	Oriente fault-Eastern	IX ^(c)	7.5 ^(b)	7.3 ^(c)	7.33
August 1856	Offshore N Honduras	Swan Islands fault — Western		8.3 ^(b)		7.69
January 1880	North Cuba	Cuba	VIII ^(c)	6.6 ^(b)	6.0 ^(c)	6.13
September 1887	W offshore Haiti	Septentrional fault	IX ^(b)	7.9 ^(e)	7.75 ^(b)	7.93
January 1907	N Jamaica	Walton-Duanvale fault		7 ^(b)	6.5 ^(d)	6.64
January 1910	Caribbean Sea	Swan Islands — Western		7.0 ^(b)		7.10
February 1914	East-Central Cuba	Cuba		6.2 ^(e)		6.29
February 1917	Offshore S Cuba	Oriente fault — Eastern	VI ^(b)	7.1 ^(b)	7.0 ^(f)	7.20
February 1932	Offshore Santiago de Cuba	Oriente fault — Eastern		6.8 ^(b)	6.75 ^(c)	6.83
April 1941	Offshore SW Jamaica	Plantain Garden-Enriquillo fault		7 ^(b)	6.9 ^(f)	7.03
August 1946	Offshore Hispaniola	Northern Hispaniola — Eastern		8.1 ^(g)	7.8 ^(b)	7.90
August 1947	Offshore Santiago de Cuba	Oriente fault — Eastern		6.8 ^(b)	6.6 ^(f)	6.83
May 1953	Offshore Hispaniola	Northern Hispaniola — Western		7.0 ^(f)	6.9 ^(b)	6.93
March 1957	W Jamaica	Walton-Duanvale fault		6.9 ^(f)	6.6 ^(b)	6.61
May 1992	Cabo Cruz	Oriente fault — Western	VII ^(c)	7.0 ^(f)	6.8 ^(c)	6.80

- (a) McCann ([Reference 283](#)).
(b) McCann ([Reference 282](#)).
(c) Garcia et al. ([Reference 254](#)).
(d) DeMets and Wiggins-Grandison ([Reference 229](#)).
(e) Cotilla et al. ([Reference 226](#)).
(f) van Dusen and Doser ([Reference 331](#)).
(g) Dolan and Wald ([Reference 236](#)).

Notes:

MMI = Modified Mercalli Intensity; M, high = Upper estimate from literature (magnitude scale unspecified); M, low = Lower estimate from literature (magnitude scale unspecified).

M_w = Estimate of moment magnitude from seismicity update performed for Units 6 & 7.

Turkey Point Units 6 & 7
COL Application
Part 2 — FSAR

PTN COL 2.5-2

Table 2.5.2-216
Empirical Relations between Rupture Area (A) and Moment Magnitude (M_w)
and Rupture Length (L) and M_w Used to Determine Mmax for Cuba and
Northern Caribbean Sources

Source	Equation (A and M_w)	Use
Wells and Coppersmith (Reference 334), all slip types	$M_w = 0.98 \text{ Log } A + 4.07$	All faults
Wyss (Reference 339) ^(a)	$M_w = \text{Log } A + 4.15$	All faults
Hanks and Bakun (Reference 262) ^(b)	$M_w = 4/3 \text{ Log } A + 3.07$	Strike-slip faults
WGCEP (Reference 337), equation 4.5b	$M_w = \text{Log } A + 4.2$	Strike-slip faults
Abe (References 201 and 202)	$M_w = \text{Log } A + 3.99$	Subduction zones
Geomatrix (Reference 257)	$M_w = 0.81 \text{ Log } A + 4.7$	Subduction zones

Source	Equation (L and M_w)	Use
Wells and Coppersmith (Reference 334), all slip types	$M_w = 1.49 \text{ Log } L + 4.38$	All faults
Geomatrix (Reference 257)	$M_w = 1.39 \text{ Log } L + 4.94$	Subduction zones

- (a) Valid for $M_w > 5.6$
(b) Valid for $A > 537 \text{ km}^2$

Turkey Point Units 6 & 7
COL Application
Part 2 — FSAR

PTN COL 2.5-2

Table 2.5.2-217
Summary of Cuba and Northern Caribbean Source Model

Area Source	Closest Distance to Units 6 & 7 (mi)	Mmax (M _w)
1. Cuba	140	7.0 [0.5] 7.25 [0.5]

Fault Source	Closest Distance to Units 6 & 7 (mi)	Fault Type/ Dip	Slip Rate (mm/r)	Seismic Coupling	Mmax (M _w)
2. Oriente – Western	420	Strike-slip/ 90°	8 [0.1] 11 [0.7] 13 [0.2]	0.6 [0.2] 0.8 [0.2] 1.0 [0.6]	7.5 [0.3] 7.7 [0.4] 8.0 [0.3]
3. Oriente – Eastern	445	Strike-slip/ 90°	8 [0.1] 11 [0.7] 13 [0.2]	1.0 [1.0]	7.5 [0.2] 7.7 [0.6] 7.9 [0.2]
4. Septentrional	545	Strike-slip/ 90°	6 [0.2] 9 [0.6] 12 [0.2]	1.0 [1.0]	8.0 [0.5] 8.25 [0.5]
5. Northern Hispaniola — Western	550	Thrust/ 20-25° south	4 [0.2] 6 [0.7] 8 [0.1]	1.0 [1.0]	7.8 [0.2] 8.0 [0.6] 8.3 [0.2]
6. Northern Hispaniola — Eastern	760	Thrust/ 20-25° south	4 [0.2] 6 [0.7] 8 [0.1]	1.0 [1.0]	8.0 [0.2] 8.3 [0.6] 8.6 [0.2]
7. Swan Islands — Western	620	Strike-slip/ 90°	18 [0.2] 19 [0.6] 20 [0.2]	1.0 [1.0]	7.8 [0.2] 8.0 [0.7] 8.3 [0.1]
8. Swan Islands — Eastern	540	Strike-slip/ 90°	18 [0.2] 19 [0.6] 20 [0.2]	0.6 [0.2] 0.8 [0.2] 1.0 [0.6]	7.2 [0.4] 7.5 [0.5] 7.7 [0.1]
9. Walton — Duanvale	490	Strike-slip/ 90°	6 [0.2] 8 [0.6] 10 [0.2]	0.8 [0.3] 1.0 [0.7]	7.3 [0.3] 7.6 [0.6] 7.8 [0.1]
10. Plantain Garden — Enriquillo	560	Strike-slip/ 90°	6 [0.2] 8 [0.6] 10 [0.2]	1.0 [1.0]	7.5 [0.2] 7.7 [0.6] 7.9 [0.2]

Turkey Point Units 6 & 7
COL Application
Part 2 — FSAR

PTN COL 2.5-2

Table 2.5.2-218
Geographic Coordinates of Cuba Source

Latitude	Longitude
21.207	-74.814
20.377	-73.219
19.834	-77.659
19.995	-77.919
20.506	-78.637
20.892	-79.345
21.259	-80.143
21.385	-80.609
21.429	-81.290
21.358	-82.724
21.295	-83.549
21.331	-84.024
21.483	-84.643
21.609	-84.975
21.686	-85.518
22.087	-85.457
22.251	-85.347
22.963	-84.450
23.179	-83.983
23.285	-83.634
23.506	-82.095
23.505	-81.043
23.421	-80.497
22.760	-78.456
21.207	-74.814

Note: Coordinates in decimal degrees.

Turkey Point Units 6 & 7
COL Application
Part 2 — FSAR

PTN COL 2.5-2

Table 2.5.2-219
Geographic Coordinates of Cuba and Northern Caribbean
Model Line Sources

Source No.:	2		3		4	
Source Name	Oriente-Western		Oriente-Eastern		Septentrional	
	Latitude	Longitude	Latitude	Longitude	Latitude	Longitude
	18.951	-81.483	19.663	-77.134	19.990	-74.120
	19.247	-79.991	19.674	-77.037	20.005	-72.979
	19.563	-77.138	19.733	-76.518	19.936	-72.606
	—	—	19.819	-75.012	19.718	-71.775
	—	—	19.959	-74.472	19.562	-70.998
	—	—	19.982	-74.205	19.151	-69.689
	—	—	—	—	19.081	-68.741

Source No.:	5		6		7	
Source Name	Northern Hispaniola-Western		Northern Hispaniola-Eastern		Swan Islands-Western	
	Latitude	Longitude	Latitude	Longitude	Latitude	Longitude
	20.415	-73.267	19.843	-70.026	15.905	-88.280
	20.400	-72.755	19.555	-68.531	17.346	-84.602
	20.165	-71.530	19.759	-66.270	—	—
	19.907	-70.025	—	—	—	—

Source No.:	8		9		10	
Source Name	Swan Islands-Eastern		Walton-Duanvale		Plantain Garden-Enriquillo	
	Latitude	Longitude	Latitude	Longitude	Latitude	Longitude
	17.190	-84.572	17.740	-81.480	17.990	-76.672
	17.758	-81.940	18.335	-79.295	17.927	-76.188
	—	—	18.467	-78.244	18.174	-75.026
	—	—	18.351	-77.429	18.296	-74.420
	—	—	—	—	18.438	-71.807
	—	—	—	—	18.347	-71.104

Note: Coordinates in decimal degrees.

Turkey Point Units 6 & 7
COL Application
Part 2 — FSAR

PTN COL 2.5-2

Table 2.5.2-220 (Sheet 1 of 5)
Mean and Fractile Rock Seismic Hazard Curves

Ampl. (g)	MEAN (a.f.e.)	0.05 (a.f.e)	0.16 (a.f.e)	0.50 (a.f.e)	0.84 (a.f.e)	0.95 (a.f.e)
PGA Hazard Curves						
0.001	4.39E-02	1.38E-02	2.24E-02	4.17E-02	6.31E-02	7.24E-02
0.0015	3.14E-02	7.94E-03	1.38E-02	2.95E-02	4.79E-02	5.89E-02
0.002	2.34E-02	5.62E-03	9.77E-03	2.24E-02	3.89E-02	4.47E-02
0.003	1.42E-02	3.02E-03	5.25E-03	1.38E-02	2.40E-02	2.95E-02
0.005	6.45E-03	1.27E-03	2.14E-03	6.03E-03	1.12E-02	1.48E-02
0.007	3.51E-03	6.84E-04	1.15E-03	3.24E-03	5.62E-03	7.94E-03
0.01	1.73E-03	3.67E-04	6.17E-04	1.51E-03	2.82E-03	3.72E-03
0.015	7.42E-04	1.72E-04	2.69E-04	6.17E-04	1.15E-03	1.62E-03
0.02	4.04E-04	9.89E-05	1.45E-04	3.31E-04	6.17E-04	8.71E-04
0.03	1.75E-04	4.62E-05	6.31E-05	1.26E-04	2.51E-04	3.94E-04
0.05	6.44E-05	1.82E-05	2.40E-05	4.47E-05	8.91E-05	1.45E-04
0.07	3.49E-05	1.05E-05	1.48E-05	2.48E-05	5.13E-05	8.04E-05
0.1	1.89E-05	5.43E-06	7.94E-06	1.43E-05	2.75E-05	4.47E-05
0.15	9.67E-06	2.54E-06	3.98E-06	7.41E-06	1.48E-05	2.32E-05
0.2	6.02E-06	1.37E-06	2.46E-06	4.57E-06	9.12E-06	1.48E-05
0.3	3.02E-06	5.19E-07	1.00E-06	2.21E-06	4.57E-06	7.67E-06
0.5	1.18E-06	1.18E-07	2.51E-07	7.85E-07	2.14E-06	3.47E-06
0.7	5.92E-07	3.63E-08	8.32E-08	3.31E-07	1.15E-06	1.93E-06
1	2.65E-07	8.51E-09	2.40E-08	1.35E-07	5.37E-07	9.33E-07
1.5	9.39E-08	1.32E-09	4.90E-09	3.27E-08	1.66E-07	3.67E-07
2	4.10E-08	2.99E-10	1.23E-09	1.12E-08	6.31E-08	1.78E-07
3	1.09E-08	2.66E-11	1.35E-10	1.86E-09	1.59E-08	5.50E-08
5	1.49E-09	7.85E-13	6.03E-12	1.45E-10	2.00E-09	8.22E-09
7	3.26E-10	6.31E-14	6.61E-13	2.09E-11	3.55E-10	1.74E-09
10	5.30E-11	2.63E-15	4.79E-14	2.00E-12	5.13E-11	2.69E-10
25 Hz Hazard Curves						
0.001	5.06E-02	1.70E-02	2.75E-02	5.13E-02	7.24E-02	8.32E-02
0.0015	3.85E-02	1.05E-02	1.82E-02	3.89E-02	5.89E-02	7.24E-02
0.002	3.05E-02	7.41E-03	1.29E-02	3.16E-02	4.79E-02	5.89E-02
0.003	2.05E-02	4.57E-03	7.41E-03	2.09E-02	3.16E-02	4.17E-02
0.005	1.11E-02	2.29E-03	3.72E-03	1.12E-02	1.70E-02	2.24E-02
0.007	6.93E-03	1.41E-03	2.46E-03	6.92E-03	1.12E-02	1.38E-02
0.01	4.03E-03	9.02E-04	1.51E-03	3.72E-03	6.46E-03	7.94E-03
0.015	2.12E-03	5.19E-04	8.13E-04	1.74E-03	3.47E-03	4.42E-03
0.02	1.34E-03	3.43E-04	4.68E-04	1.07E-03	2.14E-03	2.82E-03
0.03	7.08E-04	1.66E-04	2.34E-04	5.37E-04	1.07E-03	1.57E-03
0.05	3.20E-04	7.24E-05	9.55E-05	2.19E-04	4.68E-04	7.08E-04
0.07	1.89E-04	4.17E-05	5.50E-05	1.18E-04	2.51E-04	4.37E-04
0.1	1.07E-04	2.40E-05	3.16E-05	6.31E-05	1.35E-04	2.34E-04
0.15	5.49E-05	1.25E-05	1.70E-05	3.16E-05	7.76E-05	1.18E-04
0.2	3.40E-05	7.67E-06	1.12E-05	2.02E-05	4.79E-05	7.24E-05
0.3	1.73E-05	3.72E-06	6.03E-06	1.12E-05	2.40E-05	3.89E-05

Turkey Point Units 6 & 7
COL Application
Part 2 — FSAR

PTN COL 2.5-2

Table 2.5.2-220 (Sheet 2 of 5)
Mean and Fractile Rock Seismic Hazard Curves

Ampl. (g)	MEAN (a.f.e.)	0.05 (a.f.e)	0.16 (a.f.e)	0.50 (a.f.e)	0.84 (a.f.e)	0.95 (a.f.e)
25 Hz Hazard Curves (cont.)						
0.5	7.26E-06	1.37E-06	2.29E-06	4.90E-06	1.20E-05	1.82E-05
0.7	4.06E-06	6.38E-07	1.15E-06	2.82E-06	6.92E-06	1.08E-05
1	2.14E-06	2.43E-07	4.68E-07	1.41E-06	3.72E-06	6.03E-06
1.5	9.98E-07	7.50E-08	1.55E-07	5.96E-07	2.00E-06	3.13E-06
2	5.60E-07	2.75E-08	6.31E-08	2.88E-07	1.15E-06	2.00E-06
3	2.33E-07	5.82E-09	1.59E-08	9.55E-08	4.37E-07	8.71E-07
5	6.73E-08	5.56E-10	1.86E-09	1.76E-08	1.02E-07	3.31E-07
7	2.68E-08	9.89E-11	3.80E-10	4.90E-09	3.16E-08	1.55E-07
10	8.99E-09	1.38E-11	5.13E-11	1.15E-09	8.51E-09	5.50E-08
10 Hz Hazard Curves						
0.001	5.99E-02	2.09E-02	3.63E-02	5.89E-02	8.32E-02	9.55E-02
0.0015	4.80E-02	1.38E-02	2.57E-02	4.79E-02	6.76E-02	8.32E-02
0.002	3.96E-02	1.05E-02	1.95E-02	3.89E-02	5.89E-02	7.24E-02
0.003	2.84E-02	6.46E-03	1.12E-02	2.75E-02	4.47E-02	5.50E-02
0.005	1.65E-02	3.47E-03	5.25E-03	1.59E-02	2.57E-02	3.63E-02
0.007	1.06E-02	2.00E-03	3.24E-03	1.05E-02	1.70E-02	2.24E-02
0.01	6.21E-03	1.19E-03	1.86E-03	6.03E-03	9.77E-03	1.38E-02
0.015	3.09E-03	6.17E-04	1.00E-03	2.82E-03	5.25E-03	6.46E-03
0.02	1.80E-03	3.80E-04	6.17E-04	1.51E-03	3.02E-03	3.72E-03
0.03	8.03E-04	1.97E-04	2.88E-04	6.61E-04	1.41E-03	1.74E-03
0.05	2.79E-04	7.24E-05	1.10E-04	2.04E-04	4.68E-04	5.96E-04
0.07	1.39E-04	3.76E-05	5.13E-05	1.10E-04	2.04E-04	2.99E-04
0.1	6.71E-05	1.88E-05	2.75E-05	5.13E-05	9.55E-05	1.45E-04
0.15	3.06E-05	9.77E-06	1.38E-05	2.40E-05	4.47E-05	7.00E-05
0.2	1.80E-05	5.62E-06	7.94E-06	1.48E-05	2.75E-05	4.17E-05
0.3	8.70E-06	2.63E-06	3.72E-06	6.92E-06	1.38E-05	2.09E-05
0.5	3.46E-06	8.41E-07	1.41E-06	2.72E-06	5.62E-06	8.51E-06
0.7	1.81E-06	3.67E-07	6.61E-07	1.37E-06	3.02E-06	4.42E-06
1	8.64E-07	1.40E-07	2.69E-07	6.17E-07	1.51E-06	2.21E-06
1.5	3.39E-07	3.63E-08	7.76E-08	2.19E-07	5.75E-07	9.33E-07
2	1.63E-07	1.25E-08	2.95E-08	9.55E-08	2.88E-07	4.68E-07
3	5.16E-08	2.29E-09	6.03E-09	2.57E-08	8.91E-08	1.72E-07
5	9.83E-09	1.97E-10	6.61E-10	3.98E-09	1.70E-08	3.76E-08
7	2.87E-09	3.06E-11	1.26E-10	1.00E-09	4.90E-09	1.29E-08
10	6.86E-10	3.72E-12	1.95E-11	1.78E-10	1.07E-09	3.24E-09
5 Hz Hazard Curves						
0.001	6.55E-02	2.75E-02	4.47E-02	6.31E-02	8.91E-02	9.55E-02
0.0015	5.32E-02	1.70E-02	3.16E-02	5.13E-02	7.76E-02	8.91E-02
0.002	4.43E-02	1.29E-02	2.40E-02	4.47E-02	6.31E-02	7.76E-02
0.003	3.21E-02	7.67E-03	1.48E-02	3.16E-02	5.13E-02	6.31E-02
0.005	1.88E-02	3.72E-03	6.92E-03	1.82E-02	3.16E-02	3.89E-02
0.007	1.20E-02	2.29E-03	3.98E-03	1.12E-02	2.09E-02	2.66E-02
0.01	6.86E-03	1.23E-03	2.00E-03	6.46E-03	1.20E-02	1.59E-02
0.015	3.24E-03	5.37E-04	8.71E-04	3.02E-03	5.62E-03	7.41E-03

Turkey Point Units 6 & 7
COL Application
Part 2 — FSAR

PTN COL 2.5-2

Table 2.5.2-220 (Sheet 3 of 5)
Mean and Fractile Rock Seismic Hazard Curves

Ampl. (g)	MEAN (a.f.e.)	0.05 (a.f.e.)	0.16 (a.f.e.)	0.50 (a.f.e.)	0.84 (a.f.e.)	0.95 (a.f.e.)
5 Hz Hazard Curves (cont.)						
0.02	1.77E-03	2.99E-04	5.01E-04	1.62E-03	2.82E-03	3.98E-03
0.03	6.98E-04	1.30E-04	2.19E-04	6.17E-04	1.15E-03	1.51E-03
0.05	1.99E-04	4.17E-05	7.24E-05	1.66E-04	3.09E-04	4.22E-04
0.07	8.67E-05	2.09E-05	3.39E-05	6.76E-05	1.35E-04	1.78E-04
0.1	3.72E-05	9.77E-06	1.38E-05	2.95E-05	5.50E-05	8.04E-05
0.15	1.52E-05	4.27E-06	6.03E-06	1.16E-05	2.24E-05	3.39E-05
0.2	8.39E-06	2.29E-06	3.24E-06	6.24E-06	1.20E-05	1.95E-05
0.3	3.71E-06	9.02E-07	1.32E-06	2.82E-06	5.62E-06	9.12E-06
0.5	1.29E-06	2.43E-07	3.80E-07	9.33E-07	2.14E-06	3.35E-06
0.7	6.11E-07	8.61E-08	1.55E-07	4.22E-07	1.07E-06	1.74E-06
1	2.59E-07	2.57E-08	5.13E-08	1.66E-07	4.37E-07	7.59E-07
1.5	8.87E-08	5.43E-09	1.20E-08	4.79E-08	1.55E-07	2.79E-07
2	3.87E-08	1.51E-09	4.27E-09	1.70E-08	7.76E-08	1.40E-07
3	1.09E-08	2.11E-10	6.61E-10	3.98E-09	2.09E-08	4.47E-08
5	1.80E-09	1.29E-11	4.79E-11	4.22E-10	2.82E-09	8.51E-09
7	4.86E-10	1.51E-12	7.41E-12	7.50E-11	7.08E-10	2.29E-09
10	1.08E-10	1.18E-13	7.59E-13	1.12E-11	1.35E-10	4.68E-10
2.5 Hz Hazard Curves						
0.001	6.52E-02	3.16E-02	4.47E-02	6.31E-02	8.32E-02	9.55E-02
0.0015	5.20E-02	1.95E-02	3.16E-02	5.13E-02	7.24E-02	8.32E-02
0.002	4.26E-02	1.29E-02	2.24E-02	4.17E-02	6.31E-02	7.24E-02
0.003	3.02E-02	7.41E-03	1.38E-02	2.75E-02	4.79E-02	5.50E-02
0.005	1.71E-02	3.24E-03	6.03E-03	1.38E-02	3.16E-02	3.63E-02
0.007	1.06E-02	1.74E-03	3.47E-03	7.94E-03	2.09E-02	2.40E-02
0.01	5.82E-03	8.41E-04	1.62E-03	4.27E-03	1.20E-02	1.48E-02
0.015	2.56E-03	3.31E-04	6.61E-04	1.86E-03	5.25E-03	6.46E-03
0.02	1.30E-03	1.72E-04	3.09E-04	1.00E-03	2.63E-03	3.47E-03
0.03	4.46E-04	6.10E-05	1.02E-04	3.55E-04	8.71E-04	1.15E-03
0.05	9.94E-05	1.53E-05	2.57E-05	7.76E-05	1.55E-04	2.19E-04
0.07	3.60E-05	6.03E-06	1.12E-05	2.75E-05	5.13E-05	7.00E-05
0.1	1.28E-05	2.37E-06	3.98E-06	9.12E-06	1.70E-05	2.57E-05
0.15	4.37E-06	7.33E-07	1.32E-06	2.82E-06	6.46E-06	1.05E-05
0.2	2.15E-06	2.88E-07	5.37E-07	1.37E-06	3.24E-06	5.82E-06
0.3	8.15E-07	7.50E-08	1.55E-07	4.84E-07	1.41E-06	2.46E-06
0.5	2.38E-07	1.12E-08	2.75E-08	1.26E-07	4.68E-07	8.41E-07
0.7	1.01E-07	2.72E-09	8.51E-09	4.47E-08	2.04E-07	4.07E-07
1	3.87E-08	5.01E-10	1.74E-09	1.38E-08	7.24E-08	1.78E-07
1.5	1.18E-08	5.69E-11	2.34E-10	2.92E-09	1.82E-08	5.89E-08
2	4.77E-09	1.05E-11	4.79E-11	9.02E-10	6.92E-09	2.24E-08
3	1.19E-09	7.85E-13	4.27E-12	1.45E-10	1.62E-09	5.25E-09
5	1.68E-10	1.88E-14	1.55E-13	1.12E-11	1.91E-10	6.84E-10
7	4.03E-11	1.04E-15	1.38E-14	1.51E-12	3.63E-11	1.45E-10
10	7.81E-12	4.47E-16	6.61E-16	1.55E-13	4.90E-12	2.40E-11

Turkey Point Units 6 & 7
COL Application
Part 2 — FSAR

PTN COL 2.5-2

Table 2.5.2-220 (Sheet 4 of 5)
Mean and Fractile Rock Seismic Hazard Curves

Ampl. (g)	MEAN (a.f.e.)	0.05 (a.f.e)	0.16 (a.f.e)	0.50 (a.f.e)	0.84 (a.f.e)	0.95 (a.f.e)
1 Hz Hazard Curves						
0.0001	1.04E-01	8.91E-02	9.55E-02	1.02E-01	1.10E-01	1.18E-01
0.0003	8.45E-02	6.31E-02	7.24E-02	8.32E-02	9.55E-02	1.02E-01
0.0005	7.06E-02	4.79E-02	5.50E-02	7.24E-02	8.32E-02	8.91E-02
0.0006	6.53E-02	4.17E-02	5.13E-02	6.76E-02	7.76E-02	8.91E-02
0.0007	6.07E-02	3.63E-02	4.47E-02	6.31E-02	7.76E-02	8.32E-02
0.0008	5.67E-02	3.16E-02	3.89E-02	5.89E-02	7.24E-02	7.76E-02
0.001	5.01E-02	2.40E-02	3.16E-02	5.13E-02	6.31E-02	7.24E-02
0.0015	3.85E-02	1.38E-02	1.95E-02	3.89E-02	5.50E-02	6.31E-02
0.002	3.08E-02	8.51E-03	1.29E-02	2.95E-02	4.79E-02	5.50E-02
0.003	2.09E-02	4.27E-03	6.46E-03	1.82E-02	3.63E-02	4.17E-02
0.005	1.10E-02	1.41E-03	2.63E-03	7.41E-03	1.95E-02	2.95E-02
0.007	6.39E-03	6.61E-04	1.32E-03	3.72E-03	1.12E-02	2.09E-02
0.01	3.19E-03	2.60E-04	5.37E-04	1.74E-03	5.62E-03	1.20E-02
0.015	1.23E-03	7.76E-05	1.55E-04	7.08E-04	2.00E-03	5.62E-03
0.02	5.58E-04	3.16E-05	6.31E-05	3.31E-04	8.71E-04	2.63E-03
0.03	1.59E-04	7.67E-06	1.48E-05	8.32E-05	2.19E-04	8.13E-04
0.05	2.73E-05	1.11E-06	2.29E-06	1.12E-05	3.89E-05	1.26E-04
0.07	8.24E-06	2.79E-07	7.59E-07	2.82E-06	1.12E-05	2.75E-05
0.1	2.41E-06	6.10E-08	1.91E-07	7.08E-07	3.24E-06	5.43E-06
0.15	6.38E-07	7.94E-09	2.24E-08	1.91E-07	8.13E-07	1.74E-06
0.2	2.61E-07	1.68E-09	7.41E-09	6.31E-08	3.55E-07	9.33E-07
0.3	7.85E-08	1.50E-10	1.00E-09	1.48E-08	1.26E-07	3.80E-07
0.5	1.86E-08	5.62E-12	5.89E-11	2.00E-09	3.16E-08	9.23E-08
0.7	7.21E-09	5.56E-13	7.94E-12	5.01E-10	1.12E-08	3.16E-08
1	2.53E-09	3.63E-14	7.08E-13	8.91E-11	2.82E-09	1.01E-08
0.5 Hz Hazard Curves						
0.0001	8.85E-02	7.24E-02	7.76E-02	8.91E-02	9.55E-02	1.02E-01
0.0003	6.30E-02	4.47E-02	5.13E-02	6.31E-02	7.24E-02	7.76E-02
0.0005	5.14E-02	2.75E-02	3.89E-02	5.13E-02	6.31E-02	6.76E-02
0.0006	4.73E-02	2.24E-02	3.16E-02	4.79E-02	5.89E-02	6.31E-02
0.0007	4.39E-02	1.82E-02	2.75E-02	4.47E-02	5.89E-02	6.31E-02
0.0008	4.09E-02	1.48E-02	2.40E-02	4.17E-02	5.50E-02	5.89E-02
0.001	3.58E-02	1.05E-02	1.82E-02	3.63E-02	5.13E-02	5.50E-02
0.0015	2.69E-02	5.25E-03	1.05E-02	2.75E-02	4.47E-02	5.13E-02
0.002	2.09E-02	2.92E-03	6.92E-03	1.95E-02	3.89E-02	4.47E-02
0.003	1.35E-02	1.23E-03	3.24E-03	1.05E-02	2.95E-02	3.63E-02
0.005	6.60E-03	3.31E-04	9.33E-04	3.47E-03	1.48E-02	2.40E-02
0.007	3.64E-03	1.26E-04	3.55E-04	1.41E-03	7.94E-03	1.59E-02
0.01	1.71E-03	3.76E-05	1.02E-04	5.37E-04	3.72E-03	9.12E-03
0.015	6.07E-04	7.94E-06	2.40E-05	1.45E-04	1.15E-03	3.47E-03
0.02	2.60E-04	2.29E-06	8.51E-06	5.50E-05	4.37E-04	1.62E-03
0.03	6.84E-05	4.37E-07	1.74E-06	1.16E-05	8.32E-05	4.37E-04
0.05	1.13E-05	4.03E-08	1.78E-07	1.46E-06	1.12E-05	5.13E-05
0.07	3.62E-06	6.68E-09	3.89E-08	4.68E-07	2.82E-06	9.77E-06

Turkey Point Units 6 & 7
COL Application
Part 2 — FSAR

PTN COL 2.5-2

Table 2.5.2-220 (Sheet 5 of 5)
Mean and Fractile Rock Seismic Hazard Curves

Ampl. (g)	MEAN (a.f.e.)	0.05 (a.f.e)	0.16 (a.f.e)	0.50 (a.f.e)	0.84 (a.f.e)	0.95 (a.f.e)
0.5 Hz Hazard Curves (cont.)						
0.1	1.13E-06	9.33E-10	7.94E-09	8.91E-08	8.13E-07	1.57E-06
0.15	2.91E-07	6.76E-11	9.33E-10	1.29E-08	1.35E-07	3.94E-07
0.2	1.06E-07	8.81E-12	1.26E-10	3.98E-09	4.79E-08	1.66E-07
0.3	2.42E-08	3.55E-13	1.20E-11	5.37E-10	1.38E-08	5.50E-08
0.5	4.02E-09	2.29E-15	1.66E-13	3.16E-11	2.14E-09	1.20E-08
0.7	1.36E-09	3.16E-17	8.51E-15	3.72E-12	5.75E-10	3.85E-09
1	4.46E-10	1.02E-28	1.91E-16	4.37E-13	1.26E-10	9.33E-10

a.f.e. = annual frequency of exceedance

Turkey Point Units 6 & 7
COL Application
Part 2 — FSAR

PTN COL 2.5-2

Table 2.5.2-221
Mean Hard Rock UHRS Accelerations (g)

Frequency, Hz	Mean 1E-04	Mean 1E-05	Mean 1E-06
PGA	0.0399	0.147	0.542
25	0.104	0.414	1.50
10	0.0822	0.278	0.932
5	0.0661	0.184	0.561
2.5	0.0499	0.110	0.275
1	00.0343	0.0663	0.131
0.5	0.0267	0.0519	0.104

UHRS = Uniform hazard response spectra
PGA = Peak ground acceleration

Turkey Point Units 6 & 7
COL Application
Part 2 — FSAR

PTN COL 2.5-2

Table 2.5.2-222 (Sheet 1 of 3)
Percent Contribution to Deaggregation

Percent Contribution to Low-Frequency Deaggregation for 1E-04								
R \ M	Percent Contribution By Moment Magnitude [M] — Distance [R, km] Bin							
	5.25	5.75	6.25	6.75	7.25	7.75	8.25	8.75
0–20	3.358	0.6060	0.2397	0.02748	8.323E-3	9.539E-4	1.104E-20	1.104E-20
20–40	2.196	0.8873	0.4379	0.05555	0.01653	1.935E-3	1.682E-20	1.682E-20
40–60	0.8486	0.6860	0.4743	0.06720	0.02084	2.372E-3	2.673E-20	2.673E-20
60–80	0.3818	0.4289	0.4089	0.07140	0.02415	2.839E-3	2.672E-20	2.672E-20
80–100	0.2062	0.3388	0.3626	0.07307	0.02675	3.208E-3	2.553E-20	2.553E-20
100–210	0.3826	0.8812	1.295	0.3402	0.1589	0.02034	6.516E-20	6.516E-20
210–330	0.07032	0.6397	3.239	8.021	3.472	0.01310	3.978E-20	3.978E-20
>330	4.096E-3	0.08651	0.9054	6.256	27.78	32.16	1.977	0.03270

Percent Contribution to High-Frequency Deaggregation for 1E-04								
R \ M	Percent Contribution By Moment Magnitude [M] — Distance [R, km] Bin							
	5.25	5.75	6.25	6.75	7.25	7.75	8.25	8.75
0–20	9.682	0.8214	0.2675	0.02847	8.420E-3	9.426E-4	5.424E-21	5.424E-21
20–40	12.53	1.835	0.6223	0.06477	0.01742	1.948E-3	1.236E-20	1.236E-20
40–60	7.102	1.940	0.8323	0.08947	0.02330	2.589E-3	2.163E-20	2.163E-20
60–80	3.856	1.452	0.8217	0.1040	0.02850	3.106E-3	2.235E-20	2.235E-20
80–100	2.539	1.306	0.7968	0.1130	0.03231	3.550E-3	2.268E-20	2.268E-20
100–210	5.533	3.894	3.092	0.5538	0.1957	0.02274	6.059E-20	6.059E-20
210–330	0.7292	2.440	6.396	9.927	3.393	0.01361	3.864E-20	3.864E-20
>330	0.02732	0.1954	1.027	3.831	8.740	3.003	0.06259	1.947E-4

Turkey Point Units 6 & 7
COL Application
Part 2 — FSAR

PTN COL 2.5-2

Table 2.5.2-222 (Sheet 2 of 3)
Percent Contribution to Deaggregation

Percent Contribution to Low-Frequency Deaggregation for 1E-05								
R \ M	Percent Contribution By Moment Magnitude [M] — Distance [R, km] Bin							
	5.25	5.75	6.25	6.75	7.25	7.75	8.25	8.75
0–20	12.15	3.879	1.943	0.2549	0.08261	9.658E-3	1.464E-19	1.464E-19
20–40	3.472	3.102	2.368	0.4021	0.1452	0.01803	1.866E-19	1.866E-19
40–60	0.7056	1.364	1.664	0.3581	0.1528	0.01961	2.652E-19	2.652E-19
60–80	0.2055	0.5543	0.9977	0.2854	0.1481	0.02069	2.418E-19	2.418E-19
80–100	0.08325	0.3335	0.6990	0.2373	0.1433	0.02116	2.153E-19	2.153E-19
100–210	0.1133	0.6144	1.742	0.7683	0.6158	0.1023	4.922E-19	4.922E-19
210–330	6.898E-3	0.1182	1.198	5.745	4.268	0.04352	2.548E-19	2.548E-19
>330	1.738E-4	7.247E-3	0.1672	3.428	28.87	15.48	0.8831	8.244E-3

Percent Contribution to High-Frequency Deaggregation for 1E-05								
R \ M	Percent Contribution By Moment Magnitude [M] — Distance [R, km] Bin							
	5.25	5.75	6.25	6.75	7.25	7.75	8.25	8.75
0–20	40.80	6.066	2.324	0.2676	0.08196	9.276E-3	1.094E-19	1.094E-19
20–40	15.35	5.979	3.210	0.4532	0.1469	0.01742	1.475E-19	1.475E-19
40–60	3.048	2.545	2.122	0.3819	0.1490	0.01923	2.246E-19	2.246E-19
60–80	0.8306	0.9665	1.146	0.2708	0.1341	0.01861	2.141E-19	2.141E-19
80–100	0.3785	0.6072	0.8052	0.2195	0.1229	0.01816	1.993E-19	1.993E-19
100–210	0.5505	1.159	1.927	0.6413	0.4498	0.07458	4.284E-19	4.284E-19
210–330	0.01752	0.1130	0.6067	1.879	1.253	0.02071	1.728E-19	1.728E-19
>330	2.546E-4	3.359E-3	0.03420	0.3020	2.390	0.09811	8.617E-4	6.446E-7

Turkey Point Units 6 & 7
COL Application
Part 2 — FSAR

PTN COL 2.5-2

Table 2.5.2-222 (Sheet 3 of 3)
Percent Contribution to Deaggregation

Percent Contribution to Low-Frequency Deaggregation for 1E-06								
R \ M	Percent Contribution By Moment Magnitude [M] — Distance [R, km] Bin							
	5.25	5.75	6.25	6.75	7.25	7.75	8.25	8.75
0–20	19.29	13.59	10.37	1.814	0.7091	0.08862	1.680E-18	1.680E-18
20–40	1.613	4.002	6.005	1.678	0.9085	0.1309	1.744E-18	1.744E-18
40–60	0.1375	0.8059	2.227	0.8867	0.6630	0.1078	2.006E-18	2.006E-18
60–80	0.02297	0.1897	0.8379	0.4697	0.4684	0.08811	1.618E-18	1.618E-18
80–100	6.569E-3	0.08325	0.4397	0.2939	0.3611	0.07376	1.354E-18	1.354E-18
100–210	6.415E-3	0.1091	0.7689	0.6570	1.050	0.2427	2.846E-18	2.846E-18
210–330	1.432E-4	7.221E-3	0.1538	1.234	1.759	0.06449	1.203E-18	1.203E-18
>330	1.425E-6	2.598E-4	0.01353	0.9716	21.14	3.306	0.1628	7.440E-4

Percent Contribution to High-Frequency Deaggregation for 1E-06								
R \ M	Percent Contribution By Moment Magnitude [M] — Distance [R, km] Bin							
	5.25	5.75	6.25	6.75	7.25	7.75	8.25	8.75
0–20	53.64	17.36	9.988	1.553	0.5884	0.07252	1.248E-18	1.248E-18
20–40	3.143	3.754	4.109	1.060	0.5958	0.08899	1.408E-18	1.408E-18
40–60	0.1753	0.4668	0.9073	0.3421	0.3022	0.05753	1.586E-18	1.586E-18
60–80	0.02240	0.07983	0.2270	0.1166	0.1499	0.03383	1.176E-18	1.176E-18
80–100	6.819E-3	0.03427	0.1105	0.06464	0.09602	0.02359	9.290E-19	9.290E-19
100–210	6.744E-3	0.04374	0.1743	0.1210	0.2085	0.05592	1.688E-18	1.688E-18
210–330	5.549E-5	9.710E-4	9.667E-3	0.03550	0.05705	6.170E-3	4.768E-19	4.768E-19
>330	1.102E-7	1.140E-5	2.378E-4	2.641E-3	0.1054	8.841E-4	3.100E-19	3.100E-19

Turkey Point Units 6 & 7
COL Application
Part 2 — FSAR

PTN COL 2.5-2

Table 2.5.2-223
Controlling Magnitudes and Distances from Deaggregation

Struct. Frequency	Annual Freq. Exceed.	Overall Hazard		Hazard from R > 100 km	
		M	R, km	M	R, km
1 & 2.5 Hz	1E-04	7.1	400	7.3	570
5 & 10 Hz	1E-04	5.9	110	6.5	290
1 & 2.5 Hz	1E-05	6.7	190	7.2	560
5 & 10 Hz	1E-05	5.5	31	6.7	250
1 & 2.5 Hz	1E-06	6.3	61	7.2	600
5 & 10 Hz	1E-06	5.5	17	6.9	180

Notes:

Shaded cells indicate values used to construct UHRS
"M" is moment magnitude; "R" is epicentral distance

PTN COL 2.5-2

Table 2.5.2-224
Assigned Strong Motion Durations in P-SHAKE

Set of Runs	Description	Recurrence	Input Rock Spectra	
			Moment Magnitude	Duration [sec]
LF4	Low Freq.	1E-04	7.3	13
HF4	High Freq.	1E-04	5.9	6
LF5	Low Freq.	1E-05	7.2	13
HF5	High Freq.	1E-05	5.5	6

Turkey Point Units 6 & 7
COL Application
Part 2 — FSAR

PTN COL 2.5-3

Table 2.5.2-225 (Sheet 1 of 2)
HF and LF Horizontal 1E-04 Rock Spectra, Amplification Factors, Site Spectra, and Raw and Smoothed Envelope Spectra

Horizontal 1E-04 Rock and Site Spectra UHRS (g)								
Freq,	Rock UHRS		Transfer Function		Surface UHRS		Raw Envelope	Smooth Spectrum
Hz	LF SA(g)	HF SA(g)	LF Amp	HF Amp	LF SA(g)	HF SA(g)	SA(g)	SA(g)
100	3.99E-02	3.99E-02	1.302	0.870	5.20E-02	3.47E-02	5.20E-02	5.20E-02
90	4.39E-02	4.40E-02	1.186	0.793	5.21E-02	3.49E-02	5.21E-02	5.21E-02
80	5.05E-02	5.07E-02	1.035	0.693	5.23E-02	3.52E-02	5.23E-02	5.23E-02
70	6.06E-02	6.10E-02	0.871	0.587	5.28E-02	3.58E-02	5.28E-02	5.28E-02
60	7.36E-02	7.43E-02	0.730	0.500	5.37E-02	3.71E-02	5.37E-02	5.37E-02
50	8.66E-02	8.76E-02	0.636	0.445	5.51E-02	3.90E-02	5.51E-02	5.51E-02
45	9.20E-02	9.31E-02	0.612	0.440	5.64E-02	4.09E-02	5.64E-02	5.65E-02
40	9.65E-02	9.77E-02	0.607	0.455	5.85E-02	4.44E-02	5.85E-02	5.86E-02
35	9.98E-02	1.01E-01	0.619	0.491	6.18E-02	4.96E-02	6.18E-02	6.18E-02
30	1.02E-01	1.03E-01	0.642	0.540	6.57E-02	5.57E-02	6.57E-02	6.55E-02
25	1.04E-01	1.04E-01	0.642	0.542	6.67E-02	5.64E-02	6.67E-02	6.65E-02
20	1.00E-01	1.02E-01	0.644	0.523	6.44E-02	5.33E-02	6.44E-02	6.43E-02
15	9.34E-02	9.58E-02	0.677	0.544	6.32E-02	5.21E-02	6.32E-02	6.29E-02
12.5	8.86E-02	9.02E-02	0.710	0.575	6.29E-02	5.19E-02	6.29E-02	6.28E-02
10	8.22E-02	8.22E-02	0.821	0.701	6.74E-02	5.76E-02	6.74E-02	6.71E-02
9	8.01E-02	8.05E-02	0.869	0.755	6.96E-02	6.07E-02	6.96E-02	6.99E-02
8	7.75E-02	7.81E-02	0.950	0.847	7.37E-02	6.62E-02	7.37E-02	7.32E-02
7	7.45E-02	7.50E-02	1.010	0.897	7.52E-02	6.73E-02	7.52E-02	7.52E-02
6	7.07E-02	7.11E-02	1.100	0.994	7.78E-02	7.07E-02	7.78E-02	7.84E-02
5	6.61E-02	6.61E-02	1.310	1.216	8.65E-02	8.03E-02	8.65E-02	8.63E-02
4	5.96E-02	5.60E-02	1.437	1.302	8.57E-02	7.29E-02	8.57E-02	8.69E-02
3	5.29E-02	4.40E-02	2.147	2.047	1.14E-01	9.01E-02	1.14E-01	1.11E-01
2.5	4.99E-02	3.69E-02	2.060	1.888	1.03E-01	6.97E-02	1.03E-01	1.02E-01
2	4.54E-02	2.88E-02	1.787	1.625	8.11E-02	4.69E-02	8.11E-02	8.07E-02
1.5	4.05E-02	2.00E-02	1.988	1.828	8.06E-02	3.65E-02	8.06E-02	8.02E-02
1.25	3.71E-02	1.55E-02	2.376	2.213	8.82E-02	3.43E-02	8.82E-02	8.84E-02
1	3.43E-02	1.12E-02	3.022	2.859	1.04E-01	3.21E-02	1.04E-01	1.05E-01
0.9	3.41E-02	9.61E-03	3.461	3.325	1.18E-01	3.20E-02	1.18E-01	1.15E-01
0.8	3.32E-02	8.06E-03	3.401	3.247	1.13E-01	2.62E-02	1.13E-01	1.12E-01
0.7	3.18E-02	6.59E-03	3.019	2.867	9.59E-02	1.89E-02	9.59E-02	9.72E-02
0.6	2.96E-02	5.21E-03	3.014	2.877	8.92E-02	1.50E-02	8.92E-02	8.86E-02
0.5	2.67E-02	3.92E-03	2.752	2.653	7.34E-02	1.04E-02	7.34E-02	7.17E-02
0.4	2.14E-02	3.14E-03	2.057	1.967	4.39E-02	6.17E-03	4.39E-02	4.46E-02
0.3	1.60E-02	2.35E-03	1.864	1.784	2.99E-02	4.20E-03	2.99E-02	3.00E-02
0.2	1.07E-02	1.57E-03	1.888	1.771	2.02E-02	2.78E-03	2.02E-02	2.01E-02
0.15	8.01E-03	1.18E-03	1.599	1.519	1.28E-02	1.79E-03	1.28E-02	1.29E-02

Turkey Point Units 6 & 7
COL Application
Part 2 — FSAR

PTN COL 2.5-3

Table 2.5.2-225 (Sheet 2 of 2)
HF and LF Horizontal 1E-04 Rock Spectra, Amplification Factors, Site Spectra, and Raw and Smoothed Envelope Spectra

Horizontal 1E-04 Rock and Site Spectra UHRS (g)								
Freq, Hz	Rock UHRS		Transfer Function		Surface UHRS		Raw Envelope	Smooth Spectrum
	LF SA(g)	HF SA(g)	LF Amp	HF Amp	LF SA(g)	HF SA(g)	SA(g)	SA(g)
0.125	6.64E-03	9.75E-04	1.421	1.377	9.44E-03	1.34E-03	9.44E-03	9.37E-03
0.1	4.27E-03	6.27E-04	1.323	1.268	5.65E-03	7.95E-04	5.65E-03	5.65E-03

UHRS = Uniform hazard response spectra
 LF = Low frequencies
 HF = High frequencies
 SA = Spectral acceleration
 Amp = Amplitude

Turkey Point Units 6 & 7
COL Application
Part 2 — FSAR

PTN COL 2.5-3

Table 2.5.2-226 (Sheet 1 of 2)
HF and LF horizontal 1E-05 Rock Spectra, Amplification Factors, Site Spectra, and Raw and Smoothed Envelope Spectra

Horizontal 1E-05 Rock and Site Spectra UHRS (g)								
Freq, Hz	Rock UHRS		Transfer Function		Surface UHRS		Raw Envelope	Smooth Spectrum
	LF SA(g)	HF SA(g)	LF Amp	HF Amp	LF SA(g)	HF SA(g)	SA(g)	SA(g)
100	1.47E-01	1.47E-01	0.767	0.646	1.13E-01	9.49E-02	1.13E-01	1.13E-01
90	1.63E-01	1.63E-01	0.694	0.584	1.13E-01	9.55E-02	1.13E-01	1.13E-01
80	1.89E-01	1.90E-01	0.601	0.507	1.13E-01	9.65E-02	1.13E-01	1.14E-01
70	2.29E-01	2.31E-01	0.501	0.427	1.14E-01	9.85E-02	1.14E-01	1.15E-01
60	2.80E-01	2.84E-01	0.415	0.361	1.16E-01	1.02E-01	1.16E-01	1.16E-01
50	3.33E-01	3.39E-01	0.360	0.323	1.20E-01	1.09E-01	1.20E-01	1.20E-01
45	3.56E-01	3.62E-01	0.347	0.322	1.23E-01	1.17E-01	1.23E-01	1.24E-01
40	3.75E-01	3.82E-01	0.346	0.338	1.30E-01	1.29E-01	1.30E-01	1.32E-01
35	3.91E-01	3.98E-01	0.359	0.376	1.40E-01	1.50E-01	1.50E-01	1.50E-01
30	4.04E-01	4.09E-01	0.384	0.426	1.55E-01	1.74E-01	1.74E-01	1.73E-01
25	4.14E-01	4.14E-01	0.394	0.436	1.63E-01	1.80E-01	1.80E-01	1.79E-01
20	3.85E-01	3.93E-01	0.407	0.426	1.57E-01	1.68E-01	1.68E-01	1.67E-01
15	3.42E-01	3.52E-01	0.448	0.453	1.53E-01	1.59E-01	1.59E-01	1.58E-01
12.5	3.14E-01	3.20E-01	0.481	0.483	1.51E-01	1.54E-01	1.54E-01	1.54E-01
10	2.78E-01	2.78E-01	0.588	0.606	1.64E-01	1.68E-01	1.68E-01	1.67E-01
9	2.63E-01	2.64E-01	0.647	0.665	1.70E-01	1.75E-01	1.75E-01	1.76E-01
8	2.47E-01	2.47E-01	0.732	0.757	1.81E-01	1.87E-01	1.87E-01	1.86E-01
7	2.29E-01	2.29E-01	0.813	0.822	1.86E-01	1.88E-01	1.88E-01	1.88E-01
6	2.08E-01	2.08E-01	0.903	0.908	1.88E-01	1.89E-01	1.89E-01	1.91E-01
5	1.84E-01	1.84E-01	1.118	1.131	2.06E-01	2.08E-01	2.08E-01	2.07E-01
4	1.60E-01	1.51E-01	1.271	1.228	2.03E-01	1.86E-01	2.03E-01	2.05E-01
3	1.29E-01	1.14E-01	1.919	1.925	2.48E-01	2.20E-01	2.48E-01	2.42E-01
2.5	1.10E-01	9.37E-02	2.005	1.855	2.21E-01	1.74E-01	2.21E-01	2.19E-01
2	9.82E-02	7.11E-02	1.734	1.588	1.70E-01	1.13E-01	1.70E-01	1.69E-01
1.5	8.51E-02	4.77E-02	1.852	1.744	1.58E-01	8.33E-02	1.58E-01	1.57E-01
1.25	7.66E-02	3.64E-02	2.221	2.119	1.70E-01	7.72E-02	1.70E-01	1.70E-01
1	6.63E-02	2.58E-02	2.844	2.742	1.89E-01	7.09E-02	1.89E-01	1.91E-01
0.9	6.60E-02	2.19E-02	3.292	3.230	2.17E-01	7.07E-02	2.17E-01	2.13E-01
0.8	6.45E-02	1.81E-02	3.360	3.223	2.17E-01	5.84E-02	2.17E-01	2.13E-01
0.7	6.17E-02	1.46E-02	3.041	2.859	1.88E-01	4.17E-02	1.88E-01	1.90E-01
0.6	5.76E-02	1.13E-02	3.036	2.862	1.75E-01	3.23E-02	1.75E-01	1.74E-01
0.5	5.19E-02	8.26E-03	2.784	2.645	1.44E-01	2.19E-02	1.44E-01	1.41E-01
0.4	4.15E-02	6.61E-03	2.073	1.948	8.61E-02	1.29E-02	8.61E-02	8.74E-02
0.3	3.11E-02	4.96E-03	1.866	1.753	5.81E-02	8.69E-03	5.81E-02	5.83E-02
0.2	2.08E-02	3.30E-03	1.882	1.767	3.91E-02	5.84E-03	3.91E-02	3.90E-02
0.15	1.56E-02	2.48E-03	1.602	1.523	2.49E-02	3.78E-03	2.49E-02	2.51E-02

Turkey Point Units 6 & 7
COL Application
Part 2 — FSAR

PTN COL 2.5-3

Table 2.5.2-226 (Sheet 2 of 2)
HF and LF horizontal 1E-05 Rock Spectra, Amplification Factors, Site Spectra, and Raw and Smoothed Envelope Spectra

Horizontal 1E-05 Rock and Site Spectra UHRS (g)								
Freq, Hz	Rock UHRS		Transfer Function		Surface UHRS		Raw Envelope	Smooth Spectrum
	LF SA(g)	HF SA(g)	LF Amp	HF Amp	LF SA(g)	HF SA(g)	SA(g)	SA(g)
0.125	1.29E-02	2.06E-03	1.423	1.377	1.84E-02	2.83E-03	1.84E-02	1.82E-02
0.1	8.30E-03	1.32E-03	1.324	1.268	1.10E-02	1.68E-03	1.10E-02	1.10E-02

UHRS = Uniform hazard response spectra
 LF = Low frequencies
 HF = High frequencies
 SA = Spectral acceleration
 Amp = Amplitude

Turkey Point Units 6 & 7
COL Application
Part 2 — FSAR

PTN COL 2.5-3

Table 2.5.2-227
Horizontal 1E-04 and 1E-05 Site Spectra, Values of A_R and DF, and GMRS

Freq. Hz	Horizontal 1E-04 (g)	Horizontal 1E-05 (g)	A_R	DF	Horizontal GMRS (g)
100	5.20E-02	1.13E-01	2.17	1.11	5.79E-02
90	5.21E-02	1.13E-01	2.17	1.11	5.81E-02
80	5.23E-02	1.14E-01	2.17	1.11	5.83E-02
70	5.28E-02	1.15E-01	2.17	1.11	5.89E-02
60	5.37E-02	1.16E-01	2.17	1.11	5.98E-02
50	5.51E-02	1.20E-01	2.18	1.12	6.16E-02
45	5.65E-02	1.24E-01	2.19	1.12	6.35E-02
40	5.86E-02	1.32E-01	2.25	1.15	6.72E-02
35	6.18E-02	1.50E-01	2.43	1.22	7.53E-02
30	6.55E-02	1.73E-01	2.64	1.30	8.54E-02
25	6.65E-02	1.79E-01	2.69	1.33	8.82E-02
20	6.43E-02	1.67E-01	2.60	1.29	8.28E-02
15	6.29E-02	1.58E-01	2.51	1.25	7.88E-02
12.5	6.28E-02	1.54E-01	2.45	1.23	7.72E-02
10	6.71E-02	1.67E-01	2.49	1.24	8.35E-02
9	6.99E-02	1.76E-01	2.52	1.26	8.78E-02
8	7.32E-02	1.86E-01	2.53	1.26	9.25E-02
7	7.52E-02	1.88E-01	2.50	1.25	9.38E-02
6	7.84E-02	1.91E-01	2.44	1.22	9.59E-02
5	8.63E-02	2.07E-01	2.40	1.21	1.04E-01
4	8.69E-02	2.05E-01	2.36	1.19	1.04E-01
3	1.11E-01	2.42E-01	2.18	1.12	1.24E-01
2.5	1.02E-01	2.19E-01	2.15	1.11	1.13E-01
2	8.07E-02	1.69E-01	2.10	1.08	8.75E-02
1.5	8.02E-02	1.57E-01	1.96	1.03	8.24E-02
1.25	8.84E-02	1.70E-01	1.92	1.01	8.94E-02
1	1.05E-01	1.91E-01	1.83	1.00	1.05E-01
0.9	1.15E-01	2.13E-01	1.85	1.00	1.15E-01
0.8	1.12E-01	2.13E-01	1.91	1.01	1.12E-01
0.7	9.72E-02	1.90E-01	1.95	1.03	9.96E-02
0.6	8.86E-02	1.74E-01	1.96	1.03	9.11E-02
0.5	7.17E-02	1.41E-01	1.97	1.03	7.39E-02
0.4	4.46E-02	8.74E-02	1.96	1.03	4.59E-02
0.3	3.00E-02	5.83E-02	1.95	1.02	3.06E-02
0.2	2.01E-02	3.90E-02	1.94	1.02	2.05E-02
0.15	1.29E-02	2.51E-02	1.95	1.02	1.32E-02
0.125	9.37E-03	1.82E-02	1.95	1.02	9.58E-03
0.1	5.65E-03	1.10E-02	1.95	1.02	5.78E-03

Notes:

A_R and DF are defined in Equations 2.5.2-14 and 2.5.2-15, respectively.

GMRS = Ground motion response spectrum

Turkey Point Units 6 & 7
COL Application
Part 2 — FSAR

PTN COL 2.5-3

Table 2.5.2-228
Smooth 1E-04, 1E-05, and 1E-06 Spectra at GMRS Elevation

Freq, Hz	Smooth Spectra (g)		
	1E-04	1E-05	1E-06
100	5.20E-02	1.13E-01	2.50E-01
90	5.21E-02	1.13E-01	2.51E-01
80	5.23E-02	1.14E-01	2.53E-01
70	5.28E-02	1.15E-01	2.56E-01
60	5.37E-02	1.16E-01	2.63E-01
50	5.51E-02	1.20E-01	2.77E-01
45	5.65E-02	1.24E-01	2.92E-01
40	5.86E-02	1.32E-01	3.18E-01
35	6.18E-02	1.50E-01	3.61E-01
30	6.55E-02	1.73E-01	4.19E-01
25	6.65E-02	1.79E-01	4.51E-01
20	6.43E-02	1.67E-01	4.35E-01
15	6.29E-02	1.58E-01	4.19E-01
12.5	6.28E-02	1.54E-01	4.06E-01
10	6.71E-02	1.67E-01	4.36E-01
9	6.99E-02	1.76E-01	4.63E-01
8	7.32E-02	1.86E-01	4.91E-01
7	7.52E-02	1.88E-01	5.06E-01
6	7.84E-02	1.91E-01	5.09E-01
5	8.63E-02	2.07E-01	5.45E-01
4	8.69E-02	2.05E-01	5.20E-01
3	1.11E-01	2.42E-01	5.73E-01
2.5	1.02E-01	2.19E-01	5.12E-01
2	8.07E-02	1.69E-01	3.82E-01
1.5	8.02E-02	1.57E-01	3.02E-01
1.25	8.84E-02	1.70E-01	3.11E-01
1	1.05E-01	1.91E-01	3.34E-01
0.9	1.15E-01	2.13E-01	3.77E-01
0.8	1.12E-01	2.13E-01	4.01E-01
0.7	9.72E-02	1.90E-01	3.78E-01
0.6	8.86E-02	1.74E-01	3.52E-01
0.5	7.17E-02	1.41E-01	2.93E-01
0.4	4.46E-02	8.74E-02	1.79E-01
0.3	3.00E-02	5.83E-02	1.17E-01
0.2	2.01E-02	3.90E-02	7.78E-02
0.15	1.29E-02	2.51E-02	5.05E-02
0.125	9.37E-03	1.82E-02	3.67E-02
0.1	5.65E-03	1.10E-02	2.21E-02

GMRS = Ground motion response spectrum

Turkey Point Units 6 & 7
COL Application
Part 2 — FSAR

PTN COL 2.5-3

Table 2.5.2-229
V/H Ratios, Vertical 1E-04 and 1E-05 Site Spectra, Values of A_R
and DF, and GMRS

Freq. Hz	V/H	Vertical 1E-04 (g)	Vertical 1E-05 (g)	A_R	DF	Vertical GMRS (g)
100	1.000	5.20E-02	1.13E-01	2.17	1.11	5.79E-02
90	1.000	5.21E-02	1.13E-01	2.17	1.11	5.81E-02
80	1.000	5.23E-02	1.14E-01	2.17	1.11	5.83E-02
70	1.000	5.28E-02	1.15E-01	2.17	1.11	5.89E-02
60	1.000	5.37E-02	1.16E-01	2.17	1.11	5.98E-02
50	1.000	5.51E-02	1.20E-01	2.18	1.12	6.16E-02
45	1.000	5.65E-02	1.24E-01	2.19	1.12	6.35E-02
40	1.000	5.86E-02	1.32E-01	2.25	1.15	6.72E-02
35	1.000	6.18E-02	1.50E-01	2.43	1.22	7.53E-02
30	1.000	6.55E-02	1.73E-01	2.64	1.30	8.54E-02
25	1.000	6.65E-02	1.79E-01	2.69	1.33	8.82E-02
20	1.000	6.43E-02	1.67E-01	2.60	1.29	8.28E-02
15	1.000	6.29E-02	1.58E-01	2.51	1.25	7.88E-02
12.5	1.000	6.28E-02	1.54E-01	2.45	1.23	7.72E-02
10	1.000	6.71E-02	1.67E-01	2.49	1.24	8.35E-02
9	1.000	6.99E-02	1.76E-01	2.52	1.26	8.78E-02
8	1.000	7.32E-02	1.86E-01	2.53	1.26	9.24E-02
7	1.000	7.52E-02	1.88E-01	2.50	1.25	9.38E-02
6	0.999	7.84E-02	1.91E-01	2.44	1.22	9.59E-02
5	0.999	8.62E-02	2.07E-01	2.40	1.21	1.04E-01
4	0.999	8.68E-02	2.05E-01	2.36	1.19	1.04E-01
3	0.857	9.53E-02	2.08E-01	2.18	1.12	1.07E-01
2.5	0.715	7.28E-02	1.57E-01	2.15	1.11	8.07E-02
2	0.710	5.73E-02	1.20E-01	2.10	1.08	6.22E-02
1.5	0.704	5.65E-02	1.11E-01	1.96	1.03	5.81E-02
1.25	0.701	6.19E-02	1.19E-01	1.92	1.01	6.27E-02
1	0.696	7.27E-02	1.33E-01	1.83	1.00	7.27E-02
0.9	0.694	7.97E-02	1.47E-01	1.85	1.00	7.97E-02
0.8	0.691	7.72E-02	1.47E-01	1.91	1.01	7.77E-02
0.7	0.689	6.69E-02	1.31E-01	1.95	1.03	6.86E-02
0.6	0.686	6.08E-02	1.19E-01	1.96	1.03	6.25E-02
0.5	0.682	4.89E-02	9.61E-02	1.97	1.03	5.04E-02
0.4	0.678	3.02E-02	5.92E-02	1.96	1.03	3.11E-02
0.3	0.672	2.01E-02	3.92E-02	1.95	1.02	2.06E-02
0.2	0.668	1.34E-02	2.61E-02	1.94	1.02	1.37E-02
0.15	0.668	8.60E-03	1.68E-02	1.95	1.02	8.80E-03
0.125	0.668	6.26E-03	1.22E-02	1.95	1.02	6.40E-03
0.1	0.668	3.78E-03	7.35E-03	1.95	1.02	3.86E-03

Notes:

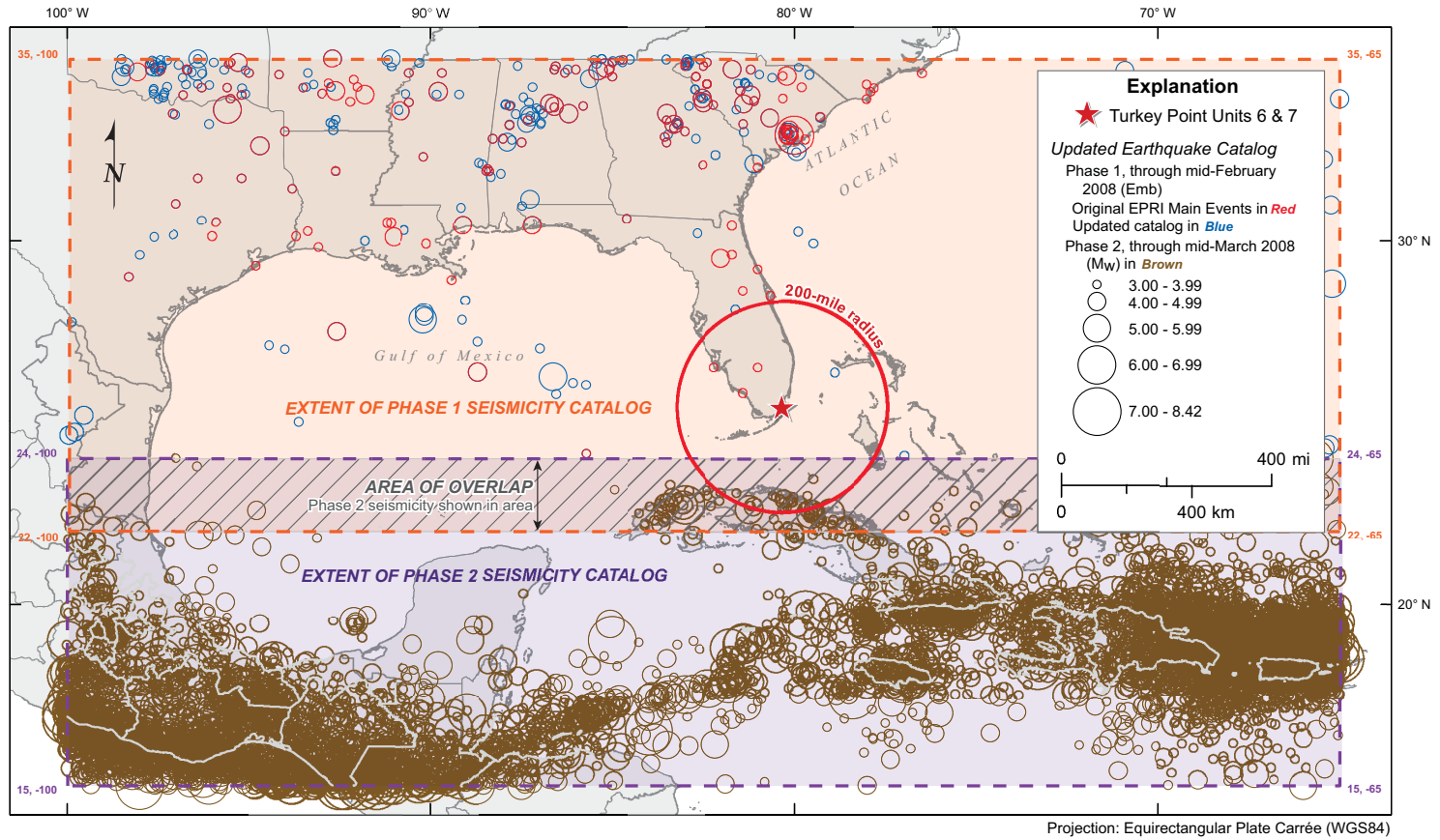
A_R and DF are defined in Equations 2.5.2-14 and 2.5.2-15, respectively.

GMRS = Ground motion response spectrum

Turkey Point Units 6 & 7
 COL Application
 Part 2 — FSAR

PTN COL 2.5-2

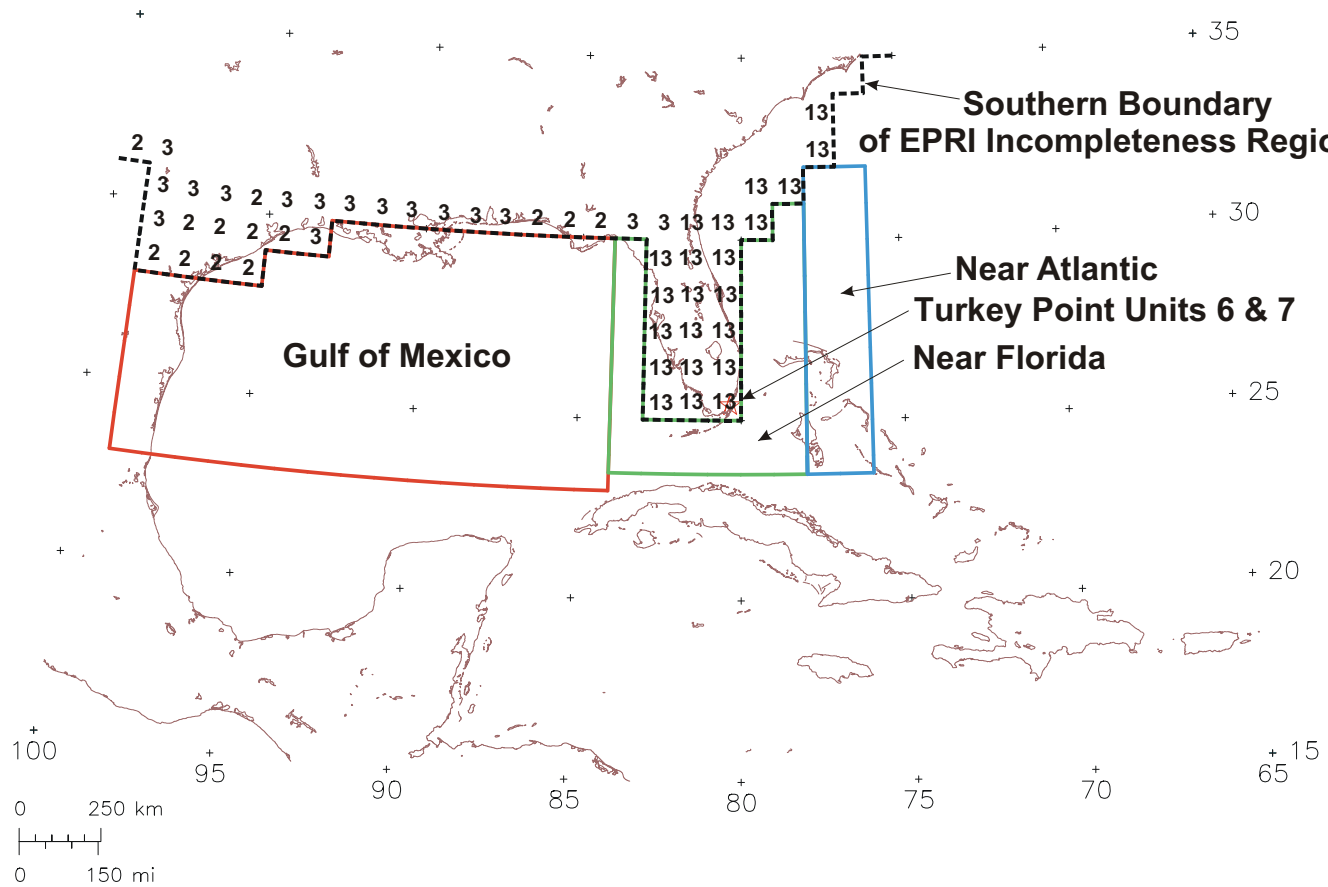
Figure 2.5.2-201 Seismicity in the Study Region, Phase 1 and Phase 2



Turkey Point Units 6 & 7
 COL Application
 Part 2 — FSAR

PTN COL 2.5-2

Figure 2.5.2-202 Supplemental Areas of Incompleteness Regions, Gulf of Mexico, Near Florida, and Near Atlantic, South of the Boundary of EPRI Incompleteness Regions



Notes:

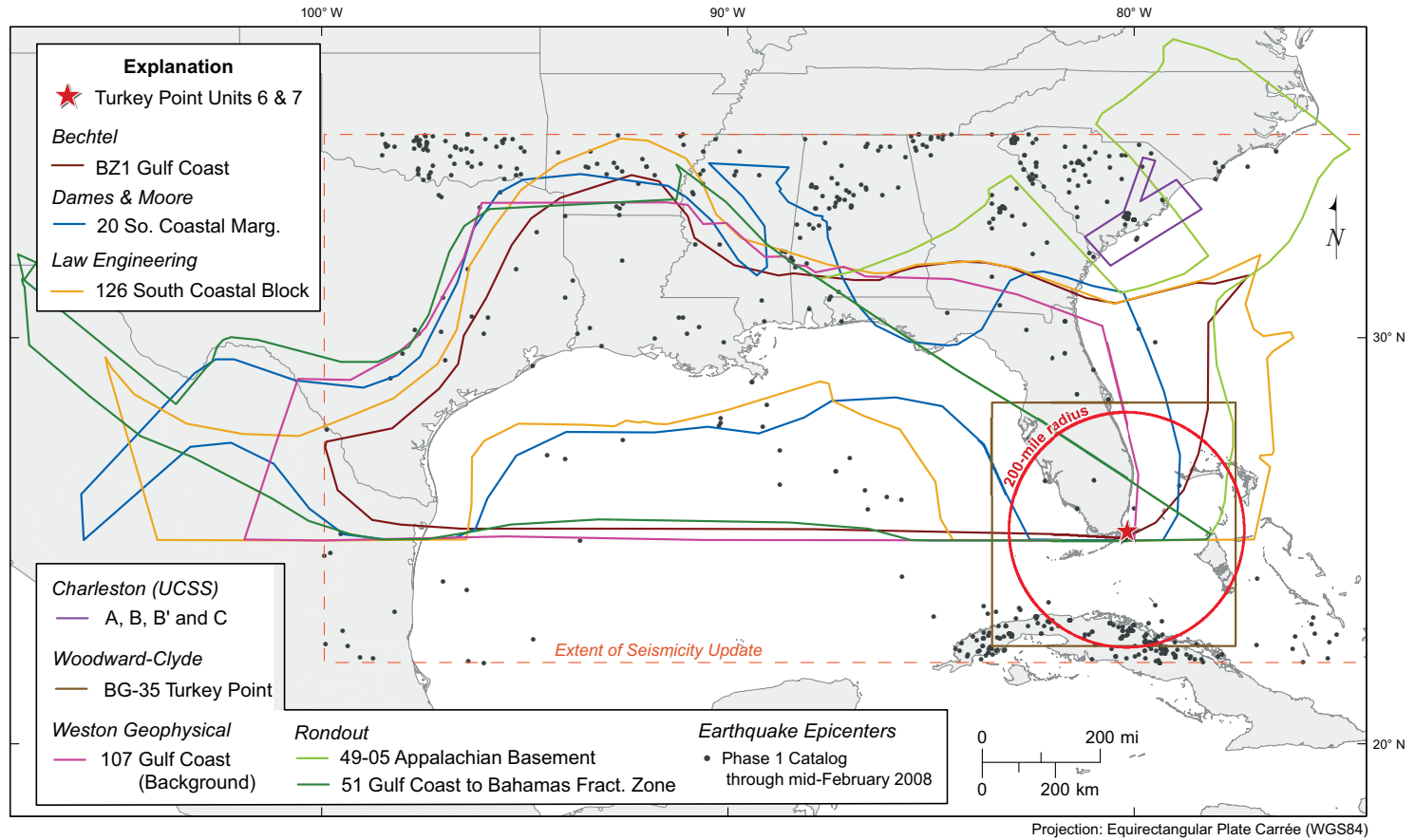
See Table 5-1 of EPRI (Reference 243) for EPRI Incompleteness Regions.

Numbers indicate the EPRI 1 degree x 1 degree regions of incompleteness along the southern border of 1989 EPRI-SOG coverage.

Turkey Point Units 6 & 7
 COL Application
 Part 2 — FSAR

PTN COL 2.5-2

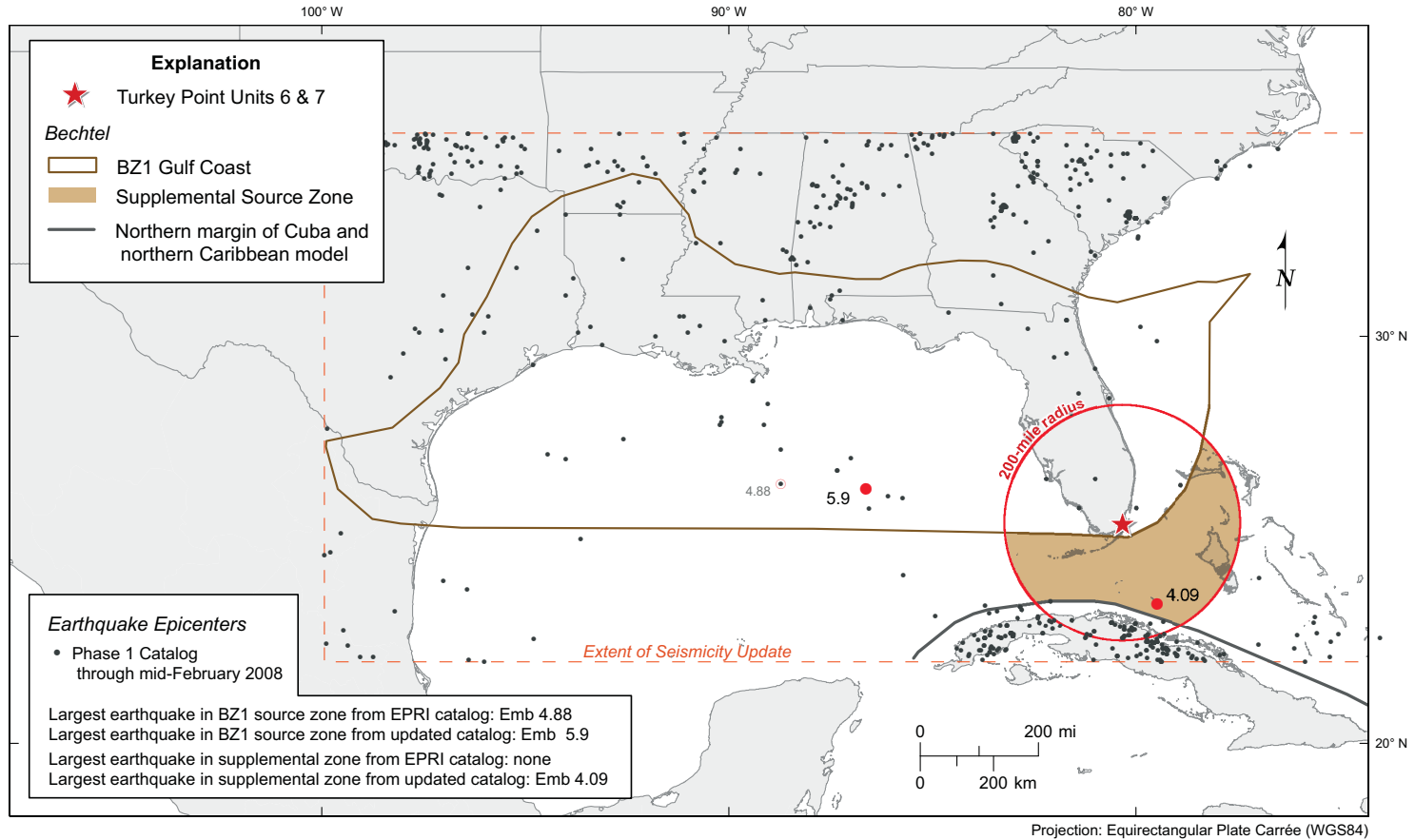
Figure 2.5.2-203 EPRI Seismic Source Zones and Updated Charleston Seismic Source (UCSS) Model Sources



Turkey Point Units 6 & 7
 COL Application
 Part 2 — FSAR

PTN COL 2.5-2

Figure 2.5.2-204 EPRI and Supplemental Source Zones — Bechtel

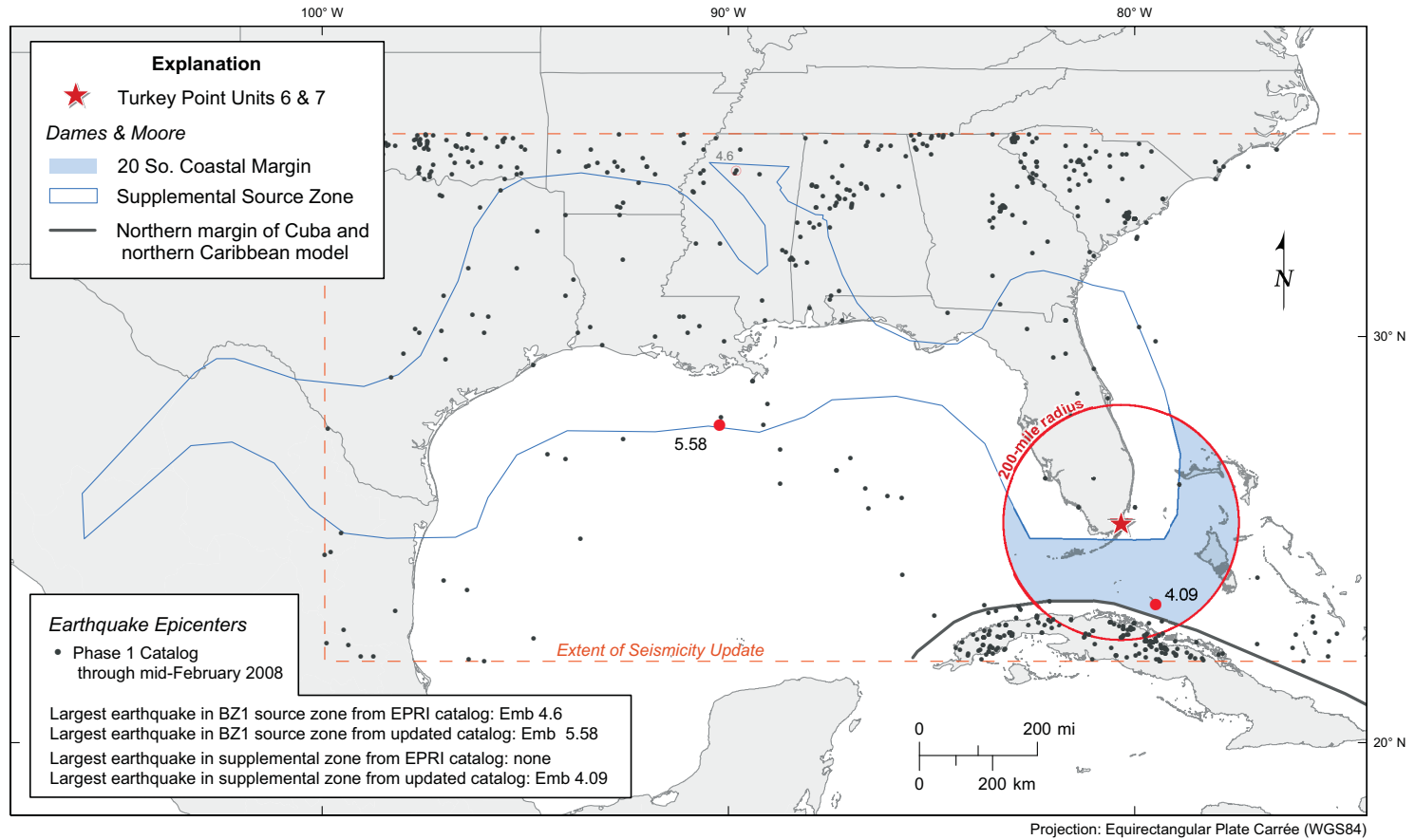


Note: Epicenters of the largest magnitude events in the seismic source zones are highlighted as red dots.

Turkey Point Units 6 & 7
COL Application
Part 2 — FSAR

PTN COL 2.5-2

Figure 2.5.2-205 EPRI and Supplemental Source Zones — Dames & Moore

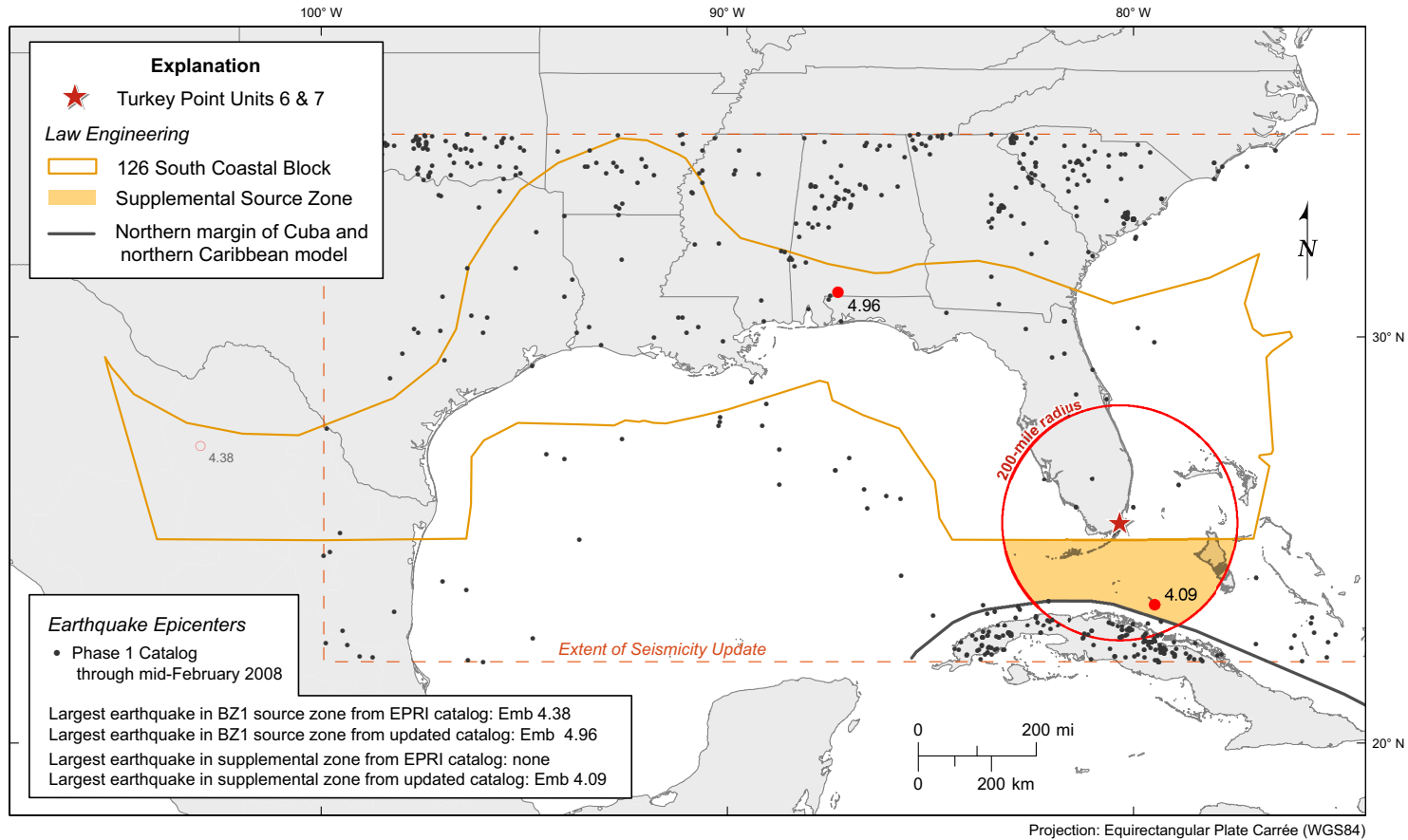


Note: Epicenters of the largest magnitude events in the seismic source zones are highlighted as red dots.

Turkey Point Units 6 & 7
 COL Application
 Part 2 — FSAR

PTN COL 2.5-2

Figure 2.5.2-206 EPRI and Supplemental Source Zones — Law Engineering

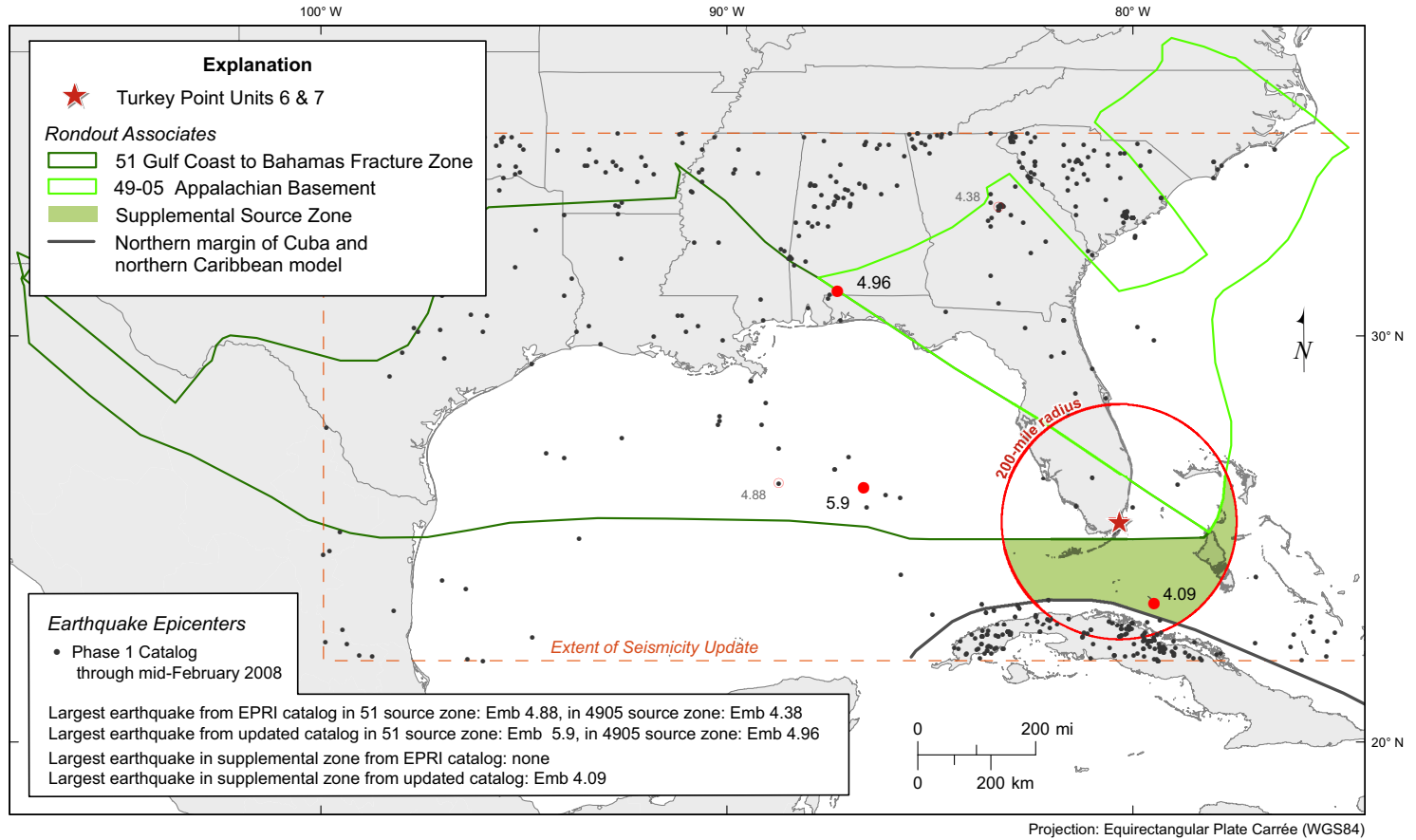


Note: Epicenters of the largest magnitude events in the seismic source zones are highlighted as red dots.

Turkey Point Units 6 & 7
COL Application
Part 2 — FSAR

PTN COL 2.5-2

Figure 2.5.2-207 EPRI and Supplemental Source Zones — Rondout Associates

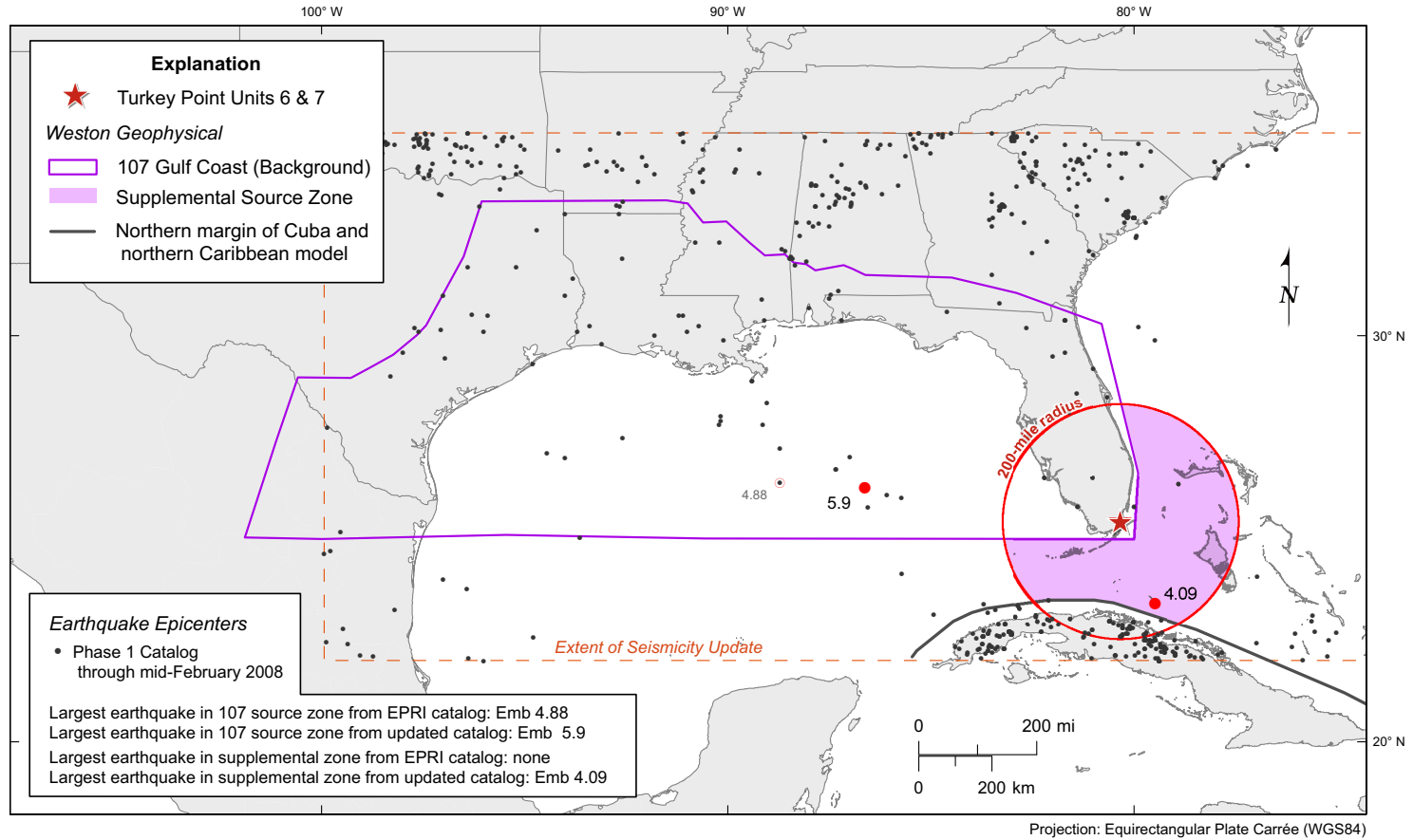


Note: Epicenters of the largest magnitude events in the seismic source zones are highlighted as red dots.

Turkey Point Units 6 & 7
COL Application
Part 2 — FSAR

PTN COL 2.5-2

Figure 2.5.2-208 EPRI and Supplemental Source Zones — Weston Geophysical

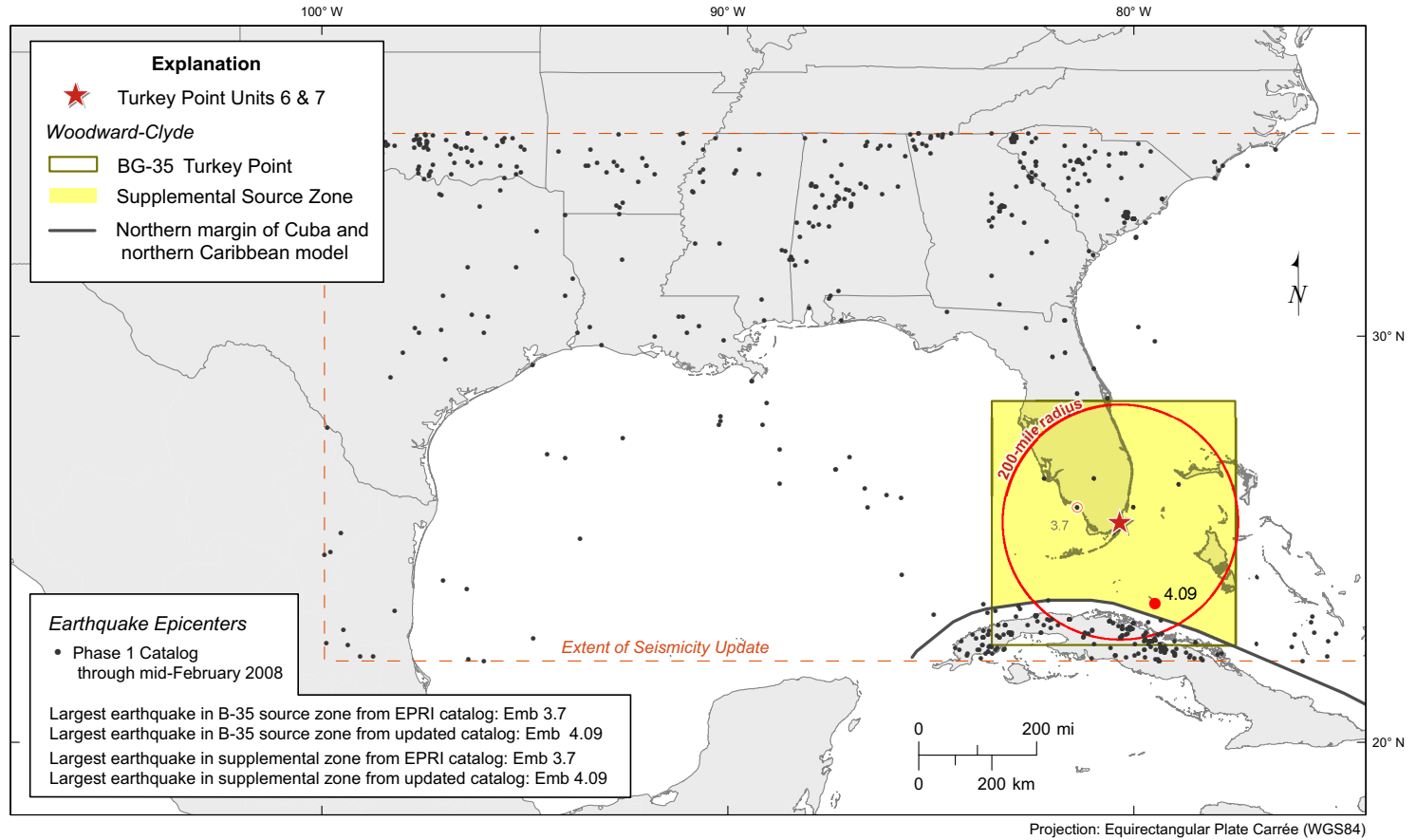


Note: Epicenters of the largest magnitude events in the seismic source zones are highlighted as red dots.

Turkey Point Units 6 & 7
COL Application
Part 2 — FSAR

PTN COL 2.5-2

Figure 2.5.2-209 EPRI and Supplemental Source Zones — Woodward-Clyde

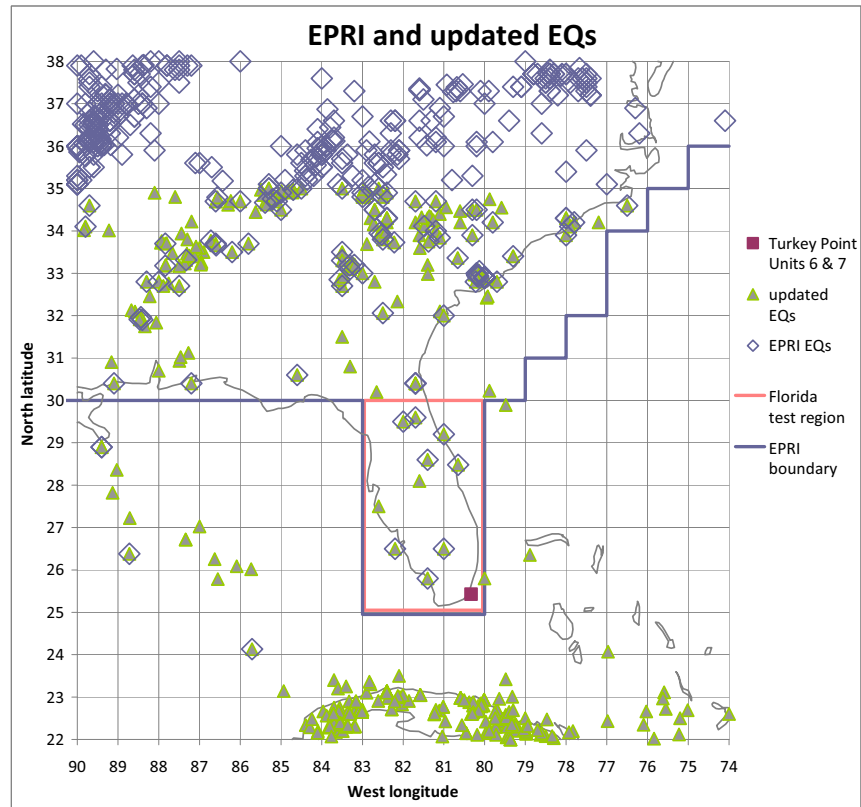


Note: Epicenters of the largest magnitude events in the seismic source zones are highlighted as red dots.

Turkey Point Units 6 & 7
COL Application
Part 2 — FSAR

PTN COL 2.5-2

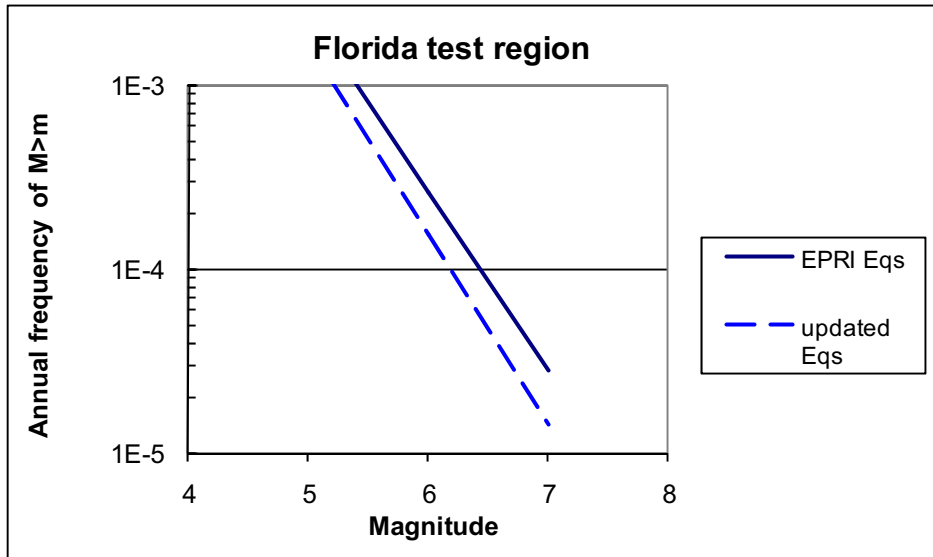
Figure 2.5.2-210 Historical Seismicity from EPRI Earthquake Catalog and from Updated Catalog (Through 2007) in Southeastern United States



Note: The boundary of the EPRI study region is shown in blue, and the Florida test region used to compare seismicity rates is shown in orange.

PTN COL 2.5-2

Figure 2.5.2-211 Earthquake Occurrence Rates for EPRI Catalog and for Updated Catalog Extended Through 2007 for Florida Test Region

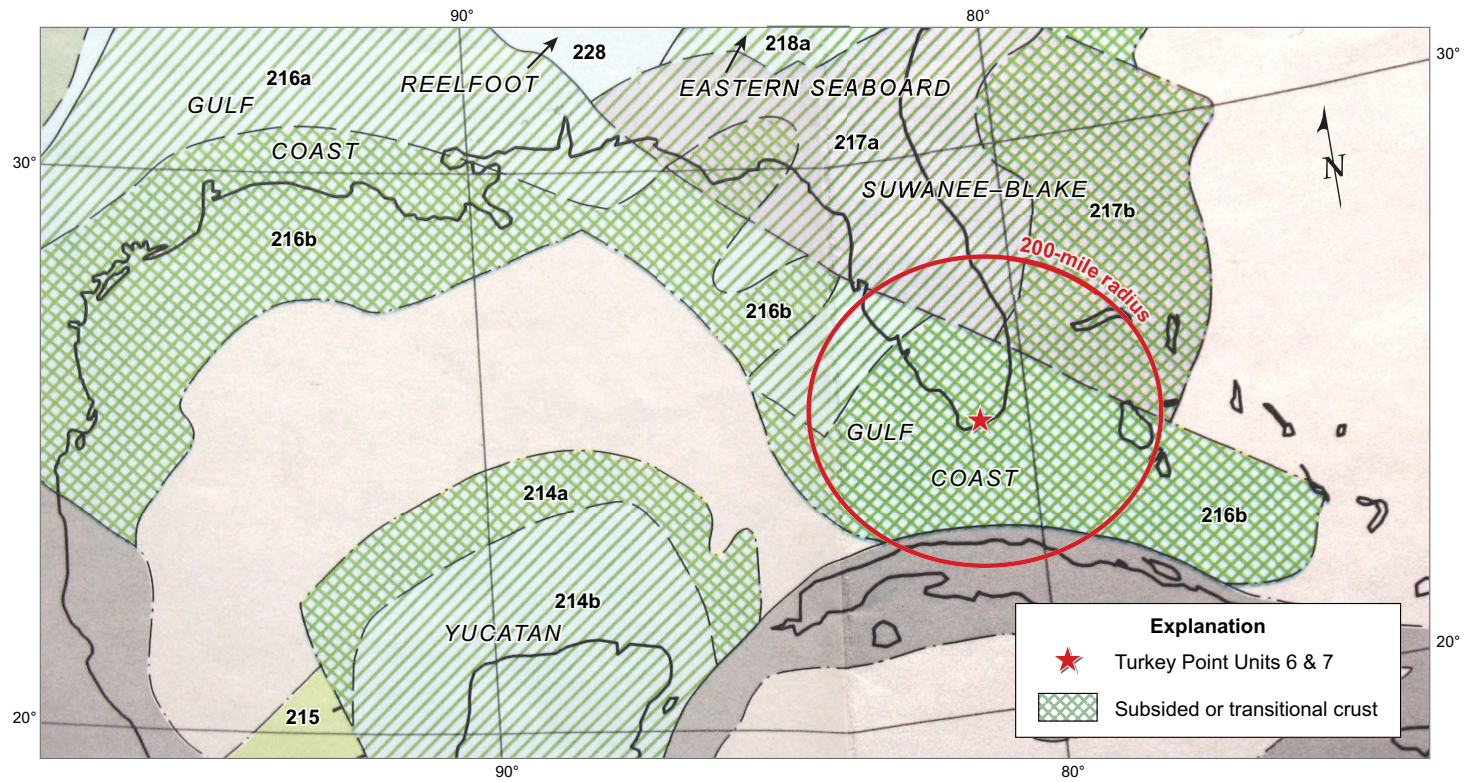


Sources: [References 245](#) and [246](#)

Turkey Point Units 6 & 7
COL Application
Part 2 — FSAR

PTN COL 2.5-2

Figure 2.5.2-212 Gulf Coast Crustal Divisions from Kanter

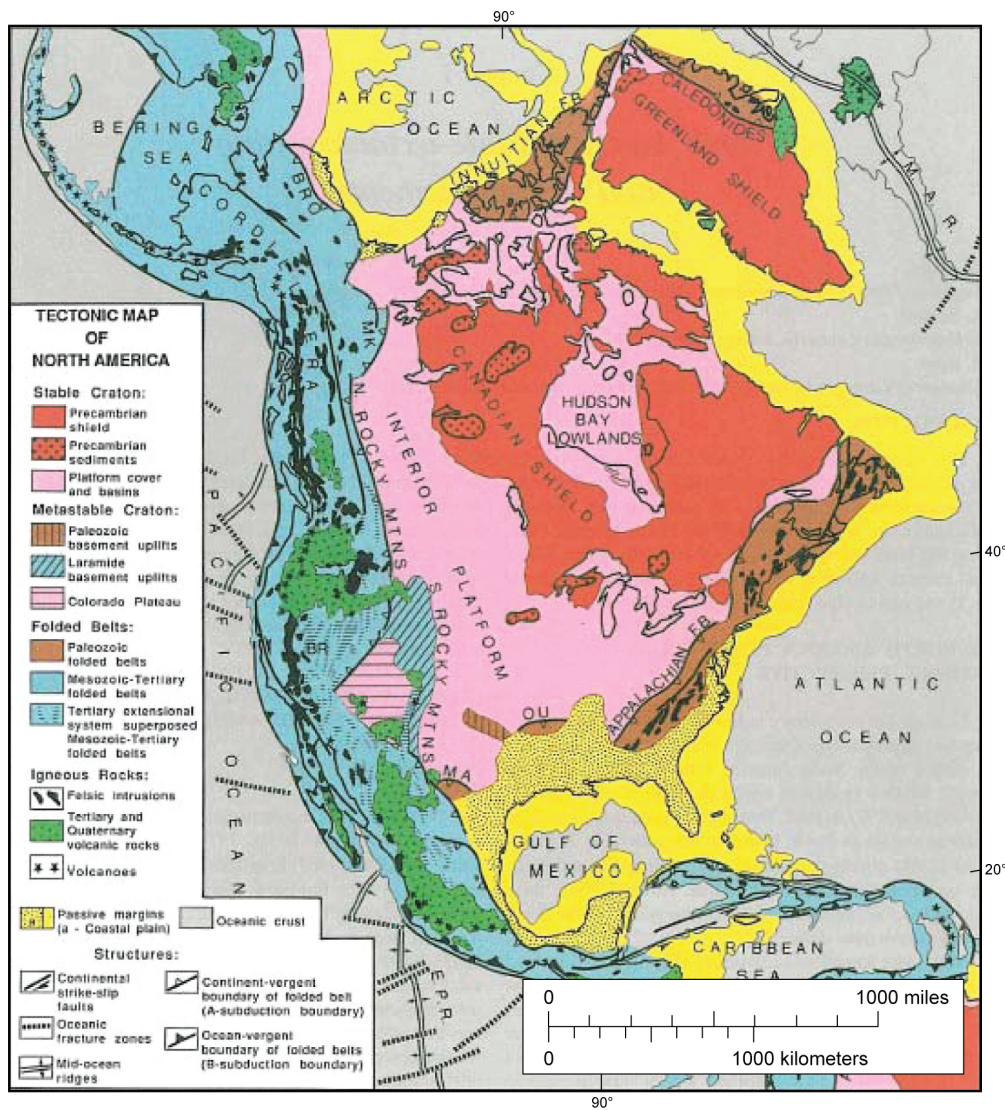


Source: Reference 270

Turkey Point Units 6 & 7
 COL Application
 Part 2 — FSAR

PTN COL 2.5-2

Figure 2.5.2-213 Passive Margin Basins on Continental and Transitional Crust from Bally et al.

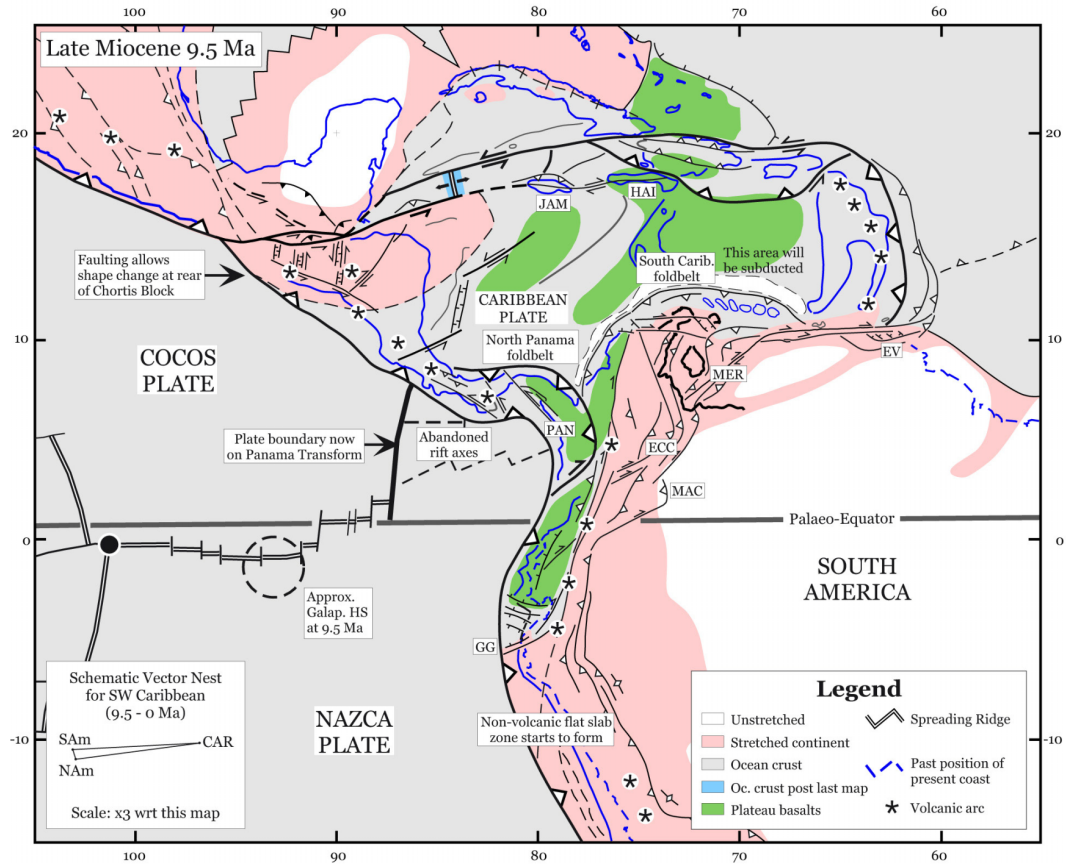


Source: Reference 239

Turkey Point Units 6 & 7
 COL Application
 Part 2 — FSAR

PTN COL 2.5-2

Figure 2.5.2-214 Plate Reconstruction Showing Stretched Continental Crust from Pindell and Kennan

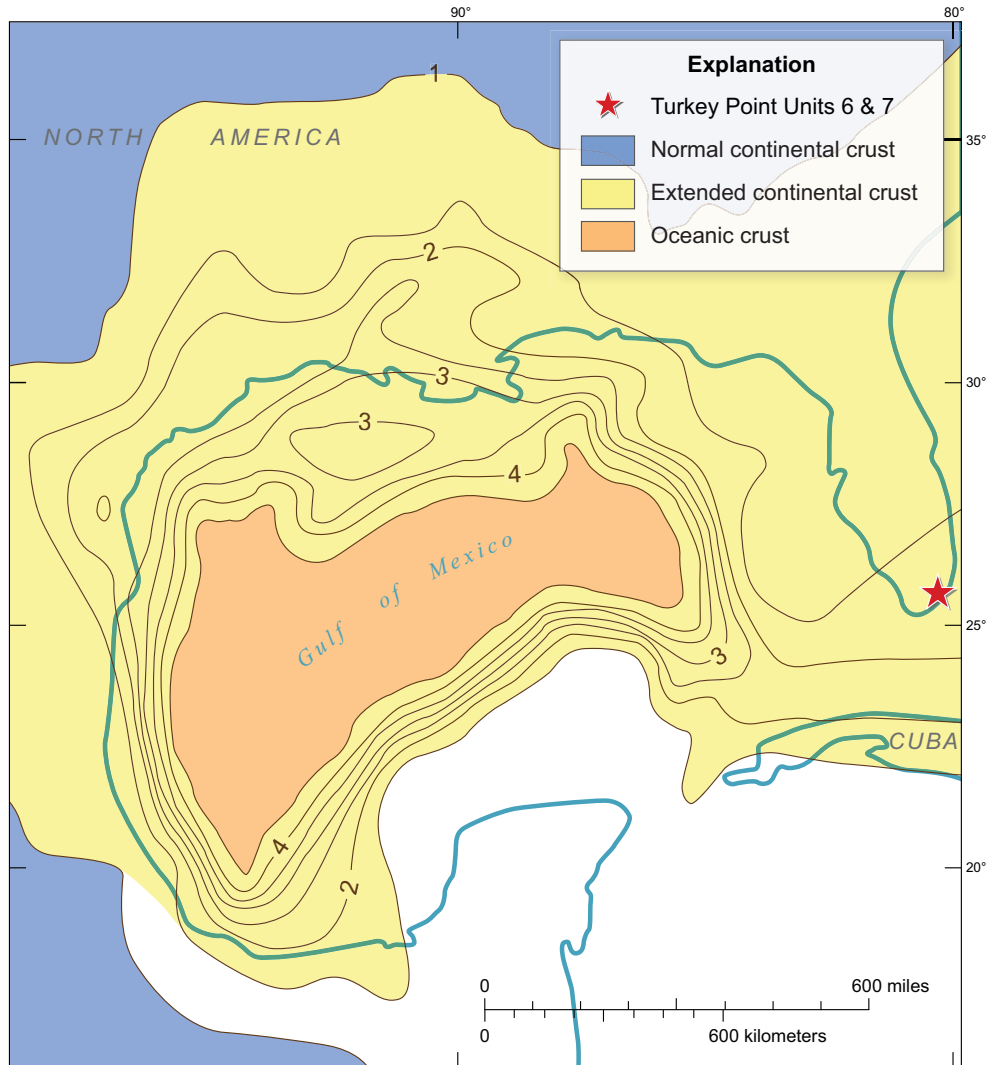


Source: Reference 302

Turkey Point Units 6 & 7
COL Application
Part 2 — FSAR

PTN COL 2.5-2

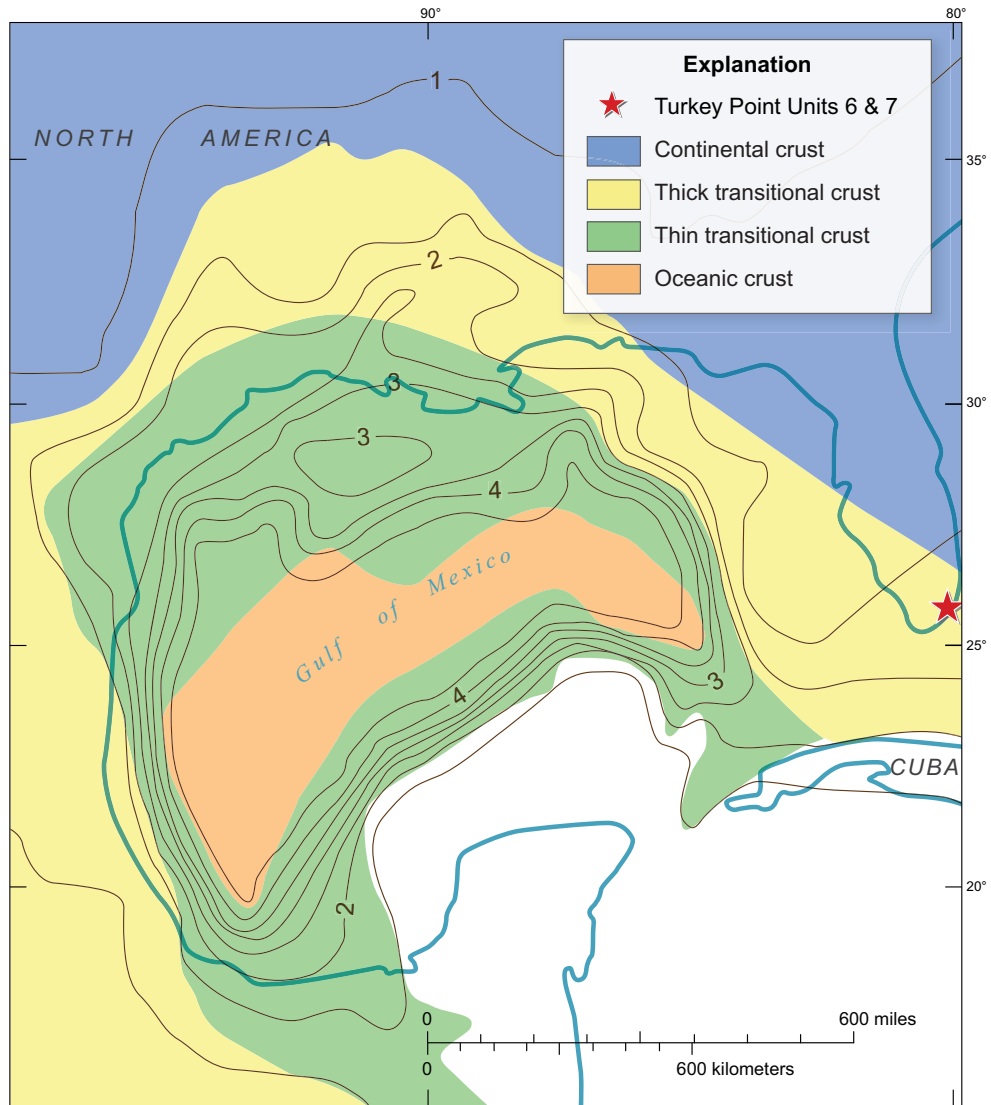
Figure 2.5.2-215 Extended Continental Crust from Dunbar and Sawyer



Source: Reference 239

PTN COL 2.5-2

Figure 2.5.2-216 Thick Transitional Crust from Sawyer et al.

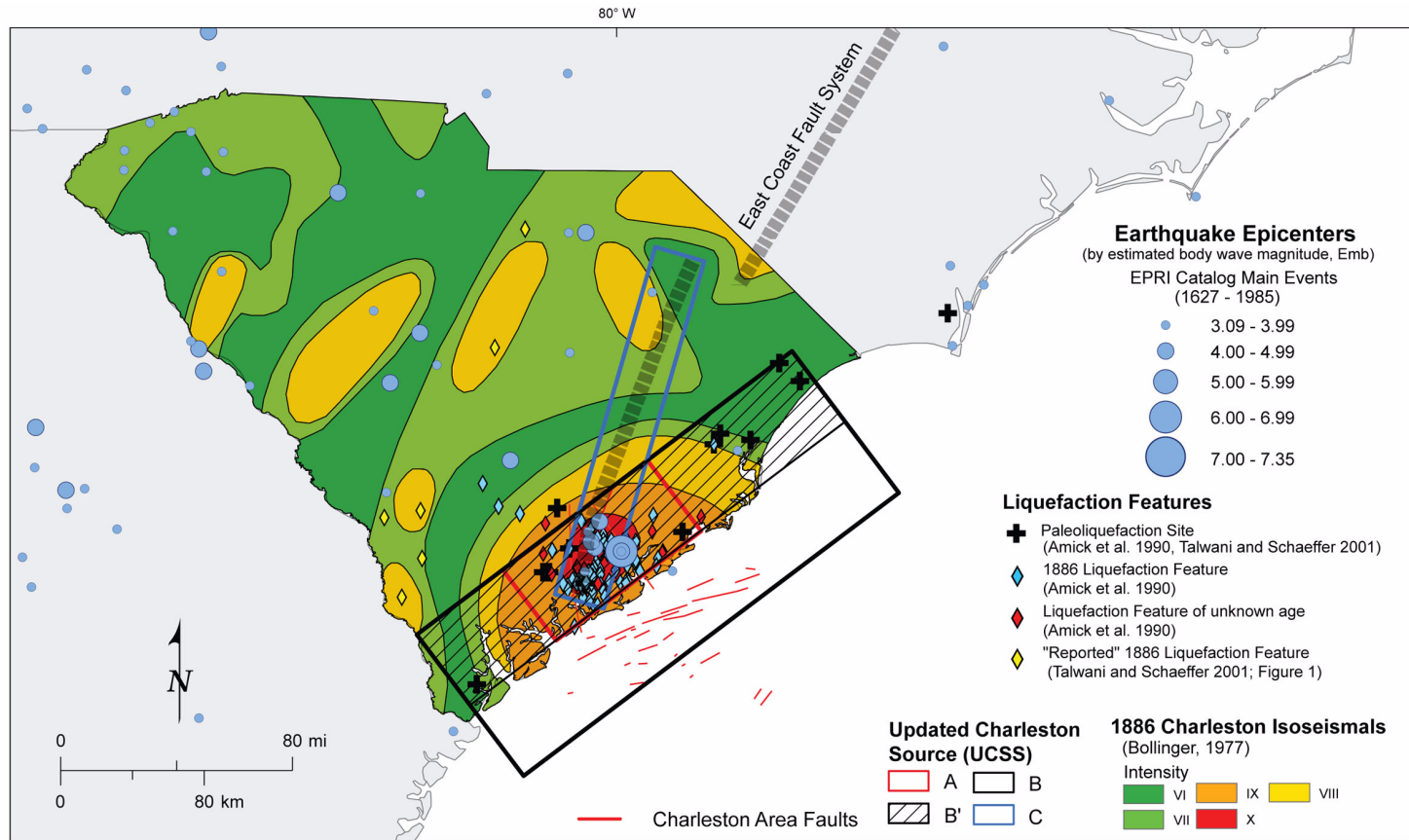


Source: Reference 315

Turkey Point Units 6 & 7
COL Application
Part 2 — FSAR

PTN COL 2.5-2

Figure 2.5.2-217 Updated Charleston Seismic Source (UCSS) Model Sources



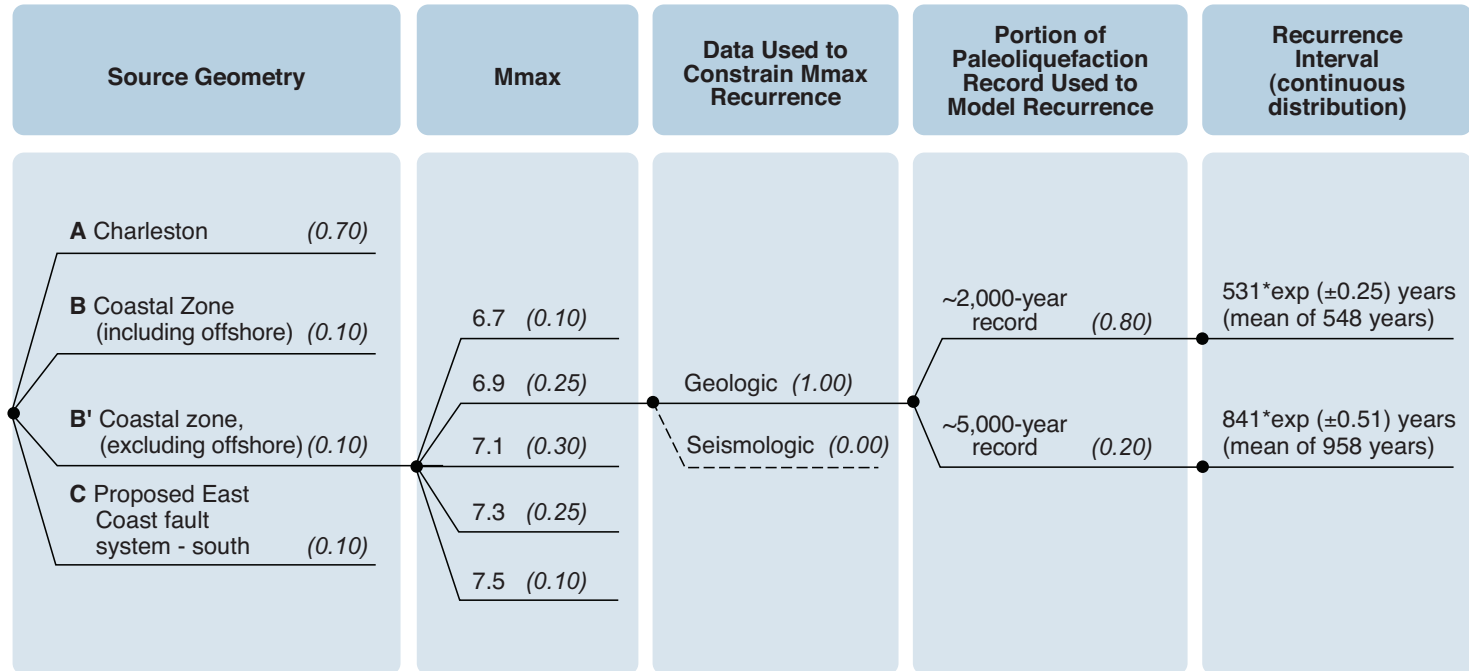
Sources of liquefaction features: [References 207, 208, and 323](#)

Source of the 1886 Charleston isoseismals: [Reference 216](#)

Turkey Point Units 6 & 7
COL Application
Part 2 — FSAR

PTN COL 2.5-2

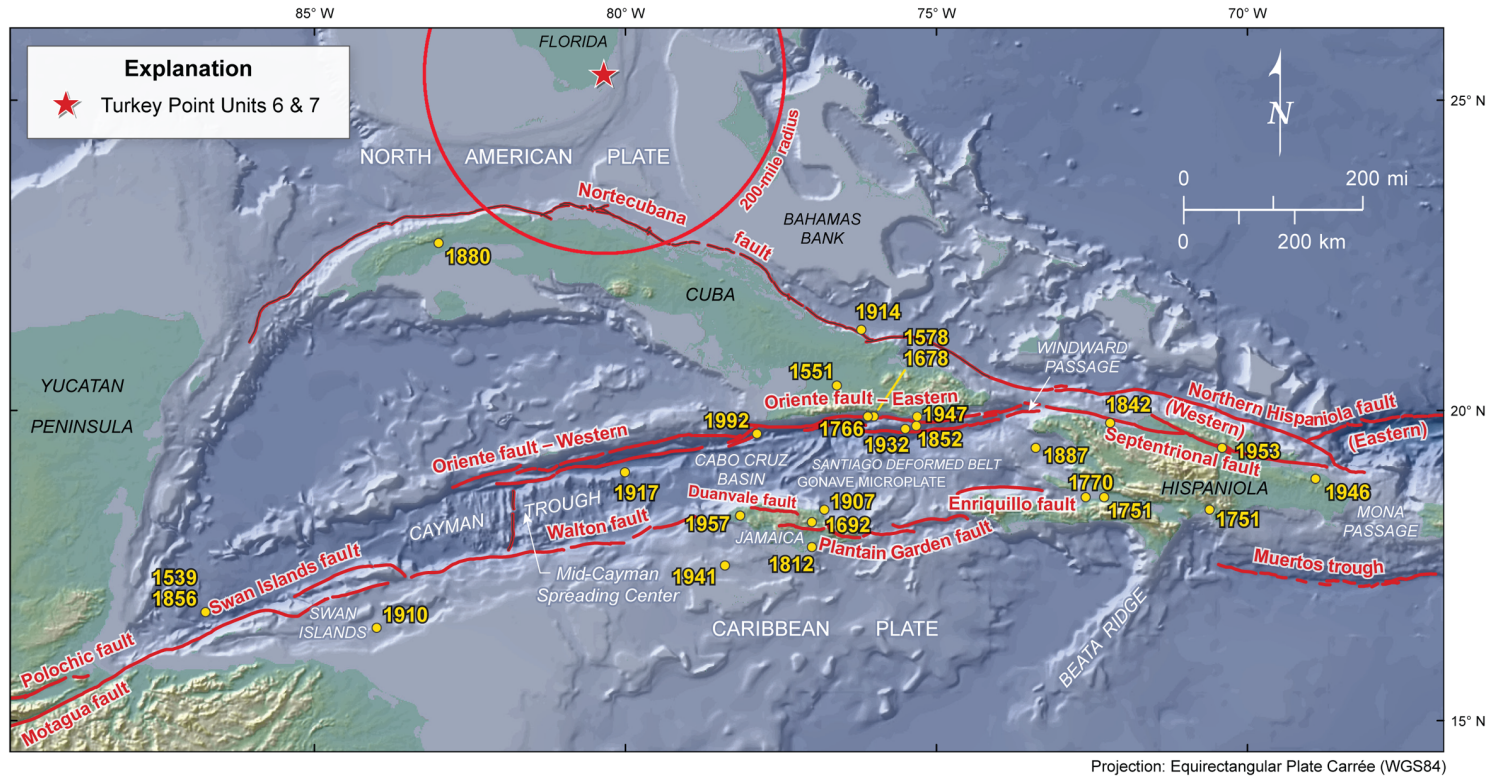
Figure 2.5.2-218 Updated Charleston Seismic Source (UCSS) Logic Tree with Weights for Each Branch



Turkey Point Units 6 & 7
 COL Application
 Part 2 — FSAR

PTN COL 2.5-2

Figure 2.5.2-219 Tectonic Features and Significant Earthquakes of Cuba and the Northern Caribbean



Turkey Point Units 6 & 7
COL Application
Part 2 — FSAR

PTN COL 2.5-2

Figure 2.5.2-220 Fault Map of Cuba from Garcia et al.

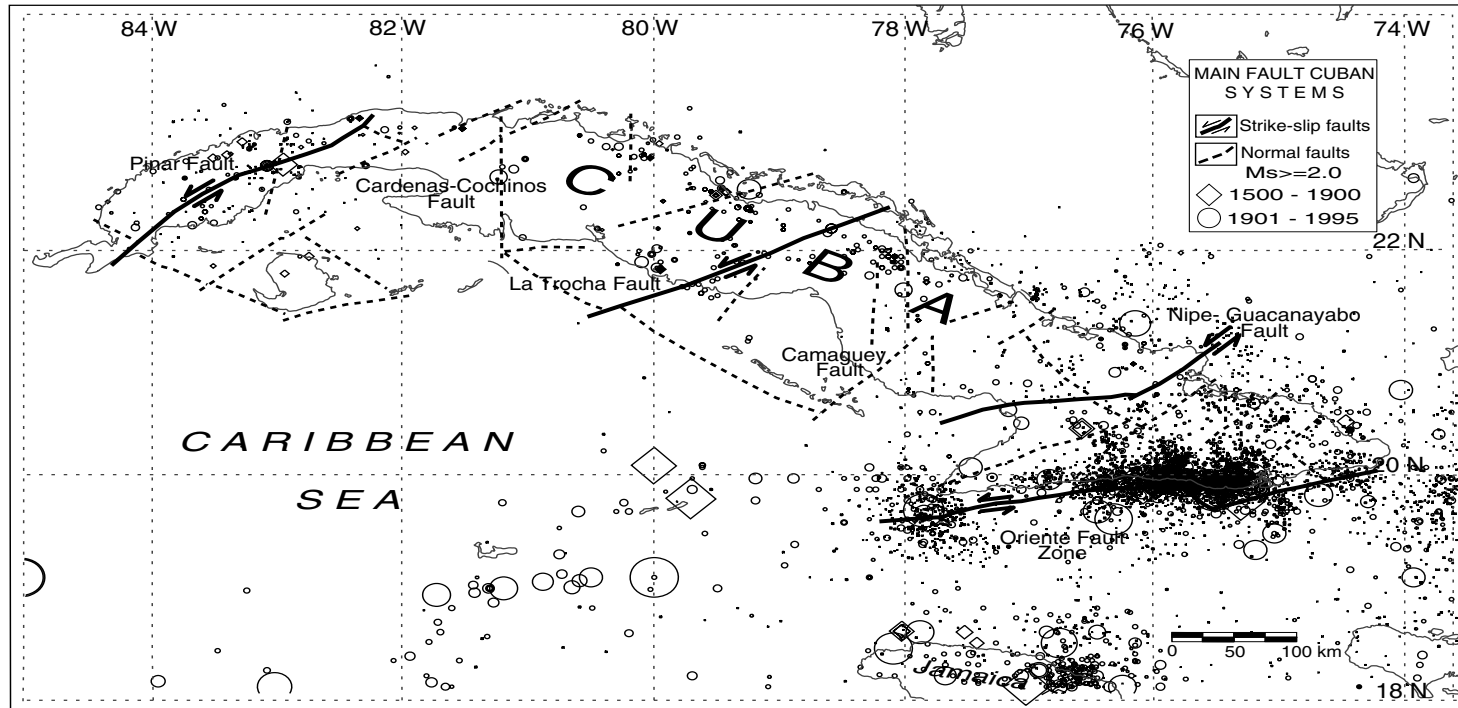


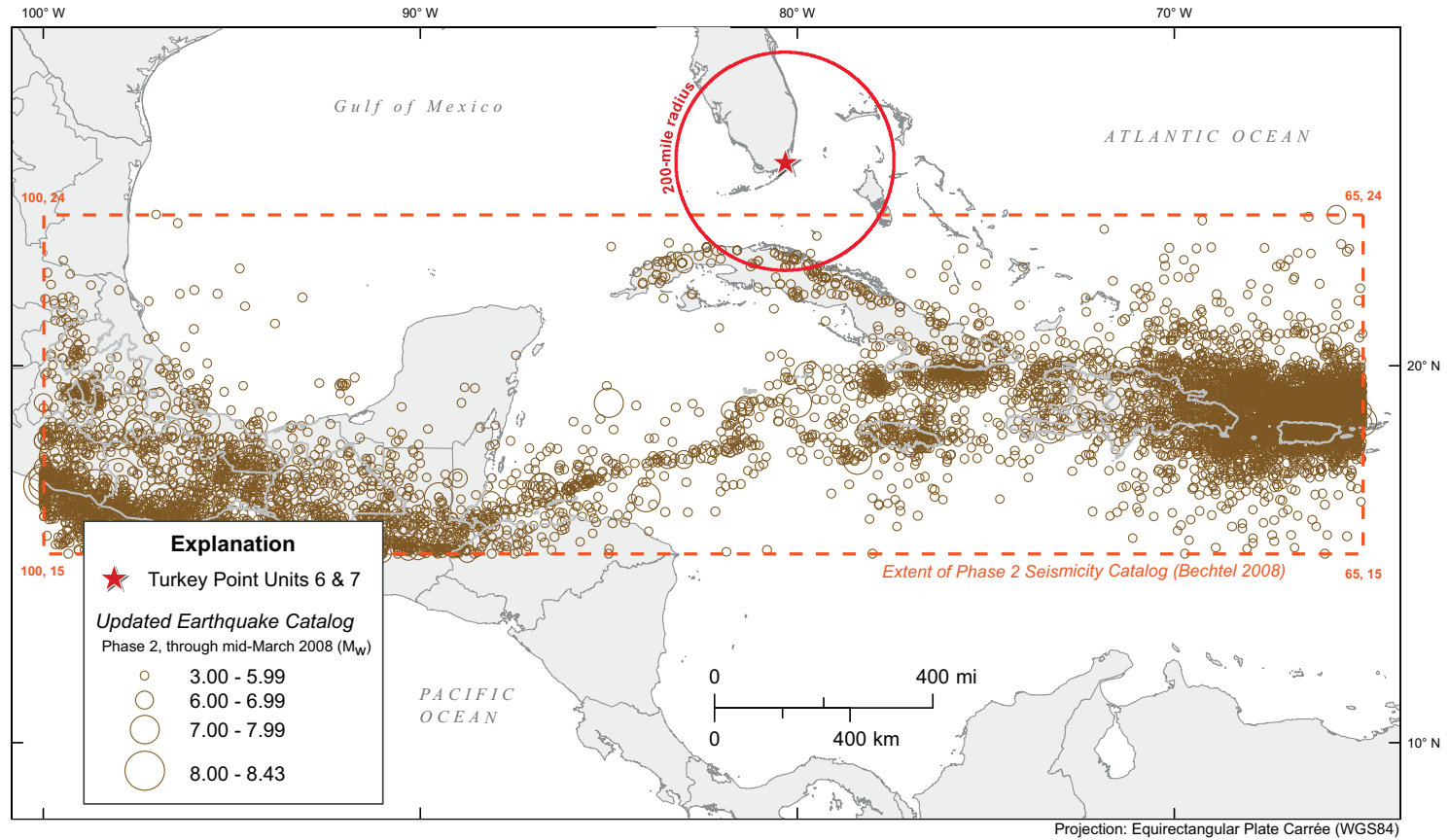
Figure 5. Map of the principal faults in Cuba (modified from Iturralde-Vinent, 1996). Solid lines show strike-slip faults; dashed lines represent normal faults. The epicenters of earthquakes (diamond, pre-1900; circles, during the twentieth century) with magnitude larger than, or equal to, 2 are reported.

Source: Reference 254

Turkey Point Units 6 & 7
COL Application
Part 2 — FSAR

PTN COL 2.5-2

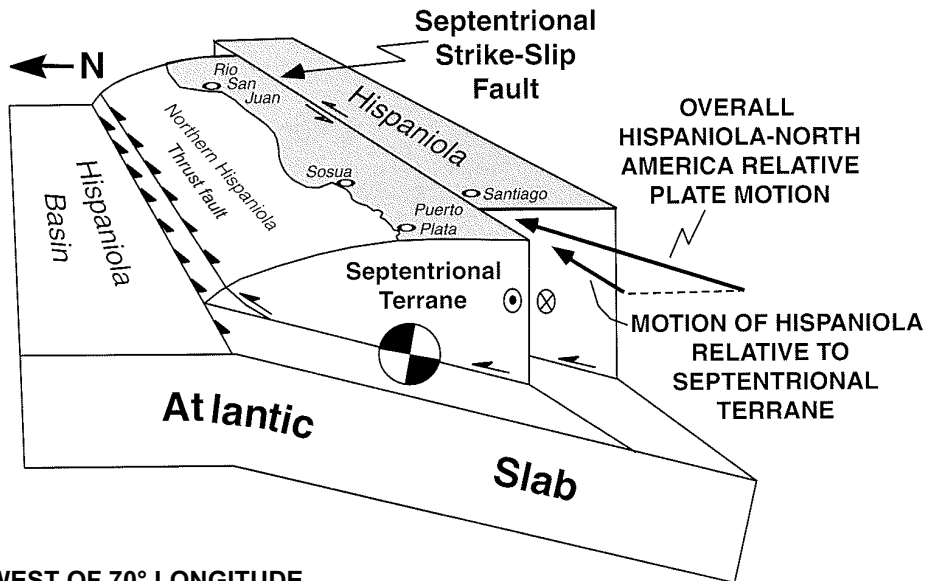
Figure 2.5.2-221 Seismicity in the Cuba and Northern Caribbean Region, 1500–2008



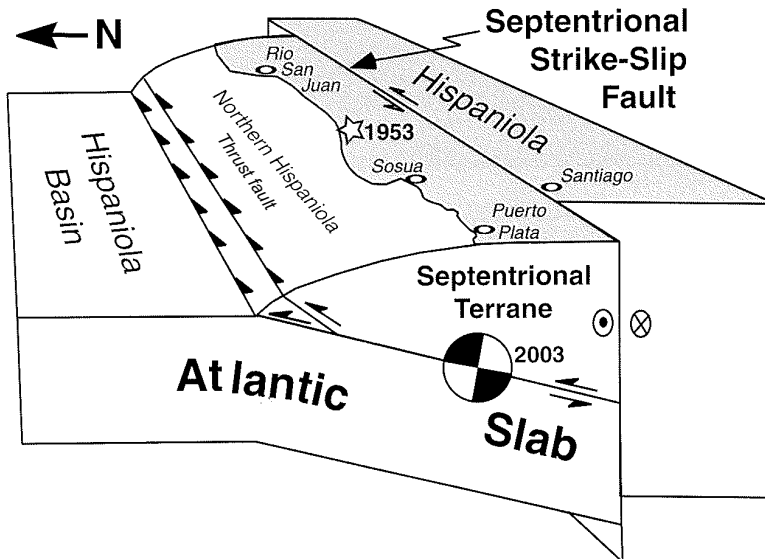
PTN COL 2.5-2

Figure 2.5.2-222 Kinematic Illustrations Showing Interactions of Septentrional and Northern Hispaniola Faults at Depth

(A) EAST OF 70° LONGITUDE



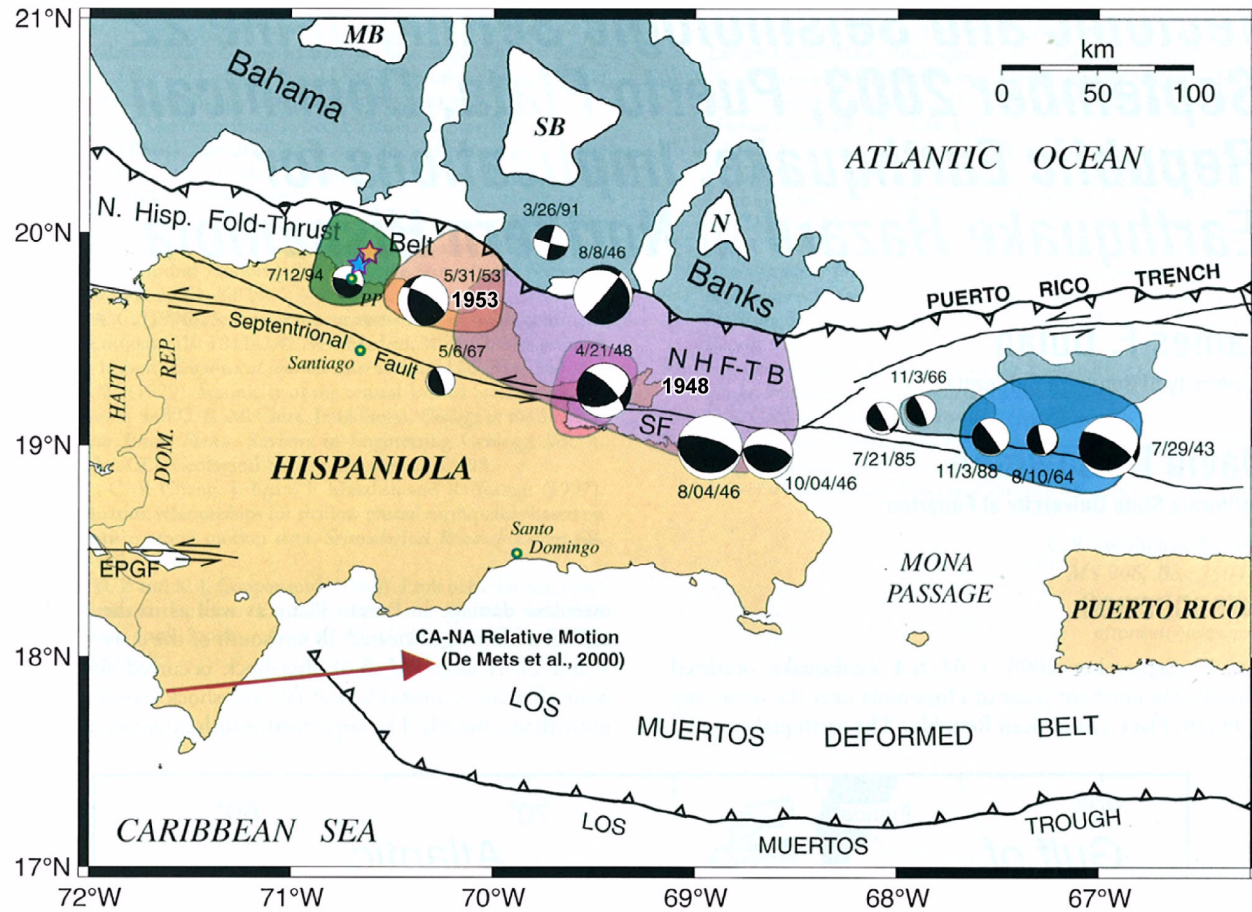
(B) WEST OF 70° LONGITUDE



Source: Reference 234

PTN COL 2.5-2

Figure 2.5.2-223 Selected Rupture Zones of Major Earthquakes on the Central North America-Caribbean Plate Boundary from Dolan and Bowman

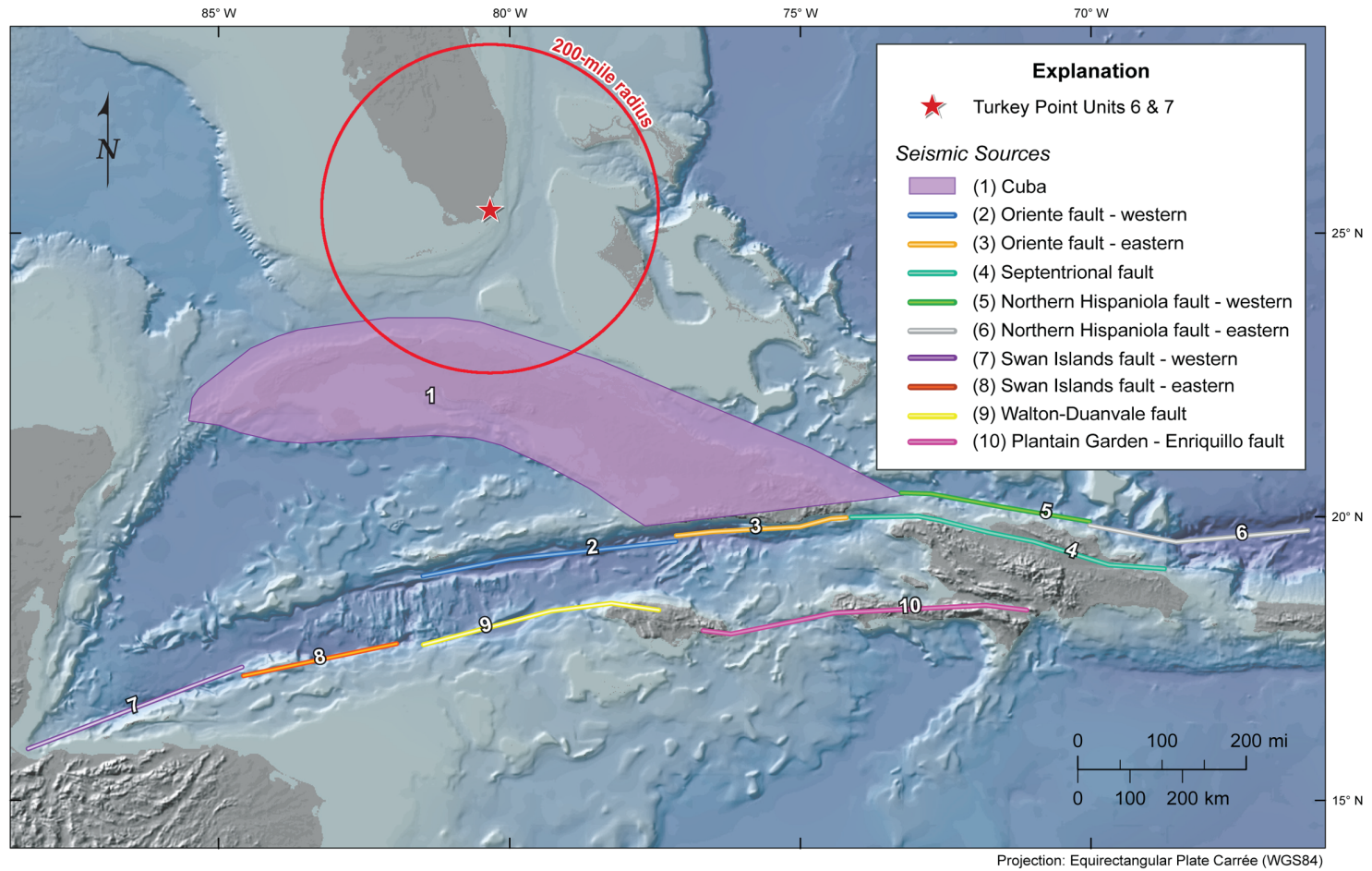


Source: Reference 234

Turkey Point Units 6 & 7
COL Application
Part 2 — FSAR

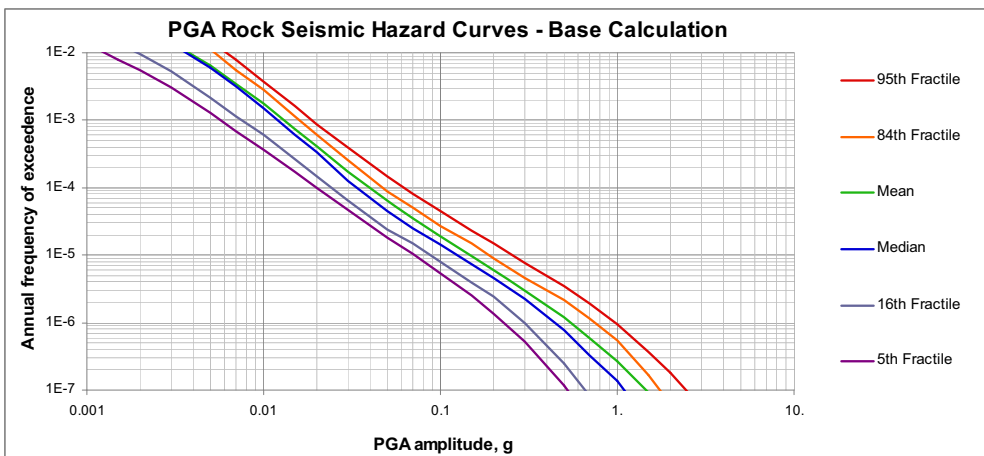
PTN COL 2.5-2

Figure 2.5.2-224 Cuba and Northern Caribbean Seismic Source Model Sources



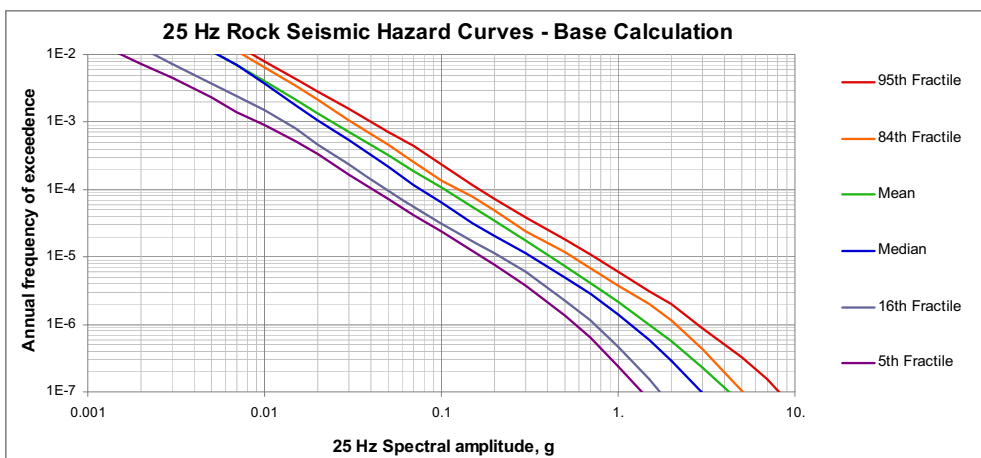
PTN COL 2.5-2

Figure 2.5.2-225 Mean and Fractile Rock PGA Seismic Hazard Curves



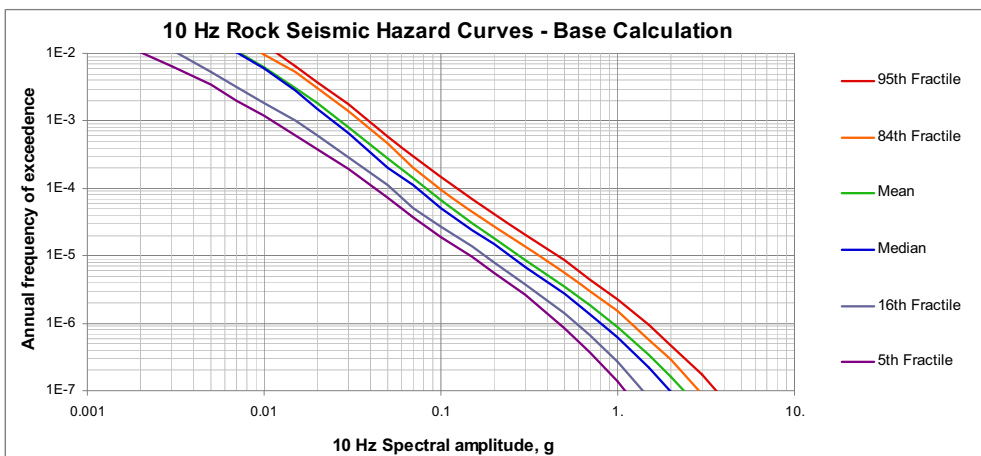
PTN COL 2.5-2

Figure 2.5.2-226 Mean and Fractile Rock 25 Hz Seismic Hazard Curves, Rock



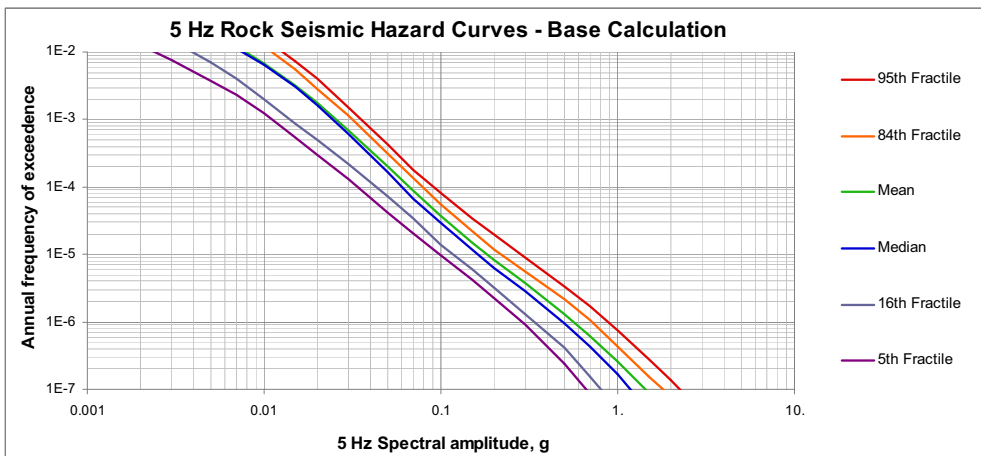
PTN COL 2.5-2

Figure 2.5.2-227 Mean and Fractile Rock 10 Hz Seismic Hazard Curves, Rock



PTN COL 2.5-2

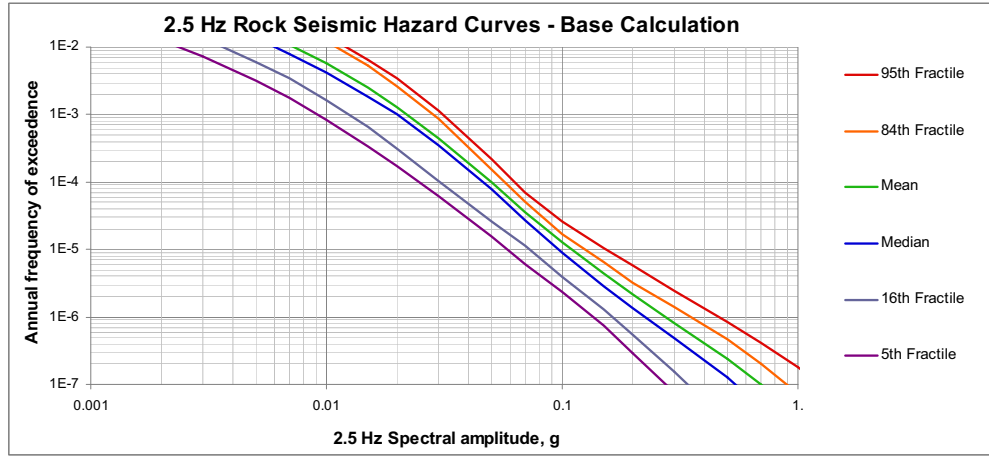
Figure 2.5.2-228 Mean and Fractile Rock 5 Hz Seismic Hazard Curves, Rock



Turkey Point Units 6 & 7
COL Application
Part 2 — FSAR

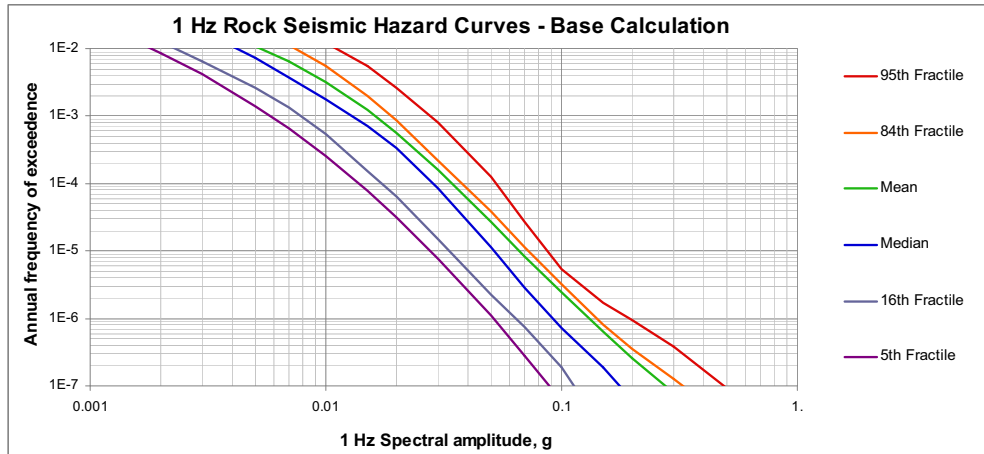
PTN COL 2.5-2

Figure 2.5.2-229 Mean and Fractile Rock 2.5 Hz Seismic Hazard Curves, Rock



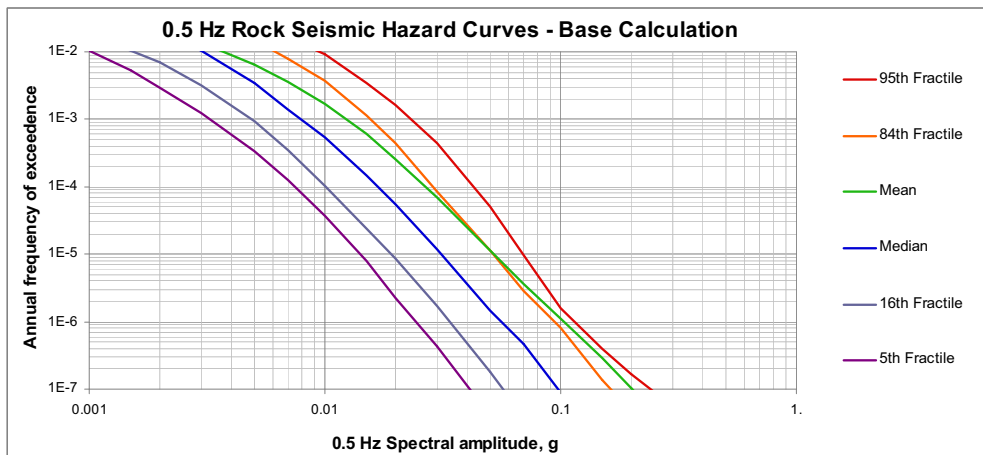
PTN COL 2.5-2

Figure 2.5.2-230 Mean and Fractile Rock 1 Hz Seismic Hazard Curves, Rock



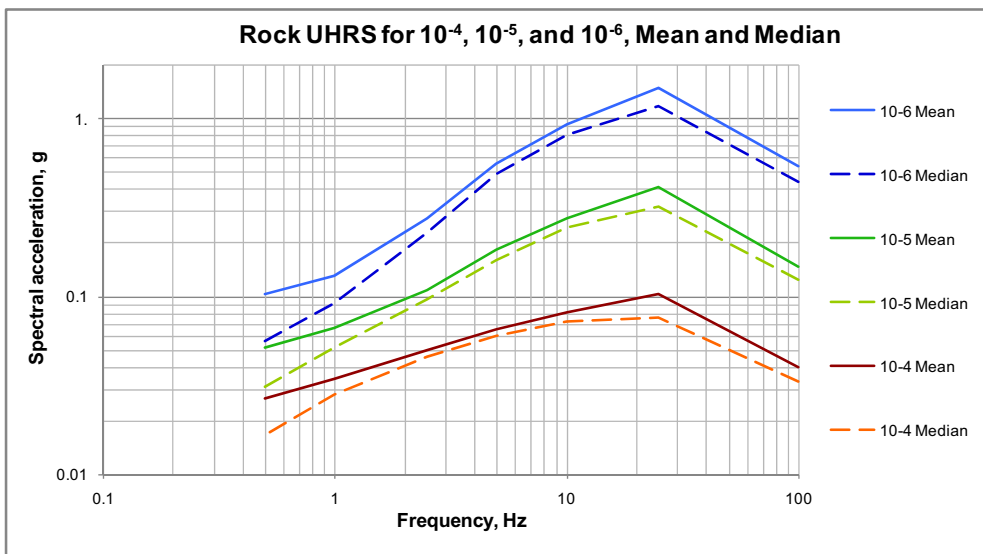
PTN COL 2.5-2

Figure 2.5.2-231 Mean and Fractile Rock 0.5 Hz Seismic Hazard Curves, Rock



PTN COL 2.5-2

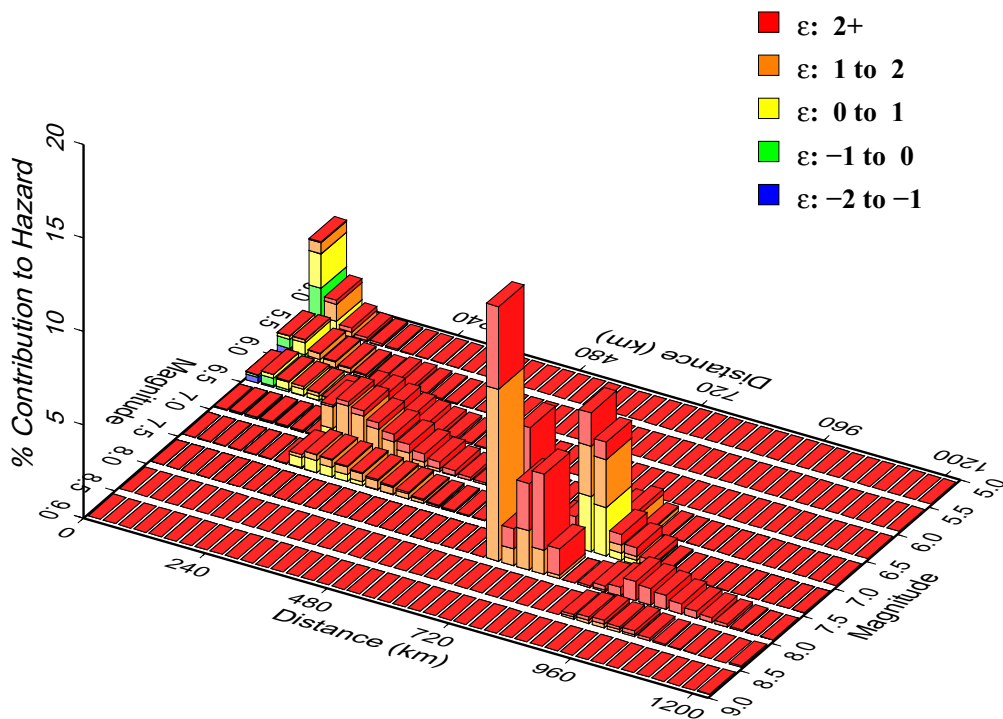
Figure 2.5.2-232 Mean and Median Rock UHRS for 1E-04, 1E-05, and 1E-06



PTN COL 2.5-2

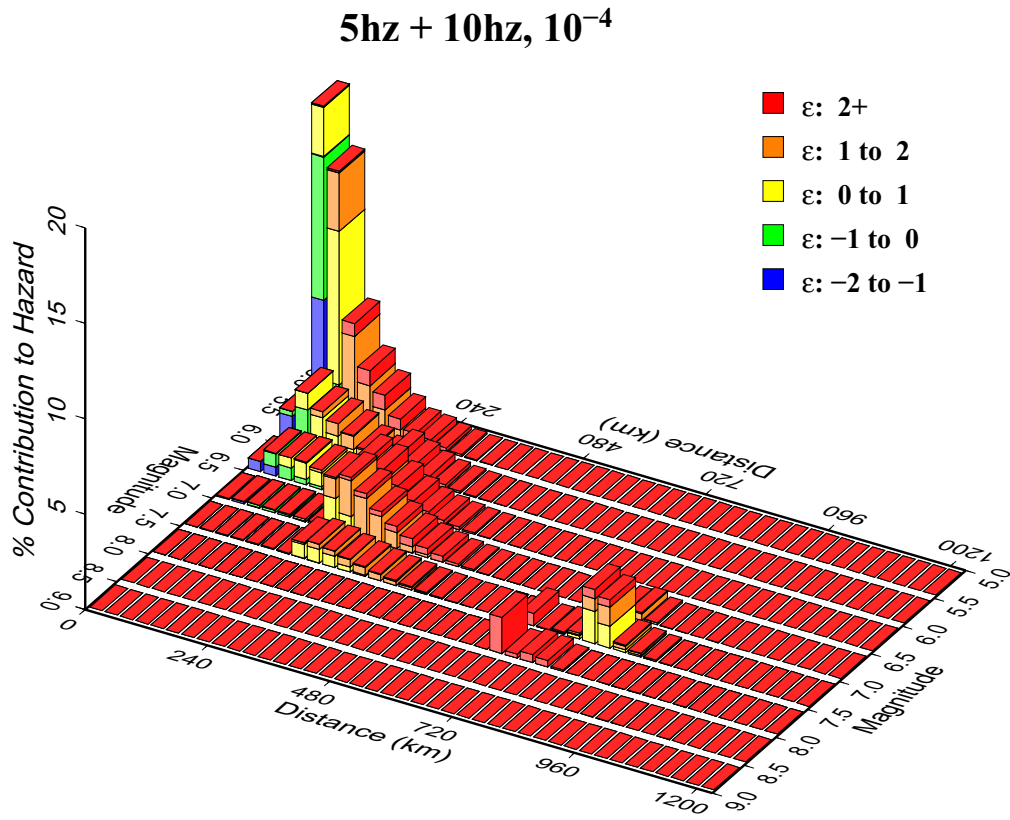
Figure 2.5.2-233 M and R Deaggregation for 1 and 2.5 Hz at 1E-04 Annual Frequency of Exceedence

1hz + 2p5hz, 10⁻⁴



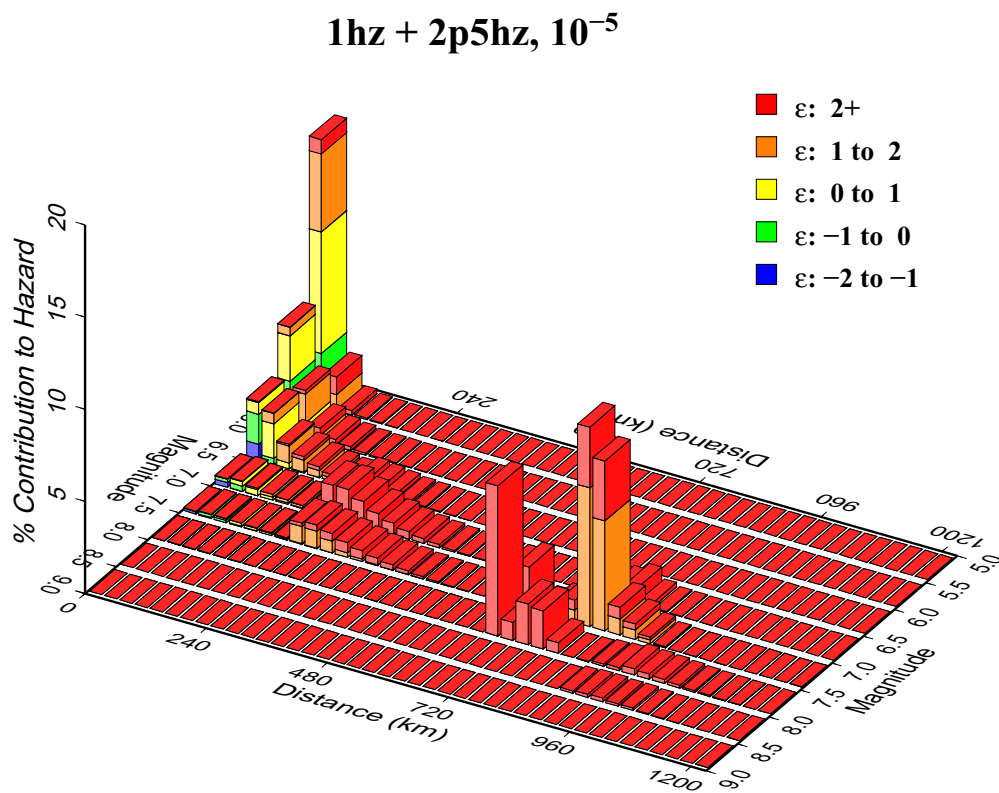
PTN COL 2.5-2

Figure 2.5.2-234 M and R Deaggregation for 5 and 10 Hz at 1E-04 Annual Frequency of Exceedence



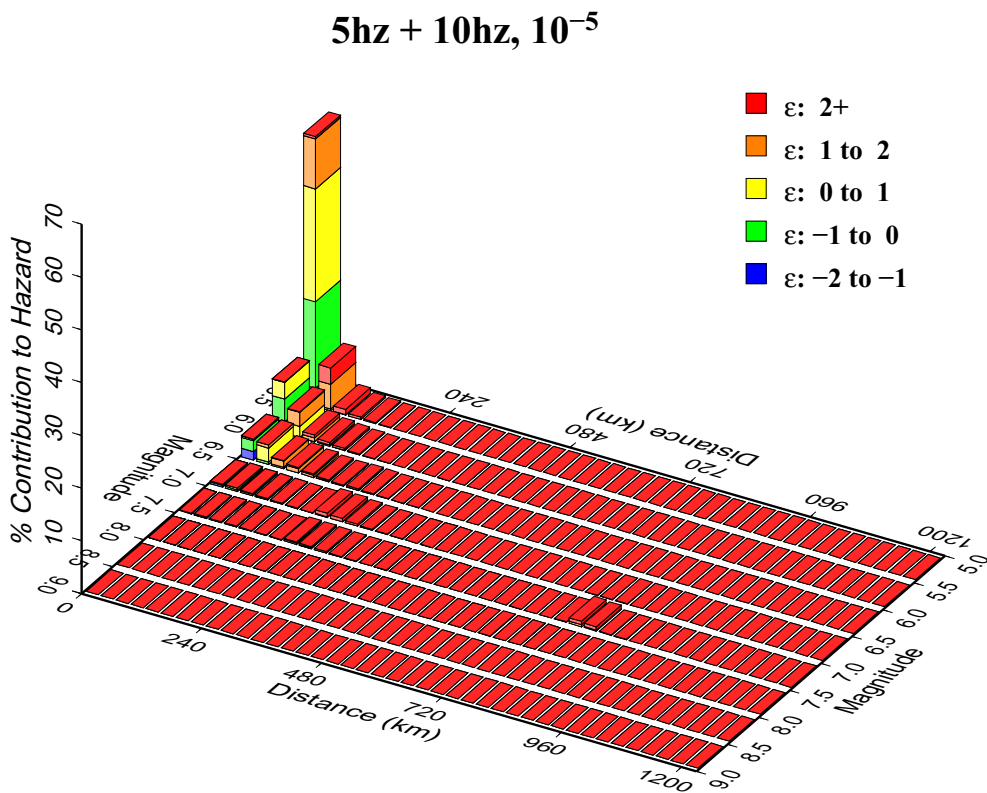
PTN COL 2.5-2

Figure 2.5.2-235 M and R Deaggregation for 1 and 2.5 Hz at 1E-05 Annual Frequency of Exceedence



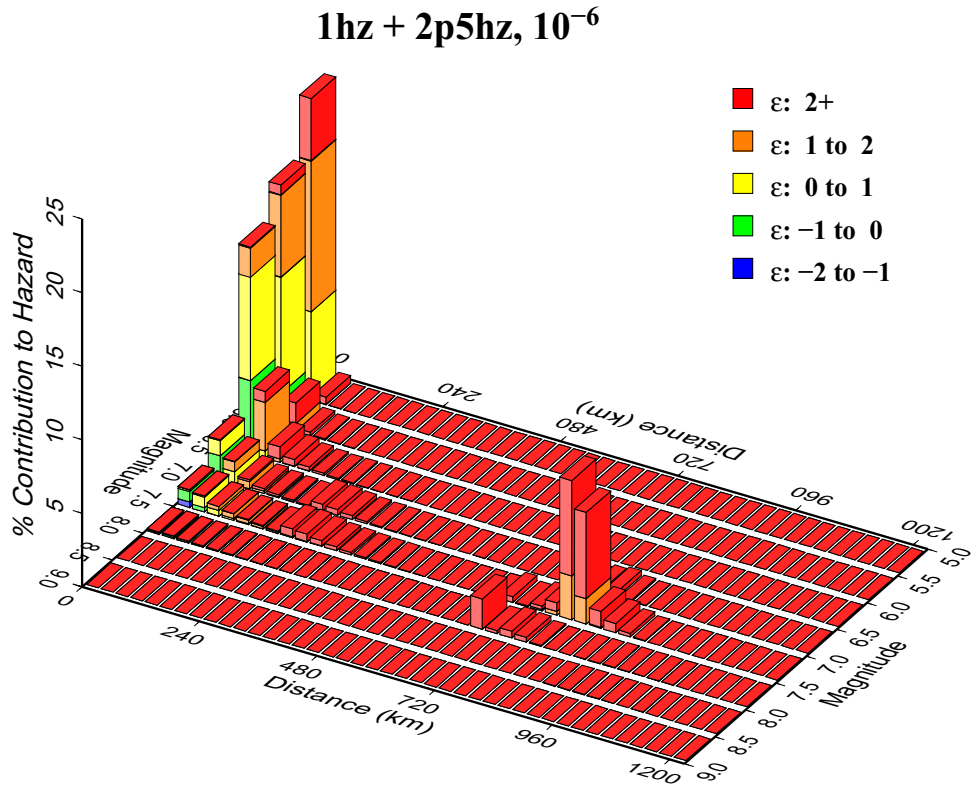
PTN COL 2.5-2

Figure 2.5.2-236 M and R Deaggregation for 5 and 10 Hz at 1E-05 Annual Frequency of Exceedence



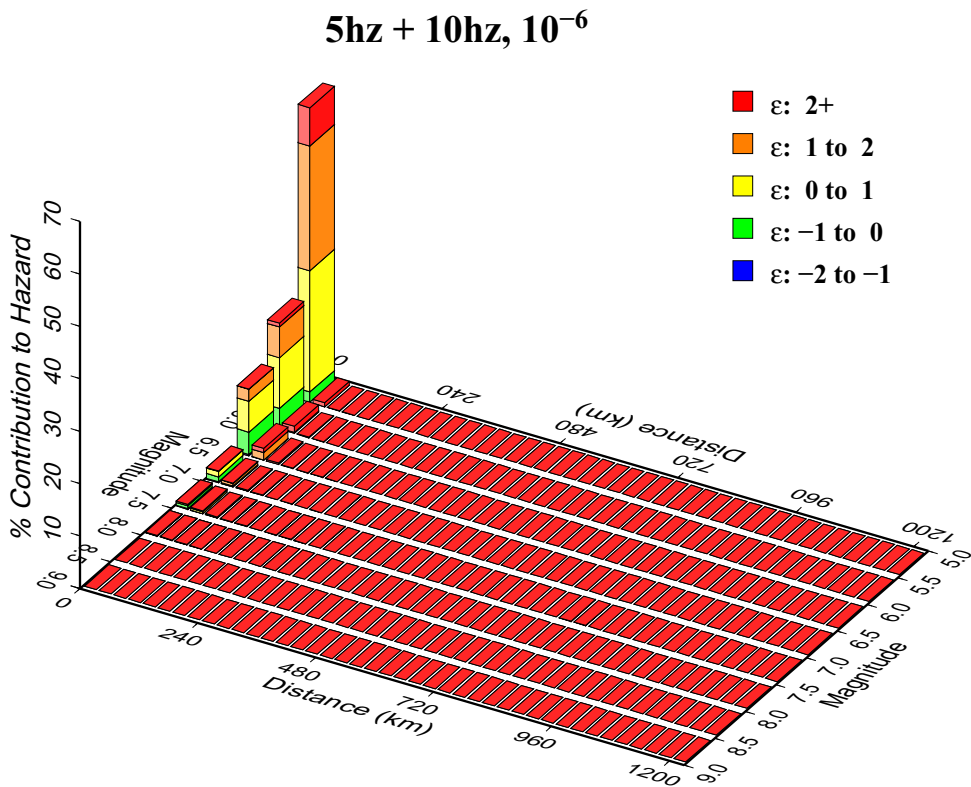
PTN COL 2.5-2

Figure 2.5.2-237 M and R Deaggregation for 1 and 2.5 Hz at 1E-06 Annual Frequency of Exceedence



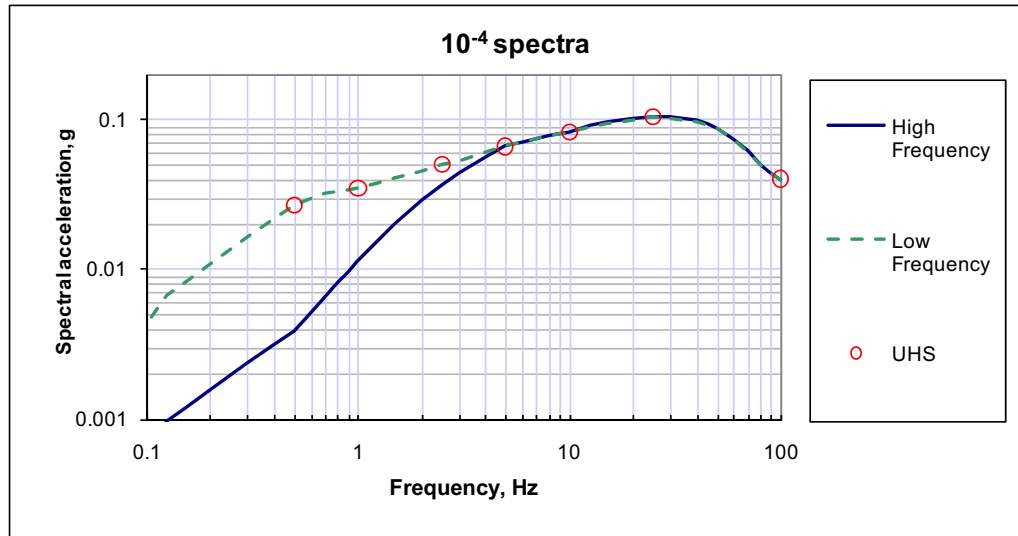
PTN COL 2.5-2

Figure 2.5.2-238 M and R Deaggregation for 5 and 10 Hz at 1E-06 Annual Frequency of Exceedence



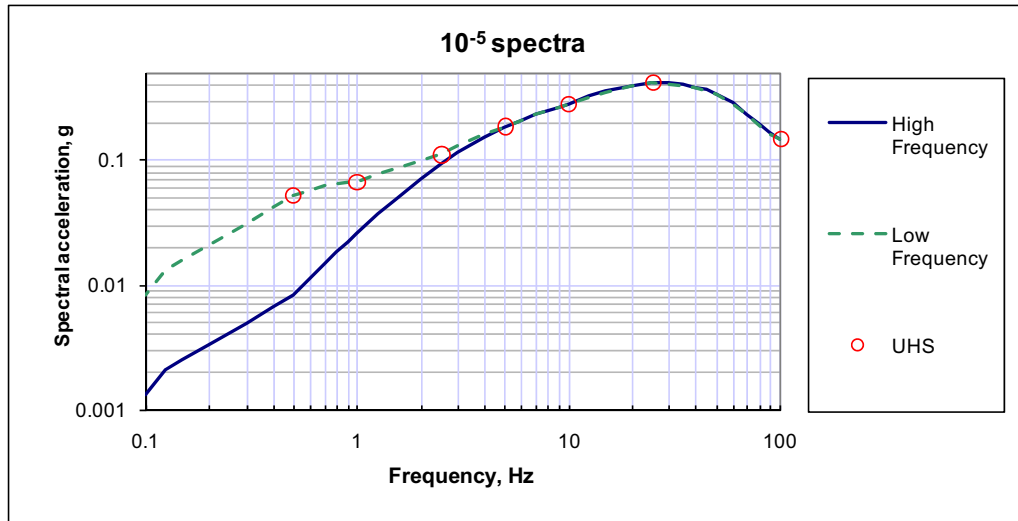
PTN COL 2.5-2

Figure 2.5.2-239 HF and LF Rock Spectra Anchored to Mean UHS Values from Hazard Calculation for 1E-04 Spectra



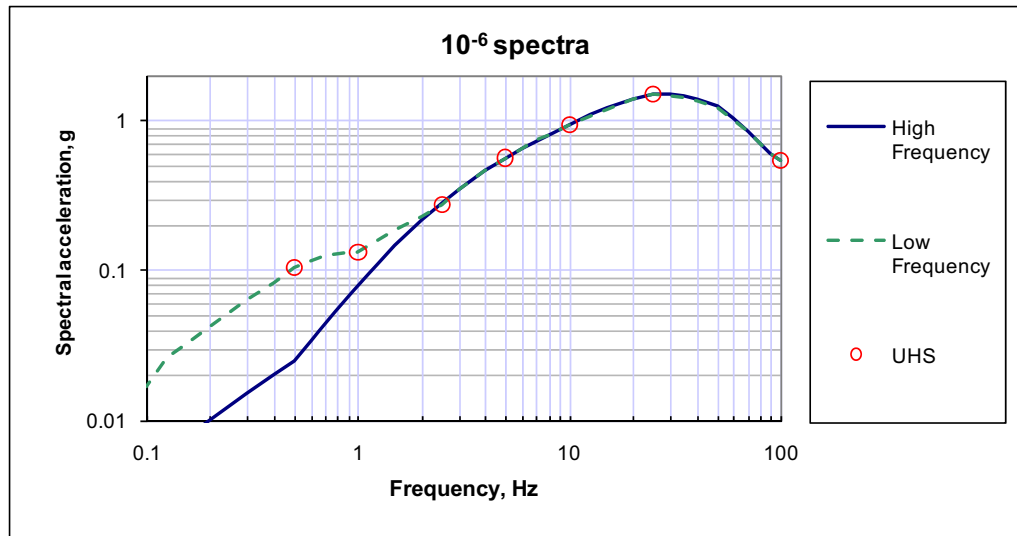
PTN COL 2.5-2

Figure 2.5.2-240 HF and LF Rock Spectra Anchored to Mean UHS Values from Hazard Calculation for 1E-05 Spectra



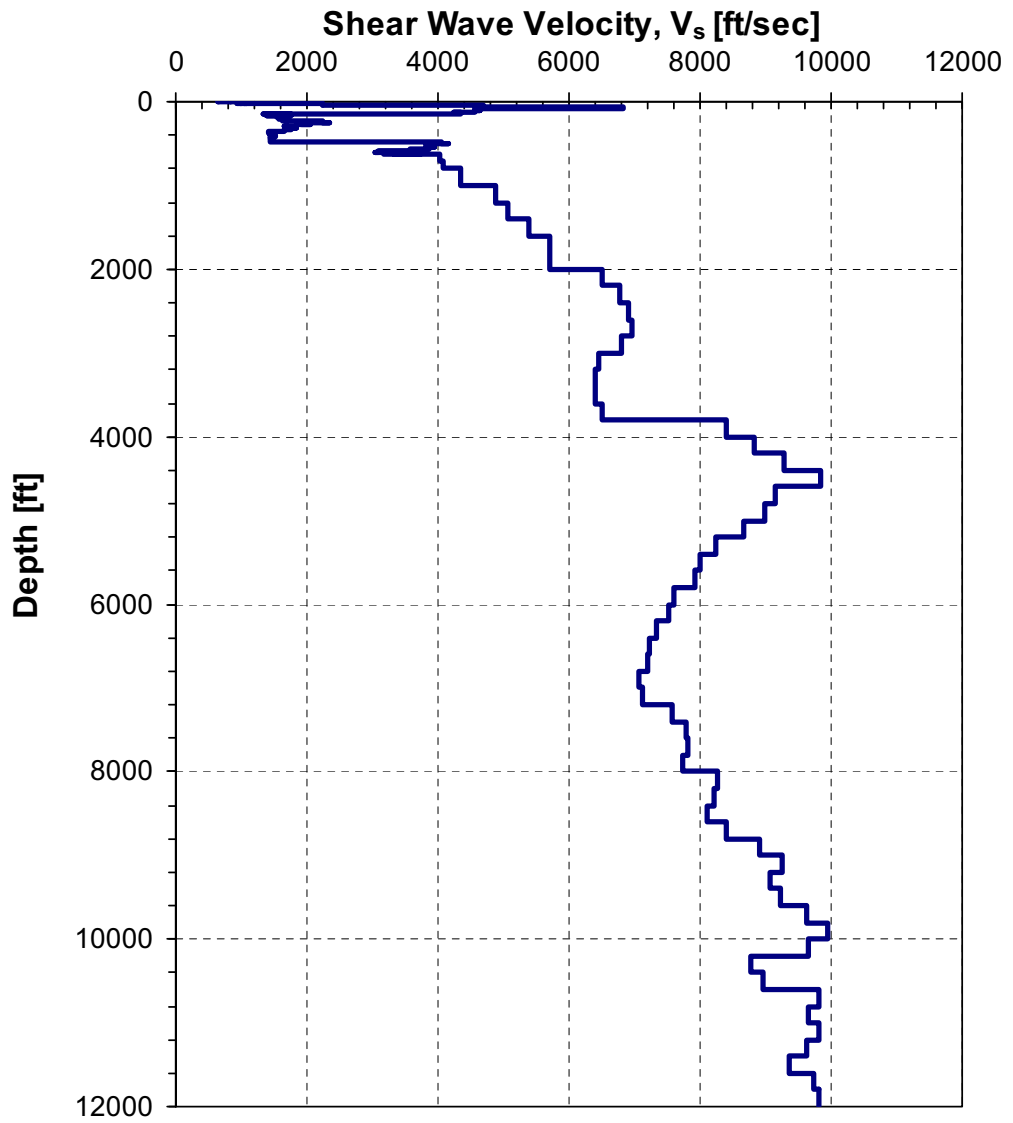
PTN COL 2.5-2

Figure 2.5.2-241 HF and LF Rock Spectra Anchored to Mean UHS Values from Hazard Calculation for 1E-06 Spectra



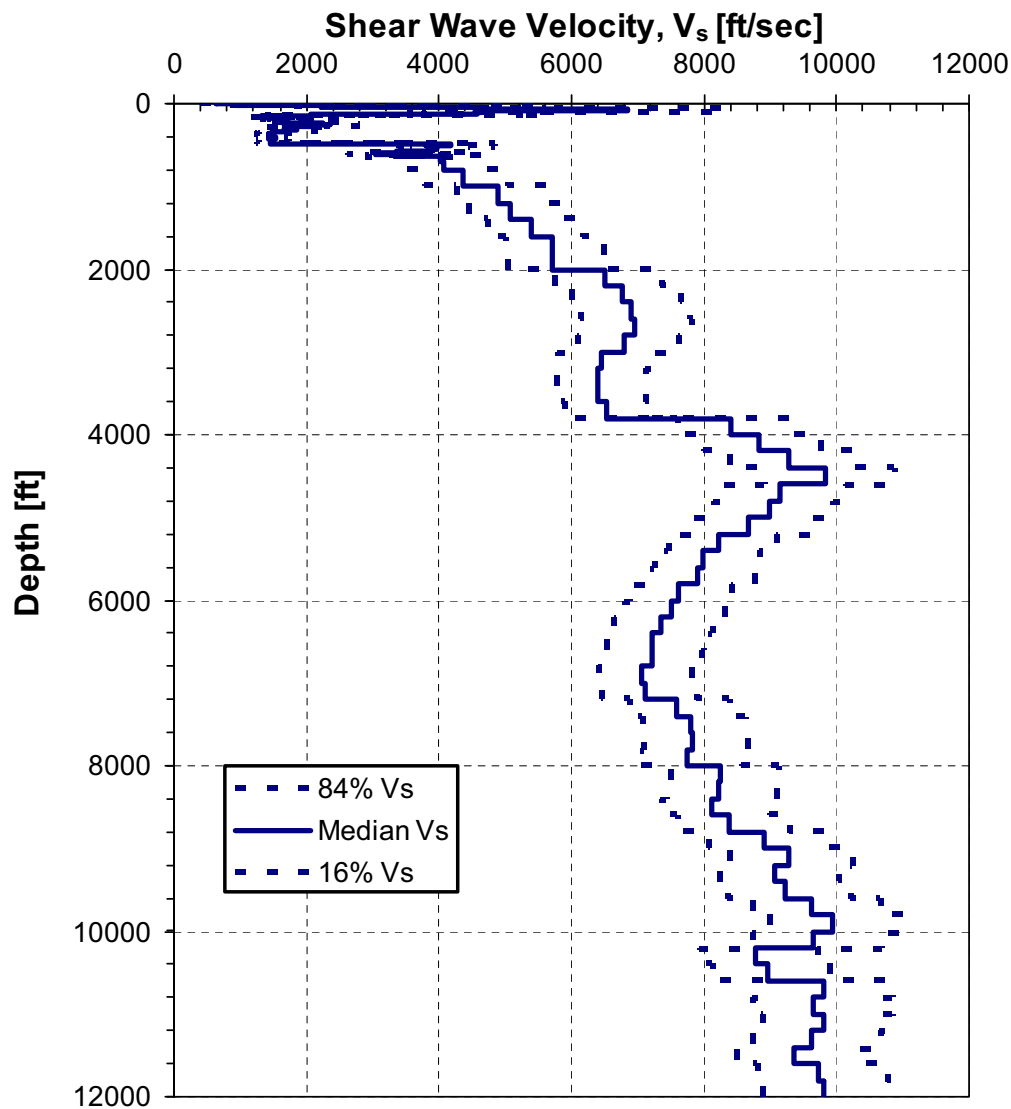
PTN COL 2.5-2

Figure 2.5.2-242 Input Base Case Shear Wave Velocity Profile



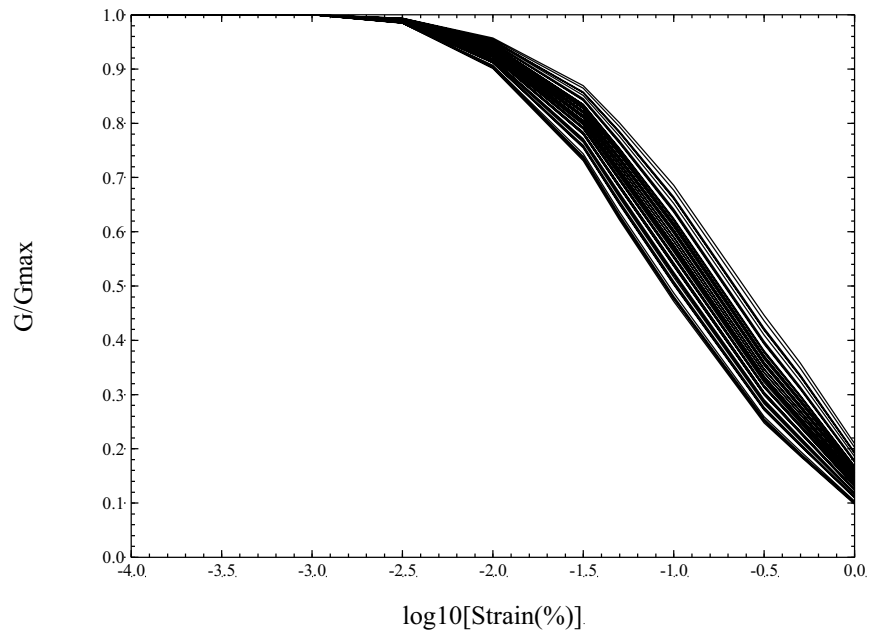
PTN COL 2.5-2

**Figure 2.5.2-243 Input Median Shear Wave Velocity Profile
(+/- One Standard Deviation) for Randomization Process**



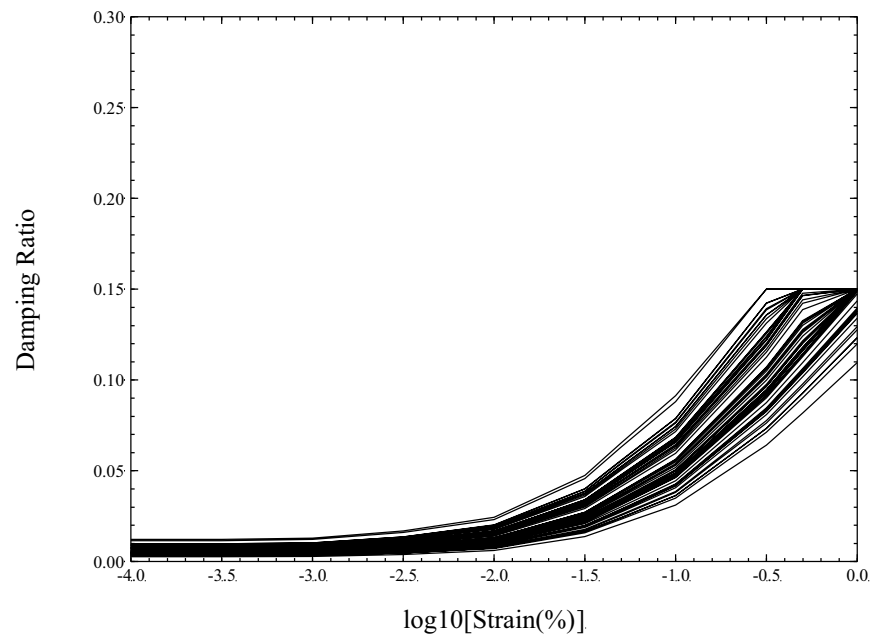
PTN COL 2.5-2

Figure 2.5.2-244 Strain Dependent Degradation Curves for Natural Soils (<150 feet)



PTN COL 2.5-2

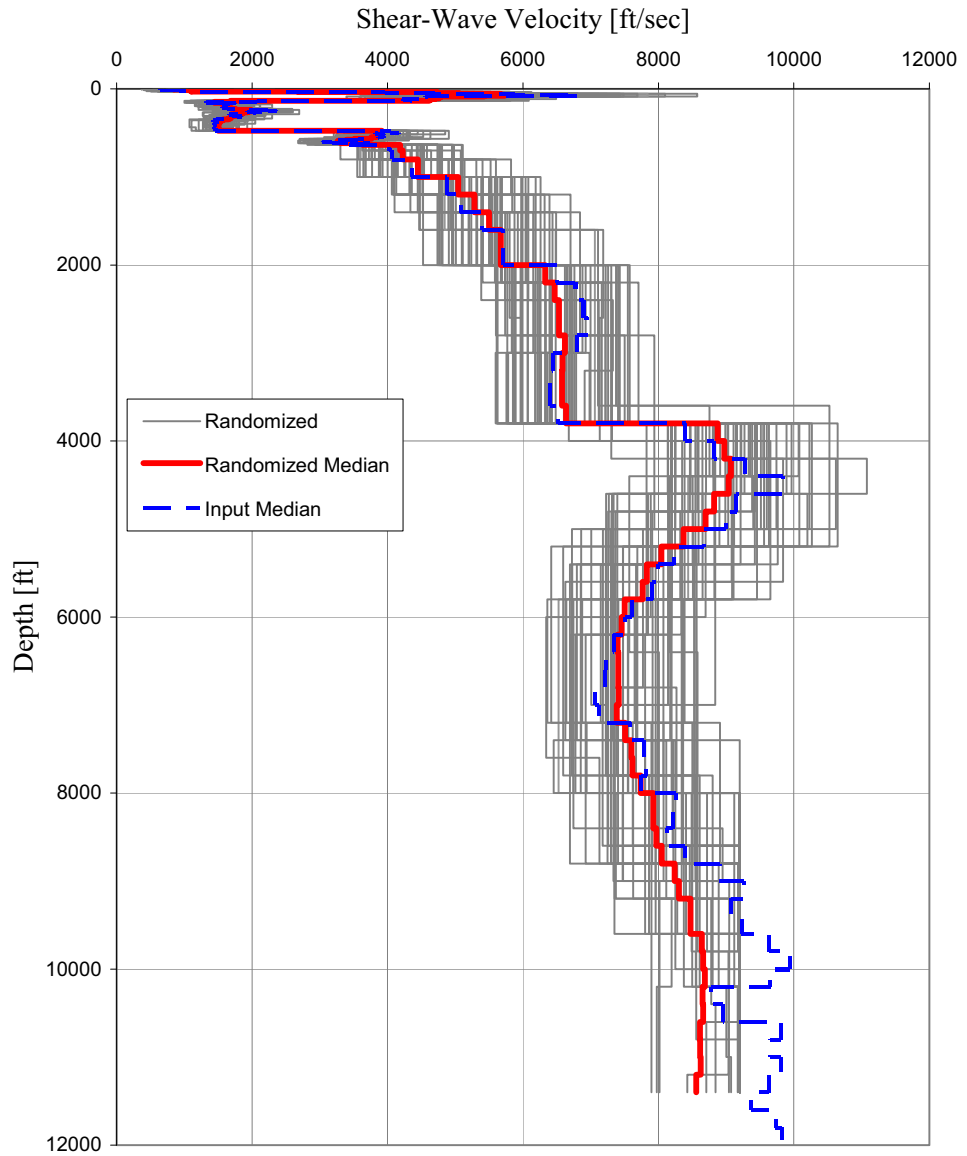
Figure 2.5.2-245 Strain Dependent Damping Ratio Properties for Natural Soils (<150 feet)



Turkey Point Units 6 & 7
COL Application
Part 2 — FSAR

PTN COL 2.5-2

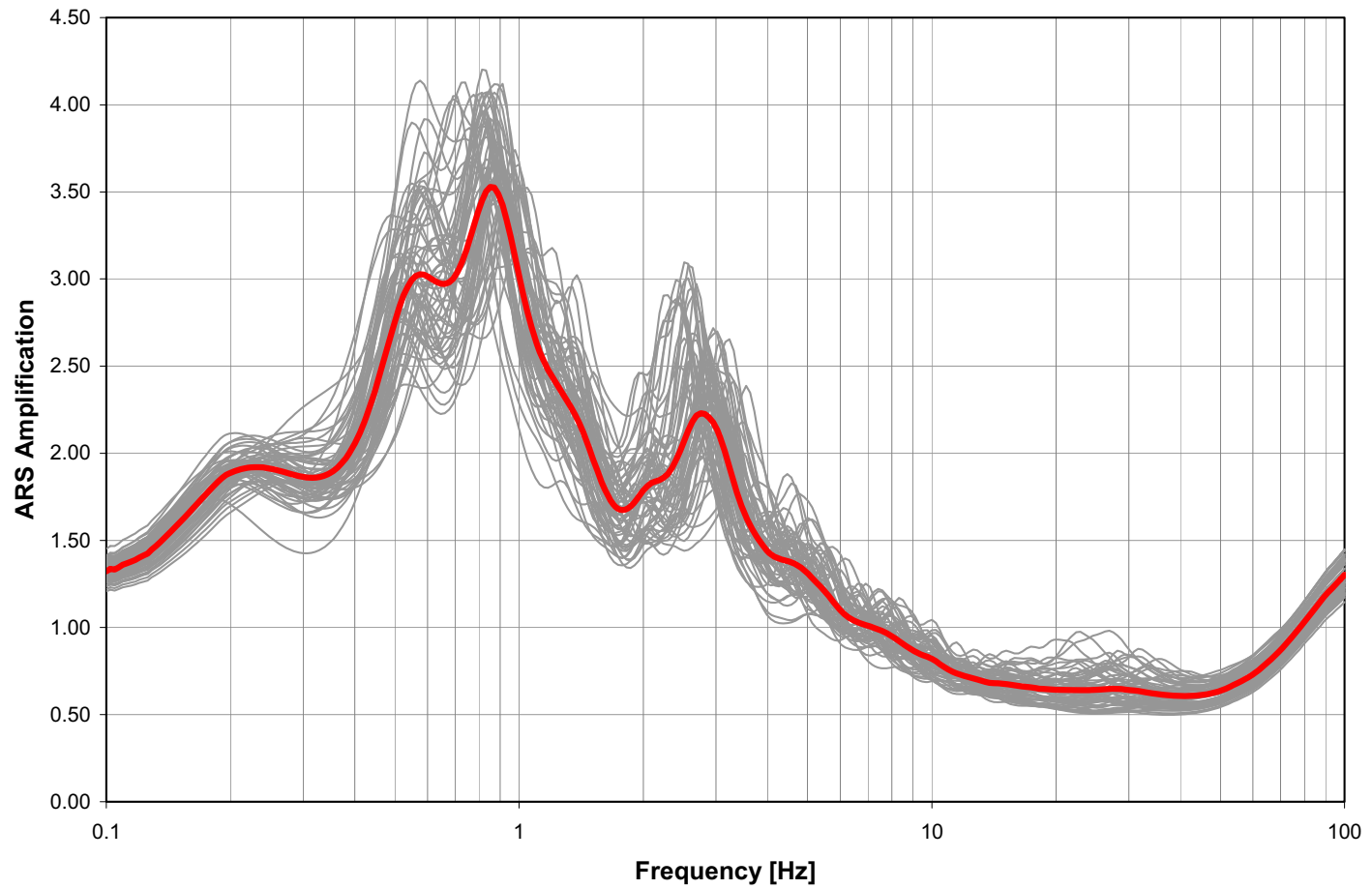
Figure 2.5.2-246 Randomized Shear Wave Velocity Profiles, Median Shear Wave Velocity Profile and the Input Median Profile Used For Randomization



Turkey Point Units 6 & 7
COL Application
Part 2 — FSAR

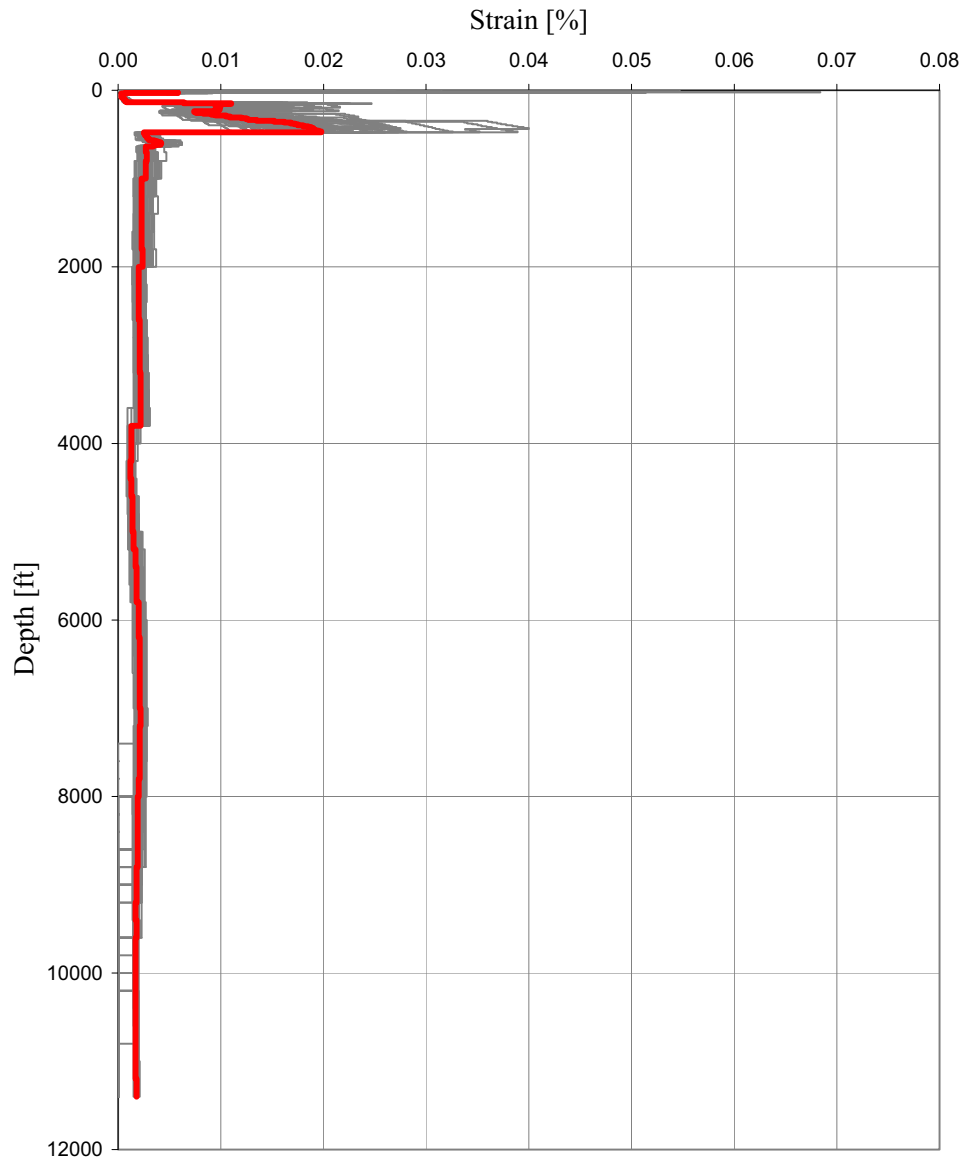
PTN COL 2.5-2

Figure 2.5.2-247 Median of Site Amplification Factor at GMRS Horizon (El. -35 feet) from Analyses of the 60 Modified Random Profiles with the 1E-04 LF Input Motion



PTN COL 2.5-2

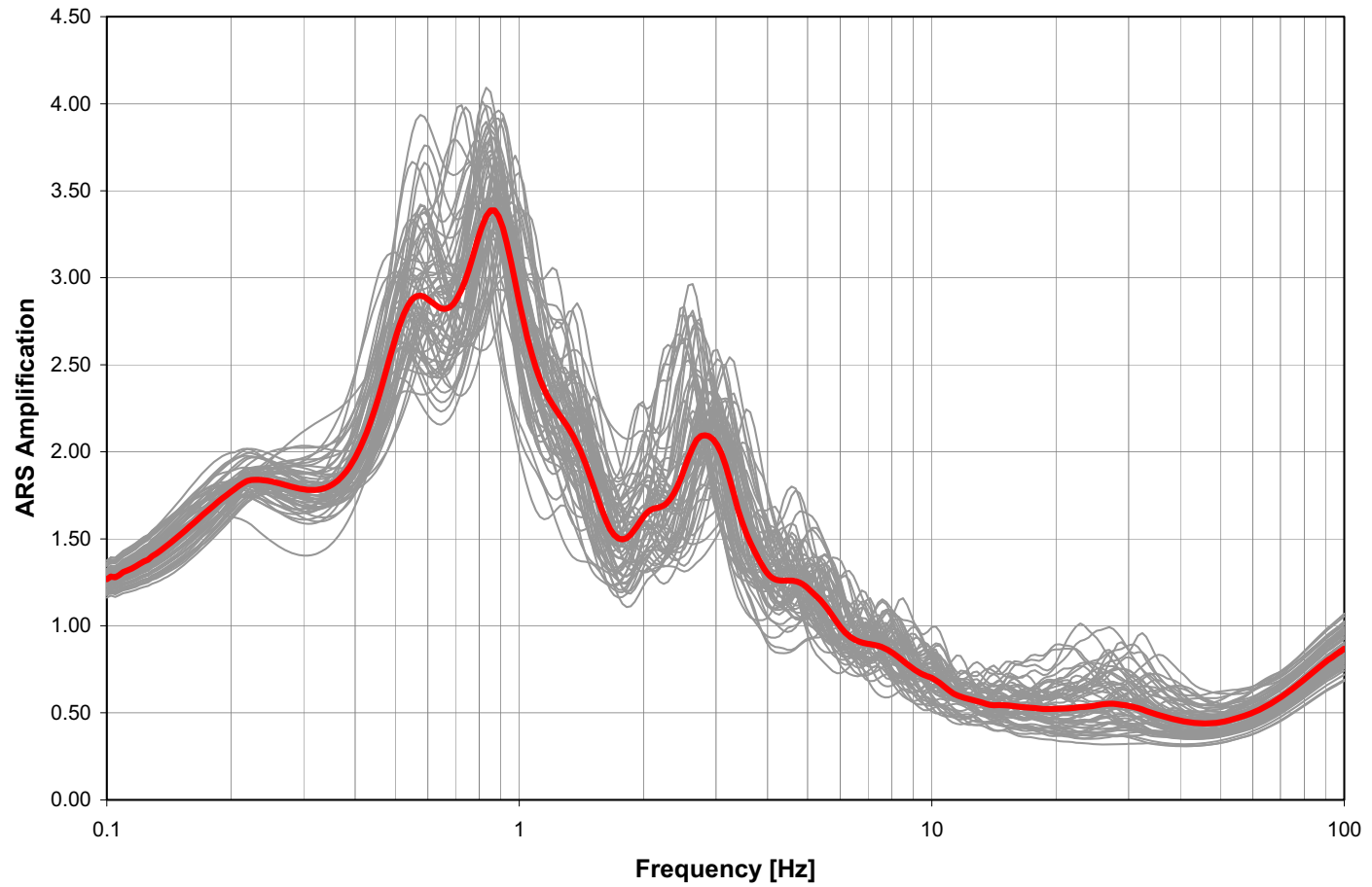
Figure 2.5.2-248 Maximum Strains Versus Depth that are Calculated for the 60 Profiles and their Median (Thick Red Line) with the 1E-04 LF Input Motion



Turkey Point Units 6 & 7
COL Application
Part 2 — FSAR

PTN COL 2.5-2

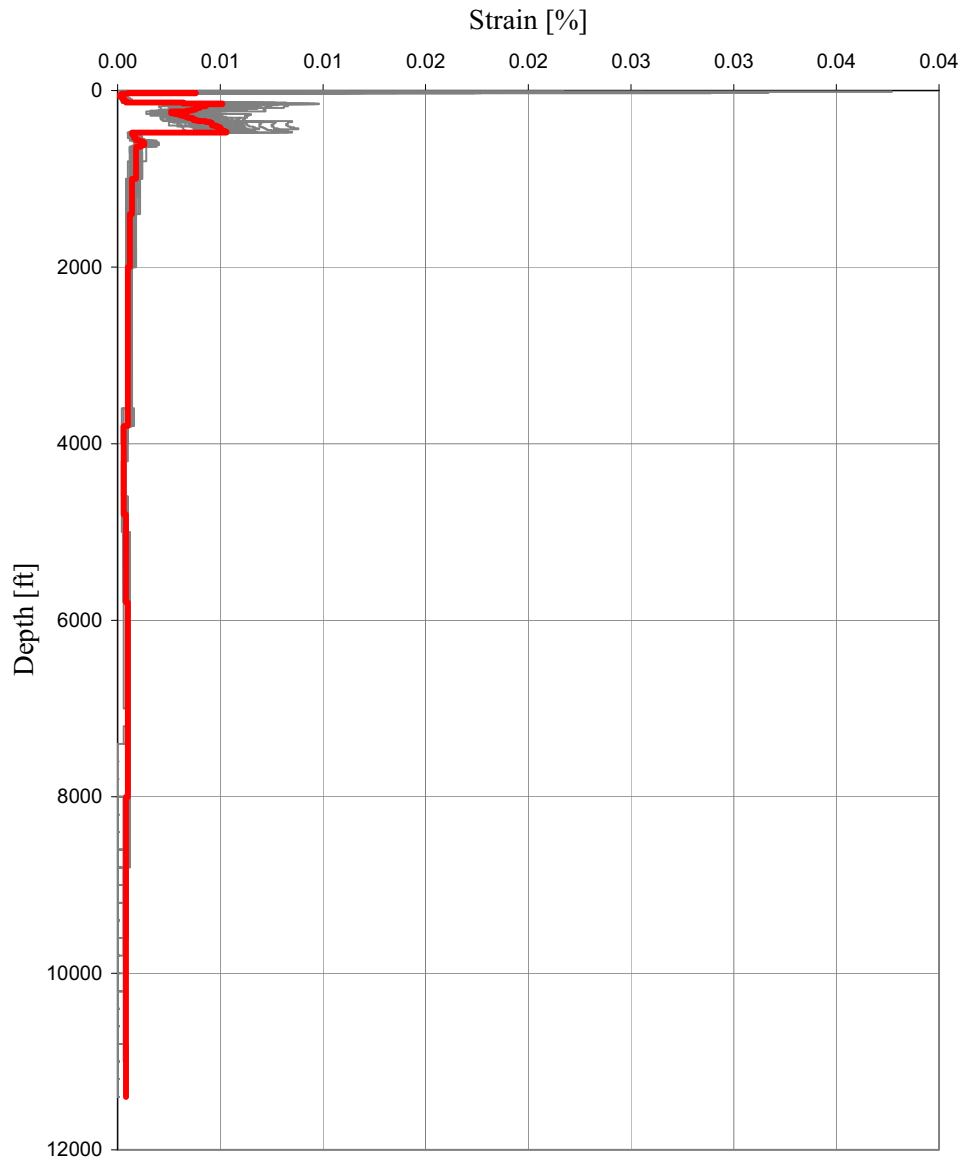
Figure 2.5.2-249 Median of Site Amplification Factor at GMRS Horizon (El. -35 feet) from Analyses of the 60 Modified Random Profiles with the 1E-04 HF Input Motion



Turkey Point Units 6 & 7
COL Application
Part 2 — FSAR

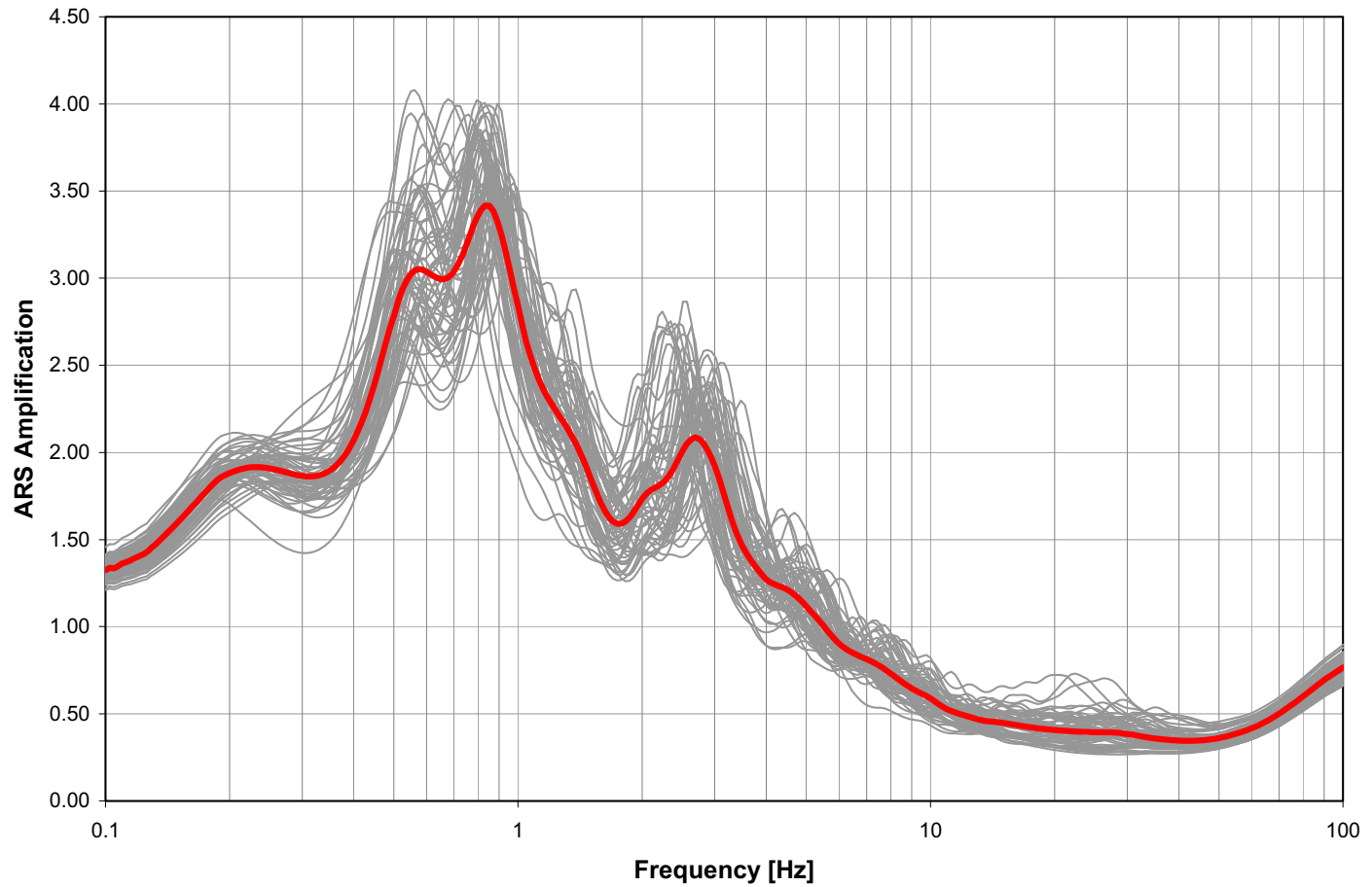
PTN COL 2.5-2

Figure 2.5.2-250 Maximum Strains Versus Depth that are Calculated for the 60 Profiles and their Median (Thick Red Line) with the 1E-04 HF Input Motion



PTN COL 2.5-2

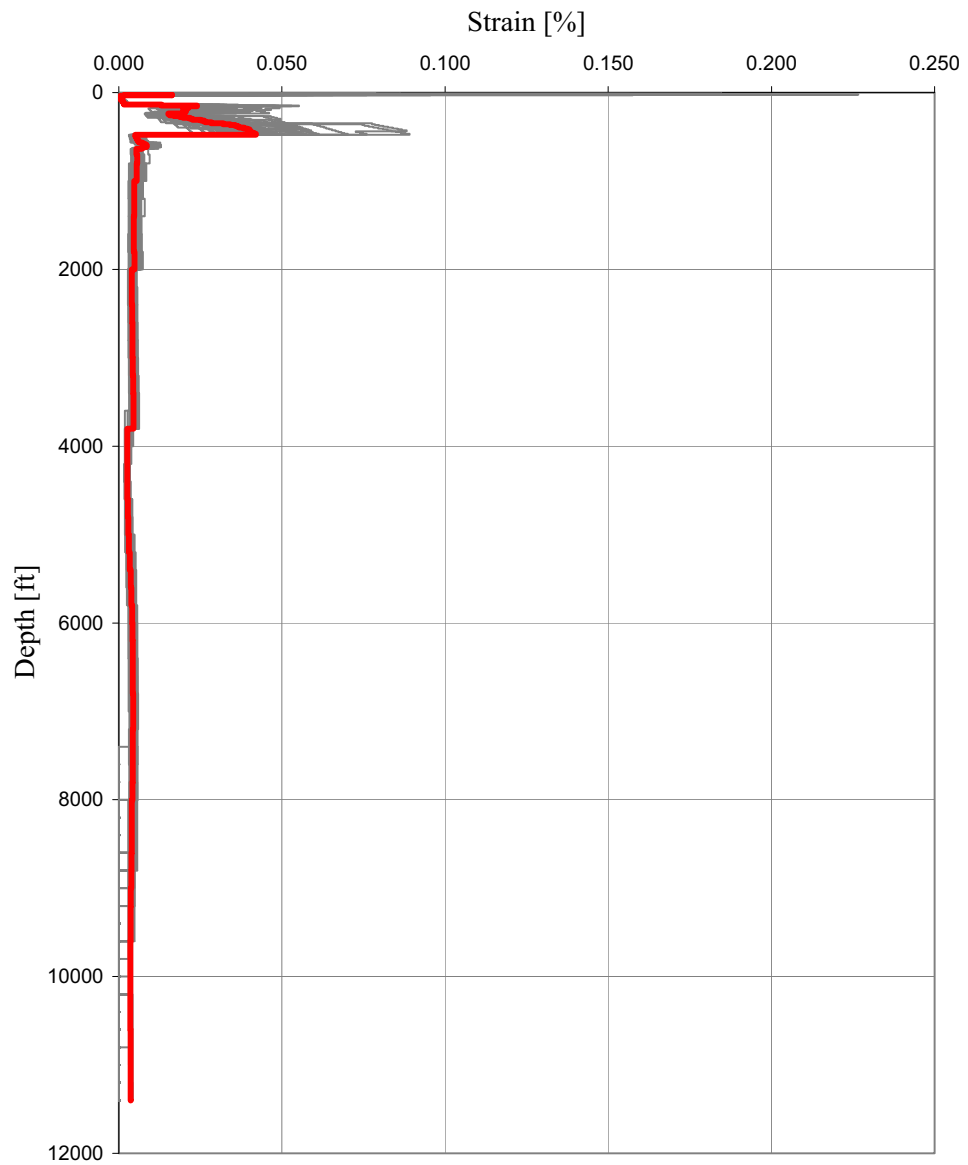
Figure 2.5.2-251 Median of Site Amplification Factor at GMRS Horizon (El. -35 feet) from Analyses of the 60 Modified Random Profiles with the 1E-05 LF Input Motion



Turkey Point Units 6 & 7
COL Application
Part 2 — FSAR

PTN COL 2.5-2

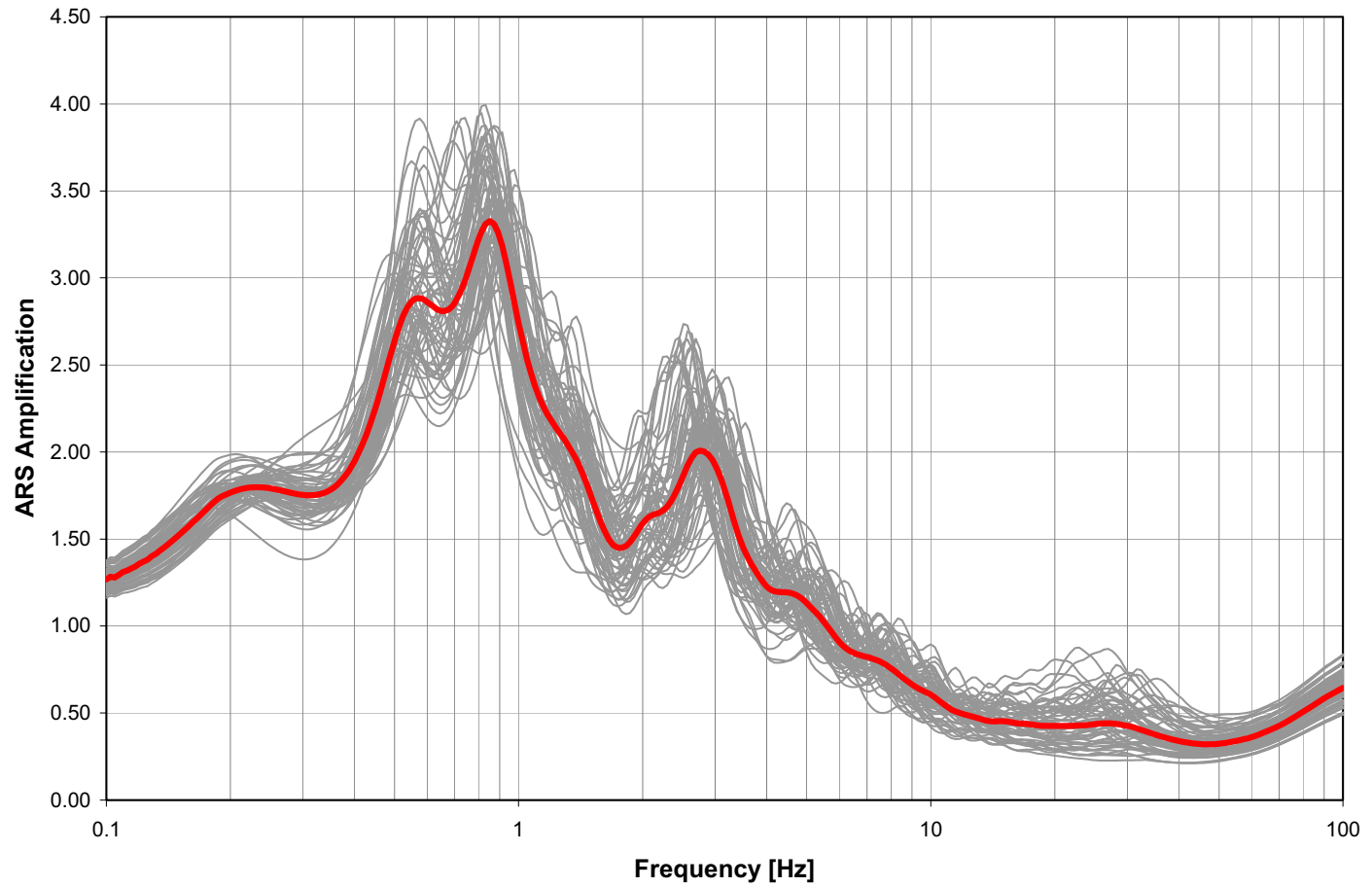
Figure 2.5.2-252 Maximum Strains Versus Depth that are Calculated for the 60 Profiles and their Median (Thick Red Line) with the 1E-05 LF Input Motion



Turkey Point Units 6 & 7
COL Application
Part 2 — FSAR

PTN COL 2.5-2

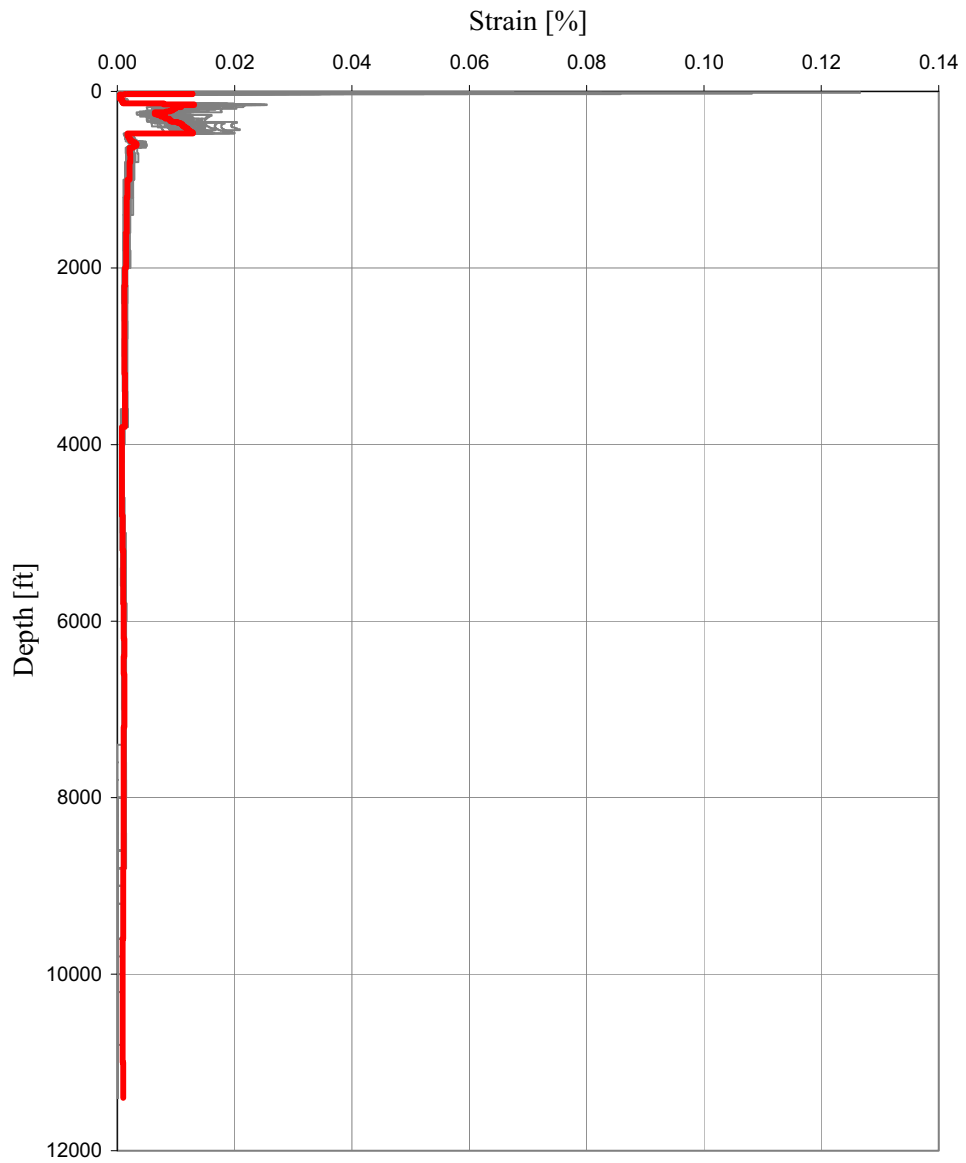
Figure 2.5.2-253 Median of Site Amplification Factor at GMRS Horizon (El. -35 feet) from Analyses of the 60 Modified Random Profiles with the 1E-05 HF Input Motion



Turkey Point Units 6 & 7
COL Application
Part 2 — FSAR

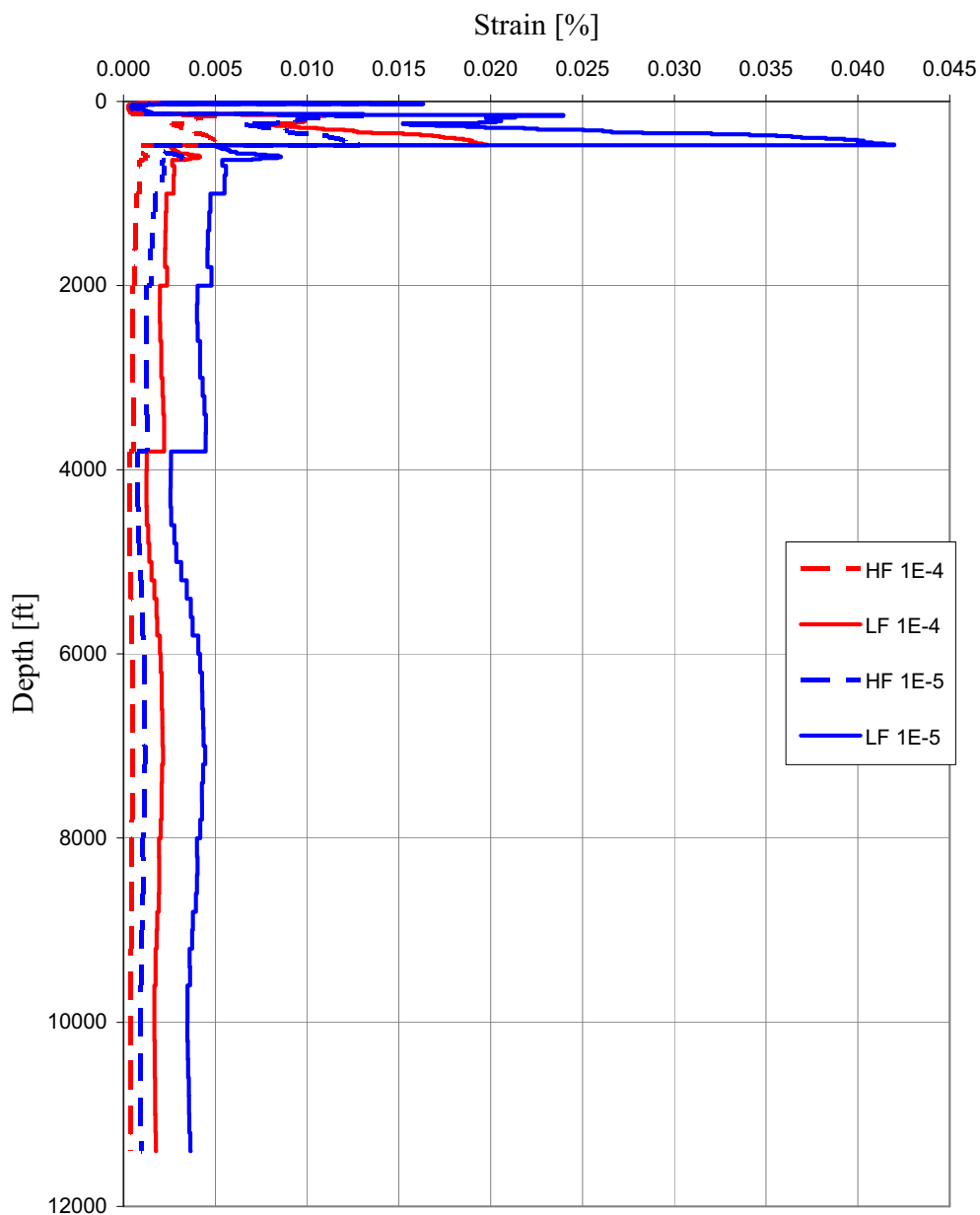
PTN COL 2.5-2

Figure 2.5.2-254 Maximum Strains Versus Depth that are Calculated for the 60 Profiles and their Median (Thick Red Line) with the 1E-05 HF Input Motion



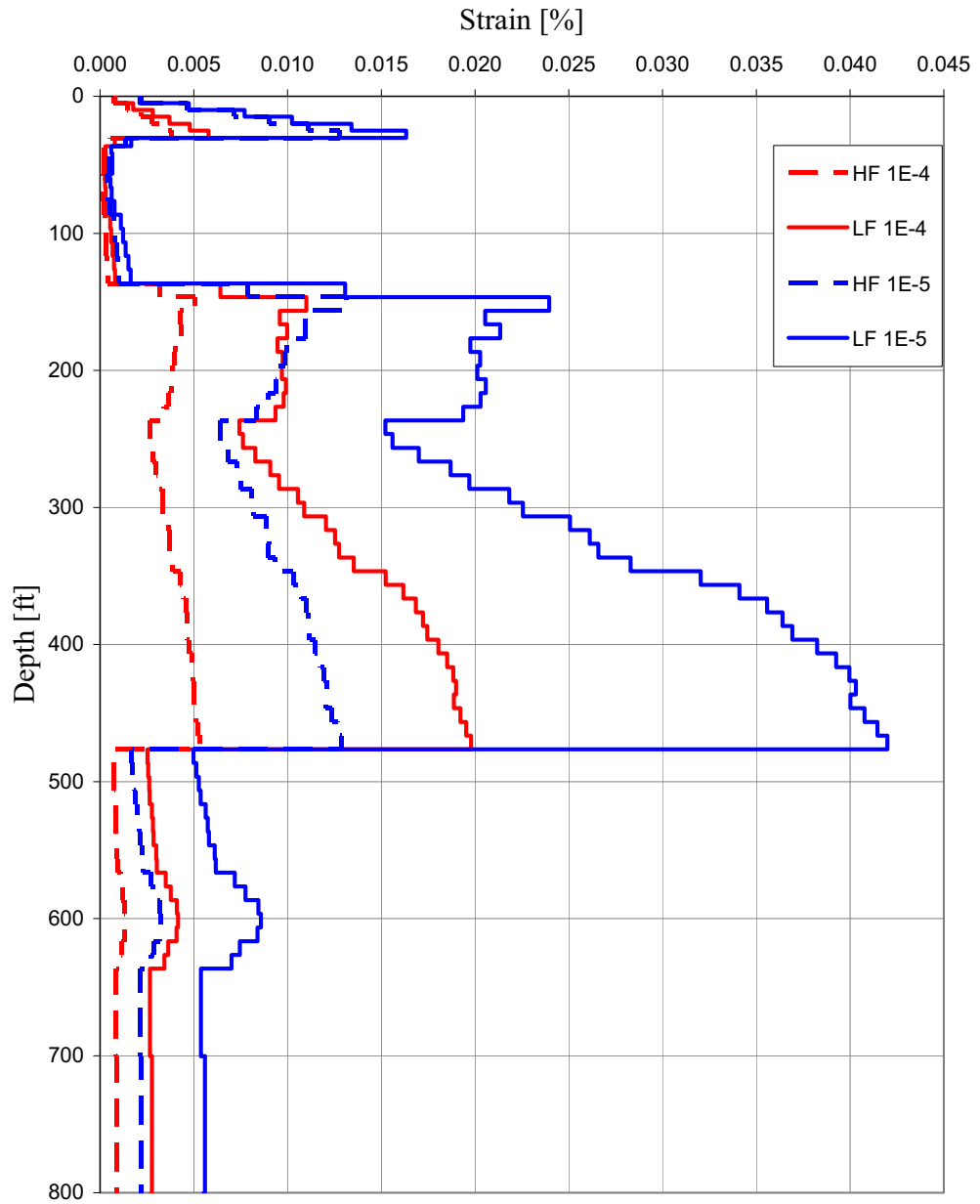
PTN COL 2.5-2

**Figure 2.5.2-255 Median Maximum Strain Profiles (Full Soil Column)
(Sheet 1 of 2)**



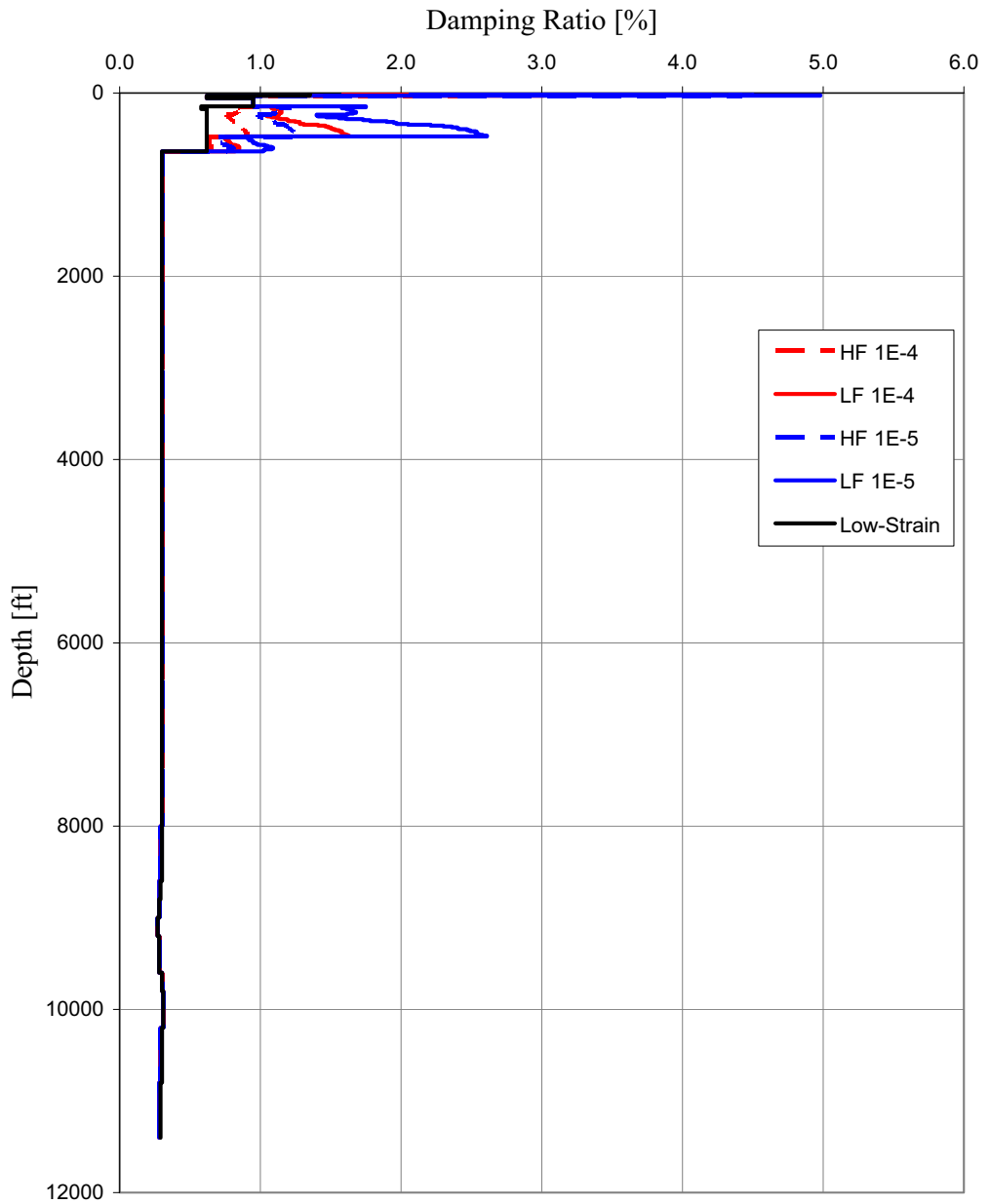
PTN COL 2.5-2

Figure 2.5.2-255 Median Maximum Strain Profiles (Upper 800 feet)
(Sheet 2 of 2)



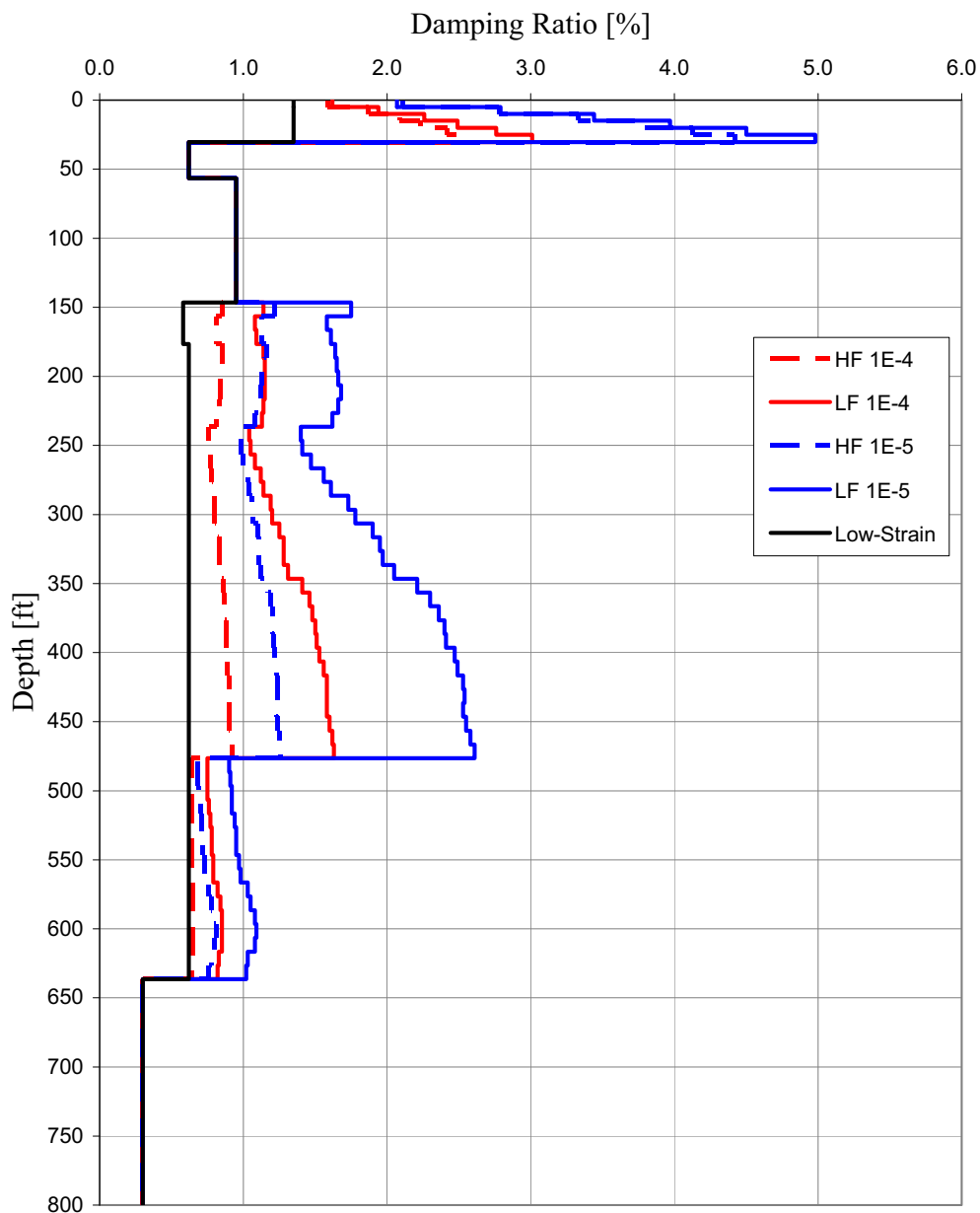
PTN COL 2.5-2

Figure 2.5.2-256 Median Profiles of Strain-Compatible Soil Damping (Full Soil Column) (Sheet 1 of 2)



PTN COL 2.5-2

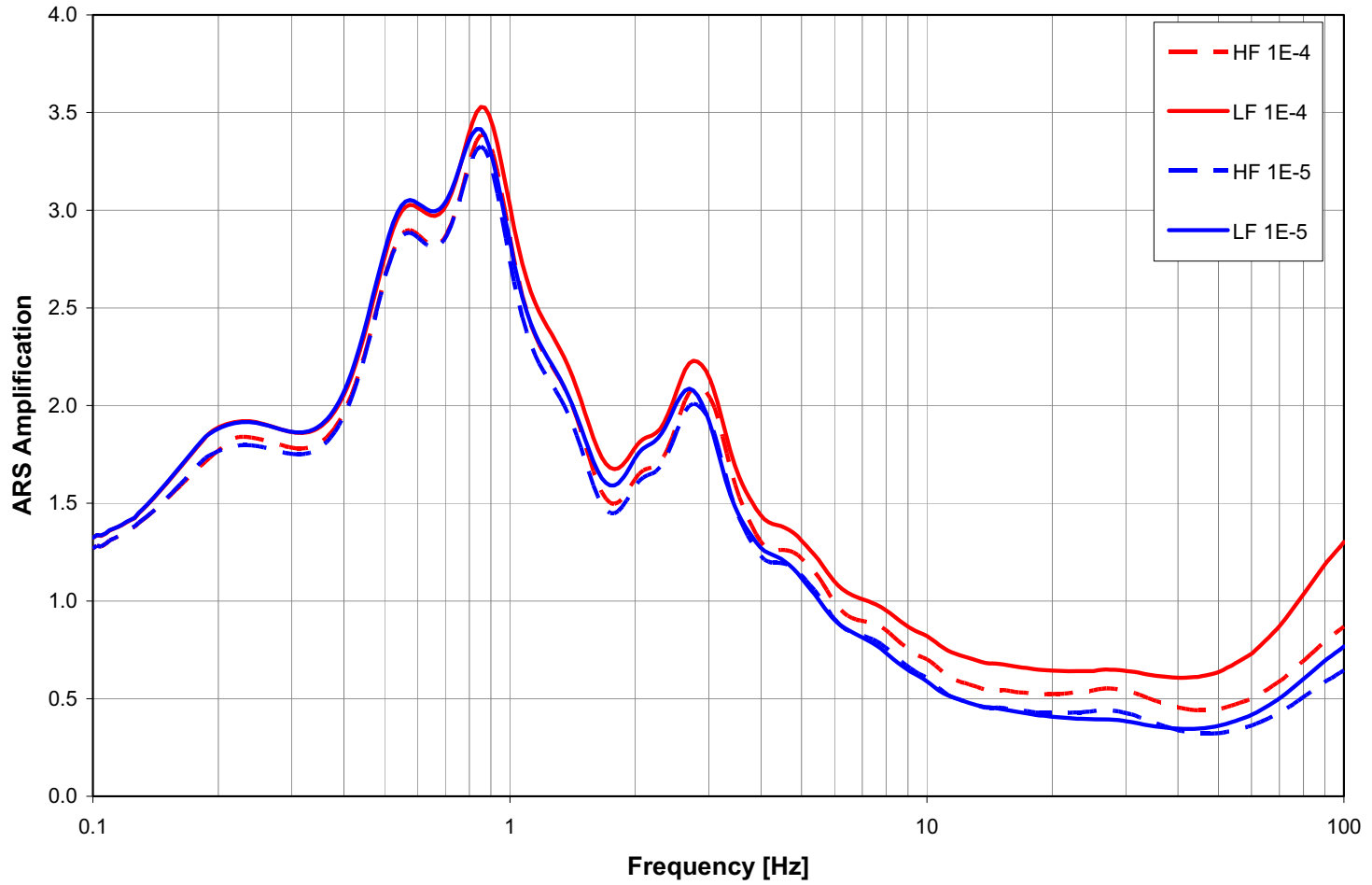
Figure 2.5.2-256 Median Profiles of Strain-Compatible Soil Damping (Upper 800 feet) (Sheet 2 of 2)



Turkey Point Units 6 & 7
COL Application
Part 2 — FSAR

PTN COL 2.5-2

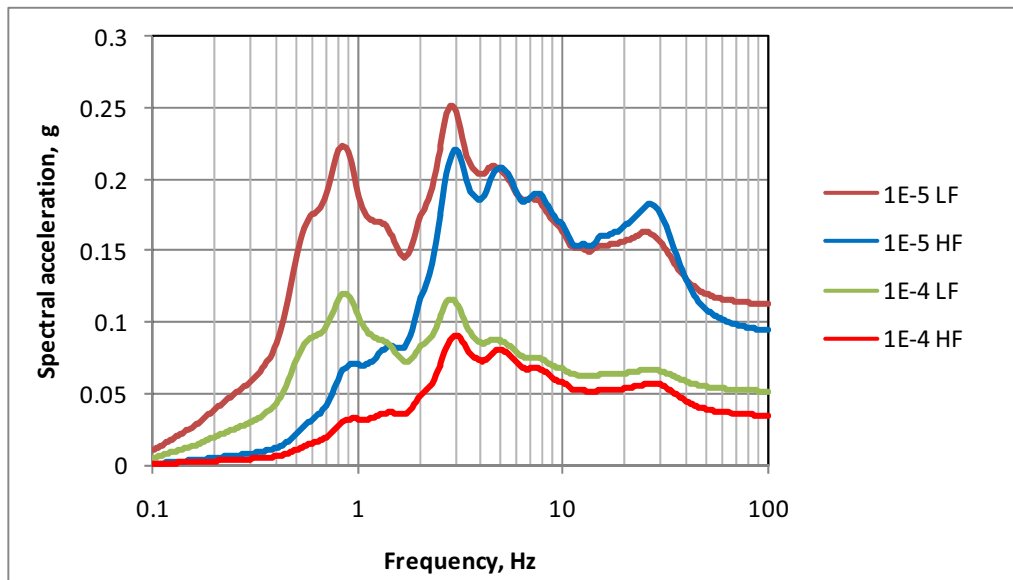
Figure 2.5.2-257 Comparison of Median Soil Amplification Factors at GMRS Horizon for LF and HF 1E-04 and 1E-05 Input Motions



Turkey Point Units 6 & 7
COL Application
Part 2 — FSAR

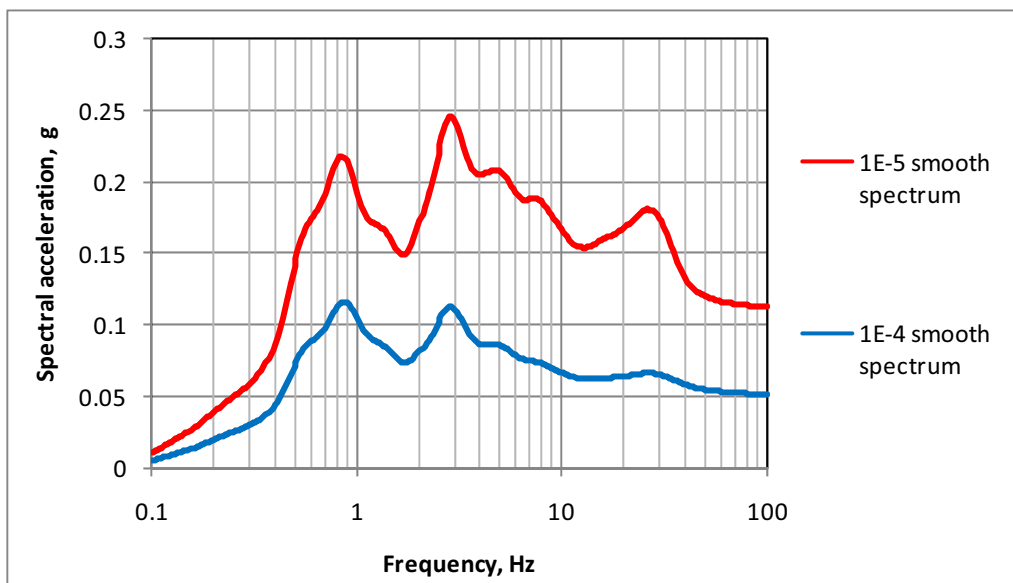
PTN COL 2.5-3

Figure 2.5.2-258 HF and LF Horizontal 1E-04 and 1E-05 Site Spectra



PTN COL 2.5-3

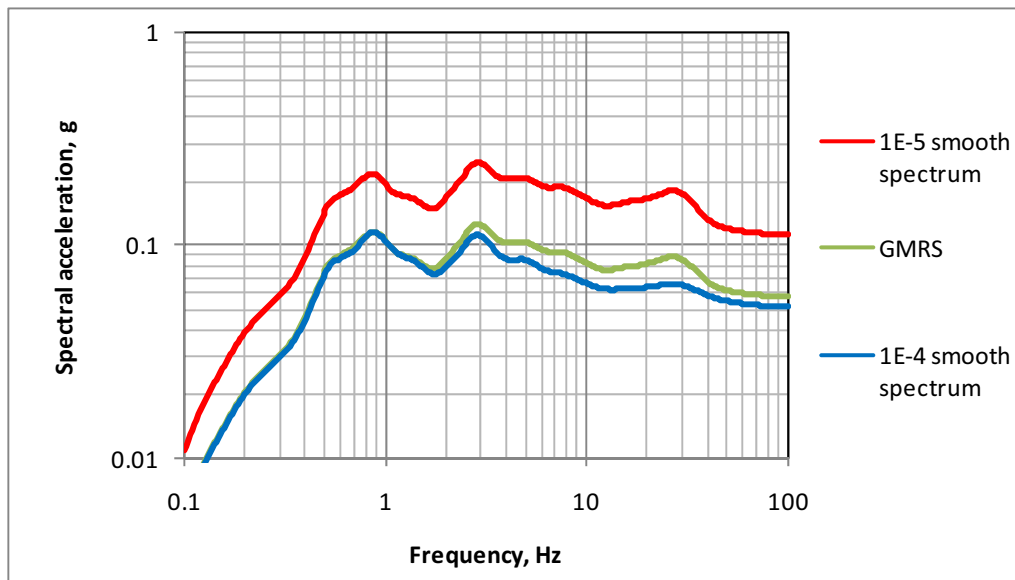
Figure 2.5.2-259 Smoothed Horizontal 1E-04 and 1E-05 Site Spectra



Turkey Point Units 6 & 7
COL Application
Part 2 — FSAR

PTN COL 2.5-3

Figure 2.5.2-260 Smoothed Horizontal 1E-04 and 1E-05 Site Spectra and GMRS



PTN COL 2.5-3

Figure 2.5.2-261 Smoothed Vertical 1E-04 and 1E-05 Site Spectra and GMRS

